Shear-Deforming Textile Reinforced Concrete

for the construction of thin double-curved freeform structures

Walter Gordon Woodington

Technische Universiteit Delft

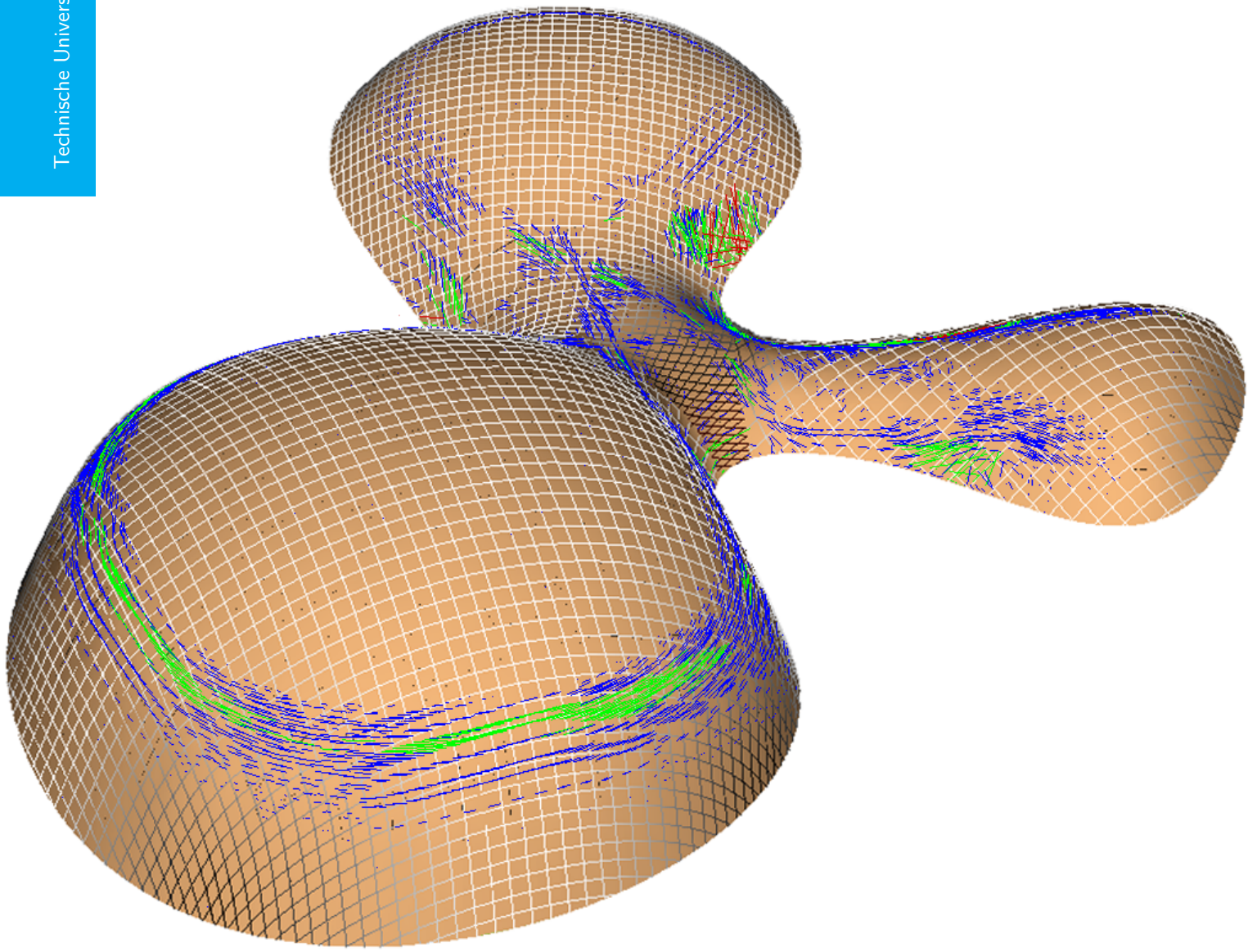

TU Delft Delft University of Technology

Challenge the future

SHEAR-DEFORMING TEXTILE REINFORCED CONCRETE

FOR THE CONSTRUCTION OF THIN DOUBLE-CURVED FREEFORM STRUCTURES

by

Walter Gordon Woodington

in partial fulfillment of the requirements for the degree of

Master of Science
in Building Engineering

at the Delft University of Technology,
to be defended publicly on Thursday, August 28, 2014.

Chairman:	Prof. dr. ir. R. Nijsse,	TU Delft
Thesis committee:	Dr. ir. O. K. Bergsma,	TU Delft
	Ir. A. Borgart,	TU Delft
	Ir. H. R. Schipper,	TU Delft

An electronic version of this thesis is available at http://repository.tudelft.nl/.

TU Delft Delft University of Technology

PREFACE

I would like to thank the course Special Structures for introducing me to concepts about freeform structures and parametric design. I am grateful to have had a diverse set of advisors to cross-pollinate this project with inspirations coming from the three departments of Civil Engineering, Architecture, and Aerospace Engineering.

Thank you to Rob Nijsse for leading the graduation committee and advising me on the project logistics. Thank you to Otto Bergsma for his patented material which was the starting point for this project and later, during the project, his enthusiasm and willingness to adapt his computer program, Drape, to the specific needs of this project. Thank you to Andrew Borgart for never being satisfied. Thank you to Roel Schipper for his interest, enthusiasm, creative suggestions, laboratory time, and unending references, which made me feel like I wasn't the only one thinking about my project.

Thank you to Peter Eigenraam for being available so often to teach me Diana and FX+.

Thank you to Kees van der Donk of Vreeberg Elastic Materials for providing me with sample materials and more importantly for giving me an in depth tour and explanation of the production process.

Thank you to my close friends for their confidence and discussions which quelled my insecurities. Finally I couldn't thank my parents enough for providing me with continual opportunities, inspirations, and encouragement. Thank you dearly.

Sincerely,

Walter Gordon Woodington
Delft, August 2014

PROJECT SUMMARY

Creating freeform architecture has been popular for a long time, at least the past century. Currently, the scale of these blobs is larger than before. As the price of labor overtook the price of materials (around the 1960's) the cost of these projects increased and has remained above normal for projects of similar scale. This project lays the groundwork to developing a material to enable the design and construction of structurally-informed freeform blob-like buildings. This is done by developing a partially-prefabricated material with significantly reduced onsite labor requirements and a method for designing with the material. Computer tools are increasingly important to the design, analysis, fabrication, and construction of these projects. Therefore the material is developed with computer tools in mind at every step of the process.

Figure 0.1: Example of realized freeform buildings, Experience Music Project and Science Fiction Museum and Hall of Fame, Seattle (left), The Sage Gateshead, Newcastle (middle top) , Kunsthaus Graz in Graz, Austria (middle bottom), Philips Pavilion, Expo 1958. [Stockton, Edkins, Aistleitner, Hagens]

A NEW MATERIAL FOR FREEFORM ARCHITECTURE

The starting point for this project is a Dutch patent for a "Sheet-like Building Material" (Chapter 2). It was created by two faculty members of the TUDelft Aerospace Composites department. It is a material that could be used to construct freeform buildings with reduced labor costs. It serves to bridge the worlds of complex small scale aerospace constructions and large scale architectural projects. This project goes beyond the properties of the patented material and construction method, while maintaining the core aspects of construction and deformation characteristics. Also from the field of aerospace composites is the computer program Drape. It models the unique deformation and layering characteristics of textiles. Therefore, even though the scale of constructions is radically different, it will be important to the structural analysis and construction of freeform buildings made from the new material.

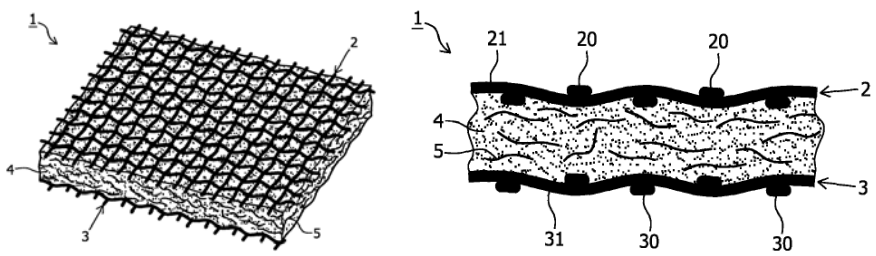

Figure 0.2: Layer configuration of the patented "Sheet-like Building Material"; two woven cloth layers and a hardenable dough-like material between them. [NL2003576C, Fig. 1 and 2]

OTHER PROJECTS ATTEMPTING TO SIMPLIFY FREEFORM CONSTRUCTION

At the architectural scale multiple projects have attempted to overcome the high cost of labor associated with constructing freeform buildings. Most of these are empowered by computers and have been developed within the last ten years. These include fabric formwork, prefabricated origami-concrete, and flexible formwork (Chapter 3). Another project called Concrete Canvas is very similar in composition to the material of this project, although it was not explicitly designed for creating freeform buildings. One key difference between the materials is Concrete Canvas's ability to meaningfully deform in shear, as textiles can. However, the strong similarities between the two show that successful fabrication and construction with the new material could be feasible. For the new material to be successful it must be developed with unique qualities to differentiate it from existing products and be paired with tools/methodologies to overcome its limitations.

Figure 0.3: Bulk roll of Concrete Canvas and close-up. [Concrete Canvas]

EXPLORATION OF CONCEPTS AND UNDERSTANDING

Background research was performed to gain insight about potential component materials, deformation possibilities, and architectural geometry (Chapter 4). This information was collected as a set of guidelines instead of as a definitive design. The development of the material will involve many more steps and could change significantly after this project, knowing the possibilities of textiles and concretes will encourage more informed decision making during development.

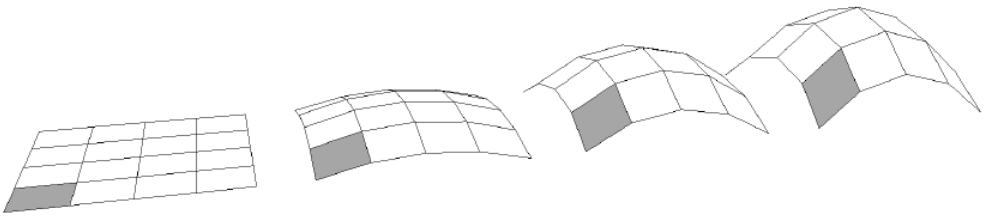

Figure 0.4: Shear deformation of a surface from flat to double-curved. [Eignraam, Figure 2-23]

ADAPTATION AND DEVELOPMENT OF THE BASIC CONCEPT

In order to begin development, multiple component materials and configurations were compared (Chapter 5). From this, a starting layered configuration was selected and potential methods for jointing elements were created. A simple structural calculation for tensile and bending cases was performed, resulting in a dimensioning and placement of the reinforcement. For demonstration purposes, physical prototype of the material was made.

The resulting material consists of two layers of glass-fiber textile reinforcement separated by a middle layer (~16mm) of dry (unhydrated) fine-grained concrete. On the bottom of this is a water- and airtight elastic foil, separated by a thin layer (~2mm) of concrete. On top is a permeable canvas layer, separated by a thin layer (~2mm) of concrete. The material can deform through shear, like textile, to create double-curved shapes. Because of this shear deformation the material thickness and reinforcement direction changes locally. Once in place the material is hydrated and allowed to harden. The material as outlined is by no means a final design, but instead merely sufficient to suggest that the material would be possible to realize, with reasonable dimensions and reinforcing. With this conceptual hurdle crossed, its dimensions and properties can be determined by investigation at a larger scale.

Figure 0.5: Photos of the physical prototype of the material showing reinforcement, concrete matrix, black elastic layer, and grey-black cloth layer, measuring approximately 20mm thick, 100mm wide, and 200mm long.

INVESTIGATION BY PHYSICAL METHODS

A basic physical test was conducted to test the most innovative feature of this new construction material: shear deformation (Chapter 8). Other properties such as the strength and behavior of textile-reinforce-concrete have been well studied (Section 4-3) Therefore priority was placed on investigating functionality of the deformation process over determining mechanical properties. The canvas, textile, and dry concrete (acting as a particulate fluid) should be able to deform through shear, given sufficient force. However, the water- and airtight elastic film layer cannot deform in shear without prestressing or buckling (in the form of winkling). Various elastic foils were subjected to shear tests using a self-made shear frame. Limited buckling occurred at small deformations but significant buckling occurred at greater shear deformation. Heating of the elastic foil layer was shown to reduce buckling.

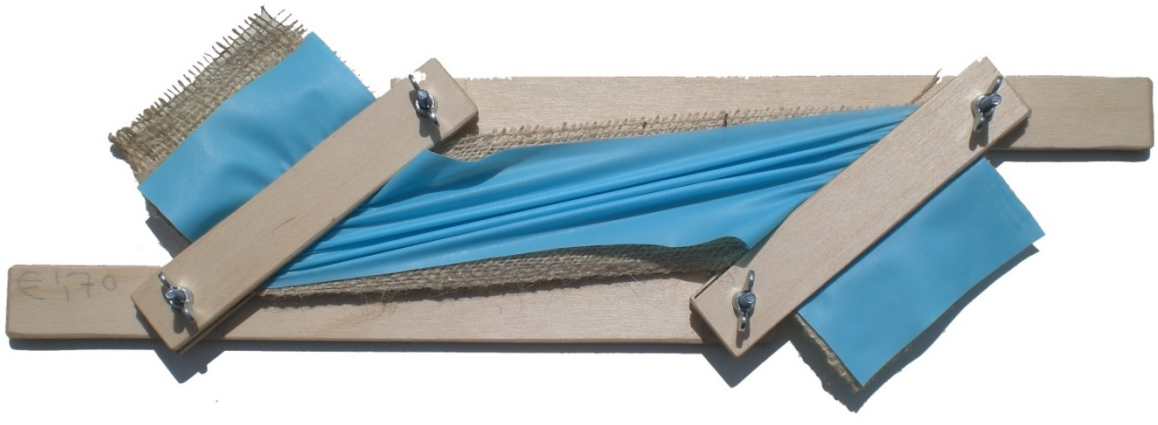

Figure 0.8: Room temperature shear deformation of a thin elastic film with burlap for comparison down to 40°.

INVESTIGATION WITH COMPUTER TOOLS

Application of the material to a larger scale construction is done using computer 3D-modeling (McNeel Rhinoceros) and structural analysis with a Finite Element Method program (Diana) (Chapter 6). To begin this process a hemispherical “test shape” building was selected. This simple shape is used instead of a more realistic freeform-blob building in order to provide confidence the computer calculations. The results are used to investigate the influence of the variable thickness and reinforcement direction as well as determine an appropriate starting thickness. It is important to understand this behavior once the material is applied to a more complex freeform building shape. Additional issues will arise when the material is applied to an actual building, such as fire safety, sustainability, and cost (Chapter 7). These topics are not core to the development of the material but are important to a well functioning building. Therefore they should be acknowledged early in the process and have been outlined.

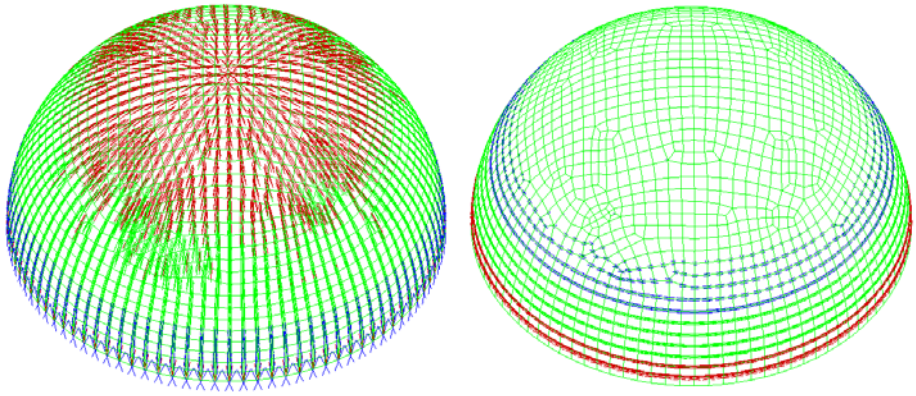

Figure 0.6: Principle stress vectors for gravity loading of the test shape, compression (left) and tension (right). Blue represents small magnitude stresses and red represents large magnitude stresses.

ADAPTATION OF EXISTING RESEARCH

With the basic thickness and reinforcement set from the test shape investigation, a more detailed analytical approach was taken to estimate the tensile (and moment) capacity of the shear-deformed material. This process takes its basis from experimental results of obliquely-loaded textile-reinforced concrete by Professor Josef Hegger of RWTH Aachen (Section 4-3-2). The approach involves modifying a coefficient in Hegger’s equation for the tensile strength of textile reinforced concrete to contain values for both directions of the weave. That coefficient is then applied to the computation of tensile strength at various shear angles and loading angles.

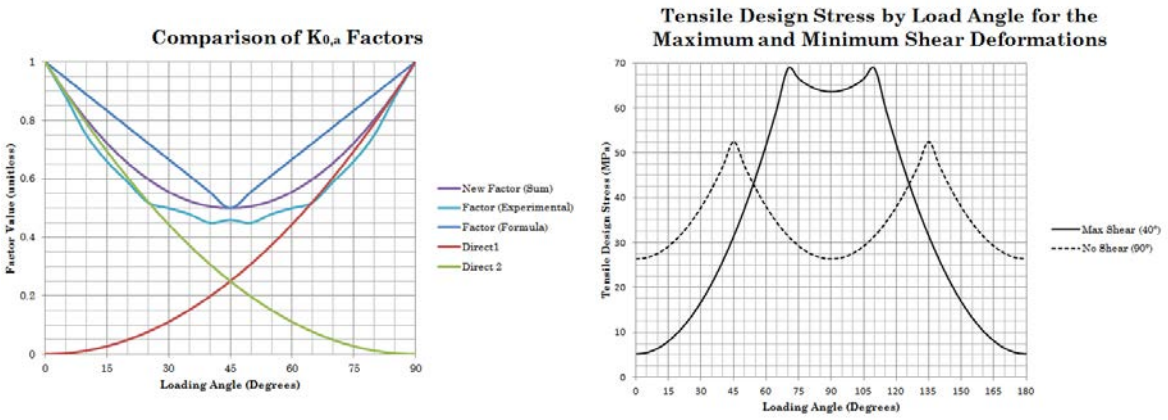

Figure 0.7: Comparison of Coefficients of Oblique-Angled Load for an orthotropic weave and the material tensile stress capacity for Orthogonal and 40-degree shear deformation cases.

FABRICATION AND CONSTRUCTION CONCEPT

The fabrication of the material limits the possible size of material elements. It is proposed, that like Concrete Canvas the new material will come in rolls. These rolls will be joined together on site where it will be deformed to create the building as designed digitally. Two methods of construction have been investigated: hanging and inflation (Chapter 9). Hanging means that temporary or permanent supports will be used to deform the joined material. Inflation means that air pressure will be used to deform the material. These methods produce very different results in appearance.

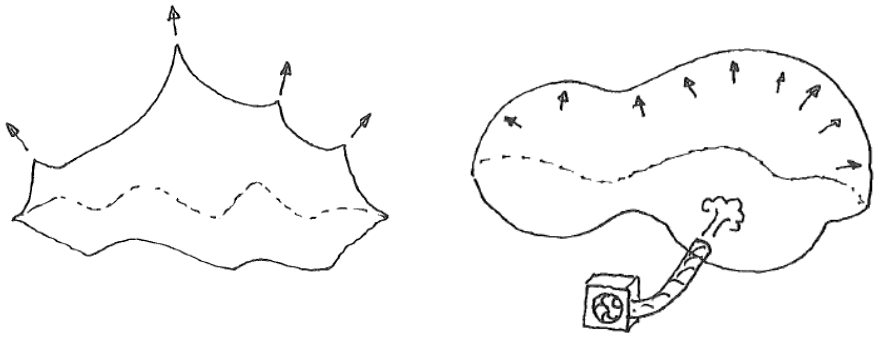

Figure 0.9: Erection methods: hanging (left) and inflation (right).

Once the supports are in place and the perimeter of the blank is secured to the corresponding foundation points, the deformation process can be performed according to the prescribed method. The deformation force (pressure or gravity) will shear-deform the material into the desired building shape. Once properly deformed the material would be structurally connected to the foundation and permanent supports. Then it should be sprayed with water to hydrate the concrete and begin the process of hardening. The force from the hanging supports or air pressure should be adjusted after hydration to insure the correct form. Once these adjustments have been made the material should be left to cure for a period of time before removing the supports or air pressure.

DIGITAL FORMFINDING

Before construction, a method of computer design must be used which takes into account the method of construction and deformation of the material. This step of formfinding is vital to creating a well constructible, efficient building from this thin material (Chapter 10). Formfinding parameters are adjusted in a parametric computer modeling environment (Grasshopper) to simulate the deformation of this material during construction with various supports and levels of air pressure and gravity. Beyond mimicking the behavior of the material, the formfinding process has the goal of creating a structurally efficient shape, meaning one with limited bending stresses. Although structural optimization is not fully integrated into the procedure, a structural analysis is performed after formfinding which can then be used to inform a successive round of formfinding. Windows, overhangs, and other “exceptions” to the solid shell of the building are analyzed after the formfinding process and are dealt with by the addition of stiffening structural elements. The result of the formfinding process is a 3D model of the building as well as a flat “blank” composed of the material. This blank is the assembled on site, in a staging area, from rolls of the material. During construction it will be deformed by hanging supports and/or air pressure to create the building.

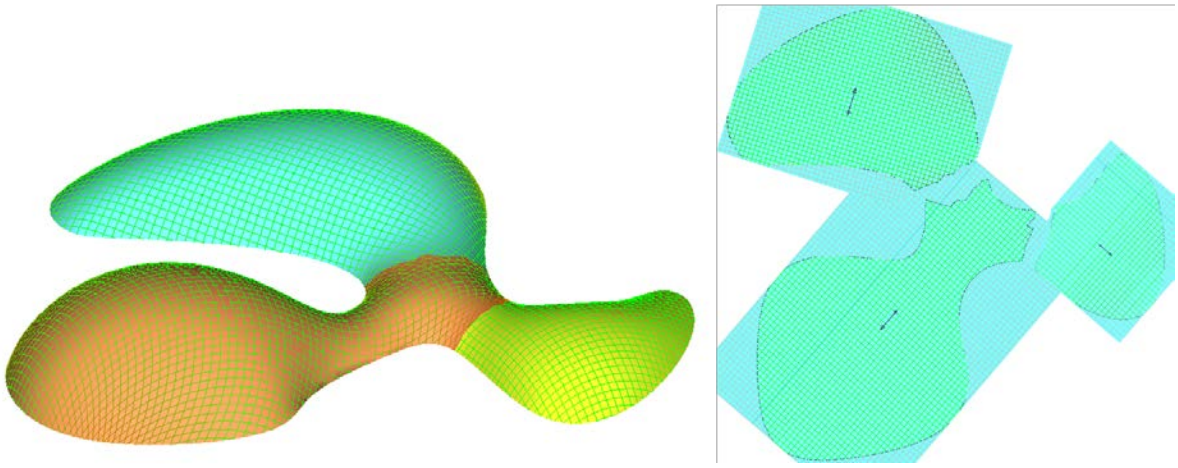

Figure 0.10: Example inflated building form divided into three structural bays (left) and three corresponding "blanks" shown at relative scale with textile orientation shown by arrows.

CASE STUDY BUILDING

As a conclusion to the project a case study building has been designed (Chapter 12). This is done to demonstrate the possibilities of the new material as well as the formfinding (Chapter 10) and construction method (Chapter 11). The building is a relatively low and wide, high profile, blob-like concert hall. This program and description matches that of other freeform buildings currently in existence. During the design process some specific solutions are proposed to overcome the limitations of the new material. For example, the structure is broken into segments (structural bays) because the material cannot shear enough to fully cover the building with one 'blank'. A series of structural analyses are performed to determine the areas in which the building would require additional layers of the material.

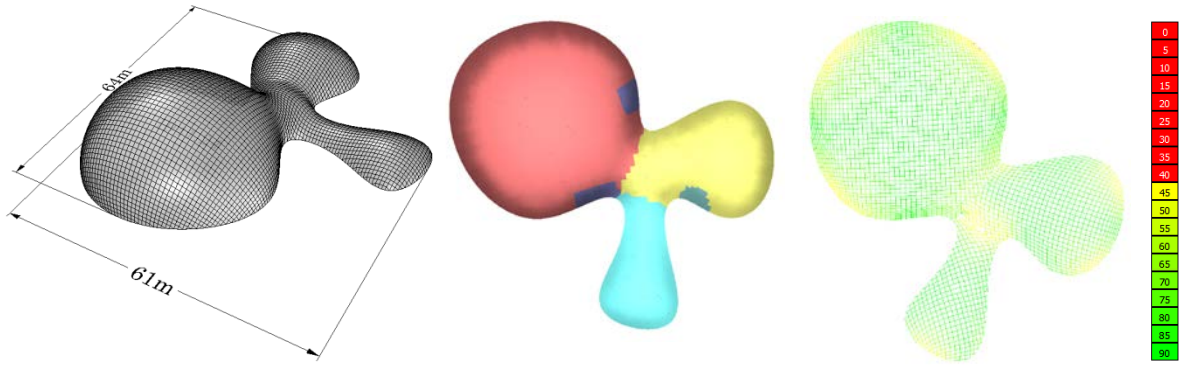

Figure 0.11: Case Study Building, dimensioned axonometric projection (left), structural bays and layers (center), and material shear angle (right).

TABLE OF CONTENTS

1 INTRODUCTION

This project captures the growing trend of freeform architecture. In order to enable this trend a composite material is developed to overcome the bottleneck to realizing these digitally produced designs: construction. This begins with a narrowing of all that is encompassed by 'freeform architecture' down to a usable definition with its own set of characteristics.

1-1 FREEFORM ARCHITECTURE

Freeform architecture is complex geometrical forms created at the building scale. These can range from complex regular, orthogonal forms to surfaces composed of non-uniform rational b-splines (NURBS) and everything in between, encompassing domes, shells, tents, blobs, and generally odd-looking buildings. Freeform architecture generally includes all non-orthogonal constructions. Blob architecture refers to a subset of these which are more complex to define geometrically, unlike spherical domes. The breadth of this definition is best understood though photographs, in Figure 1.1.

Figure 1.1: Example of realized freeform buildings, Experience Music Project and Science Fiction Museum and Hall of Fame, Seattle (left), The Sage Gateshead, Newcastle (middle top) , Kunsthaus Graz in Graz, Austria (middle bottom), Philips Pavilion, Expo 1958 [Stockton, Edkins, Aistleitner, Hagens].

Irregular freeform architecture is gaining popularity, empowered by rapid developments in three-dimensional computer design software. Starting in the 1960's these computer tools were first applied in other industries but by the year 2000 their use in architectural design had become nearly ubiquitous.

In the past buildings with curved geometries were developed analytically with mathematical expressions or experimentally through the use of physical models. Now these designs can be developed using digital techniques such as NURBS modeling, parametric design, and finite element software. With the use of these computer tools, architects and engineers have been able to realize increasingly complex freeform structures.

A summary of this trend by John Gould of Formtexx contrasts the usage of digital design and fabrication in the aerospace and construction industries.

> The late 1980s saw some radical developments in what became known as freeform, organic or zoomorphic architecture. Prior to this date most structures, with the exception of those in the craft and cultural tradition and the engineering work of the structural pioneers of the early 20th century, were constructed of planar elements in orthogonal arrangements set at regular intervals.
>
> The ability to create double-curvature forms in a controllable manner was an essential requirement of this new building typology and was enabled by borrowing the emerging 3D software platforms being developed by the film animation, aerospace and automotive industries. Here in lies a problem that has dogged the architects ever since. Their buildings are one-off "prototypes" whereas the animation industry had never intended to bring their creations into the real world and the aerospace and the auto makers were intent on making many multiples with fixed tooling.
>
> The problem for the construction industry arose when it came to transforming the creative digital data into coherent freeform buildings for which they had no obvious tools to produce large double-curvature surfaces, digitally. [Formtexx]

1-2 CONSTRUCTION BOTTLENECK

The rise of labor costs has made the construction of complex freeform buildings very expensive. Computer aided manufacturing is not yet developed enough to reduce labor costs, therefore structurally efficient freeform buildings generally have above-average budgets. Sometimes the forms are simplified in order to speed up the construction process, other times the form of the building is merely cladding concealing a more standard structure.

As seen in the photographs in Figure 1.1, freeform architecture can be made from many different materials (metal, glass, concrete, wood, etc); however concrete will be examined more closely. Of the materials that the construction industry is familiar with, concrete is the closest analog to the hardenable resins used in the freeform shapes of the aerospace industry. The history of freeform architecture is closely linked to concrete from Roman domes to later shells by Heinz Isler. Its amorphous continuous property makes it particularly well suited for freeforms. In comparison, masonry, timber, and wood are typically used in elemental methods of construction, meaning that similar discrete elements are combined onsite to create a rigid form. More complex shapes require a greater variation of elements which complicates fabrication and construction logistics.

Much of the labor and cost associated with freeform concrete construction comes from producing the curved (and sometimes double-curved) formwork. This cost can be lowered by using building forms with repeated regular curvature, but this is limiting to freeform architecture, which often requires irregular curvature to achieve the digitally produced designs and therefore has limited possibilities for repetition of formwork.

Concrete construction costs are limiting what is feasible by structural and architectural designs. The modern history of concrete shell structure construction is depicted in Figure 1.2. It shows three design techniques (analytical, experimental, and digital) as well as the limiting factor (construction, architectural design, and structural design) to the implementation of concrete shells though the century. In order to enable the efficient design and construction of freeform architecture the issue of construction must be confronted.

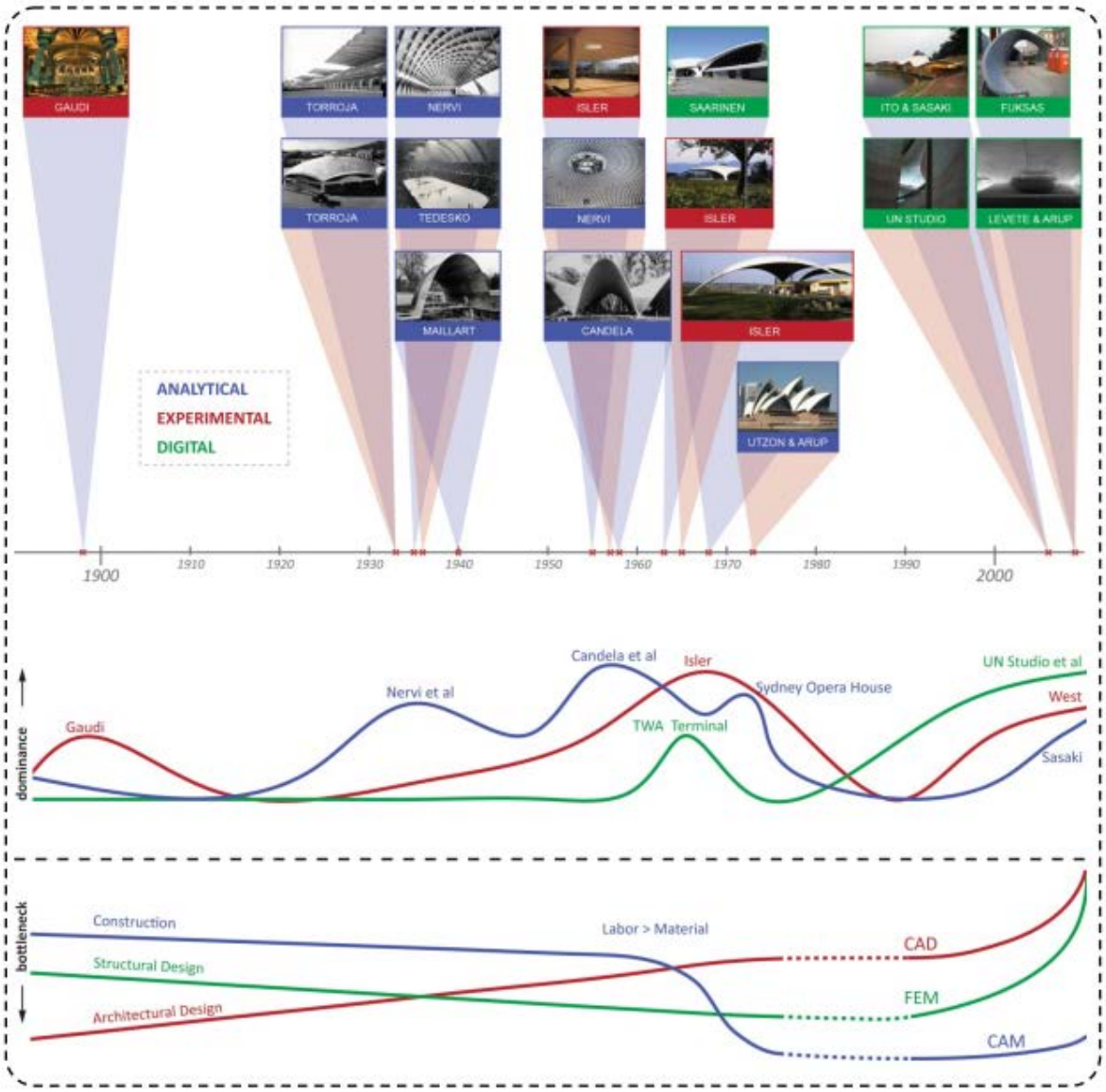

Figure 1-2: History of concrete shell structures [Huijben, Figure 8]

1-2-1 CURRENT METHODS OF CONSTRUCTION

As mentioned under the previous heading, the irregularity and high level of curvature often makes the realization of their designs cost-prohibitive. This reserves their use to special high-profile buildings. When they are built the curved form either acts as a load bearing element or simply as cladding over another main structure. Curved façade cladding elements separate the function of load bearing from expressive form creation. For this reason they can be lighter, smaller, thinner and generally easier to fabricate. Load bearing elements need to perform this additional task and are therefore larger, heavier, harder to design, and generally harder to fabricate.

An example of a double-curved façade constructed over a main bearing structure is the Louis Vuitton Foundation in Paris. It uses a primary orthogonal concrete load bearing structure and a secondary steel structure to support the curved concrete cladding. In this case it might have been possible to instead construct a freeform load bearing structure in place of the opaque façade elements. This would have required an entire structural redesign, but would have produced more voluminous interior spaces. Whether or not this would have reduced the weight of the structural elements depends of the specific form and loading of the building.

Figure 1.3: Louis Vuitton Foundation, before and after cladding [Piéton, Kapoutrocknroll].

The Neuer Zollhof is an example of a freeform building where the curved surface was loadbearing to increase the size of the interior space.

Figure 1.4: Neuer Zollhof Dusseldorf [Mayer]

Freeform load-bearing constructions can be monolithic or composed of elements. Often called grid-shells, elemental load bearing structures are composed of many smaller pieces, similar to a truss but acting as a surface. Respectively, monolithic structures are composed of a single element or extra large elements, similar to a solid beam but once again, transferring loads in two directions as a surface.

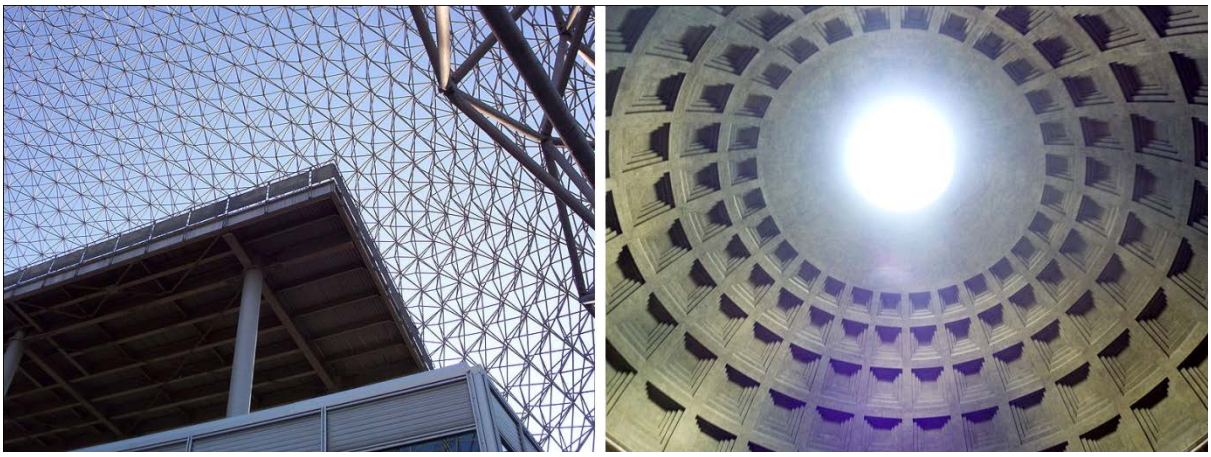

Figure 1.5: Domes as a comparison of elementized, Montreal Biosphère (left) and monolithic construction, The Roman Pantheon (right) [Colocho, Fczarnowski].

While some elemental freeform geometry can be created out of identical pieces, most require many individualized pieces. This increases costs by making on site organization and construction detailing very important. In recent years, elemental construction has been empowered by computers, meaning that digital design and fabrication can be used together with on site logistics to reduce on site labor, construction time, and therefore cost. For example, Louis Vuitton Foundation building, from Figure 1.3, was completely designed and prepared in such a computer program called Digital Project. It is an advanced BIM (building information modeling) platform made by Gehry Technologies, a spin-off company from, Gehry Partners, the firm which designed the building.

This project focuses on monolithic construction. Predominantly this means concrete construction, which can be created in-situ, prefabricated, or a combination of the two. Cast in-situ concrete construction creates strong detailed forms but requires labor intensive formwork. Prefabricated elements can be made to a greater variety of curvatures using specialty molds but require greater care during construction. A combination of the two can be used to reduce the need for skilled labor and care during construction.

1-3 SHELLS AND MEMBRANES STRUCTURES

While not all freeform buildings are designed for structural efficiency, some are able to use the curvature of these forms for their benefit. Two classes worth mentioning are shells and membrane structures. These are designed to carry loads primarily in plane, with minimal bending, allowing for a very thin cross section. Shells are designed to be in compression while membrane structures are designed to be in tension.

The structural efficiency of these structures comes at the cost of reduced freedom in the architectural form. Their shape bounded by the types and magnitudes of the stressed imposed upon the structure, sometimes classified as self-formfinding buildings.

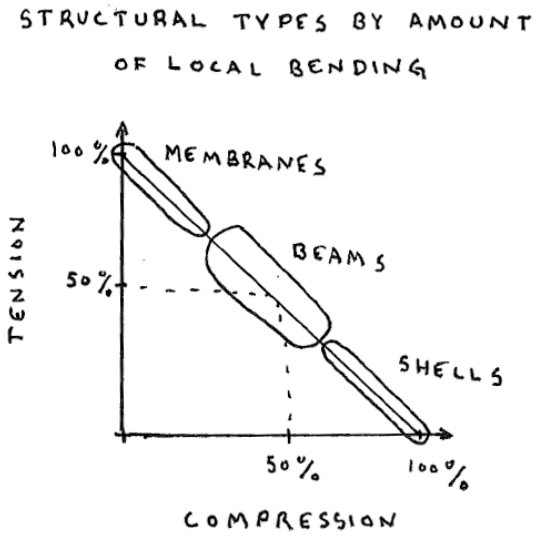

Figure 1.6: Spectrum of structural types by amount of local bending, shown as a percentage of cross section activated by type of compressive or tensile forces.

Shells treat the curved freeform shape as a load bearing surface, taking advantage of the curved or double-curved shape. Without this favorable curved form the surface may require extra thickness and weight, in which case it might be advantageous to use a regular shaped load bearing structure with a freeform cladding. This is best demonstrated by two examples from concrete construction, as seen in Figure 1.7. First the Rolex Learning Center in Lausanne, which utilizes a load bearing surface with low levels of double-curvature resulting in a thick structural cross section. Secondly, the Sicli Company building designed by Heinz Isler, which utilizes high levels of curvature resulting in a very thin cross section. This form was created using a hanging model to insure primarily in-plane loading. Both of these buildings are curved and freeform, however the difference in curvature is very noticeable and demonstrates how restricting structurally efficient but highly curved forms can be.

Figure 1.7: Examples of high, structurally efficient, curvature, Sicli Company building (left) and a thick low curvature, load bearing surface, Rolex Learning Center (right) [Unknown1, Epfll Alain Herzog].

These two example buildings represent the largest difference between structural and architecture freeform buildings. For the material being designed in the project to be more widely applicable it must find the middle ground between these two. The material will be designed as load bearing to take advantage of the curvature of freeform buildings, but not all types of freeform buildings in order to reduce its thickness and make it easier to work with. Versatility is required to make this material architecturally feasible so a suitable thickness must be found which can be the compromise between these two example buildings.

1-4 STRUCTURALLY INFORMED FREEFORM

As shown in the example from Section 1-3, the form of a building has a large influence on its internal forces and therefore the thickness of the elements from which it is constructed. This relationship is illustrated in Figure 1.8. A balance must be struck between versatility with thick elements and efficiency with thin elements, in order to create economically feasible freeform buildings. To achieve this, a new category of freeform architecture is created: structurally informed freeform. It takes on principles of shells and membrane structures (tents), however acknowledges their limitations to shape. This means two things; first that freeform building design should be guided by the principles of shells and tents, but secondly that the material will incorporate strategies to manage bending and other out of plane forces, such as punching shear from columns.

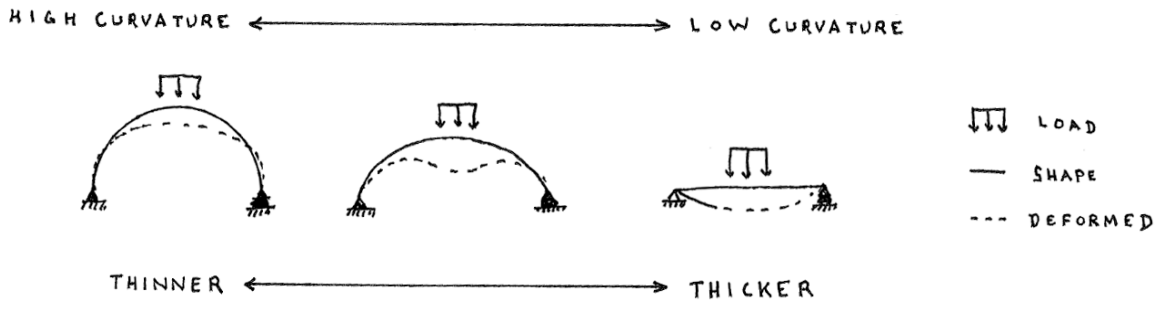

Figure 1.8: Relationship between curvature and section thickness, illustrated by three sketches.

1-5 GOAL OF THIS PROJECT

This project aims to enable the construction "structurally informed" doubly-curved freeform structures by way of developing a new building material and digital design to construction method.

This material is inspired by a patent (Chapter 2). It is being designed to perform a load bearing function; however its properties are only a compliment to the overarching structural design of a building, so an appropriate formfinding process will be investigated. It would enable the realization of freeform architecture by reducing the required labor (and costs) associated with the construction of doubly-curved load-bearing surfaces. The end result will be a prototype material, formfinding process, and construction method. This will be demonstrated by application of the material to the design of a freeform building.

1-6 CONCLUSION AND DISCUSSION

Creating freeform architecture has been popular for a long time, at least the past century. The scale of these blobs is larger than before with a focus on glass and steel. As the price of labor overtook the price of materials within these projects, methods to reduce this cost have been occasionally found, yet their cost remains above normal. A material should be found which enables a large range of freeform buildings with increased size and decreased labor costs. This is done by creating a class of structurally informed blobs. Highly curved load-bearing surfaces lack the transparent features of glass and steel constructions. While, load-bearing surfaces have beneficial structural qualities, their lack of transparency might be an issue that would prevent such a material from gaining wide acceptance.

Computer tools are increasingly important to the design, analysis, fabrication, and construction of these projects. Therefore this material should be developed with computer tools in mind. This means that information transfer between each stage should be simplified. For example, the formfinding process should include information about the material and construction method so that the found-geometry will be easy to implement during structural analysis. Additionally, architectural flexibility should be maintained as the design process progresses, for example by the use of parametric software and a cross referenced modeling environment.

Developing an appropriate material and capable computerized design process are vital to enabling large, irregular, freeform buildings with reduced labor costs.

2 SHEET-LIKE BUILDING MATERIAL PATENT

The unique deformation property of this new material is proposed and outlined in a Dutch patent from 2011. However the patented material remains unrealized. It covers a broad range of properties, some of which have been realized and exist on the market.

In this chapter the patent's key features will be summarized and the steps toward realization and application will be outlined.

2-1 DESCRIPTION

The existing patent, NL2003576C, entitled "Sheet-like building material", describes the key functions of a new type of building material and was the starting point for this project. It is held by two faculty members of the Technical University of Delft Aerospace Composite Structures department, Professor Adriaan Beukers and Dr. Otto Bergsma, an advisor on this project.

The patent describes the material and multiple construction methods that take advantage of its properties. The material is composed of multiple component materials, which vary based upon the intended application. It would be applicable as a permanent or temporary construction for the developed world, developing world, and in shelter situations such as after a major natural disaster.

In essence, the material is fabricated in flat sheets composed of layers with various properties. These connectable sheets are fabricated in a deformable state and once in position undergo a hardening process, making them rigid and able to bear compressive and perhaps bending loads.

2-1-1 MATERIAL

At the most basic level the material is "at least two sheets of woven wire cloth and a hardenable, dough-like material in between". Wherein the "two sheets of woven wire cloth substantially hold the hardenable, dough-like material at least until the dough-like material is hardened" [NL2003576C, pg. 1], meaning that the cloth acts as permanent formwork to support, deform, and contain the dough-like material from fabrication until hardening in its final form. The patent states that plastic deformation of the cloth is preferred, such as with a metal-wire-cloth to enable a greater range of self-supporting shapes before hardening. The patent proposes that the woven cloth act primarily as formwork, but leaves open the possibility of them acting as reinforcement. From reading the patent it is unknown how the cloth component will stay in place or how the specific deformation process occurs. These two matters will need to be addressed in this project.

As seen in Figure 2.1, taken directly from the patent, the dough-like material, stated to be preferably made from unsaturated polyester resins, is contained within two woven cloth layers, preferably made from metal. Presumably the resins are preferred for their light-weight, fluidity, and the authors' familiarity with them within aerospace applications. Although the figures from the patent only show these two layer types, it is open to additional functional layers or coatings to modify color, permeability, reflectivity, corrosion, adhesion, and other properties.

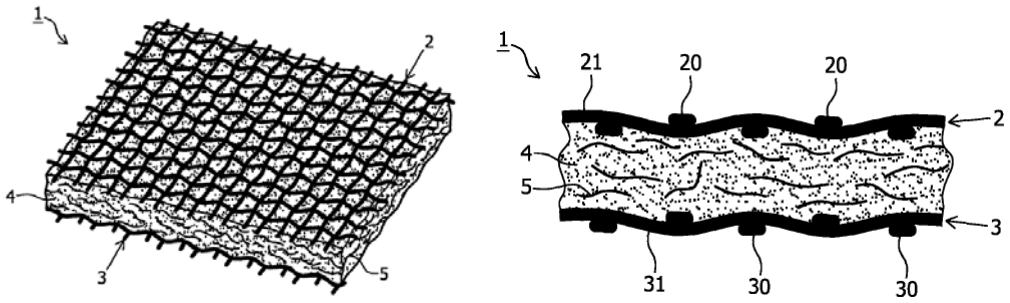

Figure 2.1: Layer configuration of the patented "Sheet-like Building Material"; two woven cloth layers and a hardenable dough-like material between them. [NL2003576C, Fig. 1 and 2]

Preferably, the patent says, the material would be available in rolled sheets of 20-50 meters long, 1-10 meters wide, and 5-50mm thick. A connected assembly of these sheets is meant to be deformed into a three-dimensional shape by locally pushing and/or pulling at least one sheet of the building material. However it may also begin as a three-dimensional shape that is "embryonic to the final [three-dimensional] shape of the construction". [NL2003576C, pg. 2]

2-1-2 CONSTRUCTION METHOD

The stated purpose of the material and construction method is to reduce construction time compared to known methods by eliminating extensive labor and major finishing. To accomplish this, the patent describes three methods for deforming the material (before hardening) to create a three-dimensional shape; (1) draping, (2) folding, and (3) inflation.

Draping means to deform the unhardened/flexible material with temporary or permanent structural supports. These supports may be poles, cables, or otherwise. Folding means to overlay the material, for example "by applying tractions at its peripheries" [NL2003576C, pg. 2]. Inflation would imply a support structure such as a balloon or other inflatable articulated structure which applies pressure to deform the material. Additionally the sheets may be anchored around the edges to allow for better deformation and to prevent it from moving. Once deformed the material is hardened, a suitable period of time, the supports are removed. Examples of draping, anchoring, and inflation can be seen in Figure 2.2.

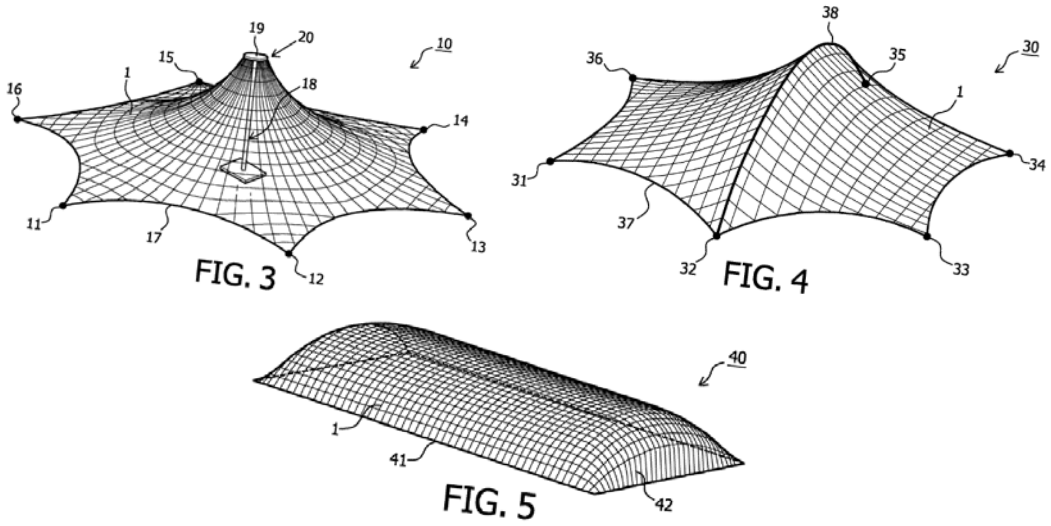

Figure 2.2: Draping, anchoring, and inflation of the patented "Sheet-like Building Material" [NL2003576C, Fig. 3, 4, and 5]

2-2 FROM PATENT TO PRODUCT

The material and construction method described by the patent are far from realization. Multiple materials and multiple configurations are proposed, consisting of varying dimensions. The patent, as written, constitutes the concept of a new building material and suggests that it might be possible to create such a material. This project covers the development of the sheet-like building material and proposes a method for its application. Inspirations for this development process come from existing products and materials.

These inspirations as well as a material development process modify the stated intent and composition of the patented material, but retain the core feature of a deformable material which begins in a flat form, embryonic to the final building shape.

This project aims to develop this material from patented concept to application within the design of a building structure, while retaining the patented innovative features. This feature is the unique fabric-like deformation abilities of the material along with the required construction method(s). This process occurs in three stages, the first being a computerized and physical investigation of the material requirements. Secondly, a formfinding study is conducted with computer modeling. Lastly, this is applied to a case study building to elaborate on the details and issues surrounding constructability and use.

2-2-1 SIMILARITIES TO AEROSPACE MATERIALS

The material being developed combines three properties of existing materials into one new material for building construction: Woven, Layered, and Changes from deformable to rigid. These properties exist together at the much smaller scale of materials for aerospace, automobile, and industrial design. And separately at larger the building scale, for example fabric tents.

WOVEN MATERIALS

The aerospace industry has been using textiles for a considerable about of time. The woven nature of these aerospace composites gives them the ability to deform, through shear, from flat to double curved during fabrication. These intricate shapes are achieved using vacuum or press-forming techniques which would be difficult to apply at the building scale. The deformation behavior, not the fabrication method, is the property most important to the development of the sheet-like building material.

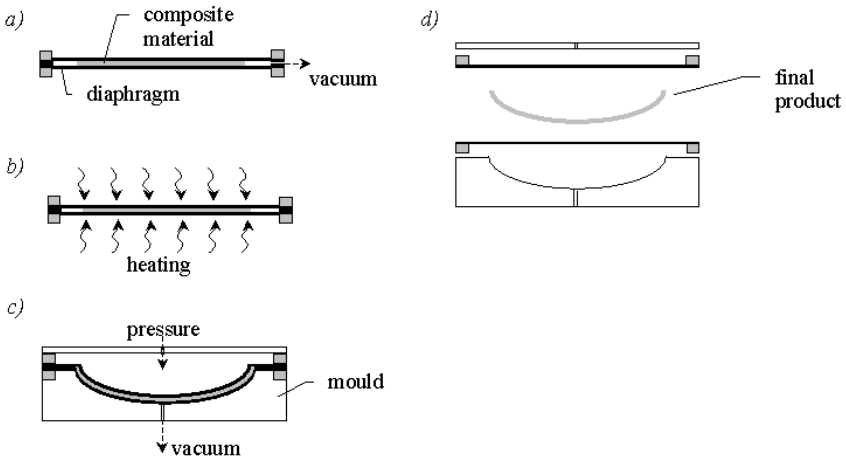

Figure 2.3: Schematic of the vacuum form process: a) material under vacuum in between elastomeric diaphragms; b) heating; c) molding under vacuum (and optional additional pressure); d) release of final product. [Lightweight Structures BV]

LAYERED MATERIALS

Aerospace composites are often composed of multiple layers of various sizes and orientations. This allows for in-plane isotropic properties and stiffness distribution dependant on the specific local requirements, instead of designing the entire product to the largest stresses. This property would also be important for multi-curved building forms and is achievable using cast-in-place or types of traditional construction techniques. In order to simplify the material development process this requirement will be minimized and handled mostly by additionally structural members or toppings. These post-erection toppings would act much like the additional layers in aerospace composites. It may be possible to develop a range of elements with different structural properties. By joining these elements into a type of quilt the specific local forces within the structure could be "embedded" within the building before erection. The specifics of this property "quilting" are slightly beyond the scope of this project because the feasibility of the material will be investigated first.

DEFORMABLE TO RIGID

In these aerospace composites the woven material provides the primary strength and stiffness. However a rigid matrix material is required to position and restrain the woven component and acquire its structural properties. The woven textile mat starts out flat. The matrix material, often an unsaturated polymer, starts as a fluid, either surrounding the textile or added later. These two components are combined and deformed by force. After some time, the matrix material hardens and the deformation force is released. Once together the matrix restrains the textile, allowing it to carry both tensile and compressive loads because of the textiles greater stiffness. The patented material differs from this standard method of aerospace composite construction. The patented form shows the matrix being sandwiched between textile layers (Figure 2.1) instead of surrounding the textile reinforcement.

This is analogous to the components in concrete construction, when the steel reinforcement is encased by the fluid concrete. After hydration and setting, the ridged concrete restrains the steel allowing force transfer. In the case of concrete construction the stiffer but more expensive steel carries tensile loads, while the less stiff and less expensive concrete carries compressive loads. A visual comparison of the differences of the matrix-reinforcement condition between concrete and aerospace composites can be seen below, in Figure 2.4.

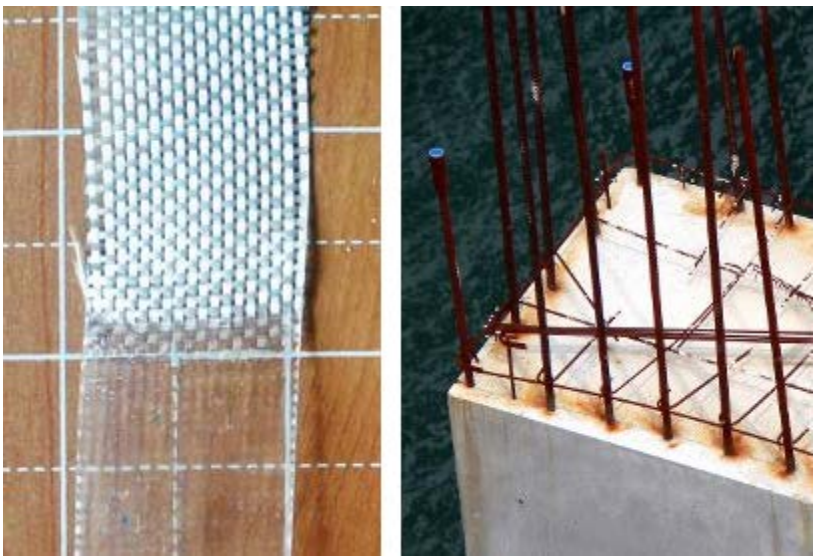

Figure 2.4: Glass fiber reinforcement partially covered by resin matrix (left) and steel reinforcement partially covered by concrete matrix (right). [GS Consulting, Emporis]

2-2-2 REALIZATION

Design decisions and experimental steps must be taken before a meaningful application of the proposed material is possible. First component materials will be investigated and then the proposed configuration will be adapted to suit the component material properties. After this has been reasonably determined, a survey of applications for the material will be undertaken. Using a test shape, this survey of application will determine the types of stresses required by the material and an idea about their relative magnitudes. With this information the specific dimensions and of each component can be outlined, given an appropriate application within building construction. This process, outlined below in Figure 2.5, will be followed, although less explicitly, within this report.

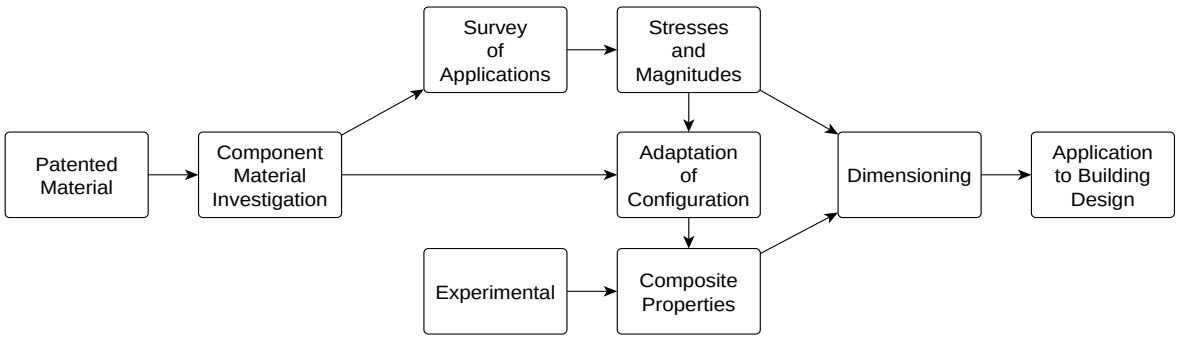

Figure 2.5: Project steps toward realization from patent to building.

2-3 DRAPE

One of the patent holders, Otto Bergsma, has created a computer program, Drape, which relates to the application of this material. Although it was designed for a more general application within the production of woven aerospace composites, it can be used to aid in the design of buildings because the new material is similar to woven materials.

An example application of drape can be seen below. This dog-bone shaped component is used to hold three ventilation ducts separate. The two side-by-side images show Drape being used to simulate the behavior of the woven material (left) and the physical product made to the same shape (right).

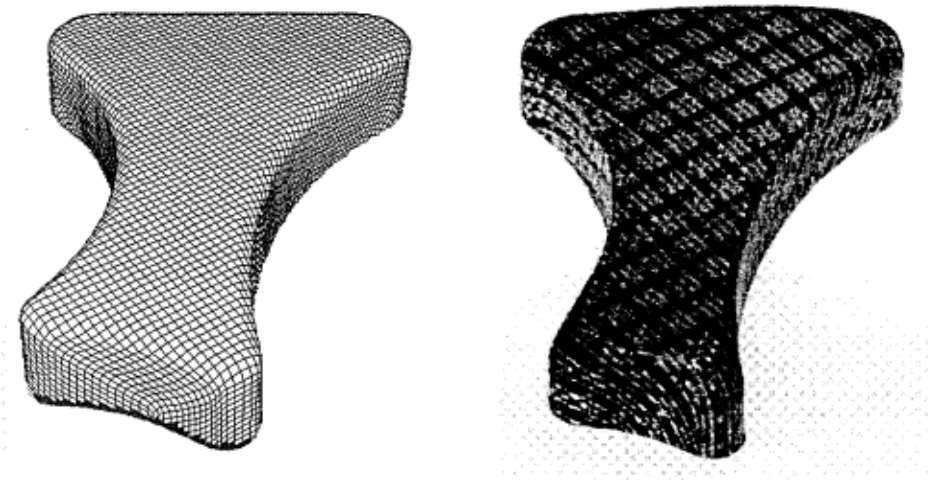

Figure 2.6: Comparison of Dog-bone designed in WinDrape (an earlier version of Drape circa 1995) and the same shape press-formed with a woven material. [Bergsma 1995, page 77, figure 6.7]

Although scale of the dog-bone is much smaller than that of a building, it could be imagined as the shape of a hall or other simple building. Drape will be used in a similar matter to aid in the design of significantly more complex buildings designed with this new material. The details of this application are outlined in Sections 5-1-3 and 10-2.

2-4 CONCLUSION AND DISCUSSION

This patent is just the starting point for the project. It serves to bridge the worlds of small scale aerospace constructions and large scale architectural projects. It outlines only the very basic material composition and range of possible architectural shapes. New irregular building forms must be conceived to properly test the benefits of such a material. This will mean that the material developed within this project will go beyond the qualities and requirements outlined within the patent. The “sheet-like building material” was conceived in the world of aerospace, from which concepts will be taken, if not the actual detail of composition and construction. For example, textile composites, although analogous to concrete construction, their composition and structural properties differ significantly from traditional building methods. The computer program Drape contains these unique properties of textile composites. Therefore, it will be important to the structural analysis and construction freeform buildings constructed with this new material, even though the scale of constructions is radically different.

3 PRECEDENTS

The development of the sheet-like building material covers multiple fields between materials engineering, fabrication, and construction. A few precedent projects are described to better understand the recent developments within these fields and how they relate to the objectives of this project.

Table 3.1: List of Precedent Projects.

Year	Precedent Project	Relation to This Project
2005	Concrete Canvas	Material usage, layers, and properties
2008	Glass Textile Reinforced Concrete	Reinforcement behavior
2009	Fabric Formwork	Fabric and concrete
2013	Flexible Mold	Double curved panels as formwork
2013	Oricrete: Foldable Concrete	Flat material to double curved building
1980	Heinz Isler's Ice Tents	Formfinding possibilities
2013	Formfinding of Funicular Funnel Shells	Structurally guided formfinding

3-1 CONCRETE CANVAS (2005)

Now sold under the name Concrete Canvas, a flexible concrete sandwich material has been invented by Peter Brewin and Will Crawford while studying Industrial Design Engineering at Imperial College and the Royal College of Art in London.

Figure 3.1: Bulk roll of Concrete Canvas and cross section. [Concrete Canvas]

The material has been very thoroughly studied in regards to use, strength, and fire. A description of the material from their website [Concrete Canvas] is as follows:

> Concrete Canvas (CC) is a flexible, concrete impregnated fabric that hardens when hydrated to form a thin, durable, water proof and fire resistant concrete layer. CC allows concrete construction without the need for plant or mixing equipment. Simply position the Canvas and just add water.
>
> CC consists of a 3-dimensional fibre matrix containing a specially formulated dry concrete mix. A PVC backing on one surface of the material ensures the material is water proof. The material can be hydrated either by spraying or by being fully immersed in water. Once set, the fibres reinforce the concrete, preventing crack propagation and providing a safe plastic failure mode.
>
> CC is available in 3 thicknesses: CC5, CC8 and CC13, which are 5, 8 and 13mm thick respectively. CC is used in a variety of civil infrastructure applications, such as ditch lining, slope protection and capping secondary containment bunds.
>
> Compared to traditional concrete solutions, CC is faster, easier and, more cost effective to install and has the additional benefit of reducing the environmental impact of concreting works by up to 95%

This material does not significantly deform in shear, does not stretch, and therefore cannot be used to create double-curved surfaces without cutting patterns. However, because of its similar composition, the mechanical properties are a good beginning estimate of how the sheet-like building material might perform. It is also a valuable precedent for fabrication procedure and element size estimations.

CC	Thickness (mm)	Batch Roll Size (sqm)	Bulk Roll Size (sqm)	Roll Width (m)
CC5	5	10	200	1.0
CC8	8	5	125	1.1
CC13	13	N/A	80	1.1

	Tensile strength (kN/m)	
	Length direction	Width direction
CC5	6.7	3.8
CC8	8.6	6.6
CC13	19.5	12.8

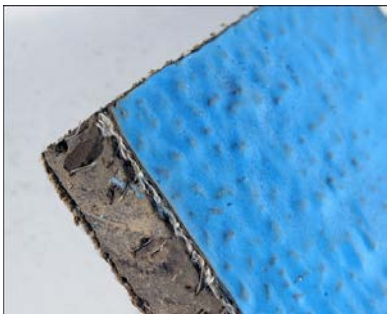

Figure 3.2: Properties of Concrete Canvas and cross section of a cured sample [Concrete Canvas]

Alongside the bulk material, the company also sells a complete inflatable shelter building constructed from the material. This inflation process is shown in Figure 3.3. It can accommodate modifications for additional windows or openings as seen in Figure 3.4.

Figure 3.3: Erection procedure of the inflatable Concrete Canvas Shelter. [Concrete Canvas]

Figure 3.4: Hole cut into Concrete Canvas Shelter. [Concrete Canvas]

3-2 GLASS TEXTILE REINFORCED CONCRETE (2008)

Non-ferrous reinforcement in concrete is being investigated for this project because it does not require a concrete cover layer to guard against corrosion. Without this cover layer requirement elements can be thinner and lighter with the same distance between layers of reinforcement.

Glass fiber is a well known in the aerospace industry as well as others. It is a strong contender for application within the sheet-like building material because of its relatively low cost, high strength, and precedented use concrete. Josef Hegger of RWTH Aachen has conducted research into the load bearing behavior of various kinds of weaves and orientations of glass fiber in concrete. Tests have also been conducted here at TUDelft by Marijn Kok into the topic of woven reinforcement of thin curved concrete elements. More information about this topic is covered in Section 4-3.

3-3 FABRIC FORMWORK (2009)

The Centre for Architectural Structures and Technology (CAST) and its director Mark West explore the use of fabric as formwork to create curved organic forms for architectural and structural elements which are not easily created with typical, rigid formwork.

Mark West and CAST at the University of Manatoba use porous textiles as formwork to create double-curved concrete elements. The fabric is hung to create structurally-informed, funicular, pure-tension forms. When inverted these hung forms become compression arches. The fabric can be backed with concrete to create rigid formwork. These concrete shapes are reinforced using carbon fibers instead of steel to reduce the required reinforcement cover layer to guard against corrosion. With this method they were able to achieve a 5.2 meter span with an element thickness of 3 centimeters.

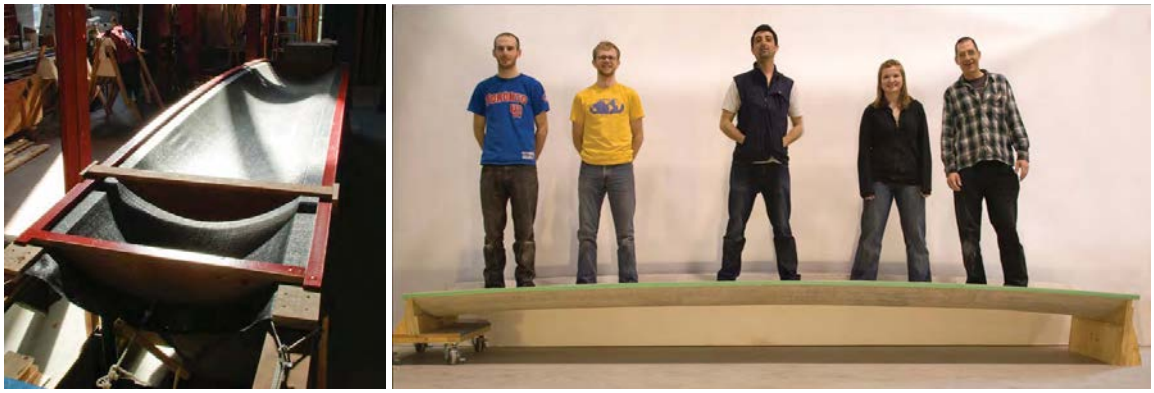

Figure 3.5: Fabric formwork and resulting double curved concrete vault element. [West]

When the hanging formwork is backed by concrete a special fabric is use which strongly adheres to the concrete. This specialty fabric was created by Fabrene Inc. It consists of a polypropylene fabric, smooth waterproof coating on one side and fuzzy non-woven fabric welded to the other side. It is not able to deform in shear or by stretching, therefore, when used as a mold it buckles resulting in wrinkled concrete forms. If the issue of shear deformation can be solved, then the two sided nature of this composite fabric would be fitting for the sheet-like building material.

Figure 3.6: Fabrene "Development Product W756" with fuzzy side bonded to concrete and mold showing buckled fabric "musculature". [West]

3-4 FLEXIBLE MOLD (2013)

A way of making double-curved load-bearing surfaces could be by directly prefabricating the rigid elements. The concrete panel elements are prefabricated on a flexible mold with variable double curvature. These individually curved panels can either act as self supporting cladding or as formwork for structural topping layers. In these ways they fulfill similar functions as the sheet-like building material.

The development of this method is being led by Roel Schipper at TUDelft. Contributors to the project have contributed research in fields including realization of a controllable mold and woven glass textile reinforcement.

Figure 3.7: Controllable mold and double-curved concrete panel with woven glass reinforcement. [Eigenraam, Kok]

The curvature of each panel is determined by dividing the building surface into quadrilateral segments and modeling the curvature of each individually.

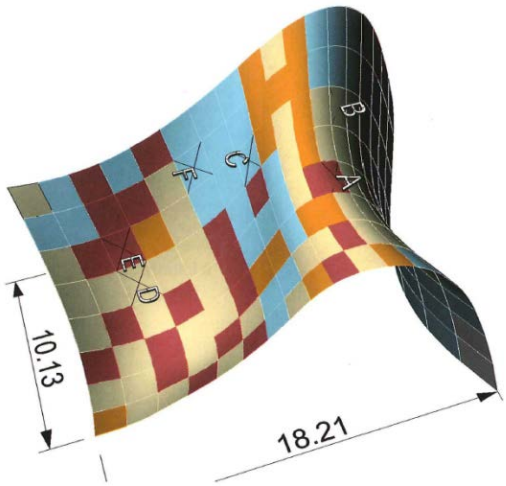

Figure 3.8: Example of a NURBS-surface of a virtual building element showing elements of similar curvature. [Schipper 2011c]

3-5 ORICRETE: FOLDABLE CONCRETE (2013)

A method for deforming a large flat element into a double curved structure by method of controlled folding has been developed by Rostislav Chudoba under Josef Hegger at RWTH Aachen. A flat concrete slab is cast with reinforced joints at prescribed locations. When erected by cranes, the slab bends at the joints taking on a new shape. After erection finishing work (grouting) and the addition of structural toppings is possible. The erected building is formed from a set of planar surface pieces and therefore not a double-curved surface. However, this project is a precedent in creating a doubly curved building from a flat prefabricated monolithic building element. The sheet-like building material would be similarly a monolithic building element that deforms using shear instead of bending.

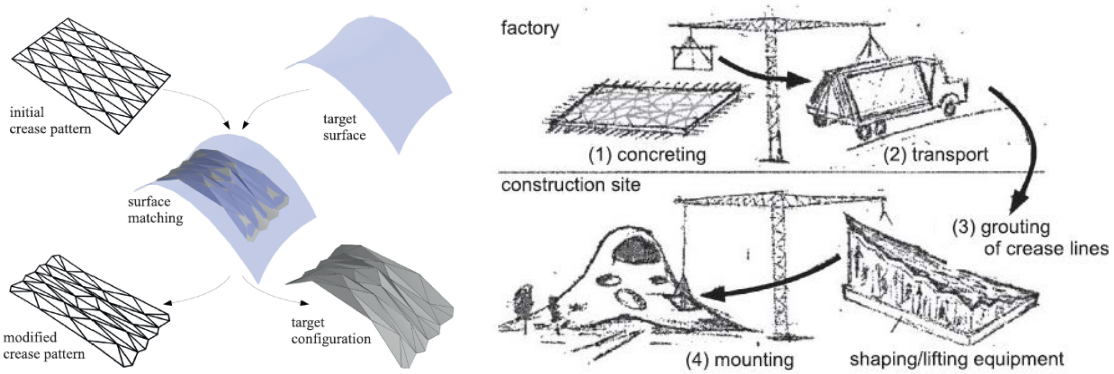

Figure 3.9: Oricrete method for folding of a concrete slab to curved building element. [Chudoba]

Figure 3.10: Physical model of the Oricrete hall made from a flat slab using Yoshimura creasing. [Chudoba]

3-6 HEINZ ISLER'S ICE TENTS (1980)

Heinz Isler, famous for his long spanning thin shell structures, primarily used physical models for formfinding and testing his designs. One set of his experimentations focused on ice and particularly interesting for this project are his experimentations with wet sheets. These wet sheets would be draped over poles or other scaffolding and left out in the cold to freeze. Once frozen, the supports could be removed, changing the load bearing behavior, and creating unusually shaped ice shells. Typically these were 1cm or thicker.

Figure 3.11: Isler ice shell tent and his wife inside for scale [Unknown2]

This draping method used as the formfinding process to create the ice shells is very similar to what was prescribed in the patent. It seems to take slight advantage of the shear deformation of woven cloth. This is only seen in the Figure 3.11 above, where the fabric creates a spherical shell connected to the peaked tent. This was created by draping the cloth over a pole and inflated sphere.

Mainly, these forms use wrinkling, which may be to increase thickness and resist bending, purposely or accidentally. This could be an alternative formfinding method for the sheet-like building material. Allowing wrinkling and also allowing shear deformation would allow a different flow of forces in the material while also allowing for the architectural versatility of smooth shapes.

3-7 FORMFINDING OF FUNICULAR FUNNEL SHELLS (2013)

The BLOCK Research Group out of ETH Zurich under Professor Block has developed a Thrust Network Analysis (TNA) tool for three-dimensional formfinding with structural principles. TNA is a computerized application of the normally two-dimensional graphic statics. As with graphic statics, the form diagram in TNA can be used to construct a force diagram, which can be used to dimension elements. Inversely, an intended force diagram can also be used to determine the form. This adds a great deal of architectural flexibility to structurally-informed formfinding.

TNA was utilized in a 2013 project entitled Ribbed Cut-Stone Funnel Vault. This freeform funnel vault was created using both compressive and tensile force vectors in the formfinding process. The tensile vectors, arranged as rings, enable architecturally important free boundaries such as overhangs. This type of formfinding process would be empowered by a material which can resist both tension and compression, such as the one being developed in this project.

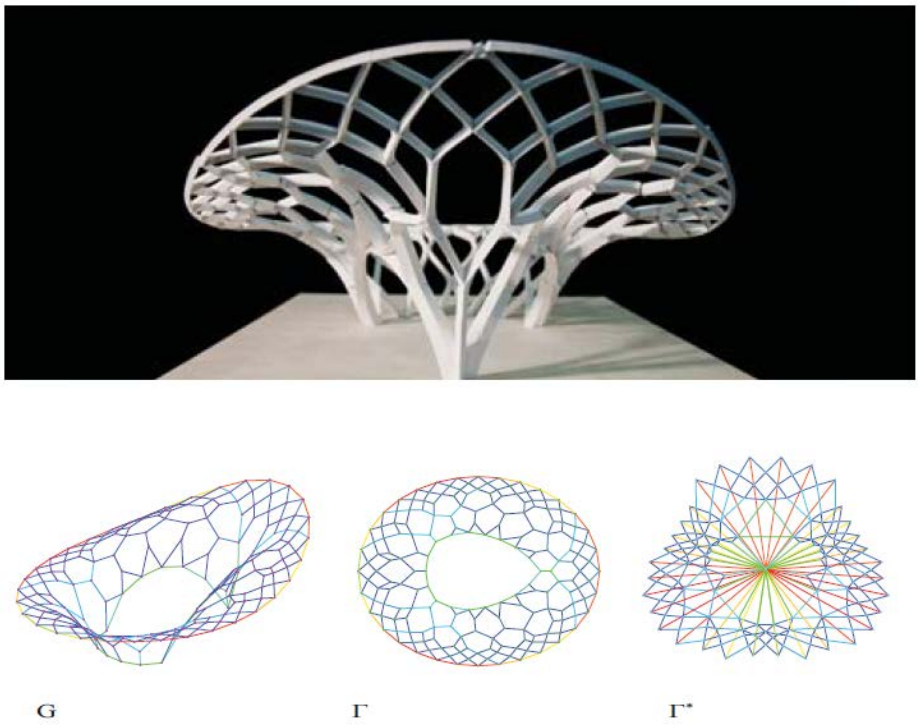

Figure 3.12: Final structure and TNA form finding result of the Ribbed Cut-stone Funnel Vault – 3D-printed Scale Model. Form diagram Γ, (reciprocal) force diagram Γ*, and thrust network G. [Rippmann]

3-8 CONCLUSION AND DISCUSSION

Many products, processes, and projects exist for creating freeform architecture. Of these the most similar to this project is Concrete Canvas. Perhaps the production methods of that material could be altered to enable the deformation properties of textiles. Collaboration with Concrete Canvas could simplify the material development process significantly. The strong similarities between that material and the one in development show that successful fabrication and construction with the new material could be within reach.

Architecturally and structurally, the new material is inspired by many projects which would serve to set it apart from Concrete Canvas. Isler's ice tents, West's fabric formwork, and Oricrete show areas in which Concrete Canvas would be applicable but has not yet been applied. While other projects, such as Schipper's flexible formwork, could not use Concrete Canvas, thereby exposing areas of architecture where new materials should be developed: smooth double-curved surfaces. Lastly, work from the BLOCK research group provides a computer tool which links material properties to formfinding. Such a tool shows the possibility of designing with building elements of known strengths instead of designing building element to match forces derived from the design. This reversal of the traditional design process would be very important to designing with the new material being developed, which has limited, predetermined properties.

For the new material to be successful it must be developed with unique qualities to differentiate it from existing products and be paired with tools/methodologies to overcome its limitations.

4 BACKGROUND CONCEPTS

Concepts about architectural geometry and material specifics are required to begin the material development process. Understanding building forms will mean controlling the flow of forces for structural efficiency and making a constructible building. Understanding the components of the material will mean cooperative and consistent properties.

4-1 ARCHITECTURAL GEOMETRY

In recent times, computers have enabled significantly more complex architectural forms. The geometry of these buildings can be modeled but not so easily constructed. A background in the geometry of curved surfaces is required to understand both how they are created and moving forward, how they could be constructed.

4-1-1 CURVATURE

Constructing irregular curvature inexpensively is the greatest blockade to realizing freeform buildings. (See Section 1-2.) Monolithic shell structures can be described as surfaces. In this way the mathematics of surfaces can be applied to analyze and design these structures. This field of mathematics is largely developed by Carl Friedrich Gauß in the 1800's. A few relevant terms and their relation to the project are described below.

Curvature – This can be quantified as the inverse of the radius of a point on a curve on a surface

Principle Curvatures – These are the maximum and minimum values of curvature, measured at a point on a surface. They are found by revolving a plane about the normal tangent vector of that point. They are geometrically related to principle strains in materials.

Mean Curvature – This is the numerical average of the two principle curvatures. Surfaces with a mean curvature of zero are minimal surfaces, meaning that they have the smallest surface area for a given set of boundaries.

Gaussian Curvature – This is the product of the two principle curvatures. For the purposes of this project it quantifies the extent of double curvature. This means that greater absolute values of Gaussian Curvature represent more curved and more difficult to construct shapes. Anticlastic surfaces such as hyperboloids have a negative Gaussian curvature, while synclastic surfaces such as hemispheres have positive values.

Double-Curvature – This is when a surface has two non-zero principle curvatures and therefore a non-zero Gaussian curvature.

Non-Developable Surfaces – This term relates to an entire surface which includes at least one point of double curvature. Because the surface includes double curvature it cannot be constructed from a single flat element through bending. Instead it would require extensile deformations (stretching) or shearing. This property is very important for this project, because the main advantage of this new material is its ability to construct surfaces which flat elements cannot.

4-1-2 CUTTING PATTERNS

Flat elements can be used to approximate the double-curvature of shapes. This is demonstrated well by a comparison of an orange peel and a beach ball. Both are spherical, meaning that they are double-curved with a Gaussian curvature of the inverse of the radius squared.

Seen in Figure 4.1 below, the double-curved orange peel is flattened to approximate a flat surface; respectively the flat segments of the beach ball are connected and inflated to approximate a double-curved surface. Most construction materials are flat or singularly curved, meaning a Gaussian curvature of zero. This is because flat things are easier to produce and to transport with existing equipment.

Figure 4.1: Orange peel and beach ball demonstrating the approximation of double curved and flat surfaces from each other. [Furuti, Unknown3]

As represented by the beach ball, one method to create double-curved surfaces from flats pieces is though the use of cutting patterns. Cutting patterns prescribe the shapes of the flat element and the manner in which to join them, just as a sewing pattern would prescribe for cloth. Cutting patterns are especially important for tents/membrane structures because the way in which they are cut affects the deformations of the structure.

4-2 TEXTILES AND DEFORMATION

Textiles are created by weaving yarns together. The yarns of the textile are composed of bundled filaments, which are made from metallic or non-metallic high-performance materials. This project will focus on alkali-resistant glass, a common structural material already used in aerospace and concrete construction. This familiarity means that there is reliable information available about its properties and the logistics for implementation within the building industry are already established.

4-2-1 TEXTILES CHARACTERISTICS

A large variety of textiles exist. Some of their important characteristics will be outlined here.

TYPES OF WEAVES

There are many different kinds of weaves, coming from the textile cloth industry, but for the purposed of this project the only weave in consideration is the plain weave. It is stable with large openings and is simple to produce and commonly used.

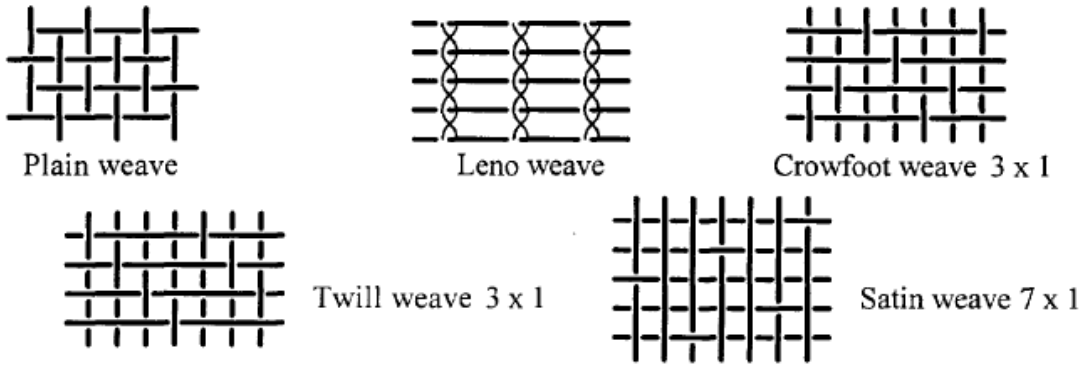

Figure 4.2: Common technical weave styles. [Bergsma, Figure 2.10]

TYPES OF BINDING

Textile reinforcement with large open areas between the yarns they are often stabilized with binding to make them easier to work with and keep the proper alignments. Two common binding types are chain and tricot binding. Chain binding involves the wrapping of one direction of yarns with smaller yarns to secure each crossover point. Tricot binding involves the knitting of smaller yarns within the weave.

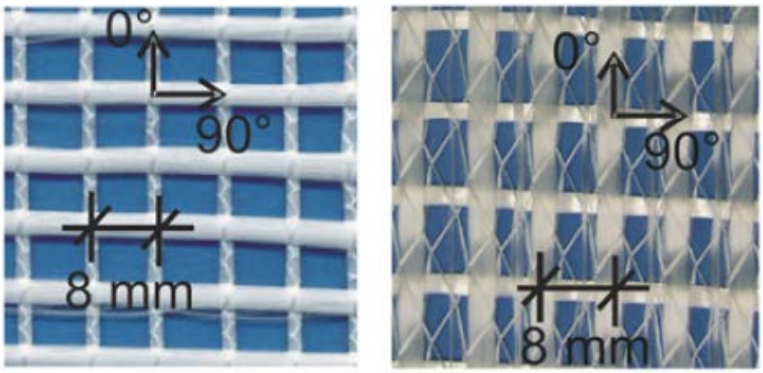

Figure 4.3: Textile reinforcement with chain binding (left) and tricot binding (right). [Hegger 2008, Figure 1]

IMPREGNATION

Friction between the filaments can be decreased by impregnation with epoxy (before or after weaving). Impregnation affects the structural efficiency of the yarns (Section 4-3-1). Impregnation should not interfere with the shear capacity of the material if the yarns can be impregnated before weaving.

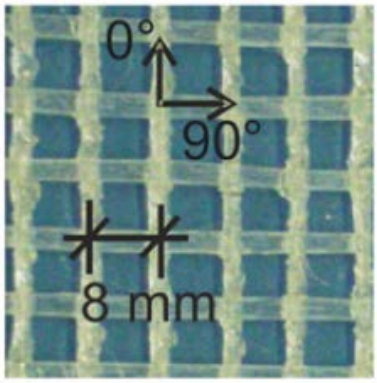

Figure 4.4: Textile reinforcement impregnated with epoxy after weaving. [Hegger 2008, Figure 1]

TEXTILE STRENGTH

The textile strength used in this project comes from the textile Hegger's experimentation, that information is reproduced in the table below. [Hegger 2006, Table 1 and 2]

Table 4.1: AR-Glass textile reinforcement properties. [Hegger 2006, Table 1 and 2]

0 ↑ → 90	Name		Roving	Mesh size [mm]	Cross-section area [mm²/m]
	MAG-07-03	0°	2400 tex	8.3	112
		90°	2400 tex	8.4	112

Table 2 Mechanical properties of the ar-glass fabric

Name		Tensile strength f_t [MPa]	Young's modulus [MPa]
MAG-07-03	0°	974	60500
	90°	533	62100

4-2-2 DEFORMATION POSSIBILITIES OF TEXTILES

Textiles have five modes of deformation, only one being considered for this project. These are (1) fiber stretching, (2) fiber straightening, (3) shear (or trellis effect), (4) shear slip, and (5) buckling. In addition to these modes, bending is of the yarns is possible. The most important is (3) shear, also known as the trellis effect. A visual description of shear and the computation of the maximum theoretical material strain caused by shear is show below, in Figure 4.5.

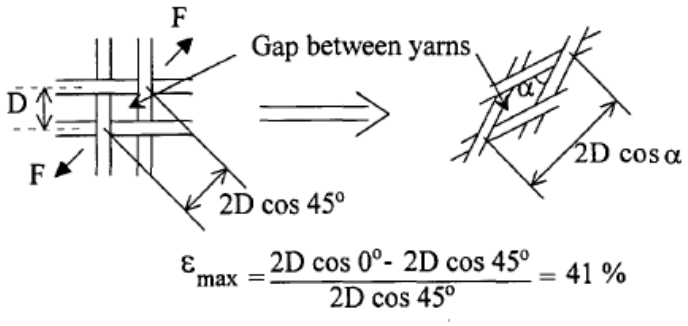

Figure 4.5: Shear deformation also known as the trellis effect. [Bergsma, Figure 2.4]

Unallowable forms of deformation are shear slip-and buckling. These forms of deformation are important for a material composed primarily of woven fabric, however these become less important for a material such as the one being developed which contains a non-fabric layer, which becomes lacks the ability to shear consistently and evenly. Never the less this mode of deformation, shear, is the most important in modeling the behavior of the material to achieve deformation from 2D to double-curved. Shear will be the guiding principle in allowing the material to create double-curved geometry. Through only shear deformation a flat surface can be deformed to create a double-curved surface. An example of a hemispherical shape formed through shear, highlighting the deformation of a single cell, is shown below in Figure 4.6.

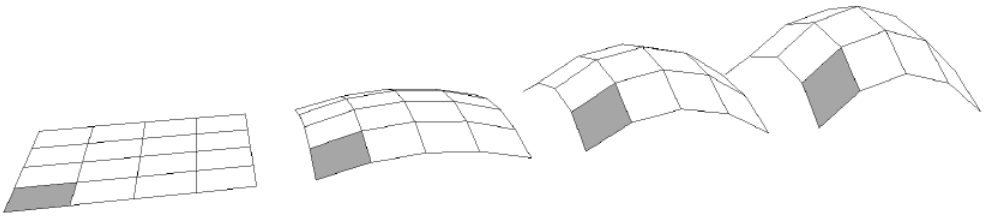

Figure 4.6: Shear deformation of a surface from flat to double-curved. [Eignraam, Figure 2-23]

This shearing changes the area of the exposed-surface of the material. In order for the volume of the material to remain constant the thickness of the material increases correspondingly. This volume increase comes from the deformation of the matrix material. The fiber length between crossovers remains constant because the fibers are assumed not to stretch. To state this geometrically the edge lengths of the exposed-surface remain constant. The thickness then increases by a factor of the inverse of the sine of the shear angle. This relationship can be seen with an example for 40 degrees, in Figure 4.7. Starting with an orthogonal weave, or a composite that acts as one, the material can only increase in thickness, not decrease.

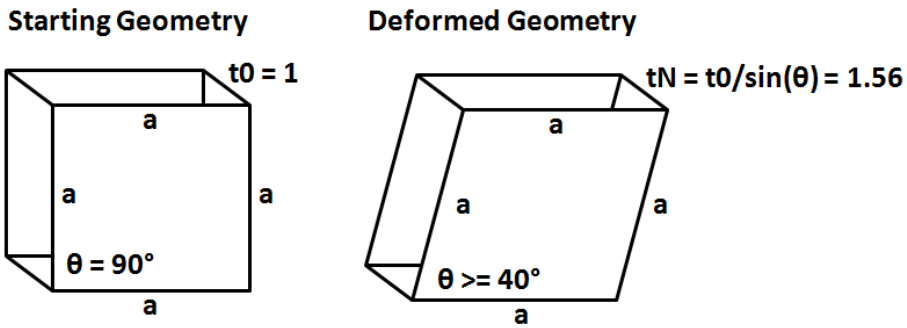

Figure 4.7: Thickness increase due to shear deformation.

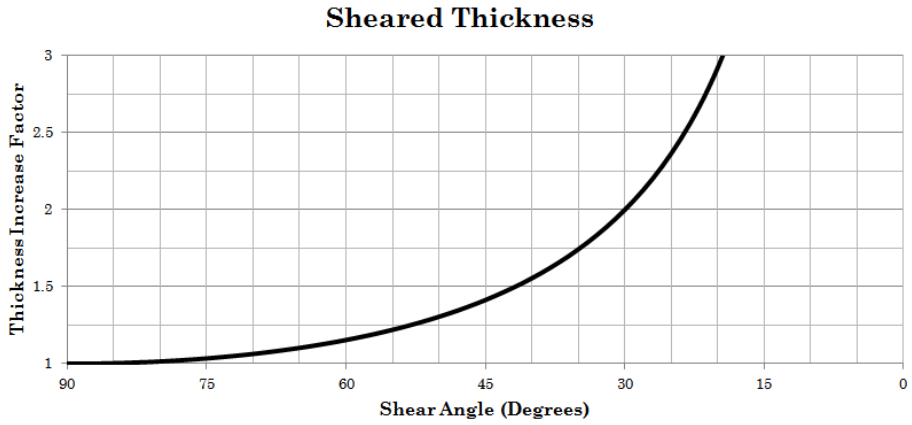

Figure 4.8: Thickness increase factor as a factor of shear angle.

If the material were to continue to shear the exposed-surface area would decrease towards zero and the thickness would increase towards infinity. However, far before this geometric maximum, the physical properties of the composite begin to increase the force associated with this shearing deformation. The point where the physical properties disallow further shearing is called the locking angle. It depends on friction between the constituent materials of the composite, therefore many factors specific to each individual material, such as layers unable to shear without buckling and its ability to accommodate the increase in thickness. The force required to shear the material increases exponentially as the shear angle approaches the locking angle. An example of this can be seen in the graph for a theoretical material in Figure 4.9.

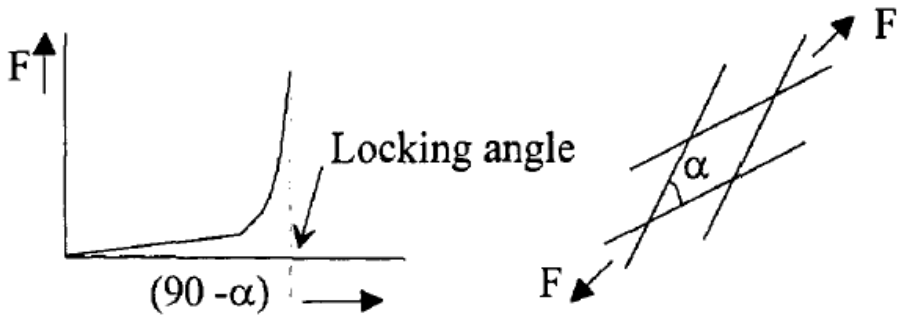

Figure 4.9: The force required for shear deformation as a textile approaches its locking angle. [Bergsma, Figure 2.5]

The locking angle of the material in development must be low enough that it can be used to construct many types of double-curved geometries. This means that attention must be given to friction between constituent materials and its ability to accommodate thickness increase. Tests with woven aerospace composites have shown that weave friction can be decreased using a matrix material (resin) to lubricate the deformation. The matrix material could be in the form of wet concrete or other flowable materials. [Bergsma, page 8]

4-3 TEXTILE REINFORCED CONCRETE

Textile reinforced concrete is a composite material made from woven yarns (textile) and concrete, which allows for thin, light-weight elements. They are often made of glass or other non-ferrous materials because they will not corrode as steel would. Glass fibers can be used as textiles, strands, or short fibers added to the concrete mix. Unlike conventional steel reinforcement, there is no profiling on the filaments which would mechanically anchor it to the concrete matrix, therefore the bond is created solely by adhesion and friction. [Hegger 2006, Page 770]

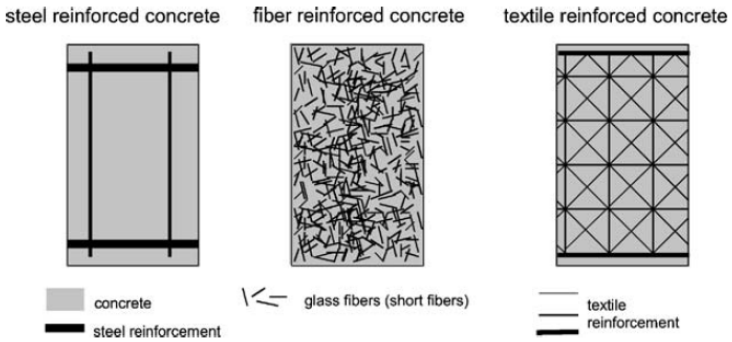

Figure 4.10: Comparison of reinforcement systems for concrete at the same scale. [Hegger 2006, Figure 1]

The textiles have benefits over other types of fiber reinforcement primarily because they can be easily applied as mats and can be oriented in the direction of tensile stresses. This type of concrete construction has been known for decades and if often applied to façade elements where light weight and high curvature are important. They can be prefabricated though lamination or cast on site with a spraying method.

4-3-1 TEXTILES AS REINFORCEMENT

The yarns of the textile are composed of bundled filaments. An important distinction between the outer and inner filaments should be made. The outer filaments are fully bonded to the concrete matrix, during the hardened stage. The inner filaments are not bonded to the concrete, but instead activated structurally because of friction between the filaments. The weaving and binding type influences the proportion of outer to inner filaments by changing the yarn (bundle) shape. Tighter bindings will have more round cross section, meaning a smaller ratio of outer to inner fibers. A looser binding has yarns with flatter, oval like cross sections, meaning a larger ratio of outer to inner filaments. Friction between the filaments can be increased by impregnation with epoxy (before or after weaving).

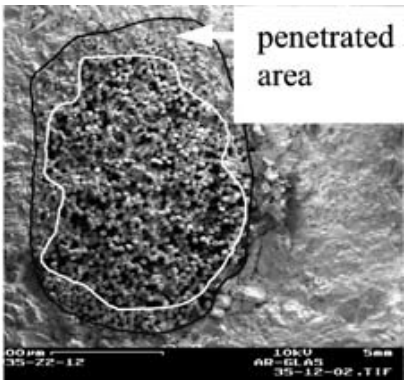

Figure 4.11: Magnified cross-section of embedded textile-bound yarn showing concrete matrix penetration depth. [Hegger 2006, Figure 13]

DURABILITY

Glass textiles are used as reinforcement for thin light weight concrete elements. Non-metallic reinforcement allows for this because the cover layer which typically protects the steel reinforcement from corrosion is no longer required. While glass textile reinforcement does not corrode it does still deteriorate due to environmental and concrete mix conditions. Moist, warm, high alkalinity conditions, either from mix design or environment causes strength losses of up to 40% over 50 years in the glass reinforcement. [Hegger 2008, page 2053] This longer lifetime is achieved by Alkali-resistant (AR) glass. It is produced by adding Zirconia (zirconium dioxide) to the glass making process, at quantities above 19% by mass.

EFFICIENCY

The yarn shape and treatment reduces the structural carrying capacity of the reinforcement below the aggregate capacity of all the filaments. This is known as efficiency, which is calculated as the ratio of the tensile stress in the reinforcement to the maximum tensile strength of the aggregate of all the filaments. Higher efficiency means an activation of a larger proportion of individual fibers. The efficiency of the textile at rupture ranges from 19% to 40% depending on binding, weave type, and up to 66% for epoxy impregnated yarns. [Hegger 2008, Table 2] When calculating this bearing strength the coefficient of efficiency plays a large role in reducing the strength of the section. Efficiency comes from understanding binding, weave, and impregnation.

OPEN AREA

The tightness of the weave can be quantified by its percentage of open area. This means the ratio of area covered by yarns to the gross surface area of the sample, when observed flat with an orthogonal weave. Open area can also relate to the size of the openings measured between the edges of yarns surround an opening. This is important for textile reinforced concrete. The openings of the textile must be large enough to enable a sufficient bond in the surrounding matrix. This is typically required to be twice width of the width of the largest aggregate within the mix design. If the textile is too open then the yarn bundle need to increase in thickness to accommodate the required loading. Large yarn bundles are associated with low efficiencies because of the decreased matrix penetration, as shown in Figure 4.11.

OBLIQUE LOADING

Textile reinforcements are sensitive to tensile loading at oblique angles because of the roving structure and the brittleness of the filament materials, i.e., glass. Hegger found a nearly linear relationship between loading angle and decrease in reinforcement bearing capacity. [Hegger 2008, page 2053] Reasons for this decrease are mainly deflection forces at crack edges leading to flexural stresses in the outer filaments and the incomplete orientation of inner filaments towards the direction of force. This is recognized in Classical Laminate Theory.

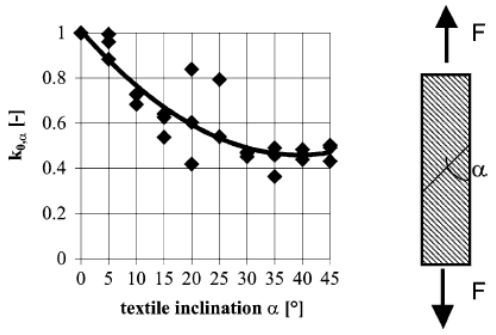

Figure 4.12: Strength reduction factor as a result of the angle between textile weave (orthogonal) and loading direction. [Hegger 2006, Figure 10]

COMPUTING ULTIMATE STRENGTH

From many experimental tests Hegger proposes an equation to calculate the tensile bearing strength of a textile reinforced composite section, seen below in Equation 4.1.

$$F_{ctu} = A_t \cdot f_t \cdot k_1 \cdot k_{0,\alpha} \cdot k_2$$

with

A_t cross-sectional area of the textile reinforcement
f_t tensile strength of the filament
k_1 coefficient of efficiency
$k_{0,\alpha}$ coefficient of oblique-angled load: $k_{0,\alpha} = 1 - \frac{\alpha}{90°}$
k_2 coefficient of biaxial load: Fabric 1:
$k_2 = 1 - 22 \cdot \sigma_{c,\text{lateral}}/\sigma_{\max} \leq 1,0.$

Equation 4.1: Hegger's equation for the tensile strength of textile reinforced concrete sections. [Hegger 2008, page 2053]

The glass textile performs better in bending than in centric tensile loading conditions due to increased filament friction at crack formations. Therefore it can be increased by a factor dependant on the weave and binding type.

$$M_u = k_{fl} \cdot F_{ctu} \cdot z$$

with

k_{fl} coefficient of the bending load depending on the fibre material:
AR-glass (chain binding): $k_{fl} = 1.0$
AR-glass (tricot binding): $k_{fl} = 1.0 + 0.15 \cdot \rho_l$
ρ_l degree of longitudinal reinforcement in %
Carbon: $k_{fl} = 1.0 + 0.4 \cdot \rho_l$
F_{ctu} according to Eq. (1)
z internal lever arm

Equation 4.2: Hegger's equation for the moment bearing capacity of textile reinforced concrete sections. [Hegger 2008, page 2054]

4-3-2 MODIFIED COEFFICIENT OF OBLIQUE-ANGLED LOAD ($K_{0,A,MODIFIED}$)

Hegger's Coefficient of Oblique-Angled Load ($k_{0,a}$), from Equation 4.1, is valid for textiles with a constant orthogonal weave. (It is sometimes referred to as a Strength Reduction Factor.) Therefore it would not be applicable for reinforcement that has been deformed by shear, which changes the weave angle. This factor must be dissected and modified so that it can be applicable to sheared textiles. The effect of each strand will be isolated and a new equation for the Strength Reduction Factor will be created ($k_{0,a,Modified}$).

COMPARISON OF COEFFICENTS OF OBLIQUE-ANGLED LOAD

Hegger's Coefficients of Oblique-Angled Load ($k_{0,a}$) is derived from experimental data (Figure 4.12) and simplified into a linear equation ($k_{0,a} = 1 - \alpha/90°$) from Equation 4.1. These two equations are plotted below in Figure 4.13 for comparison. Note the sometime large difference between the two values. The value derived from the formula is less conservative than the experimental data.

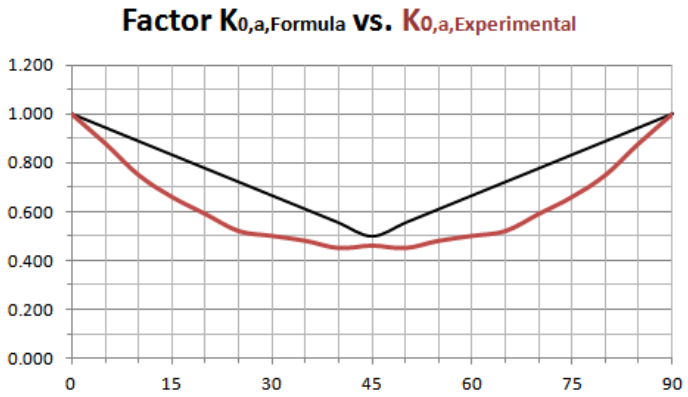

Figure 4.13: Comparison of Hegger's Coefficients of Oblique-Angled Load ($k_{0,a}$).

KEY ASSUMPTIONS

Some assumptions are required to approximate the influence of the yarns in each direction of the textile separately. Oblique tensile-loading experiments should be performed on unidirectional reinforcement and sheared reinforcement sample to validate the procedure of modifying the Coefficient of Oblique-Angled Load.

- Reinforcement contributes to the strength maximally when parallel to the loading direction.
- Reinforcement does not contribute when perpendicular to the loading direction.
- Warp and weft contribute equally when at the same angle to the loading direction (ie. 45 degrees).
- Reduction factor is 0.5 at its lowest from Hegger's data because of the difference in warp and weft strength.
- Reinforcement strength remains constant across all reinforcement ratios.
- The warp and weft directions have the same properties.

ORTHOTROPIC MODIFIED COEFFICIENT OF OBLIQUE-ANGLED LOAD ($K_{0,A,MODIFIED,ORTHO}$)

With these assumptions, three points can be plotted for the yarns in both directions of the weave, corresponding to the influence of the strength of the yarns. Point 1: Each yarn has a contributing factor of 0 when perpendicular to the loading direction. Point 2: Each yarn has contributing factor of 1 when parallel to the loading direction. Point 3: Each yarn has contributing factor of 0.25 when at 45° to the loading direction, totaling a combined factor of 0.5. A quadratic equation is fit to each set of these three points, as shown below

in Equation 4.2. The sum of both quadratic equations becomes the Modified Coefficient of Oblique-Angled Load for orthogonal weaves, ($k_{0,a,Modified,Ortho}$). This new factor as well as its contributing partial factors are compared against Hegger's factors (Figure 4.13) to show that it acceptably approximates those results, in Figure 4.14. This new factor, created from the sum of the partial factors, lies above Hegger's experimental results and below Hegger's factor from the presented formula. It is more conservative and better represents the experimental results. Therefore it will be used in this project. The value is symmetrical every 90 degrees.

$$k_{0,a,Partial,1} = 0.000123 \times \alpha_1^2$$

Equation 4.3: Quadratic equation for the influence on the Coefficient of Oblique-Angled Load for yarns in one direction of a weave, where the loading angle for direction 1, α_1 is between 0° and 90°.

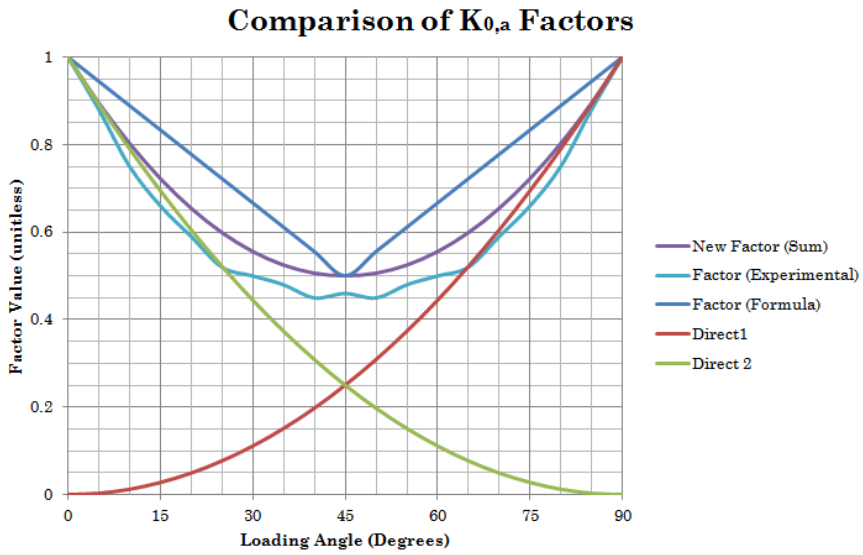

Figure 4.14: Comparison of Coefficients of Oblique-Angled Load for an orthotropic weave.

SHEAR DEFORMATION WEAVE TIGHTENING

As the material and reinforcement deforms through shear the thickness increases and the distance between reinforcement yarns (d_r) of the weave decreases. This increased density has positive effect on the strength. This value is equal to the number of reinforcement yarns per unit length ($1/d_r$). It increases the strength and is therefore equal to 1 at orthotropic weave angles and greater than 1 at all other sheared weave angles. It is computed as shown in Figure 4.15. Therefore it is possible that the Modified Coefficient of Oblique-Angled Load actually increase the strength relative to the orthotropic weave case.

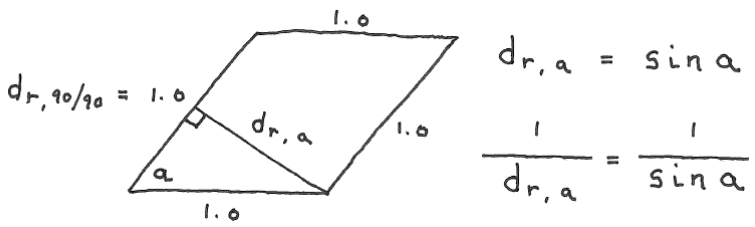

Figure 4.15: Diagram and computation of the reinforcement yarns per unit length.

MODIFIED COEFFICIENT OF OBLIQUE-ANGLED LOAD ($K_{0,A,MODIFIED}$)

The Modified Coefficient of Oblique-Angled Load ($k_{0,a,Modified}$), Equation 4.4, combines the orthotropic factor with the value for weave tightening which is valid for all angles of shear deformation. This value is plotted against the load angle over an increased range of 0 to 180 degrees. This increase is to account for non-orthogonal shear angles which are symmetrical every 180 degrees. Figure 4.16 shows this symmetry for the orthogonal case and has a value of 1.0 for weave tightening.

$$k_{0,a,Modified} = 0.000123 \times (\alpha_1^2 + \alpha_2^2) \times \frac{1}{sin(\alpha_s)}$$

Equation 4.4: Modified Coefficient of Oblique-Angled Load ($k_{0,a,Modified}$) for shear deformed textiles, where the shear angle, α_s and the loading angle for directions 1 and 2, α_1 and α_2 are between 0° and 90°.

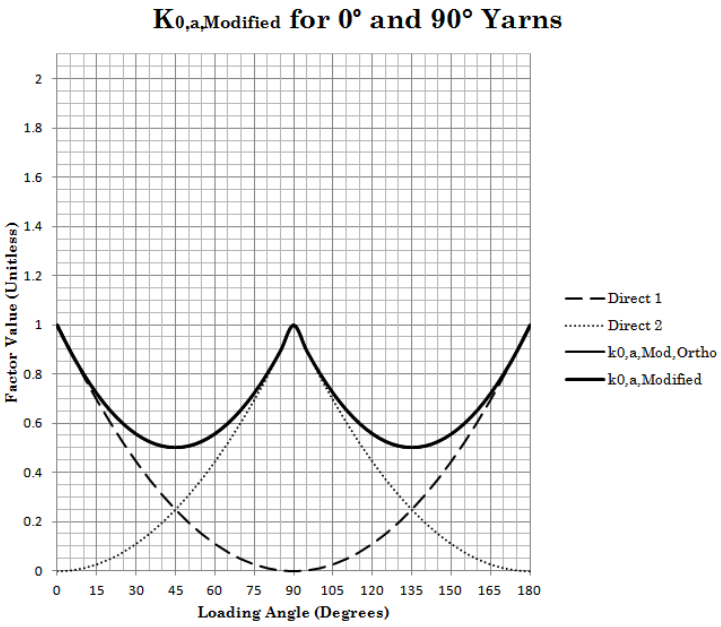

Figure 4.16: Modified Coefficient of Oblique-Angled Load for an orthotropic weave.

A highly shear-deformed case of 40-degrees between reinforcement yarns is illustrated in Figure 4.17. It shows the orientation of the reinforcement yarns relative to the loading angles. The Modified Coefficient of Oblique-Angled Load for this case is shown in Figure 4.18. This factor ranges from 0.15 at 0 degrees to 2.05 at 70 and 110 degrees. This value of 2.05 represents an increase in strength due to the reduced distance between reinforcement yarns.

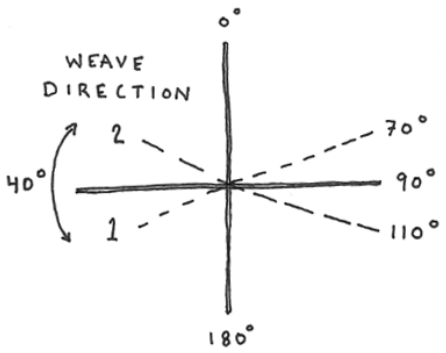

Figure 4.17: Shear-deformed case of 40 degrees between reinforcement yarns relative to the loading angles.

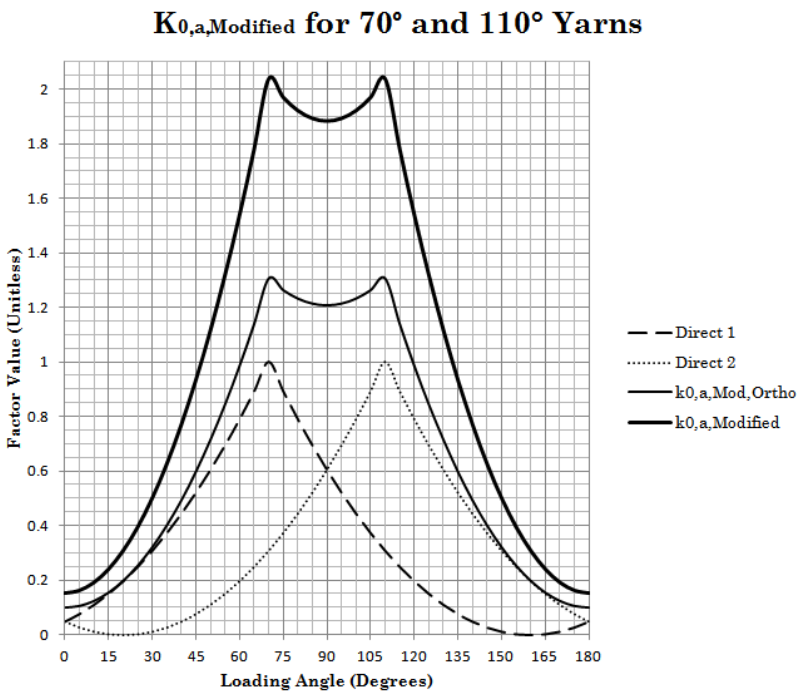

Figure 4.18: Modified Coefficient of Oblique-Angled Load for the shear-deformed case of 40° with yarns at 70° and 110° relative to the loading angles, note the symmetric peaks at these values.

4-3-2 DETERMINING A USABLE BEARING STRENGTH

Experimental information for textile reinforced concrete (TRC) has been created by Marijn Kok at TUDelft in 2013 as well as by Josef Hegger in the years prior. Kok identifies, three stages for TRC during loading until failure: Linear-elastic (LE), Crack formation (CF), and Stablized cracking (SC).

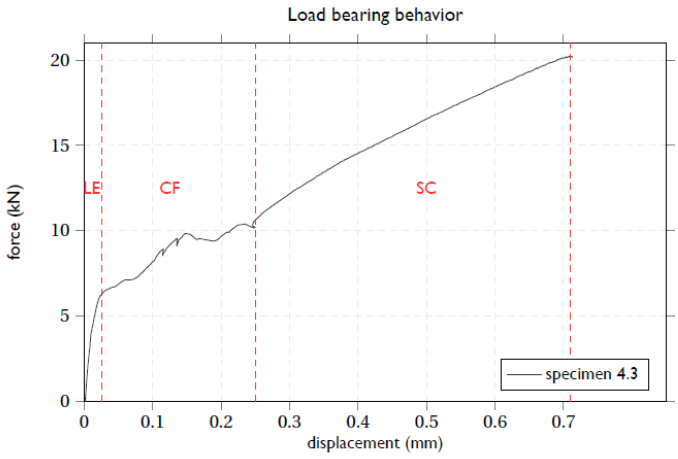

Figure 4.19: Tensile load bearing behavior of a TRC sample measuring a 25 x 100 x 450mm with 2.01% glass reinforcement. [Kok, Figure 6.11]

Textile reinforced concrete has great bearing capacity beyond the linear-elastic stage. However, this capacity comes with permanent plastic deformations, which would only be relevant as a safety buffer between normal loading conditions and collapse. If prevalent though a structure, these deformations would alter the curvature

and therefore load path within a freeform building. For freeform buildings even small local deformation would have a large, visually noticeable effect. Even small deformations, far below the ultimate bearing capacity could have a catastrophic effect because of this global curvature alteration.

During cyclic loading the deformations grow after each successive cycle, perhaps do to the cracking of single filaments and/or the detachment of the filaments from the concrete matrix. [Hegger 2008, Page 2053] The result of one such cyclic loading test on a TRC sample can be seen below, in Figure 4.20.

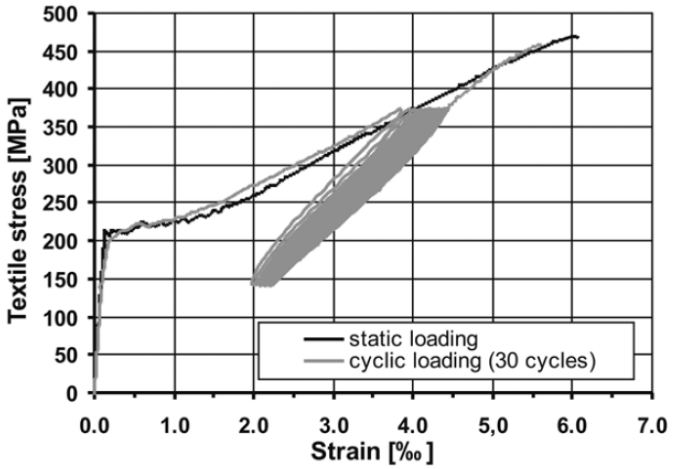

Figure 4.20: Textile stress–strain curve of tensile tests on AR-glass reinforced specimens under cyclic and static loading. [Hegger 2008, Figure 5]

Structural checks should insure that the structure stays within the linear-elastic stage during general loading conditions. Cyclical loading such as variable wind conditions outside of the linear-elastic stage, would not be bearable. However cyclic loading within the linear-elastic stage may be acceptable, as long as it doesn't cause significant cracking of individual fibers. This might occur, dependent on the fiber-matrix bonding.

4-4 CONCRETE TECHNOLOGY

Textile reinforced concrete requires special attention to concrete technology. The grain size distribution of the concrete mix related to the penetration depth of the matrix into the glass yarns and therefore the reinforcement efficiency.

Concrete able to bear greater strains has been developed using special mix designs and distributed fiber reinforcement. This concrete can be called ductile concrete or classified as a strain-hardening cementitious composite (SHCC) or engineering cementitous composite. Such materials can reach higher strains (3-5%) in the range of 30 to 50 time greater than ordinary unreinforced Portland cement. Textile reinforced concrete has this property and may be useful during the structural design of a building constructed from the material being designed.

4-4-1 GRAIN SIZE

The largest grain size of components within the concrete mix for use with textile reinforcement should be half of the width of the size of the openings of the textile being used. This requirement is to guard against air voids during casting and delamination during loading. A much smaller maximum grain size is used in order to insure a strong bond and deep penetration of the matrix into the yarns (filament bundles) of the textile. An adequate maximum width ranges from 0.6 to 2.0 millimeters. Additives such as fly ash and super plasticizers can be used to achieve flowable concrete, which also assists the matrix in penetrating the textile. [Hegger 2006, Page 766]

4-4-2 CONCRETE STRAIN

Unreinforced concrete is poor in tension. Therefore it is paired with a stiffer reinforcing material such as steel or glass fiber that is able to carry more tension at lower strains.

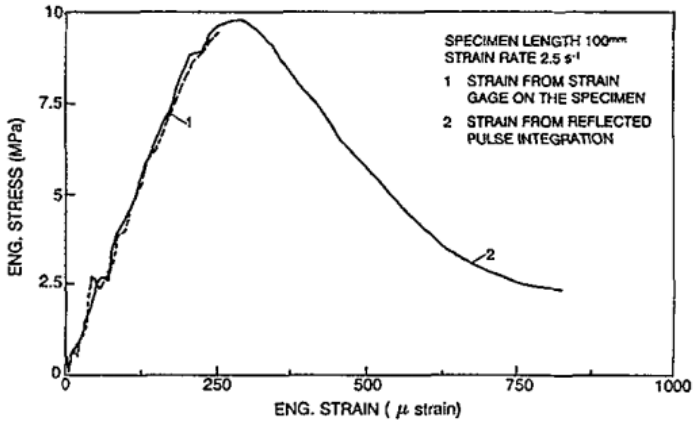

Figure 4.21: Stress-strain curves for regular concrete in tension. [Albertini, Figure 3]

Concrete behaves well in compression, but many different kinds of concrete exist, each with its own properties. Fine grained concrete, the type used with textile reinforcement has the stress-strain properties seen below, in Figure 4.22.

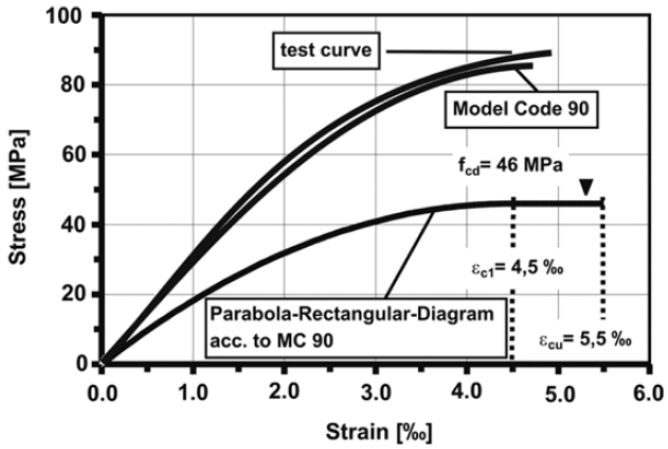

Figure 4.22: Stress-strain curves for fine grained concrete in compression. [Hegger 2008, Figure 2]

4-4-3 SHORT GLASS FIBERS

TRC has good stress-strain behavior. It is able to carry large tensile loads at large deformations, due to many fine cracks. This is good for dynamic loading and preventing failure. However for the service state the smallest cracks are acceptable, meaning that the service state of TRC is considerably lower than its measured tensile strength. The addition of short-fibers to the mix design might be able to increase the acceptable tensile load bearing capacity of TRC. [Barham, page 1]

Dispersed short glass fibers (SGF) distribute themselves in the water of the mix and become thousands of monofilaments. Alternatively, integral short glass fibers remain together as yarns, i.e., bundles of filaments. The water within the concrete mixture aids in the distribution of fibers. Following the example of Concrete Canvas, a prefabricated material with the dry components of concrete may not fully benefit from the use of short fibers. For this reason, integral fibers would be preferred over distributed fibers.

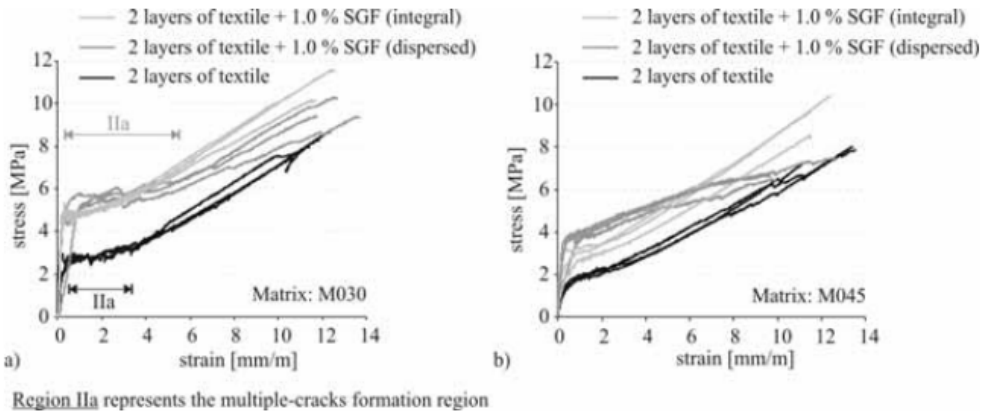

Figure 4.23: Effect of short glass fibers (1.0% by volume) on the tensile stress-strain behavior of TRC for concrete of two water cement ratios, 30% on the left and 45% on the left. [Barham, Figure 3]

The short dispersed fibers are more effective than the integral fibers, during the crack formation stage, however both increase the tensile bearing capacity with lower strains.

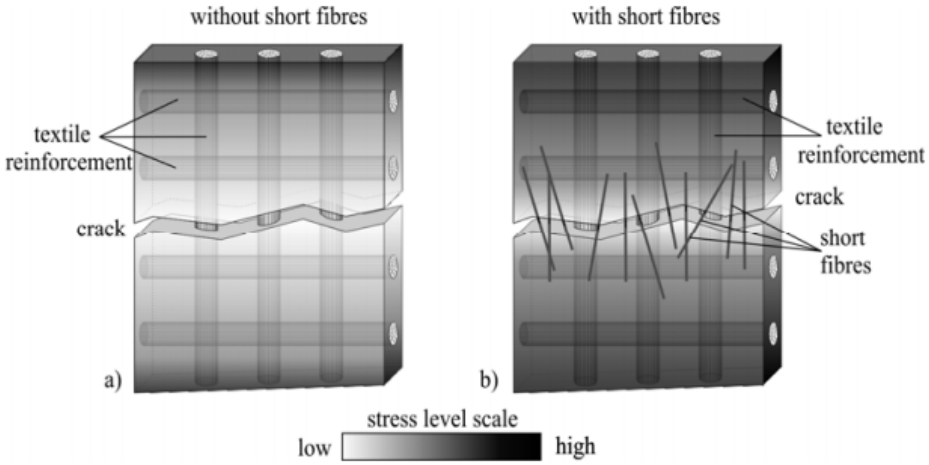

Figure 4.24: Stress gradient distribution in the vicinity of a macro-crack [Barham, Figure 7]

4-4-4 CONCRETE PROPERTIES

The concrete strength used in this project comes from the textile Hegger's experimentation, that information is reproduced in the table below. [Hegger 2006, Table 3]

Table 4.2: Fine-grained concrete properties. [Hegger 2006, Table 3]

Compression strength [MPa]	Tensile strength [MPa]	Young's Modulus [MPa]
78.3	4.4	34000

4-5 CONCLUSION AND DISCUSSION

The material being developed is wholly about geometry. It is created to make smooth double-curved surfaces. These surfaces are in turn empowered by highly curved geometry, which serves to control internal forces. The material is also a physical entity and must be composed of existing constituents. It is valuable to understand the material behavior and gain insight into the sort of stresses which it may be able to bear. This information is stated as a set of guidelines instead of a definitive design. The development of the material will involve many more steps and could change significantly after this project, knowing the possibilities of textiles and concretes will encourage more informed decision making during this process.

5 MATERIAL DEVELOPMENT

The material begins as a concept based on patent figures and a description of its deformation function. From this information a class of applications (structurally-informed freeform) has been created to determine required properties. The core functional properties are distributed among a set of layers, then individually the layers are realized with existing products. Finally the core functions of the multi-layer material are analyzed qualitatively and experimentally. Additional functions and properties are discussed and potential solutions are proposed, but not deeply investigated.

5-1 CONFIGURATION

The configuration prescribed by the patent consists of two layer types: a hardenable dough-like material and a deformable woven material for containment of the dough. Both layers are assumed to have a structural function. Presumably, like fiber reinforced plastics from the aerospace industry, the woven material would the stiffer and more load-bearing element of the construction. The prescribed configuration can be seen in diagrams from the patent reproduced in Figure 5.1.

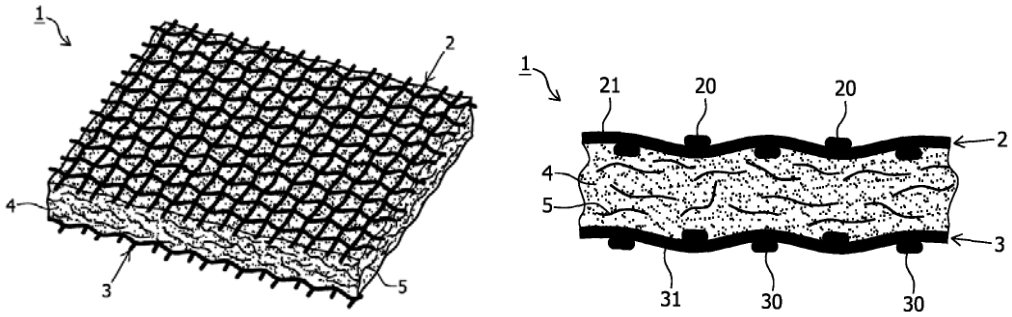

Figure 5.1: Configuration of the "Sheet-like Building Material". [NL2003576C, Fig. 1 and 2]

For the purposes of the investigation, new configurations and new functional layers have been considered. While the configuration and layer functions may change, the functional aspects of the patented material remain the same. As in the patent, the project presumes this material to be at least partially prefabricated in order to reduce onsite labor during construction.

5-1-1 COMPOSITE MATERIAL PROPERTIES

Aside from fabrication and transportation, the material as a whole must have two functional states: deformable for construction and rigid for use. During construction the material must be able to deform to enable double curvature and must be contained so that the layers remain in the same relative positions without delamination. During use the material must be rigid and able to resist loads imposed upon it. These properties could be attributed by one homogeneous material or divided among multiple layers. The only property that must be in common to each layer is its ability to deform sufficiently.

Other "luxury" properties important to a well functioning building could be attributed to the material or auxiliary finishing layers. These include resistance to fire, matters of acoustics, heat transfer, and moisture transport. These are not vital to the material's core functionality. Therefore those properties are only minor considerations during the phase of its development covered in this project.

After the useable life of the building has come to an end another set of properties will come into play. These are important for dismantling, reuse, and recycling/disposing of the structure.

Table 5.1: Minimum, 'luxury', and end-of-life properties the composite material.

Construction	Service Life	Luxury Properties	End-of-Life
Deformation Matrix Containment Air-tightness Water-tightness Force Resistance	Rigidity Force Resistance	Fire Resistance Acoustic Insulation Heat Insulation Moisture Transport	Easy of Separation Recyclability Re-usability

5-1-2 FORCES

This realization of the patented material is intended for 'structurally informed' building forms. For this reason, the loading can be restricted primarily to in-plane loading (tension, compression, and shear), while only minimally accounting for out of plane loading (bending and punching shear). Out of plane loading is required for non-uniform loading cases, such as wind, but also to allow for greater design flexibility over the building form.

While the building curvature and form determine the expected forces, the material configuration and composition determine the resistance to these forces. The thickness of the material determines the maximum in-plane load resistance. The placement of the reinforcement determines the maximum out-of-plane load resistance.

Corrugation, folding, or waves in the material increase curvature locally. More importantly they increase the structural depth of the construction, thereby changing the distribution of forces when such a section is loaded out of plane. More about this topic in Section 5-4-1.

5-1-3 MINIMUM SHEAR ANGLE

The ability of textiles to form double curved surfaces depends on its ability to deform. While multiple modes of deformation are possible, the mode of primary concern is shear deformation, otherwise known as the trellis effect (see Section 4-2-2). The extent of this effect can be quantified by the change in textile weave angle between the warp and weft yarns. For most textile applications, including this material, the initial weave angle is 90 degrees.

Shapes with double curvature will require the trellis effect in order to be constructed. The extent of double curvature does not directly correlate to the change in textile weave angle. Instead the angle is determined by many factors including weave direction, initial contact point, and most importantly the complexity of the desired shape. Therefore creating a material which can deform to smaller angles, thus increasing the change in textile weave angle will enable the creation of more complex shapes. This is for the standard width material sheet without requiring specific cutting patterns.

In order to approximate the smallest feasible angle for the material a combination of rudimentary physical tests and computerized draping calculations were preformed for this project. Shear deformations were imposed on various materials and the angle before buckling was measured. The minimum angles ranged from 35 degrees for foam to 45 for woven metal.

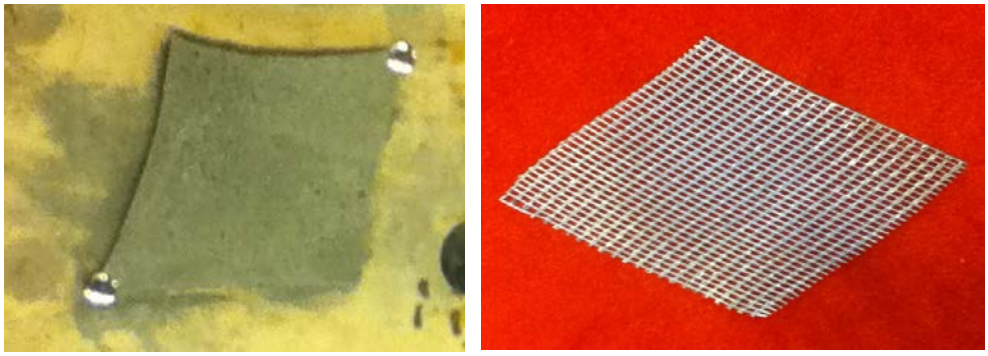

Figure 5.2: Physical shear deformation investigation, foam with concrete (left), woven metal (right).

Draping calculations for the hemispherical test-shape required a minimum angle of 39.2 degrees. These results fit conveniently with the minimum recommended element mesh shape (40-140 degrees) in TNO Diana, the FEM program used for this project.

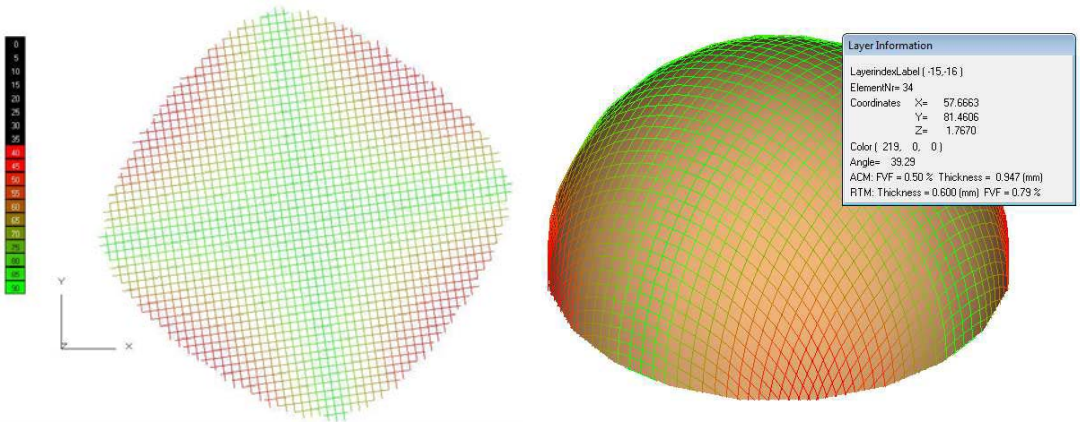

Figure 5.3: Computerized shear deformation investigation on a hemisphere using Drape, green showing the warp-weft yarn angle to be near 90° and red showing near 40°.

From this investigation the benchmark shear angle for physical and computer investigations will be 40 degrees.

As discussed in Section 4-2-2, the locking angle of material is the smallest angle to which it can deform, but before reaching this angle the force required for deformation increases exponentially. This force comes from the yarns of the weave deforming or from friction between the component materials.

As discussed in Section 4-2-2, a very open fabric would be required for adhesion with the concrete. The large openings of this fabric mean that it will deform to low locking angles. Friction within the unhardened matrix material, caused as the material thickness increases due to shear, would resist this deformation, therefore increasing the minimum shear angle. A way to minimize this friction would be to wet the dry concrete immediately before deformation. Such shear measurements have been performed of sands and soils at varying amounts of moisture, so it would be possible to find data relating to the required shear force. This mode of shear could be significant and warrants further investigation with physical testing. However, such tests will not be performed during this project.

Another component which would limit shear deformation is the layer required for water and air-tightness, such as an elastic foil. Instead of shear, this layer would have to rely on existential deformations and buckling. Tensile prestressing of this layer may be possible to reduce buckling. The shearing behavior of this layer will be investigated experimentally in Section 8-1.

5-1-4 WEAVE TYPES AND FOAM

As the patent acknowledges, woven materials for reinforcement come in many forms. A large distinction for this project is the difference between weaves in two-dimensions and three-dimensions, meaning yarns in X, Y, and Z directions. Two dimensional weaves have been discussed in Section 4-2. Alternatively open celled foam could be used as reinforcement, replacing all or some of the woven layers.

THREE-DIMENSIONAL TEXTILES

Three-dimensional weaves consist of warp, weft, and vertical yarns, making it orthotropic. They resemble two layers of regular textile jointed at a set distance by vertical loops. This weave was developed in the velvet and carpet industry for a non-structural purpose. These are often used to create hollow reinforced panels using epoxy as a matrix material. Their application to the concrete industry is not unprecedented. For example, very open 3D textiles are used to create light-weight prefabricated elements for heat and sound insulation. A type of 3D weave ("fiber matrix") is used in the Concrete Canvas (Section 3-1).

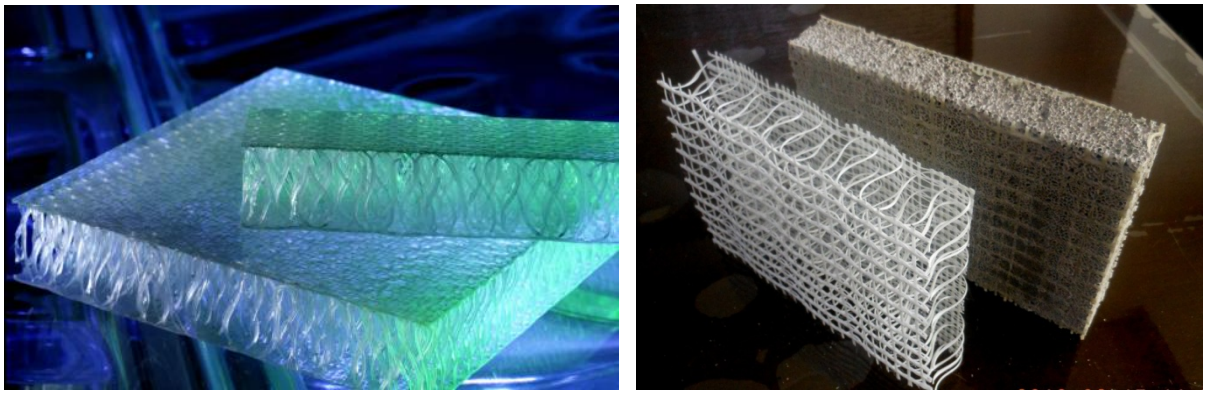

Figure 5.4: Comparison of 3D Textiles for use in boatbuilding and concrete, Parabeam 3D Glass Fabric (left) and China Beihai Fiberglass 3D GRP reinforced foam cement board (right). [Parabeam, China Beihai]

A benefit of the vertical yarns is that they maintain a set distance between layers, meaning it resists delamination. But more importantly the vertical yarns maintain a set minimum distance between the top and bottom layers of reinforcement leading to a consistent resistance against bending. The vertical yarns may, however, resist thickening and therefore increase the force required to shear the material or entirely prevent the benchmark 40 degree shear angle to be reached. This could be alleviated though two modes of thickening: yarn straightening and partial delamimation between the outer layers and the reinforcement. If delamination is restrained then an in-plane redistribution will occur, thickening areas of lesser shear and causing yarn straightening in those areas. This might be beneficial because it increases the thickness of the material more equally allowing a more even distribution of force. In reality a combination of these modes and effects would probably occur.

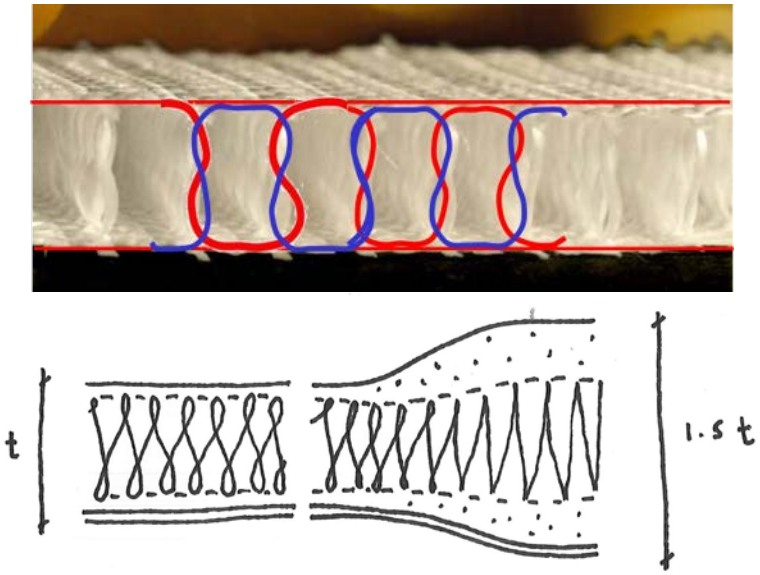

Figure 5.5: Detail of Z-direction fibers with possible mode of thickness increase (Z-direction yarn straightening with outer layer delamination). [Parabeam]

OPEN-CELLED FOAM

Open-cell foam is a non-woven material which can be made out of many materials. It is considered for this project because of its consistent thickness and large open area which could hold cry concrete or another matrix material. As with three-dimensional textiles, foam would maintain a consistent thickness between the top and bottom extents of the reinforcement. Sometimes called reticulated foam, it is produced using gas bubbles within another hardenable (synthetic) foam material. The intersections of the bubbles have thicker portions of this foam material. Therefore a chemical bath can be used to dissolve the material leaving behind these intersections, creating open cells. Another way of opening the cells is by igniting the gas within them, exploding the bubbles.

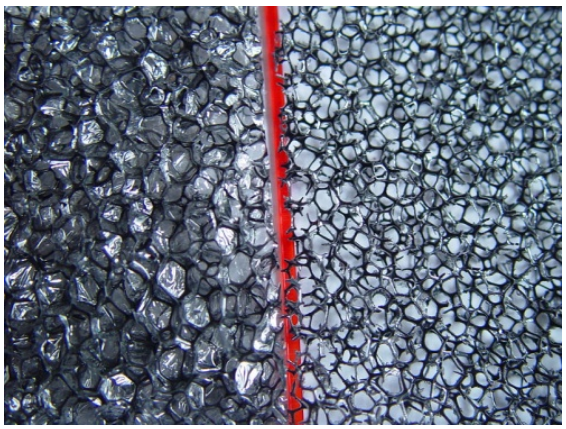

Figure 5.6: Foam before and after reticulation. [Public Domain]

Unlike woven materials it has isotropic properties, which would mean equal reinforcement properties in all directions. However, this property comes along with its inability to deform in shear. This is because the cell structure of the foam is in all direction instead of being aligned orthogonally. To approximate shear deformation the structure of the foam would have to bend and buckle locally. This buckling would occur before hardening of the concrete matrix and therefore not be detrimental. After hardening, force flow would be possible though the buckled elements because they would be supported by the hardened concrete matrix.

5-1-5 ALTERNATIVES FOR MATERIAL CONFIGURATION

Many alternative configurations for the product could be imagined. They will ultimately be judged on their mechanical performance. This performance is largely affected by reinforcement amount and placement. The amount of reinforcement should be placed far apart within the thickness of the material, to achieve the largest lever arm against bending. However, the textile reinforcement should be distributed enough that a strong bond with the matrix and high efficiencies are achieved. Presented below, in Figure 5.7, are configurations for foam, 3D textile, and multiple arrangements of 2D textile.

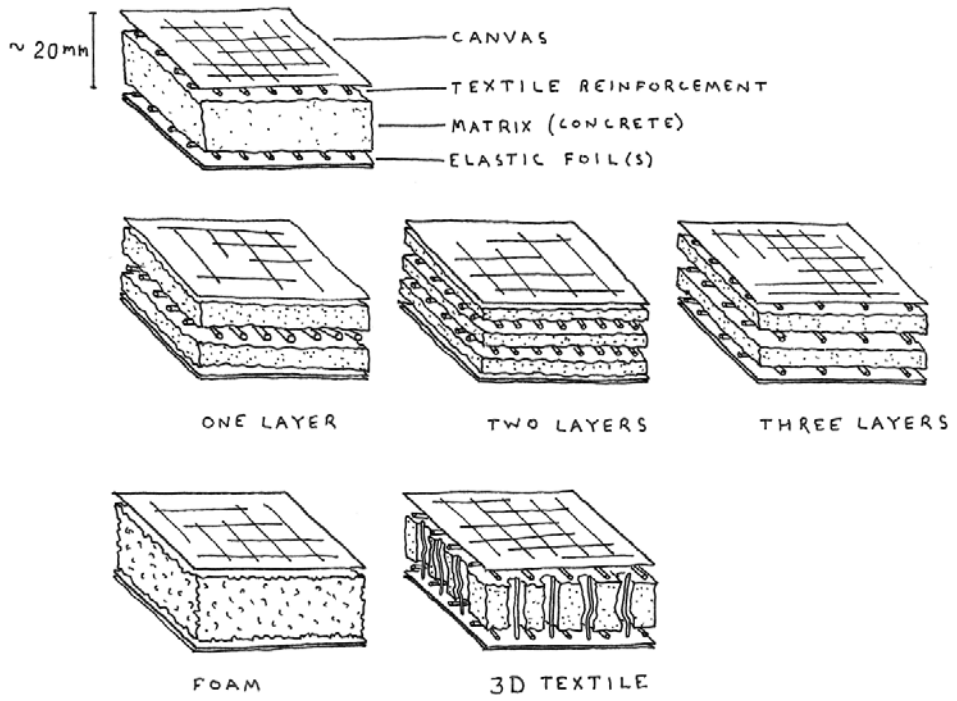

Figure 5.7: Sketches of alternative configurations for the composite material.

5-1-6 CONFIGURATION FOR DEVELOPMENT

A simple configuration was selected for the ease of design. It contains the basic qualities of each arrangement from Figure 5.7. The reinforcement distance is set to the maximum within the cross section. The reinforcement shown would be surrounded by a sufficient amount of matrix material to insure proper bonding. This basic configuration is presented below, in Figure 5.8, with each layer performing its own function, as outlined in Table 5.2.

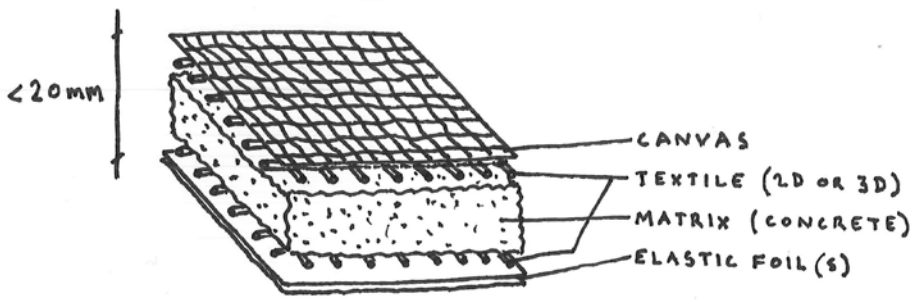

Figure 5.8: Semi-exploded view of the layers and configuration of the material in development.

Table 5.2: Layers names and functions.

Layer	Function	Notes
Canvas	Containment	Distributes water to hydrate concrete
Textile (2D or 3D)	Force Resistance	Could be one or two layers
Matrix	Rigidity + Force Resistance	Starts dry and deformable becomes rigid
Elastic Foil(s)	Containment+ Air/Water Tightness	Might need other layers for reinforcement

5-2 COMPONENT SELECTION

The preferred materials prescribed by the patent are woven metal and unsaturated polyester resin. This woven material is meant to include all types of cloths, textiles, stitched and braided, or otherwise composed of fibers or yarns. The other component, the dough-like material, includes all materials which can be changed from deformable to rigid.

The search for materials comes from two directions the aerospace industry and construction industry because this material behaves like an aerospace composite but is being applied at the larger, cruder building scale. In order to better compare this spectrum of materials a few criteria were outlined. These criteria had to account for mechanical properties (stiffness, strength), other physical properties (durability/age, temp extension), cost, required tolerances, deformability, industry familiarity, and others considerations.

Materials from the aerospace industry are typically high performing materials, which has the benefit of reducing weight and expanding the possibilities. However they have drawbacks in terms of cost, specialized manufacturing requirements (temperature/pressure), high required construction tolerances, difficulty with concentrated loads, and don't always work well with other building elements.

Materials known to the construction industry have the promise of easy implementation because of industry familiarity with their properties and working methods, as well as being inexpensive in enormous quantities. However these materials tend to be heavy and low performing.

A combination of these materials was found to balance cost and performance while increasing the ease of implementation into the construction industry.

5-2-1 REINFORCEMENT

Woven textiles have been chosen over foam because of the shear capability and its known use as a reinforcement material in the aerospace and concrete industries. Materials under consideration come from the aerospace industry or are prescribed within the patent. These are metal, glass, carbon, polymers, minerals, and natural fibers. From this list, three have been selected for their potential: galvanized steel because it would not require cover to guard against corrosion, is inexpensive, its use is precedented in ferro-cement, and could deform plastically during construction; Glass for its moderate cost and precedented use; and lastly basalt fibers for their high strength and less CO_2 intensive production.

Glass fiber is well known, moderate cost, and has precedented use as concrete reinforcement. For those simple reasons, glass has been selected for as the woven reinforcement material for the material in development.

Table 5.3: Qualitative comparison of reinforcement materials with potential materials bolded.

Material	Stiffness & Strength	Cost	Notes
Metal			
Steel	High	$$	Requires cover
Galvanized Steel	High	$$	No cover
Stainless Steel	High	$$$	No cover
Aluminum	High	$$$	Requires coating if used with concrete
Glass	High	$$$	Precedented
Basalt	High	---	New and promising
Polymers	High	$$$$	Little known
Carbon	Ultra-High	$$$$$	Too expensive
Natural Fibers	Low	$	Weak + Degrades over time

Textile reinforcement can be used in combination with chopped strands (continuous reinforcement) to create a hybrid reinforcement system. This would have the benefit of increasing ductility and reducing crack width. Hybrid reinforcement will not be investigated further during this project. It is however worth further consideration during the next stage of development, when the details of the concrete mixture are investigated.

ONE OR TWO LAYER VERSES 3D TEXTILE

The choice of textile reinforcement configuration is based on a combination of fabricatability, loading, and constructability. Fabricatability is mostly out of the scope of this project; all alternatives are considered equally feasible. Loading in bending is the most affected by the placement of reinforcement. For this case, one or two layers or a 3D textile are preferred over one layer because this enables a moment couple to be formed (between the concrete and textile) at the greatest distance apart for both directions.

Geometrically one layer of reinforcement is preferred. Large curvatures will cause a relative extension of the reinforcement. When the principle curvatures are not aligned with weave orientation then the two layers will deform differently in shear to accommodate this relative extension. However, if the principle curvatures are aligned with one or more directions of the weave orientation then the textile/yarns at the inside of the curve will cover a larger angular distance as compared to the outer textile/yarn. This effect could become a problem if the curvature of the building is primarily in one direction and the radius is very small. This will probably cause buckling (in or out of plane) of the inner textile while the material is still deformable. Once rigid, the buckled textile will affect the load bearing capacity of the reinforcement. For buildings with larger curvatures (and inherently large radii) this effect becomes less relevant because the difference in angular length of the inner and outer textiles becomes smaller in proportion to their overall lengths.

Figure 5.9: Diagrams showing the relative extension of the inner textile (left) and internal buckling when fiber extension is constrained (right) at the material scale.

5-2-2 MATRIX

The patent suggests using unsaturated polyester resin or a synthetic material which can harden in the presence of oxygen or ultraviolet light. These materials often come at high costs, work best for thin cross sections, and are unfamiliar to the construction industry. For these reasons fine grained concrete was selected as the matrix material. It is well known, highly researched, already applied to thick sections and the scale of buildings. It is rather inexpensive in large quantities and resistant to decay from ultraviolet light. Importantly it is simple and permanent, with only the addition of water and energy, to transform unhydrated particulate concrete into rigid concrete. This deformable use is precedented by Concrete Canvas (Section 4-1).

Alternatively geo-polymers or alkali-activated binders can be used much like cement as a method to reduce the CO_2 emissions which would otherwise be associated with this material if Portland cement were to be used. [Provis, page vi] These materials are currently under development and testing, so far they have been found to have noticeably different properties than traditional concrete. For example concrete made with and alkali-activate binder has high flexural and tensile strength. [Provis, page 282] For this reason their use maybe preferred over cement, not only for environmental but also structural reasons. This project will be developed using traditional concrete and leaving the option open to utilize geo-polymers or alkali-activated binders in future development.

5-2-3 CONTAINMENT AND AIRTIGHNESS

The deformable matrix needs to be confined and reinforcement kept in place before the matrix is hardened. The layer that performs this task is analogous to formwork that supports the weight and keeps the form of concrete during construction. This layer need not be entirely air or watertight for the purpose of containment. However, it should be closed enough to prevent leakage of the matrix out of the composite material. Therefore it could be a tightly woven fabric which would deform though shear.

Using a (mostly) airtight material as part of the containment layer would enable inflation, a method of construction prescribed by the patent and also used by Concrete Canvas (Section 4-1). The difficulty of having an airtight layer is getting it to shear. A woven fabric would be porous, while a metal or plastic layer wouldn't shear. An elastic layer may be a solution for low amounts of shear deformation. It could even be prestressed to increase its shear capacity. The strength of the air tight layer must be balanced; closed enough to enable a pressure differential, soft enough to approximate shear, and strong enough to contain the matrix material. An elastic layer might be used in combination with a woven canvas layer for added strength. The shearing of this layer will be investigated experimentally in Section 8-1.

5-2-4 OTHER LAYERS

Other layers could be added to the material during fabrication or added during or after erection, on either side, and to some or all areas of the construction. These might be to alter the color or texture, structural reasons, noise or heat insulation, fire, moisture transport or other reasons. These layers, coatings, or cladding materials will not be covered in this project, although some type of finishing will most likely be required to increase the durability, lifetime, and appearance of the completed building.

5-3 JOINTING

Equally important to creating a functional material section and element is creating a method to join those elements together. Joints are needed because current material fabrication methods are unable to create a singular element large enough to make an entire building. Joints must be sufficiently airtight (to enable inflation) and able to resist compression and tension. Minimizing the width of the joint will improve shear deformation capabilities. Unless special care is taken to design the orientation of the material, the joint will require some bending resistance, particularly for long flat spans. Since bending resistance will not be needed during construction, it could be provided by a topping layer or grouting. During construction the joint must be easy to form between elements as the material is unrolled after transport. Three classes of element-to-element joints have been designed and discussed. Prototyping and mechanical testing, out of the scope of this project, will be required to select the most appropriate joint.

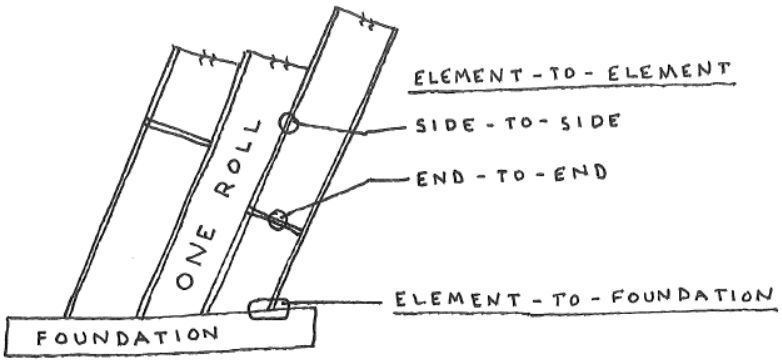

Figure 5.10: The types of joints in an elemental construction at building scale, side view.

5-3-1 ELEMENT-TO-ELEMENT

Element to Element joints will be the most prevalent type of joint. They will also be the only joint to be factory fabricated as part of the material. This joint would most probably be made from a high-performance plastic because it won't corrode and could be formed around the glass fiber reinforcement. Alternatively it could be made from stainless steel or another low-corrosion alloy. Three types of side-to-side joints have been designed. End-to-end joints are less prevalent and presumed to be simpler to design; they could even take the form of one of the proposed side-to-side joints. It may be possible to simply glue the element a top on another for all kinds of jointing. This should be tested alongside other methods of jointing.

SIDE-TO-SIDE

The side-to-side joints must resist compression, tension, and some amount of bending. In order to resist these loads the joint would be connected to the textile reinforcement during the fabrication process. They should be easy to join when handling the heavy material rolls but also be permanent.

The first option, "**Locking Hooks**", would be simple to join by placing one atop another. Bending strength would come from the stiffness of the joint material because the central hooking mechanism is the only way to transfer tensile forces.

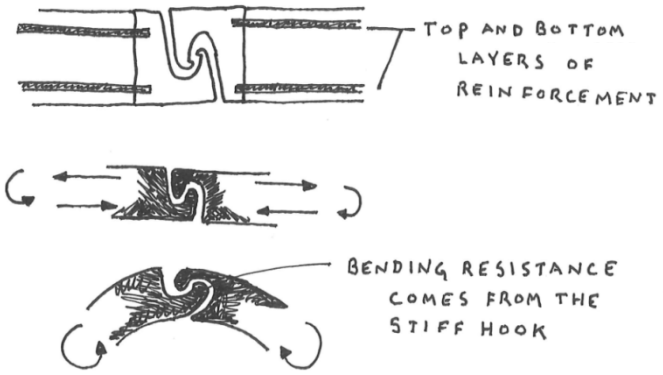

Figure 5.11: Section view of the locking hook joint, at the material scale, showing that bending resistance comes from the hook stiffness.

The second option, "**Zipper**", would function similarly to a normal zipper from the clothing industry. It would transfer tensile forces through localized shear. Slippage of the joint out of plane is accomplished by offsetting the lower half of the zipper tabs from the top half. A type of lever or joiner device would be required on site to connect the heavy rolls of material. Rails would be integrated into the joint for the joiner device to use. For increased stability a type of glue or sealant is suggest for use in combination with this joint.

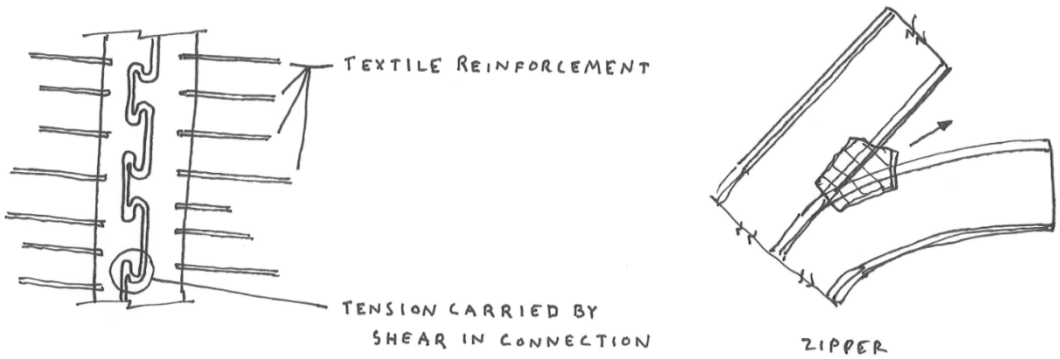

Figure 5.12: Top view of the zipper joint, at the element scale (left) and a zipper-pull component which could be used during construction to join two rolls of elements, at the element scale (right).

The third proposed option, "**Layered**", would be the simplest to produce and not require a specialty material. During fabrication the edges of the material would be flattened and joined with the bottom textile reinforcement, while the top layer of reinforcement would protrude from the joint. The flattened portioned would be connected either mechanically by some type of Velcro, stitching, or adhesive glue. This would be the

only bond used for erection, while the material is loaded only in tension. After erection the void above the joint would be filled with grout, binding together the reinforcement and enabling bending resistance for both out-of-plane directions. For high tensile strengths a large lap length would be required, since the transfer of force between each element's reinforcement is carried by shear. At low over-lapping lengths the reinforcement is liable to be pulled out of the grout or binding agent.

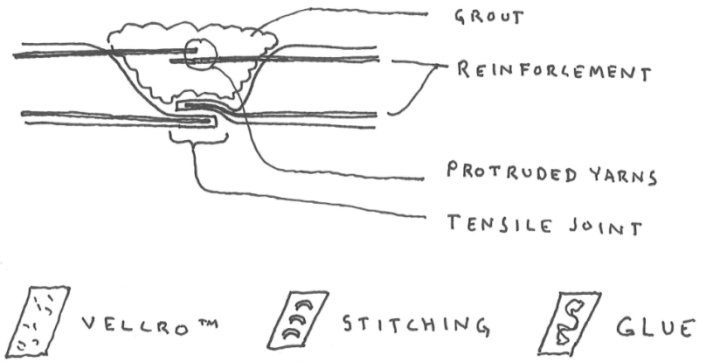

Figure 5.13: Concept section view of the layered joint and potential methods of connection in principle.

5-3-2 ELEMENT-TO-FOUNDATION

Due to the low bending resistance of the thin material, the permanent element-to-foundation connection is designed as a pinned connection. (The temporary foundation connection for erection is discussed in Section 9-3-1.) Simply casting the elements into a section of concrete would be a simple and secure way to form a connection. However this would not be a pinned connection and would probably cause the material to crack during loading. A compromise between these two concepts would be to build a double foundation. The top foundation would be a concrete beam into which the material elements are cast. The lower foundation would support this cast-in-situ beam using pivoting connectors. Never the less, these connections might have a local concentration of bending stresses.

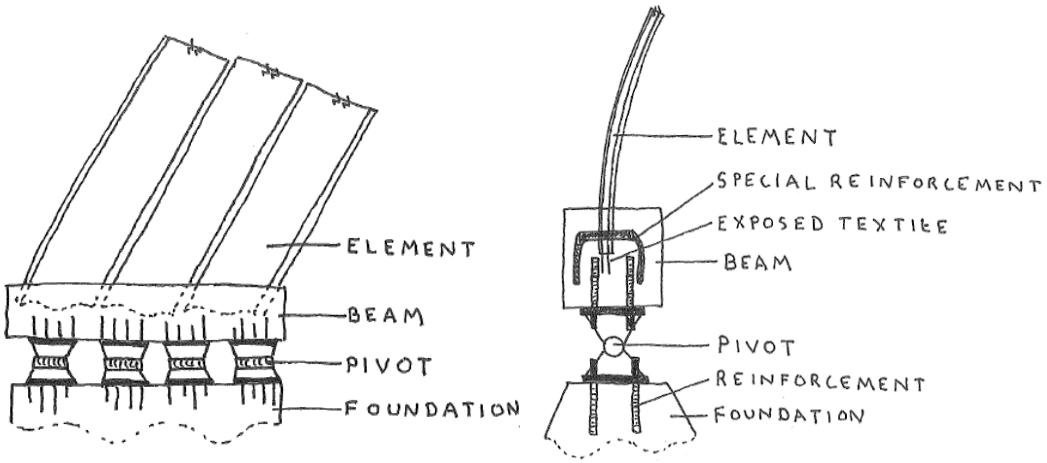

Figure 5.14: The element-to-foundation connection is formed by a beam and pivot system, side view (left) and section (right), both at the building scale.

5-4 STRATEGIES FOR OUT-OF-PLANE LOADING

Out-of-plan loading forces such as bending and punching shear are of concern for thin structural elements such as this material. Three main strategies have been conceived as potential solutions to these types of loading situations. Choosing which of the three to use will come down to a decision about which fits best with the architecture of the building both spatially and aesthetically.

5-4-1 CORRUGATION

Corrugation or other wrinkling of the material can be used to increase the structural depth of the region faced with out-of-plane loading. Effectively this moves more of the material further from the neutral-axis of bending so that more of the forces are carried in-plane. From Steiner's rule this affect works quadratically with distance, meaning that it is a very effective against even large bending loads. For example punching shear is cause by a point load normal to the curvature of the thin element. When this thin element is turned towards the direction of the force more of the punching shear is now carried by in-plane shear. Similarly this reorientation of the surface through wrinkling means that the compression and tension of bending can be distributed over a larger cross section at greater separation.

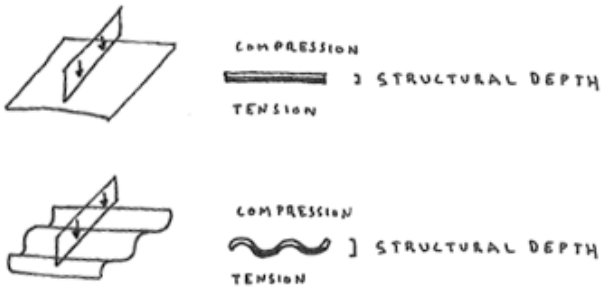

Figure 5.15: Comparison of loading a wrinkled and a flat element in bending. Corrugation increases the structural depth and therefore bending resistance of the material.

5-4-2 LAYERING OF THE MATERIAL

Increasing the structural thickness could be by using multiple layers of the same material or the material could come in multiple thicknesses. Areas of the building with higher out-of-plane forces would be constructed from multiple layers of the material or of a thicker version of the material. This would keep construction simple by enabling the material to better resist the specific local loads, without the need for additional topping layers or other elements. This method is used later in the Case Study Building (Section 11-5).

If multiple layers are used they would need to adhere to each other and water to hydrate the concrete would need to sufficiently permeate through them. For this reason it would be simpler to use multiple thickness of the material and therefore becomes a concern for fabrication more than construction.

5-4-3 ADDITIONAL STRUCTURAL ELEMENTS

Additional structural elements such as beams or columns will most likely be required for the more complex constructions using this material. This will require an additional step during construction. These other elements will allow the thin material to carry primarily in-plane-loads and therefore reduce the overall mass of the construction as compared to thickening material element globally.

5-5 PHYSICAL PROTOTYPE

A simple mock-up of the material was created in order to better communicate the concept. It was made with easy to acquire materials: Woven cloth, concrete, woven glass-fiber reinforcement, and elastic film. It measures approximately 20mm thick, 100mm wide, and 200mm long.

Figure 5.16: Photos of the physical prototype of the material showing reinforcement, concrete matrix, black elastic layer, and grey-black cloth layer, measuring approximately 20mm thick, 100mm wide, and 200mm long.

5-6 CONCLUSION AND DISCUSSION

A starting configuration was selected to progress in the project, however further inspection should be conducted. A collection of many more types of materials is required, namely types of foams and 3D woven textiles. They could be the most promising type of reinforcement because they are very stable and would resist delamination.

The few jointing options presented seem reasonable but are far from fully developed. Inspiration from other jointed systems or other industries should be searched. The next step would be to select materials and create prototypes. For these reasons no preferred joint has been selected.

This development process did not produce a confident final result because of the many topics were not fully investigated. The material as it is outline above is by no means a final prototype but instead merely sufficient to suggest that the material would be possible to realize. With this hurdle crossed, it becomes more important to investigate its application to buildings. Appling it to a building will open up new issues which can be used to guide the future material development process after the conclusion of this project.

6 TEST SHAPE

In order to translate the material from a concept with imagined properties, to a material ready for application, a simplified building form is used to refine the material properties and explore its application.

This test shape has a number of requirements that will insure that the results are meaningful for a more complex structurally informed building form. For procedural clarity and accuracy of the results, the test shape is kept simple and symmetrical without additional structural features. The requirements defining this shape relate to the types of stresses in the material as well as the geometry of how the material becomes a building.

The results of the test shape will be used to refine the composition, dimensions, and other properties of the material in development. Iteration is used within the procedure to find acceptable dimensions for the material.

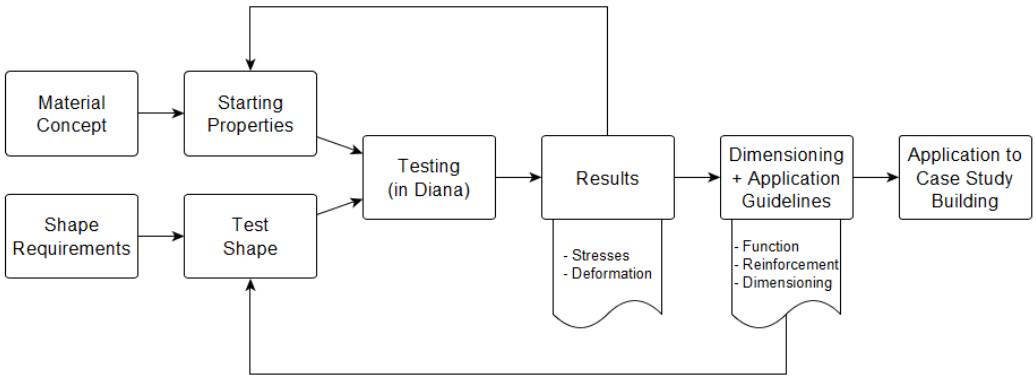

Figure 6.1: Process flowchart of the test shape development and testing.

6-1 REQUIREMENTS

The test shape will be used to dimension the sheet-like building material and investigate its behavior. Therefore the test shape geometry should require the material to be loaded in multiple ways and at reasonable spans for the application of a real building. Exceptions, such as cutting patterns or additional structural members, are not considered for the simplest test shape. Their influence should be investigated later because they would be necessary when constructing a real building.

The requirements of the test shape concerning the loading of the material are very important. The requirements regarding the similarity of the test shape to a real building are guidelines, because simplicity and verifiable accuracy, instead of reality is desired. These requirements are summarized in Table 6.1 below.

Table 6.1: Test Shape Requirements.

Material Loading	Building Geometry
In-Plane Compression	Double-Curvature
In-Plane Tension	Medium-Sized Span
Out-of-Plane Bending	Realistic Building Shape
	No Structural Exceptions
	Simple Construction

6-2 SHAPE ALTERNATIVES

Hemisphere – resembles a real building, hoop compression, hoop tension, and bending expected for all loading cases, means it's a good test of the requirements for this material that will enable versatility/many architectural possibilities, while also being simple enough to calculate by hand.

Torus hall – resembles a real building, such as a sports venue, good test of compression perhaps a bit of hoop tension, not much bending; it's double-curved meaning it would test the deformation and construction of the material; Its long shape may require multiple pieces which would mean structural exceptions.

Hung Arch – resembles a potential building element, models a method of construction unique to this material, complex, not so easy to predict the influence of geometry on load bearing behavior.

Hanging Shape – would be loaded mostly in plane, treats this material as a material for building shells, although it would like to be able to do more than just that (somewhere between membrane and shell), construction method fitted to this material

Figure 6.2: Test shape alternatives from left to right: hemisphere, torus, hung arch, and hanging shape.

6-2-1 HEMISPHERE

The hemisphere is chosen as the test shape because it fulfills most of the requirements. It represents a common shape found within classical buildings and has an appropriate double-curved architectural geometry. Therefore the results can be used to approximate more complex double-curved freeform geometry. The full range of imposed stresses is important for the versatility of the material. It includes some hoop-tension and in-plane compression. These stresses will be used to dimension the reinforcing and cross-section. These stresses in a hemisphere can be easily determined analytically (hand calculation) and checked against the numerical results (Diana FEM model). Additionally the hemisphere could be reasonably constructed by simple geometric or inflatable formwork, a method prescribed by the patented and well suited for the material in development.

Two versions of the hemisphere will be created: continuous and non-continuous. Both will be building sized, with a radius of 10 meters. The non-continuous version will have a circular opening as an additional test of the material's behavior. This opening has a radius of 2.5 meters and is located at a 45 degree angle from the center of the sphere.

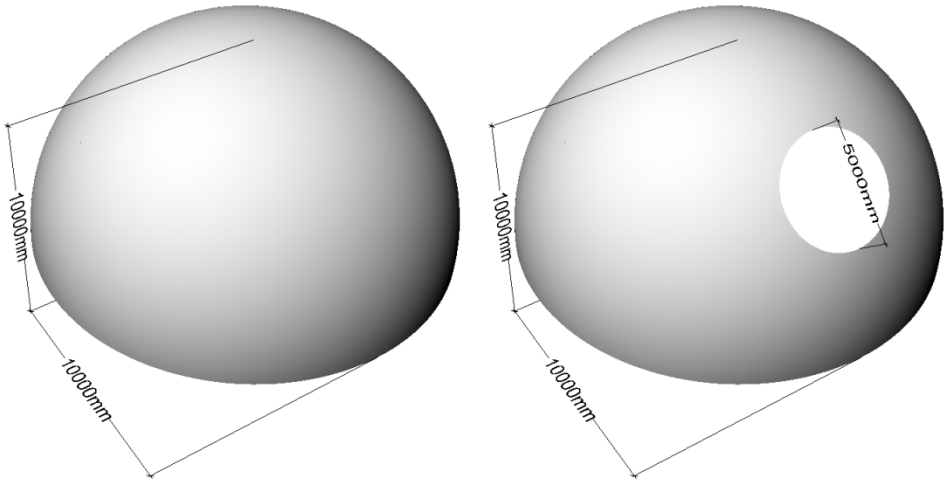

Figure 6.3: Geometry of the hemispherical test shape, continuous (left) and with hole (right).

6-3 ANALYTICAL ANALYSIS (HAND CALCULATION)

This section presents a summary of the hand calculations to determine the internal forces of the hemisphere analytically. The results of this hand calculation will be used primarily to check the accuracy of the numerical (FEM) analysis model. A simple loading case in the negative Z-direction is used for this model. This distributed load of -7.2 kN/m^2 (-0.0072 N/mm^2) represents the thickness of the material and topping or finishing layers equivalent to a constant thickness of 300mm of normal weight concrete. The calculation assumes a uniform distributed load and supports restrained in the global Z-direction while free in X and Y.

The hand calculation determines the in-plane forces for the local surface coordinate system as a function of angle of elevation. The relationship between angle of elevation (a) and the force in the local y direction (N_{yy}) are shown below, in Figure 6.4. The in-plane forces are aligned by the local surface coordinate system; therefore they represent arch forces and hoop forces respectively for y and x. The equations for these forces are shown below in Equation 6.1 and 6.2. R represents the radius (10m) and G represents the distributed load (-7.2 kN/m^2) and a represents the angle of elevation. The solution of these equations is presented, in Table 6.2, for a wide range of angle between 0° and 90°. For this load case, a change in hoop forces occurs at ~52.8°, where compression transitions to tension. A visual representation of this change from compression to tension is shown in Figure 6.5. The work for this calculation is presented in the Appendix.

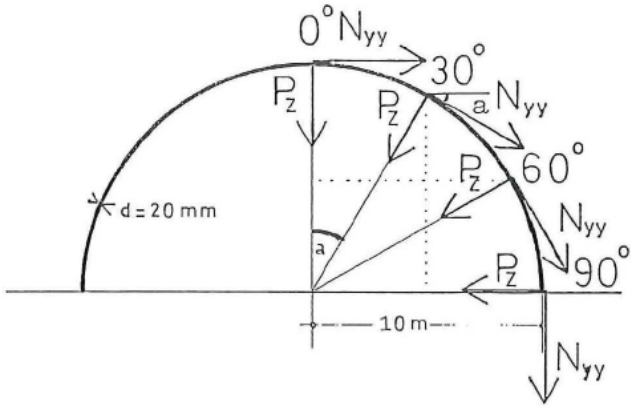

Figure 6.4: Relationship between angle of elevation (a) and the force in the local y direction (N_{yy}) for the hemispherical test shape. [Modified from: Haas]

$$N_{yy} = G \times R \times \frac{1 - \cos a}{\sin^2 a} = Arch\ Forces$$

Equation 6.1: Internal force for the hemispherical surface Y-direction, representing hemispherical arch forces.

$$N_{xx} = G \times R \times \left(\cos a - \frac{1}{1 + \cos a}\right) = Hoop\ Forces$$

Equation 6.2: Internal force for the hemispherical surface X-direction, representing hemispherical hoop forces.

Table 6.2: Internal forces by angle of elevation for a uniformly loaded hemisphere, negative values represent tension.

Angle (Deg.)	N_{yy} (kN)	N_{xx} (kN)
0	n/a	36.0
5	36.1	35.7
10	36.3	34.6
15	36.6	32.9
20	37.1	30.5
25	37.8	27.5
30	38.6	23.8
35	39.6	19.4
40	40.8	14.4
45	42.2	8.7
50	43.8	2.5
51.827	44.5	0.0
55	45.8	-4.5
60	48.0	-12.0
65	50.6	-20.2
70	53.7	-29.0
75	57.2	-38.6
80	61.3	-48.8
85	66.2	-60.0
90	72.0	-72.0

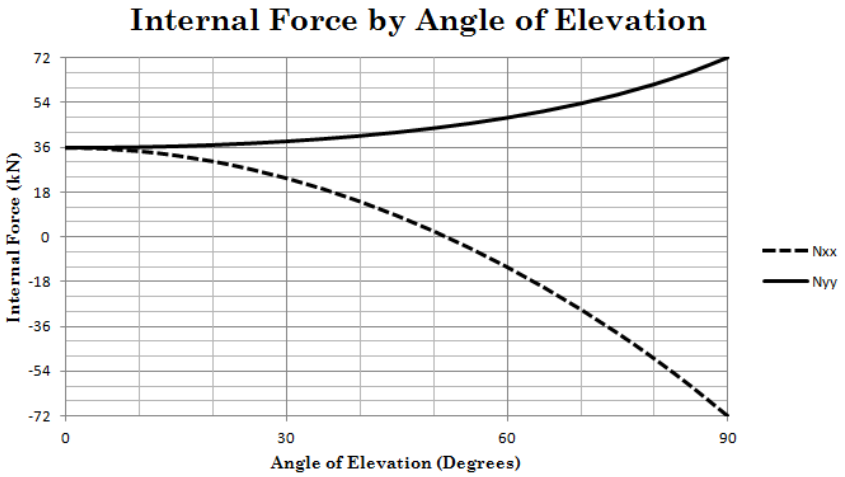

Figure 6.5: Graph of internal force by angle of elevation, analytically determined for a hemisphere, negative values represent tension.

6-4 MODELING THE TEST SHAPE GEOMETRY

The test shape geometry is first created as a 3D computer model before it can be analyzed numerically. It is created using the computer program McNeel Rhinoceros. The hemisphere is modeled as a continuous surface but uses break lines to divide it into smaller sub-surfaces. These break lines are important for two reasons. First, it enables the creation of a hole in the test shape to test the effect of non-continuities (Figure 6.3). Secondly, these break lines simplify the process of "meshing" which is required for numerical Finite element method (FEM) analysis. Meshing means to break the surface into smaller elements which are geometrically more suited for FEM. Square mesh elements are preferred (Section 6-4-3).

The hemispherical surface, divided by the break lines, seen in Figure 6.6 below, will be further used by two computer programs. The first, Midas FX+, is used to create the element mesh for FEM. The second, Drape, is used to determine how the new material might deform to create the hemispherical test shape (Section 5-1-3). Therefore the geometry is exported in two formats: an IGES (Initial Graphics Exchange Specification) file, for use in Midas FX+, and as a ".3DS" file, for use in Drape.

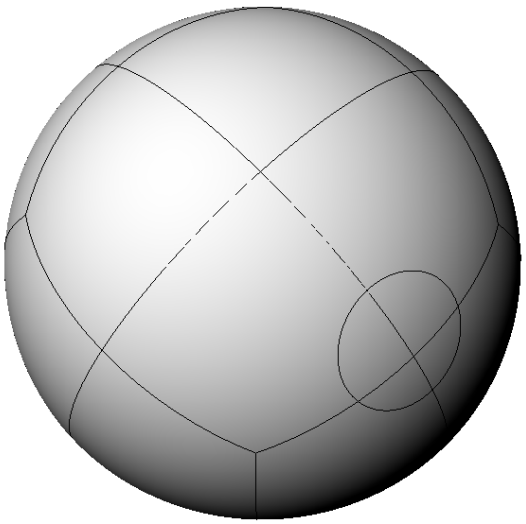

Figure 6.6: Test shape modeled in McNeel Rhinoceros, showing break lines and sub-surfaces in preparation for FEM meshing, three-quarters top-view.

6-4-1 FIELD OF POSSIBLE TEST SHAPE MODELS

Finite element method (FEM) analysis is used to determine the expected forces within the material. For the best results the model should simulate reality as closely as possible but also simplify reality as much as possible in order to reduce the chance of error. Therefore the test shape is first analyzed as a monolithic, isotropic shell, which can be compared against hand calculations. Then information about the textile is added to the model, first variable thickness, then orthotropic stiffness. These thickness and stiffness variations are caused by shearing of the material and its reinforcement. Additionally the test shape will be tested as a continuous shell, a shell with a hole, and a shell with a hole and a stiffening beam around the hole.

A field of possible models for numerical analysis is created by combining the test shape forms and the material property variables, as seen below in Table 6.3. The cell in the upper left, "isotropic, uniform, continuous", represents the simplest model, while the lower right, "orthotropic, variable, hole + stiffening beam", represents the model most closely mimicking the material properties. Each of these models has a problem: the

first is too simple to reflect the material behavior but is confirmable by hand calculations, the second is inaccurate because the material properties aren't full known but never the less reflects the behavior of the material qualitatively.

The combinations illustrated in black within the table will be modeled in the following section, Section 6-5. They represent increasing complexity within the model while retaining simplicity of either the continuity or material properties. The fields marked with an "X" will not be modeled because they don't fully represent the test shape behavior, while being too complicated to produce reliably results. Lastly, the combination illustrated in grey, represents the combination of all modeled test shapes, but will not be modeled.

Table 6.3: Field of possible test shape models showing test shape number.

Stiffness / Thickness	Isotropic Uniform	Isotropic Variable	Orthotropic Variable
Continuous	 **1**	 **4**	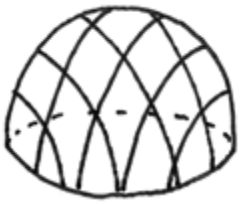 **5**
Hole	 **2**	X	X
Hole + Stiffening Beam	 **3**	X	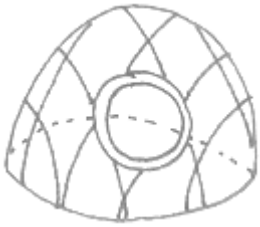

6-4-2 TEXTILE SHAPE WITH DRAPE

The ".3DS" file created in Rhinoceros is imported into Drape (Section 2-3) to investigate how the new material would deform to create the hemisphere. Shear is the only deformation mode allowed for this deformation. Therefore, Drape is being used to determine the greatest required shear deformation angle. In order to keep the structure and analysis of the test shape simple, it is important that it can be formed by reasonable deformations of the new material.

A woven material 1000 millimeters wide was selected to cover the test shape in Drape. This width based on the roll widths of Concrete Canvas, as presented later in Section 9-1-1. The width of the woven material does not affect the resulting draping angle, so the any dimensions could have been used. However this realistic width provides a clearer image of the logic behind its construction.

The results of a symmetrical draping process, seen below in Figure 6.7, show the distribution of shear deformation as well as the approximate number of sheets that would be required to create the hemisphere. The angle formed by the draping process is at its smallest value ~39 degrees. This gives a lower geometrical goal for the physical material; it must be able to shear sufficiently, down to ~39 degrees, in order to create the basic spherical test shape.

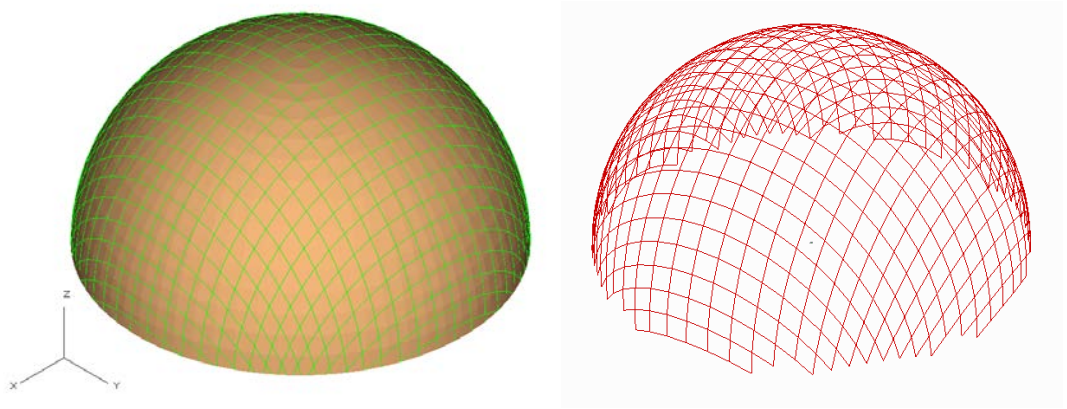

Figure 6.7: 10 meter radius hemispherical test shape draped with 1000 millimeter wide material, screenshot from Drape (left) and the same geometry exported to McNeel Rhinoceros (right).

6-4-3 COMPUTATION MESHING

A computational mesh is used to create the finite elements used by the finite element method (FEM). To insure accurate results these elements are constrained to fit assumptions made by the program. The FEM program of choice, Diana, requires the quadrilateral elements to have angles between 40 and 140 degrees. The sub-divided hemispherical surface from Rhinoceros (Figure 6.6) has been further divided using Midas FX+. The results of this meshing division and the computation accuracy of each element can be seen in below, in Figure 6.7. The accuracy of this model comes from the squareness of the meshing elements. This mesh will be used in the following steps of the process to calculate the test shape, in Diana, using multiple loading conditions.

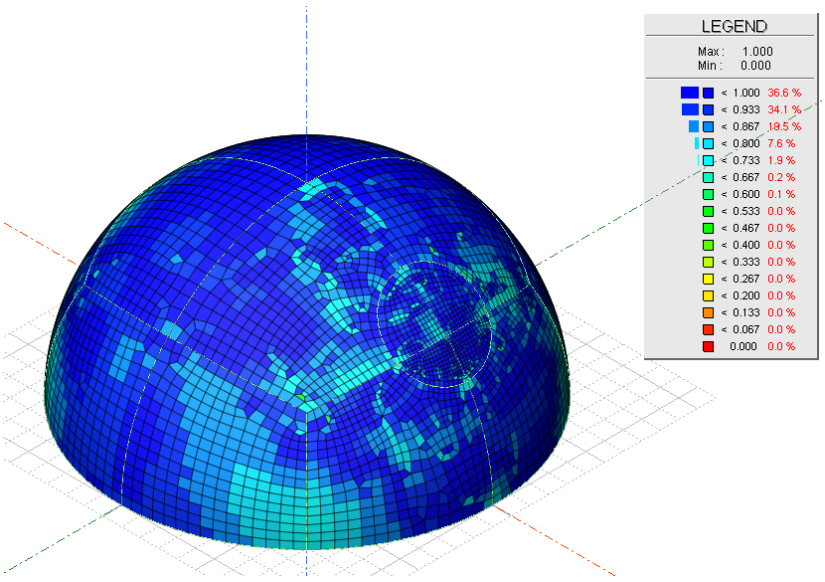

Figure 6.8: Computation mesh for FEM, created in Midas FX+, showing the mesh quality as indicated by aspect ratio, 1.000 being squarer and more accurate, also noted is the percentage of elements in each category.

6-4-4 LOAD CASES

The loading conditions and the supports are also defined using Midas FX+. The entire circular footprint of the test shape has been created as a pinned support. A simple gravity load has been applied to each element in the negative Z-direction. Additionally, for the test shape with the hole and stiffening beam, a load representing the self weight of the stiffening beam has been applied. A wind load has been applied as pressure and suction over two zones.

The foundation connection for the test shape has been modeled as a continuous pinned support around the footprint edge.

Load Case 1 was found the show the largest forces and deformations therefore it is the one discussed in this chapter, although both were investigated.

Table 6.4: Test Shape Loading Cases.

Load Case	Direction	Force	Rational
1: Gravity	Z	-0.0072 N/mm^2	Force of 300mm concrete = material + topping
	Z	-0.480 N/mm	Self weight of stiffening beam (100x200mm)
2: Wind	Surface Normal	±0.002 N/mm^2	Exaggerated pressure and suction of 2kN/m^2

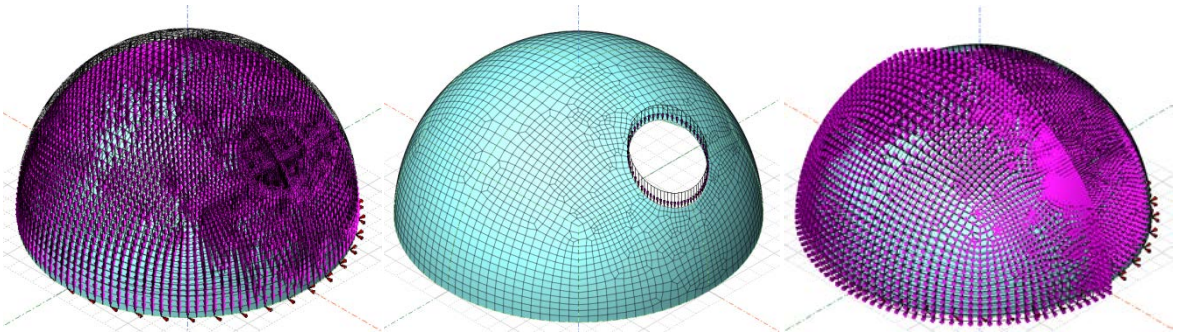

Figure 6.9: Test shape loading diagrams for load cases 1, gravity (left) with beam load (center) and 2, wind (right), from Midas FX+.

6-4-5 THICKNESS INCREASE BY SHEAR DEFORMATION

The test shape is modeled with two thicknesses: a uniform 20mm thickness and a variable shear-deformed thickness between 20 and 31mm. The initial thickness of the material is set at 20mm; a value that is reasonable for fabrication. Increasing the thickness beyond this value would make fabrication and construction more difficult. The uniform thickness model represents the simplest case and is used for comparison of the results to the analytical results (Section 6-3), while the variable thickness model represents the influence of shear-deformation thickening of the material. The thickness increase does not correspond to the angle of elevation, as the internal forces do, because it is caused by shear deformation of the material which occurs in four areas of the shape. As shear deformation increases the thickness, it also reorients the reinforcement and changes the relative stiffness and other mechanical properties of the material. This variation in thickness and reinforcement reorientation can be seen below in Figure 6.10.

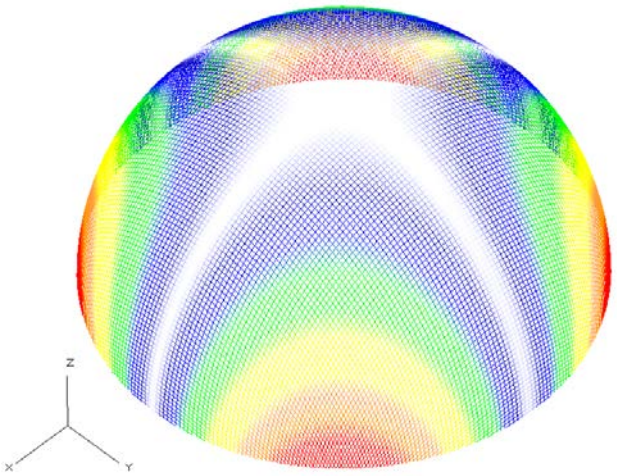

Figure 6.10: Test shape showing areas of increased thickness due to shear deformation, White = 20.0mm, Blue ≤ 20mm, Green ≤ 21mm, Yellow ≤ 23mm, Orange ≤ 26mm Red ≤ 31mm.

Shearing increased thickness, stiffness, and bearing capacity for certain regions of the structure but also added mass. This would have the result of increasing the load asymmetrically, which has a negative effect on the bearing capacity of the hemisphere, as it could increase buckling. However, this effect occurs mostly at the lower edge of the sphere, where the most shearing occurs (Figure 6.10) At these lower portions the structure is closest to vertical, meaning that an increase in mass would contribute mostly to the in-plane loading and minimally to loading normal to the surface. For comparison both models will be analyzed in Section 6-5.

6-4-6 HOLE STIFFENING BEAM

Shell structures work best without discontinuities because the force is transferred across the entire cross-section of the shell. However these discontinuities, such as windows, are important architectural features and necessary to a well functioning building. The influence of the discontinuity can be decreased by using a stiff element to allow force transfer through the discontinuity. This works similarly to the rolled ring at the lip of a paper cup, making it possible to squeeze. The test shape will use a stiffening element for this purpose of load transfer. Its properties will be estimated for the purpose of the test element, as shown below in Figure 6.11. However, for a real construction the stiffening elements should be design for the specific loading conditions at each discontinuity to reduce unneeded mass.

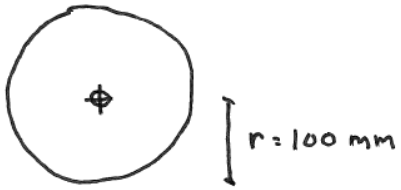

Figure 6.11: Test shape stiffening beam cross-section dimension, 100mm radius concrete beam.

6-4-7 ORTHOTROPIC STIFFNESS

A value for the stiffness of the material in the direction of the glass fiber reinforcement is required for orthotropic analysis, which takes into account the textile-like properties of the material (Section 6-5-4). This value is inputted to Drape so that the resulting stiffness can be calculated as the reinforcement orientation changes through shearing. The glass fiber is assumed to have a stiffness of 72.5GPa and the concrete is assumed to have a stiffness of 30GPa. Together these two constitute the structural layers of the material. (These material properties are different that those from Hegger, Section 4-2-1 and 4-4-4, but are close enough.)

This step in the process was actually performed after the application of the numerical analysis results (Section 6-6) but is presented here for clarity. From this later section, a preliminary reinforcement percentage has been determined. From this percentage a balanced stiffness can be calculated between the concrete and glass reinforcement. An assumed 20mm cross-section is composed of 14mm concrete, 3mm, aligned glass fiber, and 3mm unaligned glass fiber. The unaligned glass fiber is assumed not to contribute to the stiffness. The resulting balanced stiffness is 37.5GPa, as shown below in Equation 6.3. Drape then estimates the remaining elastic properties as seen below, in Figure 6.12.

$$Balanced\ Stiffness\ = \frac{E_{Conc} \times t_{Conc}\ +\ E_{Glass} \times t_{Glass}}{t_{contibuting}} = \frac{30 \times 14\ +\ 72.5 \times 3}{17} = 37.5GPa$$

Equation 6.3: Balanced stiffness calculation for orthotropic analysis.

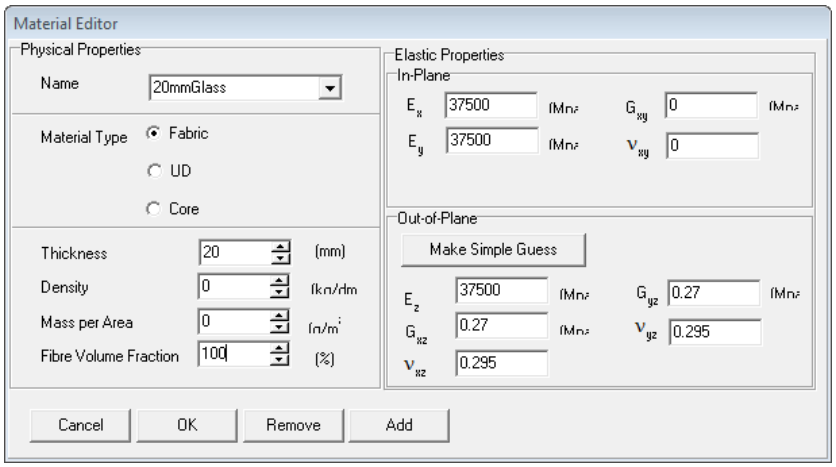

Figure 6.12: Balanced material stiffness as inputted into Drape.

6-4-8 JOINTING

In reality the test shape could not be created as a monolithic shell because the material could not be produced in large enough elements to cover an entire building. (See more about jointing in Section 5-3.) These joints are changes in the properties of the structure and have different bending stiffnesses, shear capacities, etc. The influence of joints could be significant if it causes buckling. This effect of buckling will need to be investigated further, as buckling of thin shells can be the limiting factor.

Although their influence on the structure of the test shape is unknown it is possible to continue with the analysis assuming that the joints will have sufficient stiffness in order not to influence buckling. Instead of bending, much of the load in such a hemispherical shell is carried by in-plane compression and tension. This means that joint stiffness would be an issue for flatter, less shell-like building shapes, which require more bending.

The influence of the joints could be investigated using FEM, with a slight alteration of the element meshing to account for the proper placement of the joints. Such a mesh alteration would require the combination of textile shape information (Section 6-4-2) with the geometry from Rhinoceros, as seen below in Figure 6.13. The rotational stiffness about this joint could be analyzed for multiple values, above, at, and below that of the material. This approach would yield a bench mark stiffness that the joint construction should achieve during further development. Alternatively, the joint stiffness could be estimated, by knowing the details of its construction. Such an estimate would then allow the numerical FEM analysis to determine critical loading conditions for the construction of the material as is. These joints are a concern for buckling because structural discontinuities and imperfections can increase the chance of buckling.

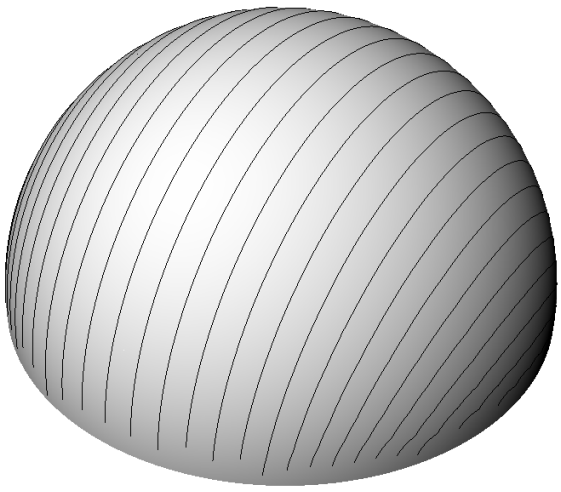

Figure 6.13: Test shape with showing joints lines between 1000mm-wide elements.

6-5 NUMERICAL ANALYSIS (FINITE ELEMENT METHOD)

Once the geometry has been created using Rhinoceros, divided using Midas FX+, and checked by Drape, another program, MeshEdit, is used to create a ".dat" file useable by TNO Diana, the Finite Element Method (FEM) analysis program. The ".dat" file contains all the information about the geometry, material properties, supports, and loading. This file can be edited using Drape or a text editor, such as Microsoft Notepad, to alter the material properties to include information about the textile behavior, namely thickness and stiffness variations. With this file, Diana runs a static linear analysis to determine the internal forces within the material as well as principle stresses and deformations. A flow chart of this procedure is shown below, in Figure 6.14.

The purpose of the FEM analysis is to get an idea of the forces in the material. From these forces a preliminary estimate for the cross-section and amount of reinforcement of the material can be determined. Additionally, Diana calculates the deformations of the structure. These deformations are a simple way to compare the behavior between each of the test shape models. The five test shapes from Table 6.3 will be analyzed for the load cases show in Table 6.4.

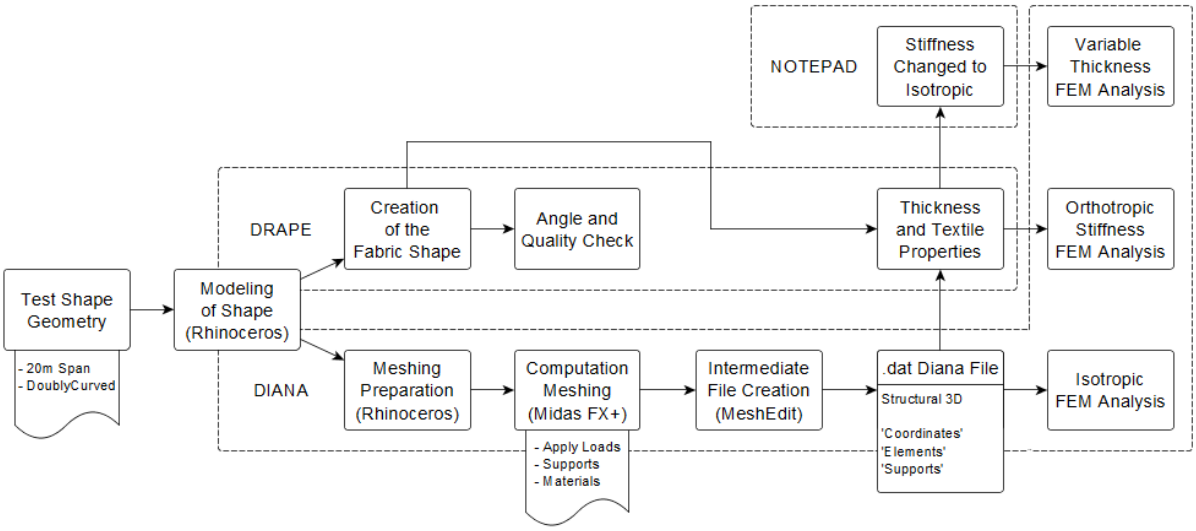

Figure 6.14: Process flow chart for the test shape from creation to FEM analysis.

6-5-1 TEST SHAPE 1: ISOTROPIC UNIFORM THICKNESS

The most simple test shape has isotropic concrete properties (Young's Modulus = 30 GPa, Poison's Ratio = 0.2) and a uniform thickness (20mm). it is loaded by the cases seen in Table 6.4. It is analyzed for principle stresses (S_3 and S_1), internal forces (N_{yy} and N_{xx}), internal moments (M_{XY}), and deformation. The internal forces are compared against the analytical calculation (Section 6-3) to validate the other results. Load Case 1, gravity, is presented in this section because it resulted in the largest internal forces, instead of Load Case 2, wind.

PRINCIPAL STRESSES (S_1 AND S_3)

Diana calculates principal stresses at each mesh element. The largest (S_1) and smallest (S_3) represent the maximum tensile and compressive stress respectively. The magnitude and direction of these stresses will later be used to dimension the reinforcement for tension and cross-sectional thickness for compression (Section 6-6). The analysis shows compression throughout and areas of hoop tension at the base of the test shape. The distribution of the principle stresses are presented as vectors below, in Figure 6.15. The largest principle stress is 3.94MPa (tension) and the smallest is 3.73MPa (compression). The image on the bottom of Figure 6.15 shows a transition from no vectors to blue vectors, this is where the hoop forces change from compression to tension (~51.8° from the top center).

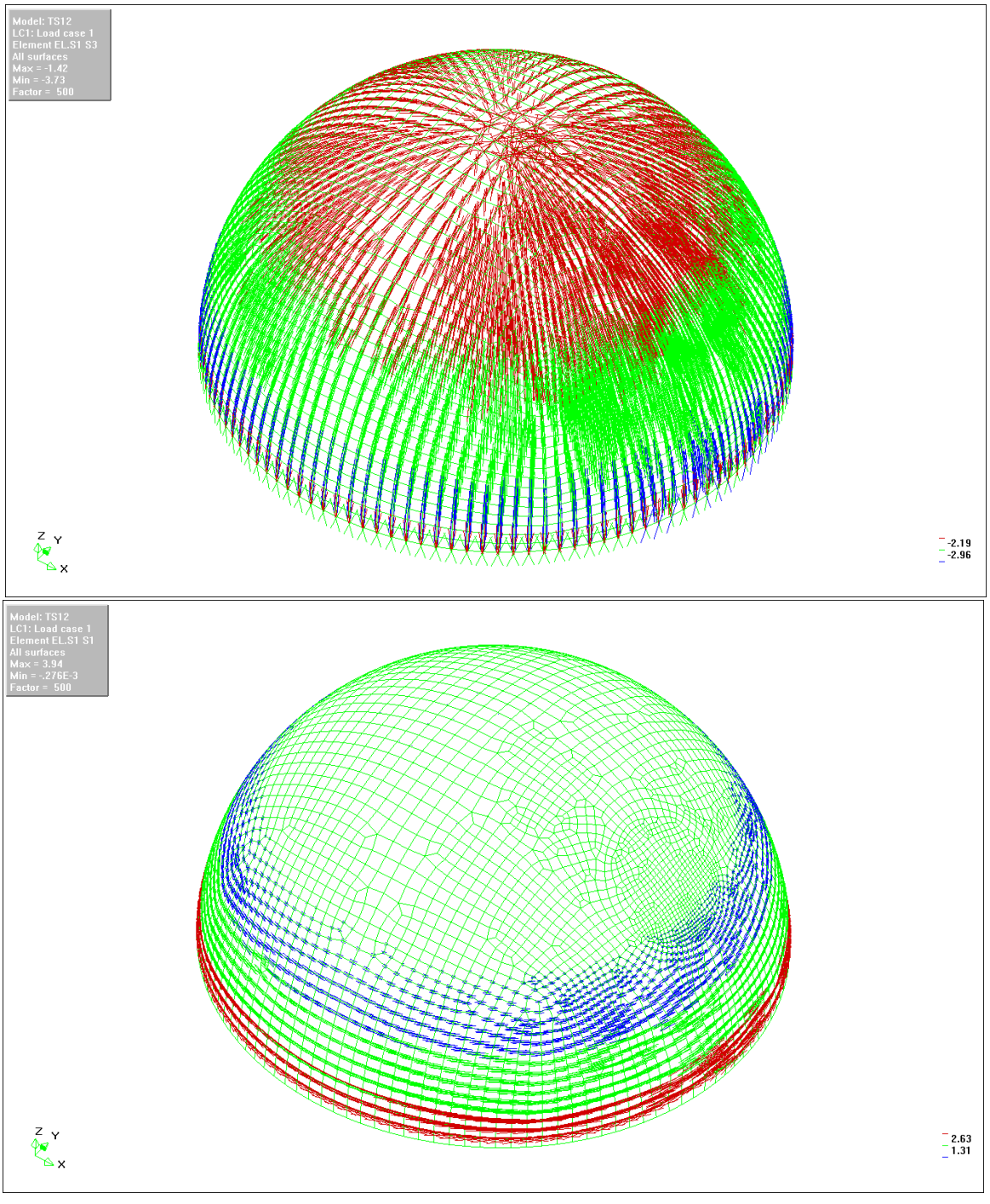

Figure 6.15: Test Shape 1, load case 1: Principle stress vectors for compression (top) and tension (bottom) in N/mm.

INTERNAL FORCES (N_{XX} AND N_{YY})

Internal (arch) forces in the surface X-direction (N_{xx}) have a maximum of 86.1kN/m in compression, as seen in Figure 6.16. Internal (hoop) forces in the surface Y-direction (N_{yy}) range from 71.1kN/m in tension to 36.9kN/m in compression, as seen in Figure 6.17.

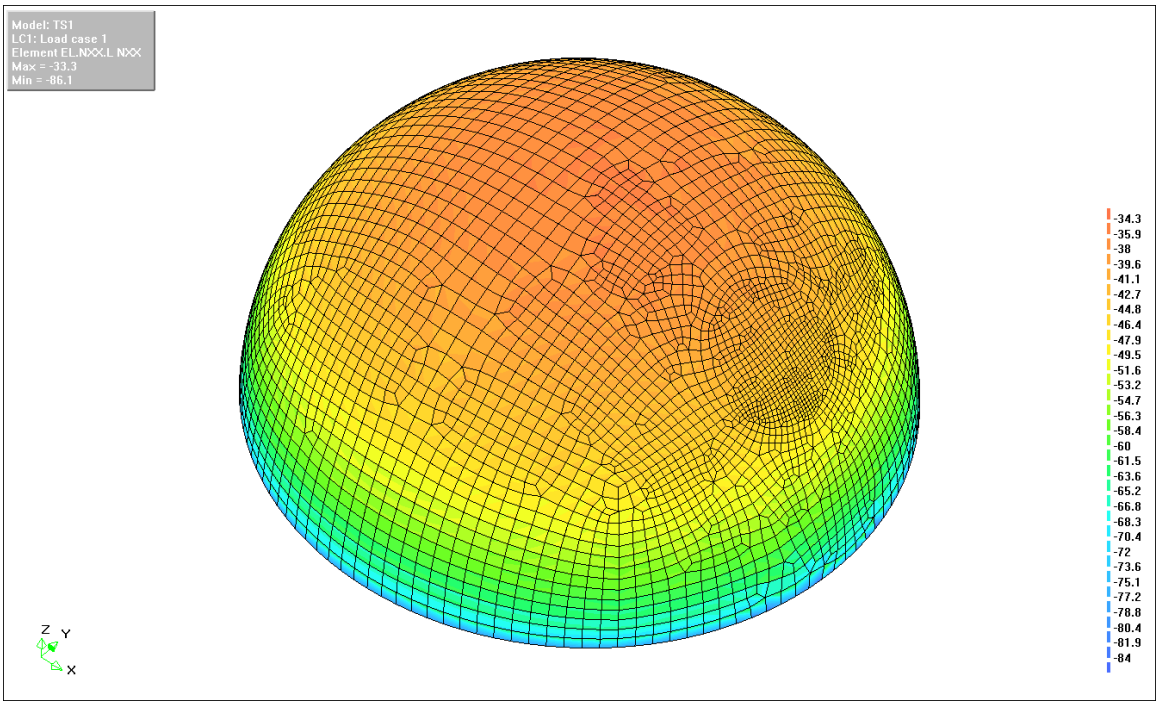

Figure 6.16: Test Shape 1, load case 1: Internal (arch) forces in the surface X-direction (N_{xx}), in kilonewtons per meter, negative values represent compression.

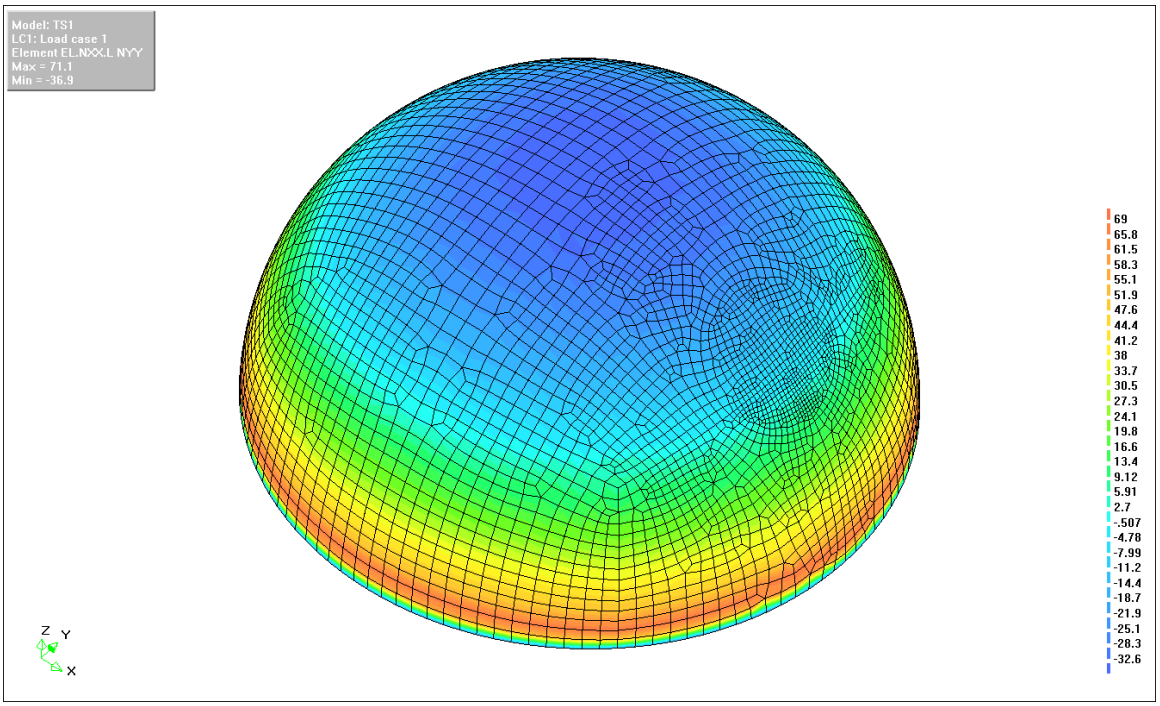

Figure 6.17: Test Shape 1, load case 1: Internal (hoop) forces in the surface X-direction (N_{yy}), in kilonewtons per meter, negative values represent compression.

INTERNAL MOMENTS (M_{XY})

The maximum (absolute) internal bending moment about the surface XY-plane (M_{xy}) is 22.4N-mm. Most of the surface has a bending moment value of 5N-mm or less. The maximum value occurs throughout the structure and inconsistently. Therefore its cause is most likely the calculation between elements within the applied meshing pattern.

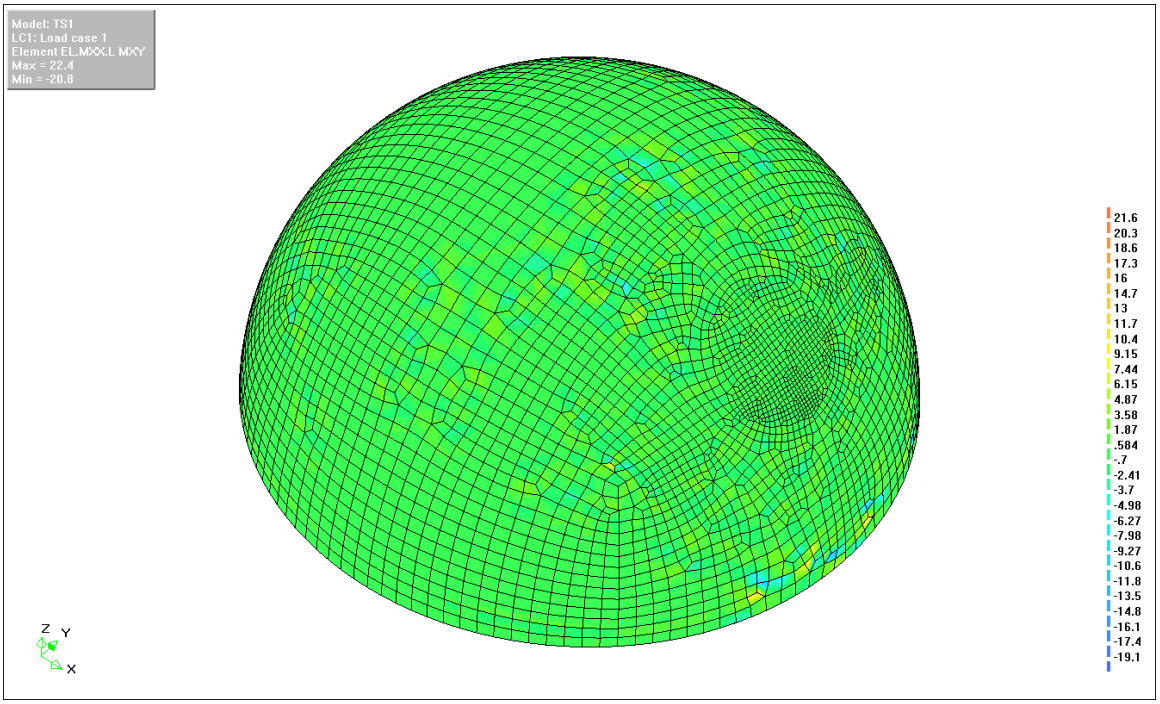

Figure 6.18: Test Shape 1, load case 1: Internal bending moments about the surface XY-plane (M_{xy}), in newton-millimeters.

DEFORMATIONS (D_{RES})

Deformations under Load Case 1 (gravity, 7.2kN/m^2) were greater than for Load Case 2 (wind, ±2kN/m^2), reaching maximums of 2.17mm and 0.85mm respectively. These small deformations are increased by a factor of 1000 to better visualize the deformed shape, as seen in Figure 6.19. It shows significant flattening suggesting that areas with large tensile hoop stresses (and therefore strains) exist. The distance of each deformation can be seen as a symmetrical heat map in Figure 6.20, increasing from 0mm in blue to 1mm in green and 2mm in red.

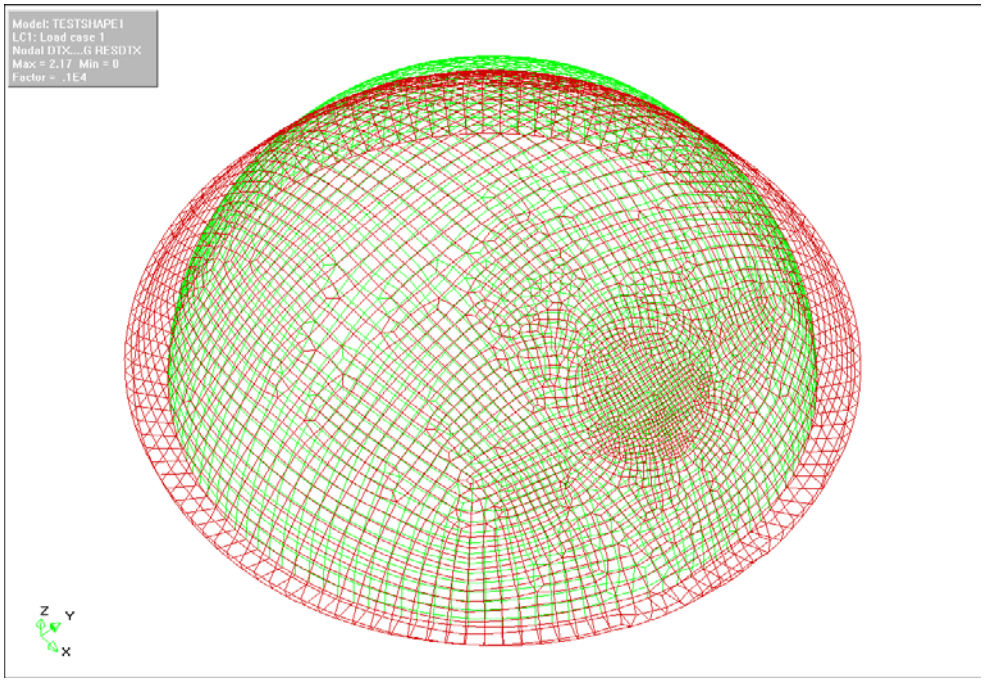

Figure 6.19: Test Shape 1, load case 1: Deformed shape resolved from each direction (D_{Res}), three-quarters top view, exaggerated by a factor of 1000.

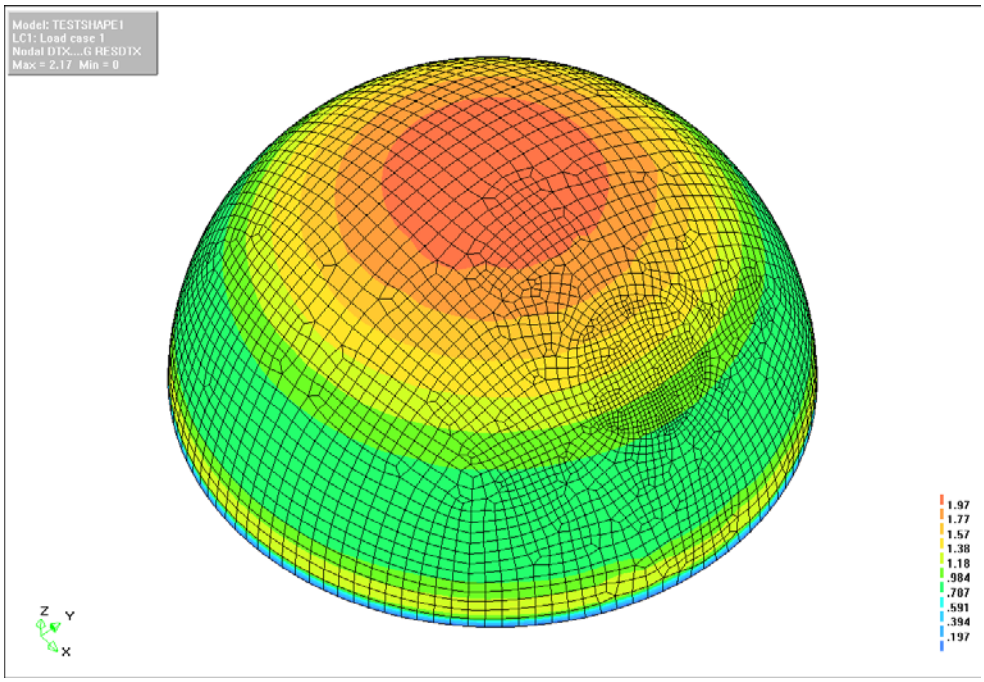

Figure 6.20: Test Shape 1, load case 1: Deformation contour heat-map resolved from each direction (D_{Res}), three-quarters top view.

COMPARISON TO ANALYTICAL ANALYSIS

The internal forces are compared against hand calculations to insure reliability of the other results. The loading in both analyses is the same however the boundary supports are different. The analytical hemisphere assumes a support which can resist only forces in the Z-direction, while the test shapes have pinned supports resisting force in all directions. Neither situation can resist rotation. For this reason, the results near the supports (a = 90 degrees) show considerable variation.

The internal force results (N_{yy} and N_{xx}) from test shape one are plotted to a graph, shown below in Figure 6.21 (using the PLOT GRAPH LINE command in iDiana). The plotted points represent the force within each element that a line cutting through the center of the hemisphere crosses. The graph is a combination of two such line-generated data sets in blue (one for each N_{yy} and N_{xx}) and two more lines in black from the analytical results (Section 6-3, Figure 6.5). The data are plotted as a function of radians of rotation from the base of the hemisphere on one side (0 radians) through the center top (pi/2 radians) to the base of the hemisphere on the other side (pi radians). In this graph blue crosses represents numerical results, black lines represent analytical results, and negative values represent compression. Overall the blue plotted points from the numerical analysis correspond very closely to the black line representing the analytical calculation. This means that the numerical analysis is as expected and the settings can be trusted for further results. One key difference between the numerical and analytical results is the significant edge disturbances, as shown by the long red lines, where the different support conditions have a strong effect on internal forces.

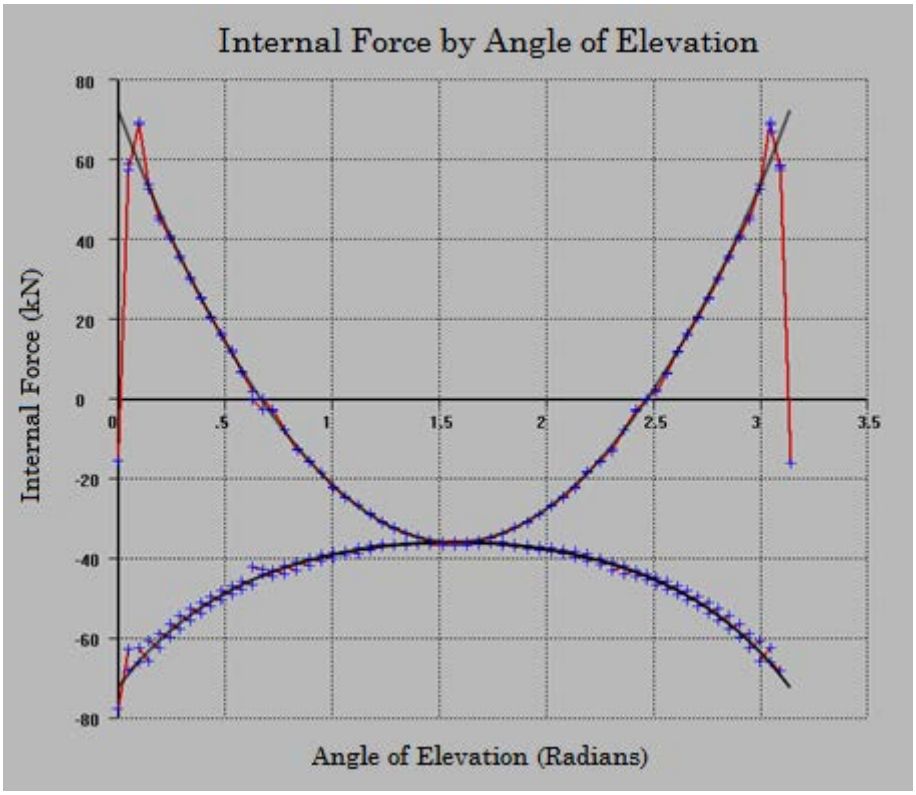

Figure 6.21: Internal forces (kN/m) as a function of radians of rotation, blue crosses represents numerical results, black lines represent analytical results, and negative values represent compression.

6-5-2 TEST SHAPE 2 AND 3: NON-CONTINUOUS

The next two test shapes represent the non-continuous shell with the circular hole. Both have isotropic concrete properties (Young's Modulus = 30 GPa, Poison's Ratio = 0.2). The first has a uniform thickness (20mm) for all elements, while the second has the same uniform thickness except for a beam around the circular hole. The properties of this beam are found in Section 6-4-6. Both are loaded by both load cases seen in Table 6.4. They are analyzed for internal forces (N_{yy} and N_{xx}), internal moments (M_{xy}), and deformation. Load case 1 is presented in this section because it resulted in the largest internal forces.

INTERNAL FORCES (N_{XX} AND N_{YY})

Internal (arch) forces for Test Shape 2 (no beam) in the surface X-direction (N_{xx}) range from 37.7kN in tension to 181kN in compression, as seen in Figure 6.22, top. Internal (arch) forces for Test Shape 3 (beam) in the surface X-direction (N_{xx}) range from 45.4kN in tension to 92.3kN in compression, as seen in Figure 6.22, bottom. This reduction in arch forces with the addition of the beam brings the values closer to those of Test Shape 1 (86.1kN) in compression. However the beam increases the tensile forces in the x-direction of the material in the area directly surrounding the beam. This suggests that the beam helps to better distribute the arch forces (and gravity load) across the cross-section of the structure, but also requires support from the surrounding material, which, with greater forces would require thickening.

Internal (arch) forces for Test Shape 2 (no beam) in the surface Y-direction (N_{yy}) range from 104kN in tension to 85.8kN in compression, as seen in Figure 6.23, top. Internal (arch) forces for Test Shape 3 (beam) in the surface Y-direction (N_{yy}) range from 79.1kN in tension to 82.4kN in compression, as seen in Figure 6.23, bottom. This reduction in hoop forces with the addition of the beam brings the values closer to those of Test Shape 1 (36.9kN in tension to 71.1kN in compression). This suggests that the beam helps to better distribute hoop forces across the cross-section of the structure.

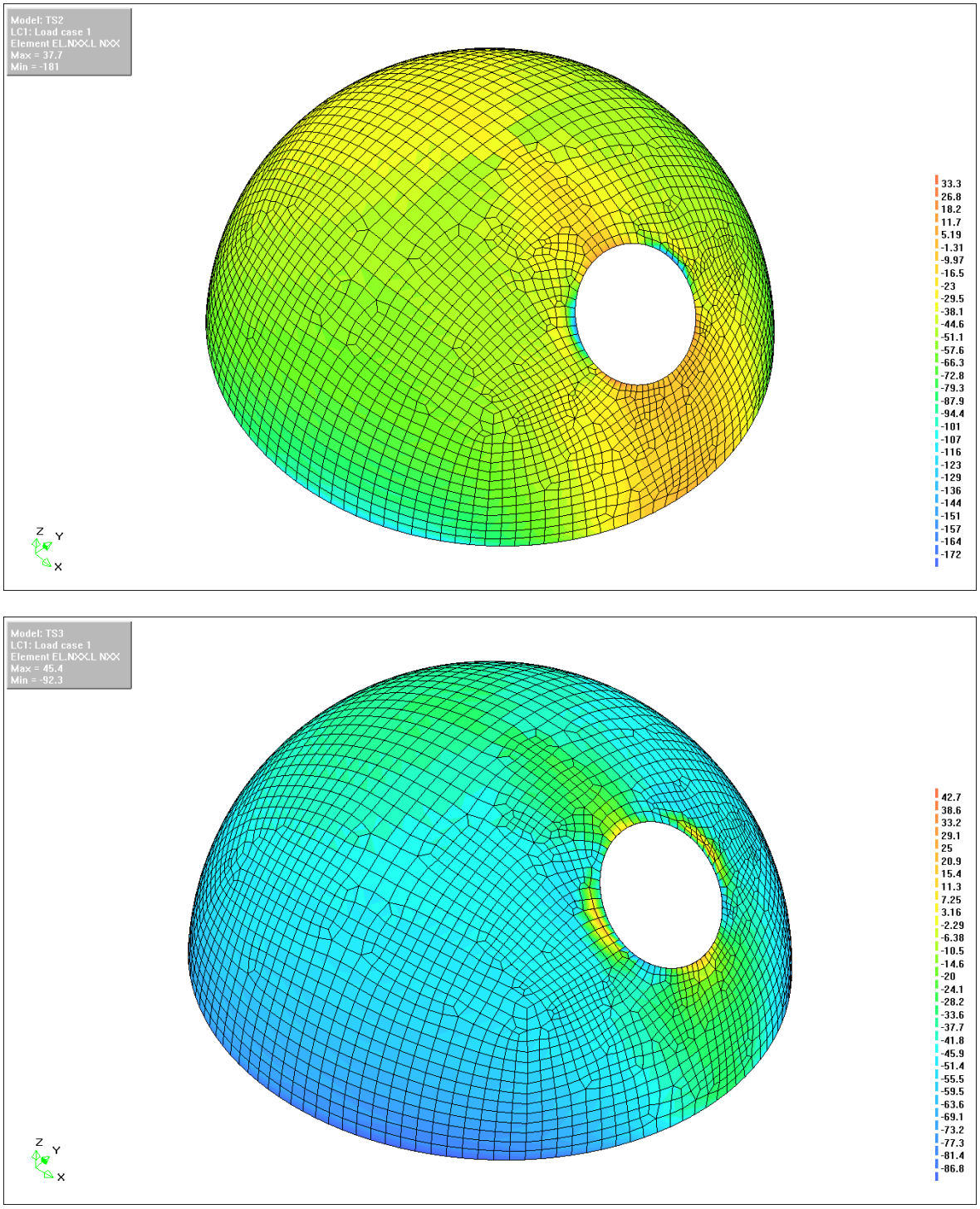

Figure 6.22: Test Shape 2 (top) and 3 (bottom), load case 1: Internal (arch) forces in the surface X-direction (N_{xx}), in kilonewtons per meter, negative values represent compression.

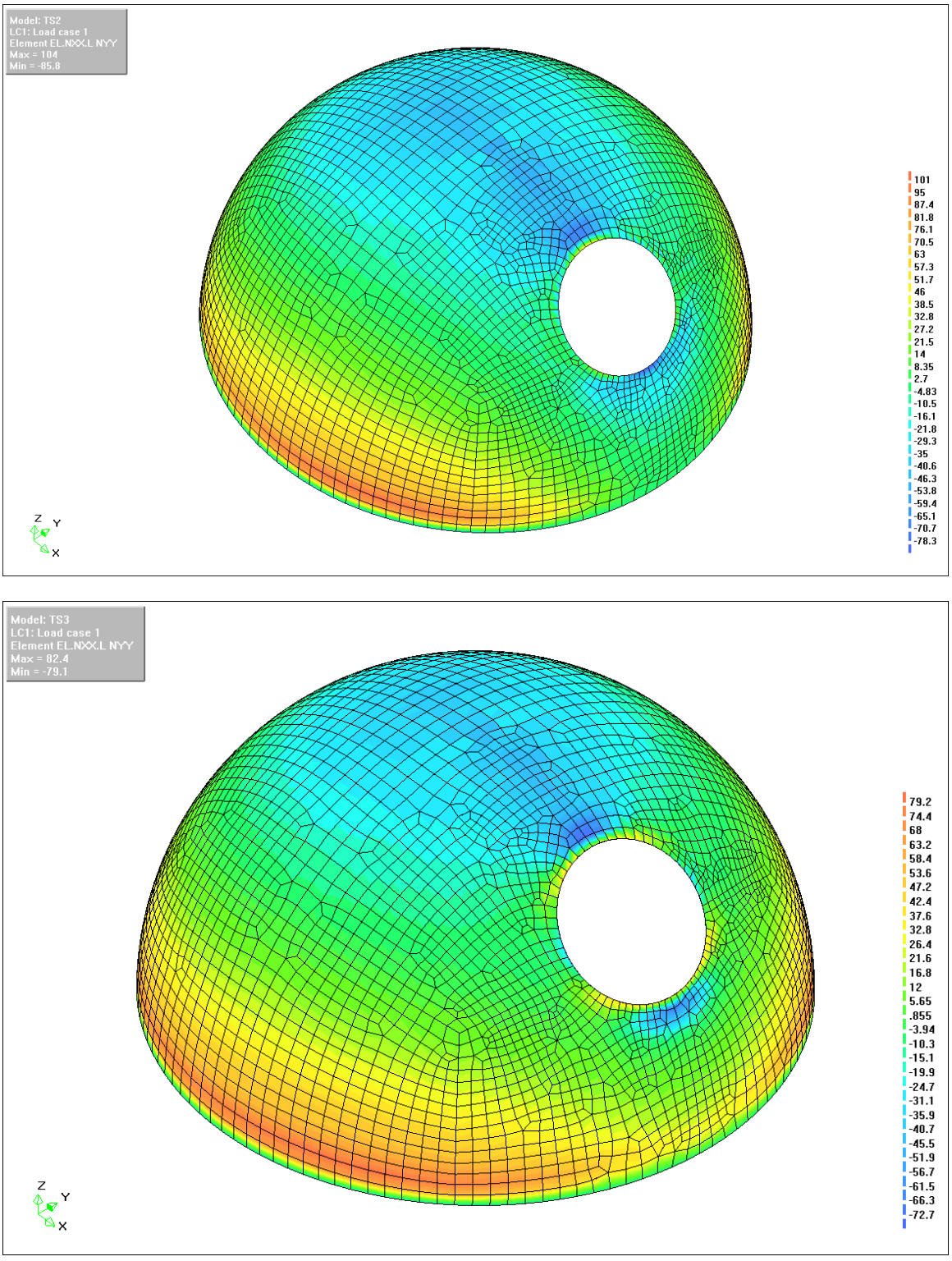

Figure 6.23: Test Shape 2 (top) and 3 (bottom), load case 1: Internal (hoop) forces in the surface Y-direction (N_{yy}), in kilonewtons per meter, negative values represent compression.

INTERNAL MOMENTS (M_{XY})

The maximum (absolute) internal bending moment about the surface XY-plane (M_{xy}) is 449N-mm for Test Shape 2 (no beam) and 189N-mm for Test Shape 3 (beam). Most of the surface of both test shapes has a bending moment value of 30N-mm or less. The maximum values occur around the circular hole, as expected. The addition of the stiffening beam has a large reduction of the maximum internal bending moment. The pattern of the moment distribution changed slightly from an alternating circular pattern to a two ringed alternating pattern. This suggests that the force transfer in the connection between the beam and material should be investigated further, especially for larger forces.

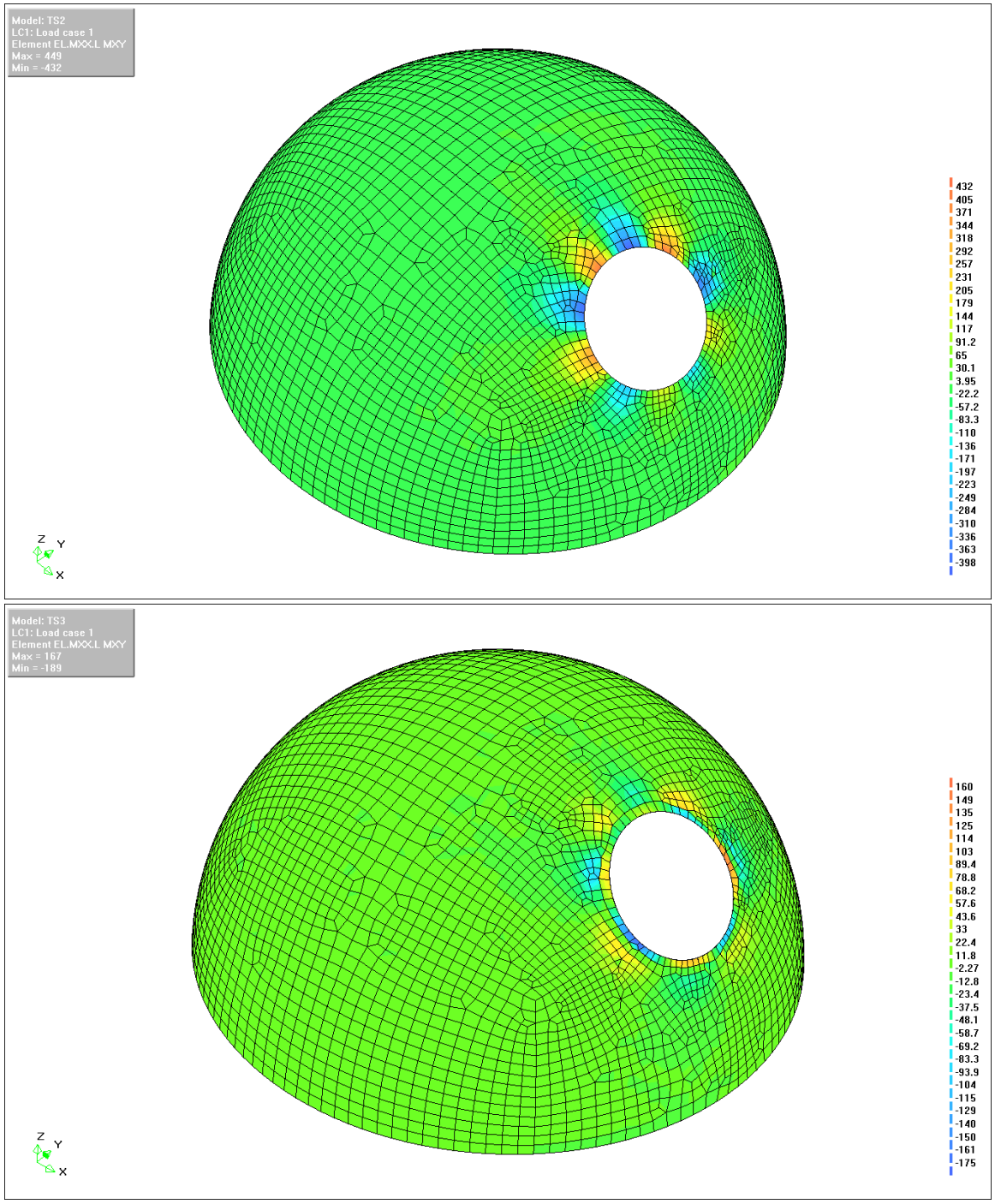

Figure 6.24: Test Shape 2 (top) and 3 (bottom), load case 1: Internal bending moments about the surface XY-plane (M_{xy}), in newton-millimeters.

DEFORMATIONS (D_{RES})

Deformations under Load Case 1 (gravity, 7.2kN/m^2) reached maximums of 34.4mm and 8.45mm for Test Shape 2 (no beam) and 3 (beam) respectively. These deformations are increased by a factor of 100 to better visualize the deformed shape, as seen in Figure 6.25. Some flattening as with Test Shape 1 is seen, but more noticeably the large twisting deformations around the circular hole. These twisting deformations represent the re-routed load path around the circular opening. The stiffening beam is able to reduce these deformations, suggesting that it maybe be aiding in load transfer around the discontinuity. The distance of each deformation can be seen as a heat map in Figure 6.26.

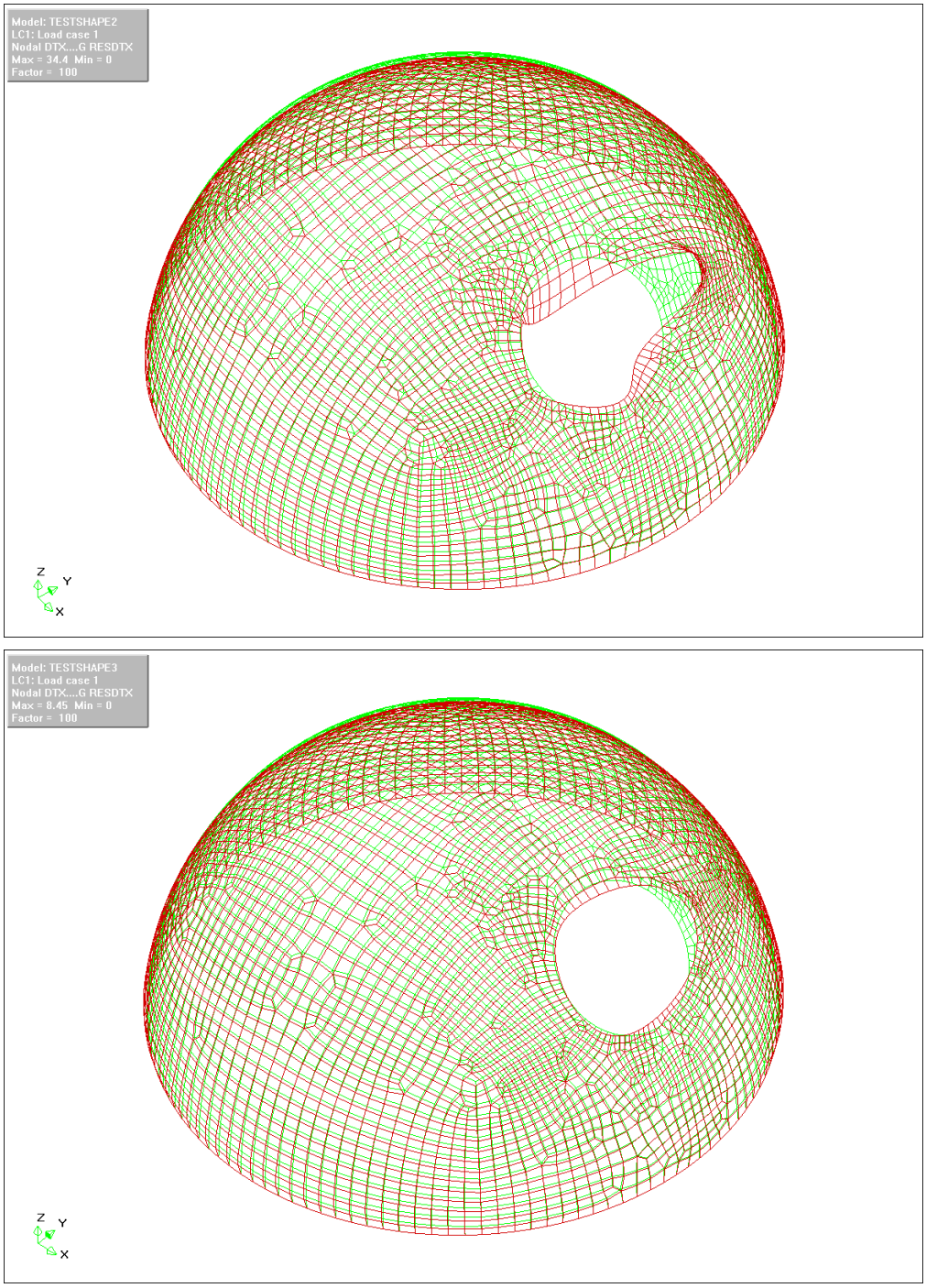

Figure 6.25: Test Shape 2 (top) and 3 (bottom), load case 1: Deformed shape resolved from each direction (D_{Res}), three-quarters top view, exaggerated by a factor of 100.

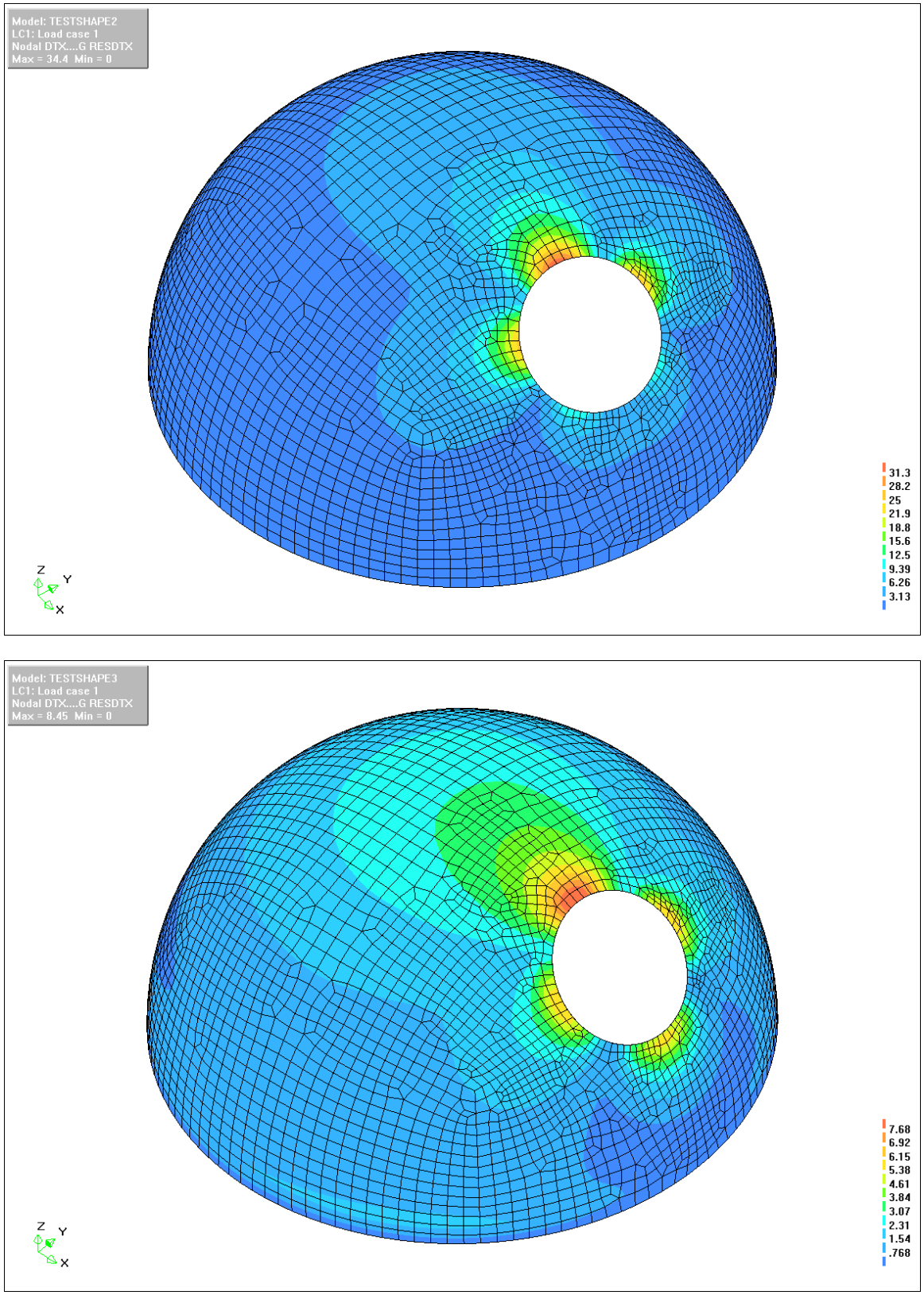

Figure 6.26: Test Shape 2 (top) and 3 (bottom), load case 1: Deformation contour heat-map resolved from each direction (D_{Res}), three-quarters top view.

6-5-3 TEST SHAPE 4 AND 5: TEXTILE PROPERTIES

The next two test shapes represent the continuous shell with variable thickness and orthotropic stiffness properties (Section 6-4-7). Both are loaded by both load cases seen in Table 6.4. They are analyzed for internal forces (N_{yy} and N_{xx}), internal moments (M_{XY}), and deformation. Load case 1 is presented in this section because it resulted in the largest internal forces. The results of this analysis will be compared against the results from the isotropic Test Shape 1.

These models are not more accurate than the previously analyzed isotropic shell model because it is more complex and estimates the yet-unknown properties of the material. It does, however, take into account the asymmetry of the material and will there for provide insight into the asymmetry's effect on the stress distribution.

The reason for the increase of maximum (absolute) values between Test Shape 4 and Test Shape 5 most likely comes from the addition of textile stiffness properties from Drape, although the specific reason is unclear. The stiffness should have increased from Test Shape 4 to Test Shape 5 due to shearing of the reinforcement. Meaning that relatively stiffer and less stiff areas would exist in Test Shape 5. It would be reasonable to assume that the stiffer areas carry more load and therefore more force. This would explain an increase the maximum internal force values, however visually this is not seen as a pattern in the Figures 6.29 and 6.30 above. Very few elements in Test Shape 5 exceed the internal forces from Test Shape 4 and no strong pattern emerges. For these two reasons the increase in internal force probably comes from the way that Drape and Diana apply element properties.

PRINCIPAL STRESSES (S_1 AND S_3)

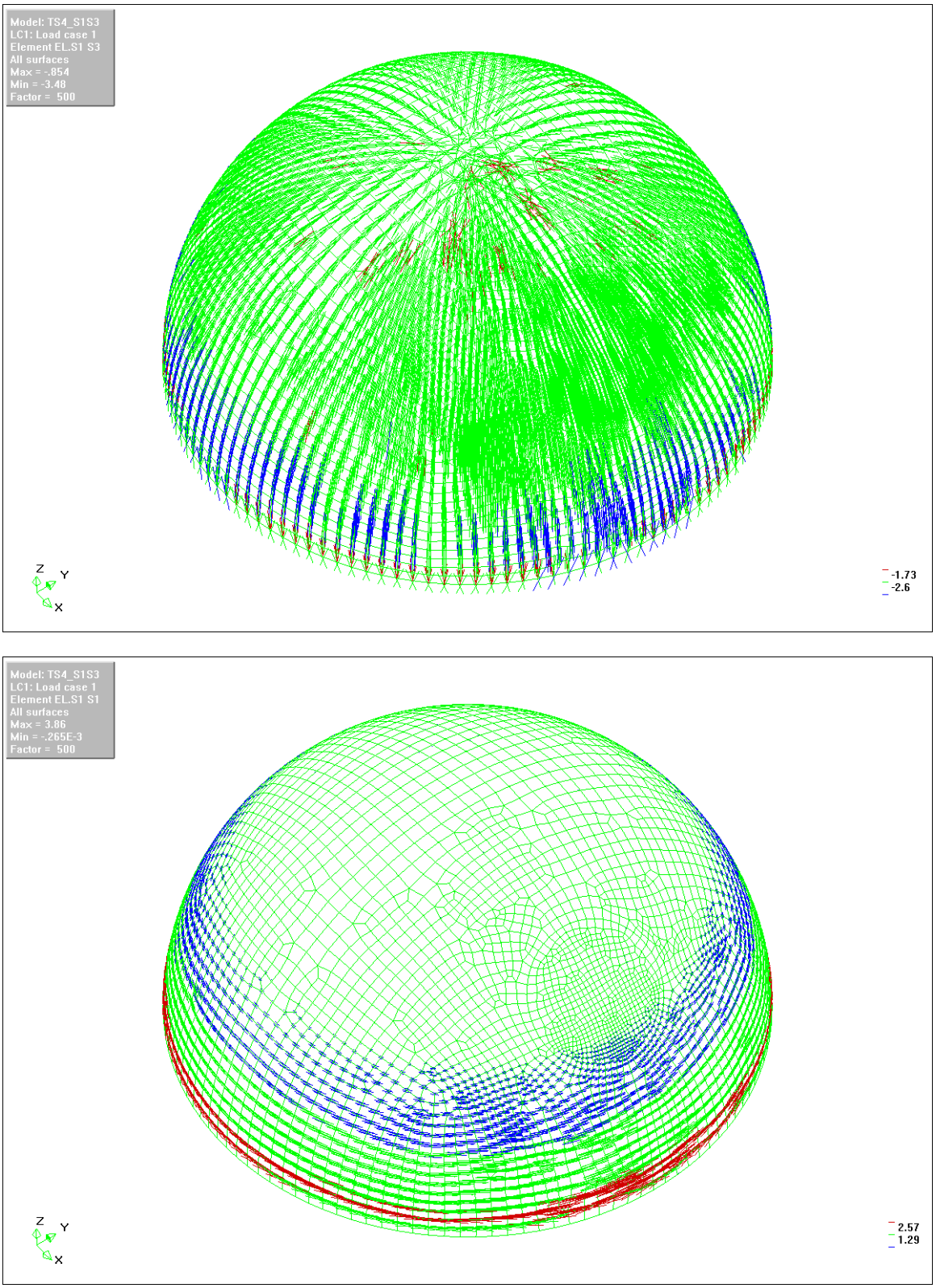

Figure 6.27: Test Shape 4, load case 1: Principle stress vectors for compression (top) and tension (bottom) in N/mm.

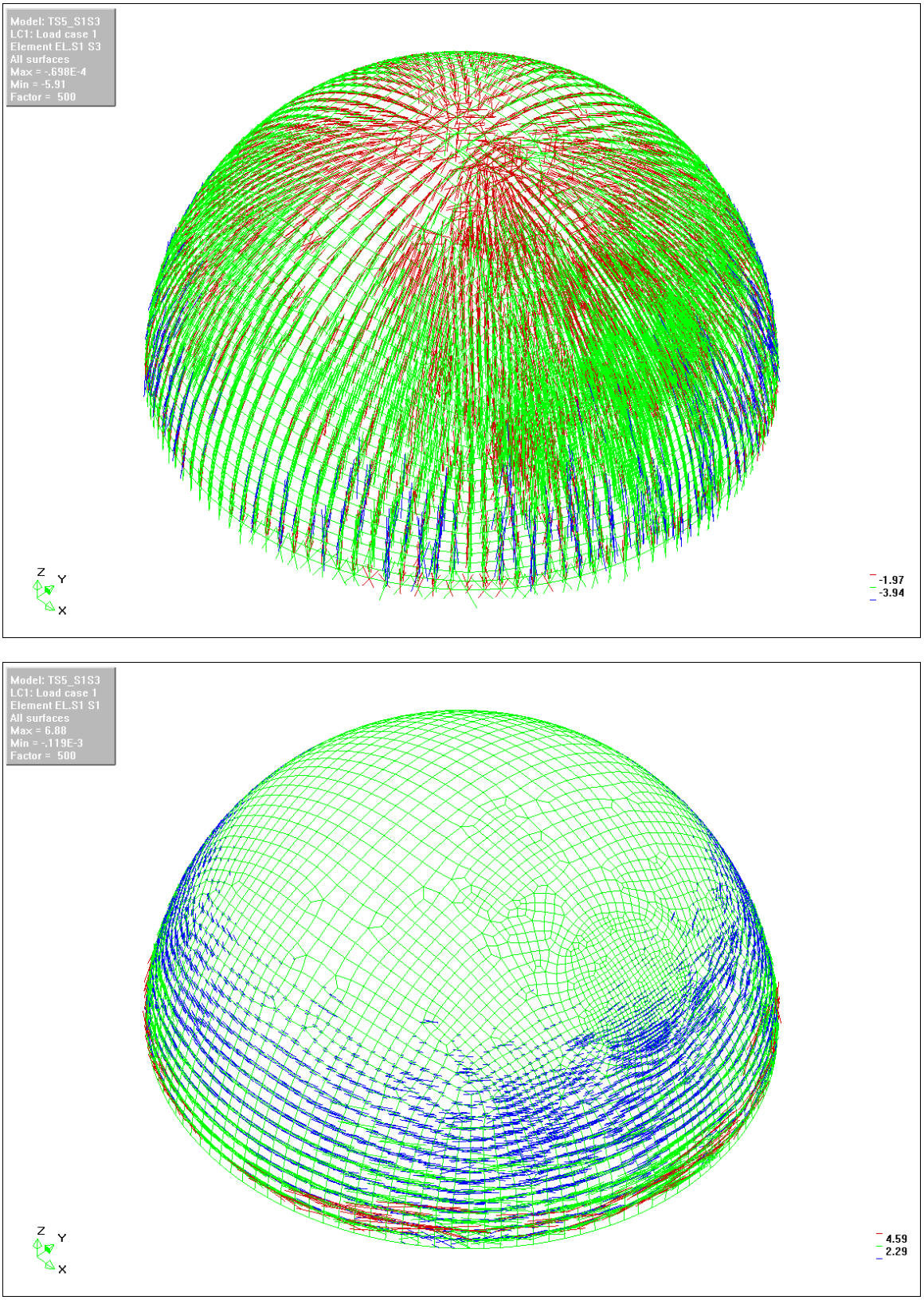

Figure 6.28: Test Shape 5, load case 1: Principle stress vectors for compression (top) and tension (bottom) in N/mm.

INTERNAL FORCES (N_{YY} AND N_{XX})

Internal (arch) force for Test Shape 4 (variable thickness) in the surface X-direction (N_{xx}) has a maximum of 93kN in compression, as seen in Figure 6.29, top. Internal (arch) forces for Test Shape 5 (orthotropic) in the surface Y-direction (N_{xx}) range from 16.1kN in tension to 175kN in compression, as seen in Figure 6.29, bottom.

Internal (hoop) forces for Test Shape 4 (variable thickness) in the surface X-direction (N_{yy}) range from 37.6kN in tension to 80kN in compression, as seen in Figure 6.30, top. Internal (hoop) forces for Test Shape 5 (orthotropic) in the surface Y-direction (N_{yy}) range from 60.4kN in tension to 163kN in compression, as seen in Figure 6.30, bottom.

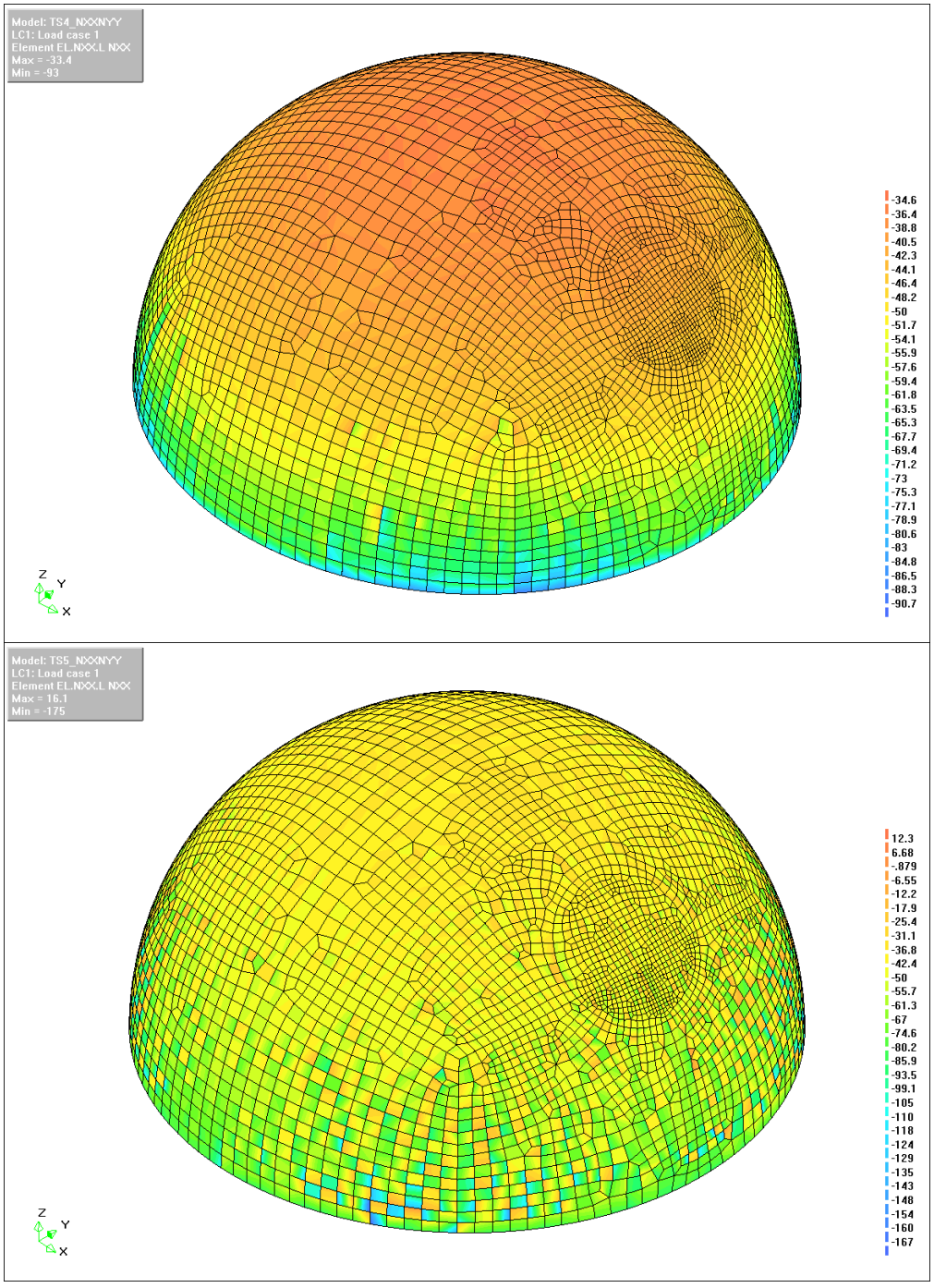

Figure 6.29: Test Shape 4 (top) and 5 (bottom), load case 1: Internal (arch) forces in the surface X-direction (N_{xx}), in kilonewtons per meter, negative values represent compression.

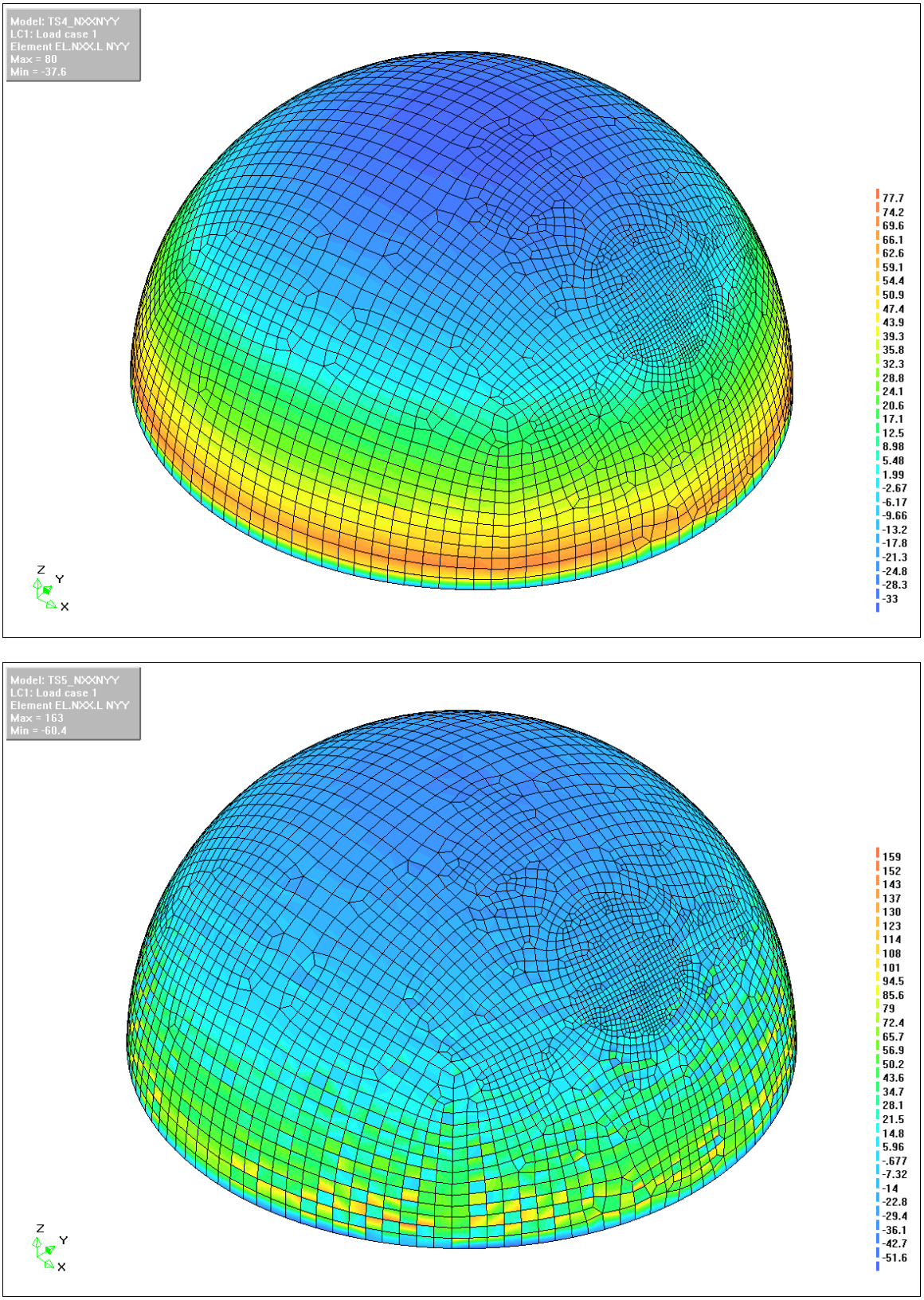

Figure 6.30: Test Shape 4 (top) and 5 (bottom), load case 1: Internal (hoop) forces in the surface Y-direction (N_{yy}), in kilonewtons per meter, negative values represent compression.

INTERNAL MOMENTS (M_{XY})

The maximum (absolute) internal bending moment about the surface XY-plane (M_{xy}) is 33.3N-mm for Shape 4 (variable thickness) and 56N-mm for Test Shape5 (orthotropic). Most of the surface of both test shapes has a bending moment value of 10N-mm or less. The maximum value occurs only near the base of the structure and inconsistently. Therefore its cause is most likely a combination of meshing pattern and the base supports which are restrained in the X and Y-directions. This increase between Test Shape 4 and Test Shape 5 presumably comes from the method in which Drape and Diana apply element properties, as seen in the previous section. This has not been investigated further.

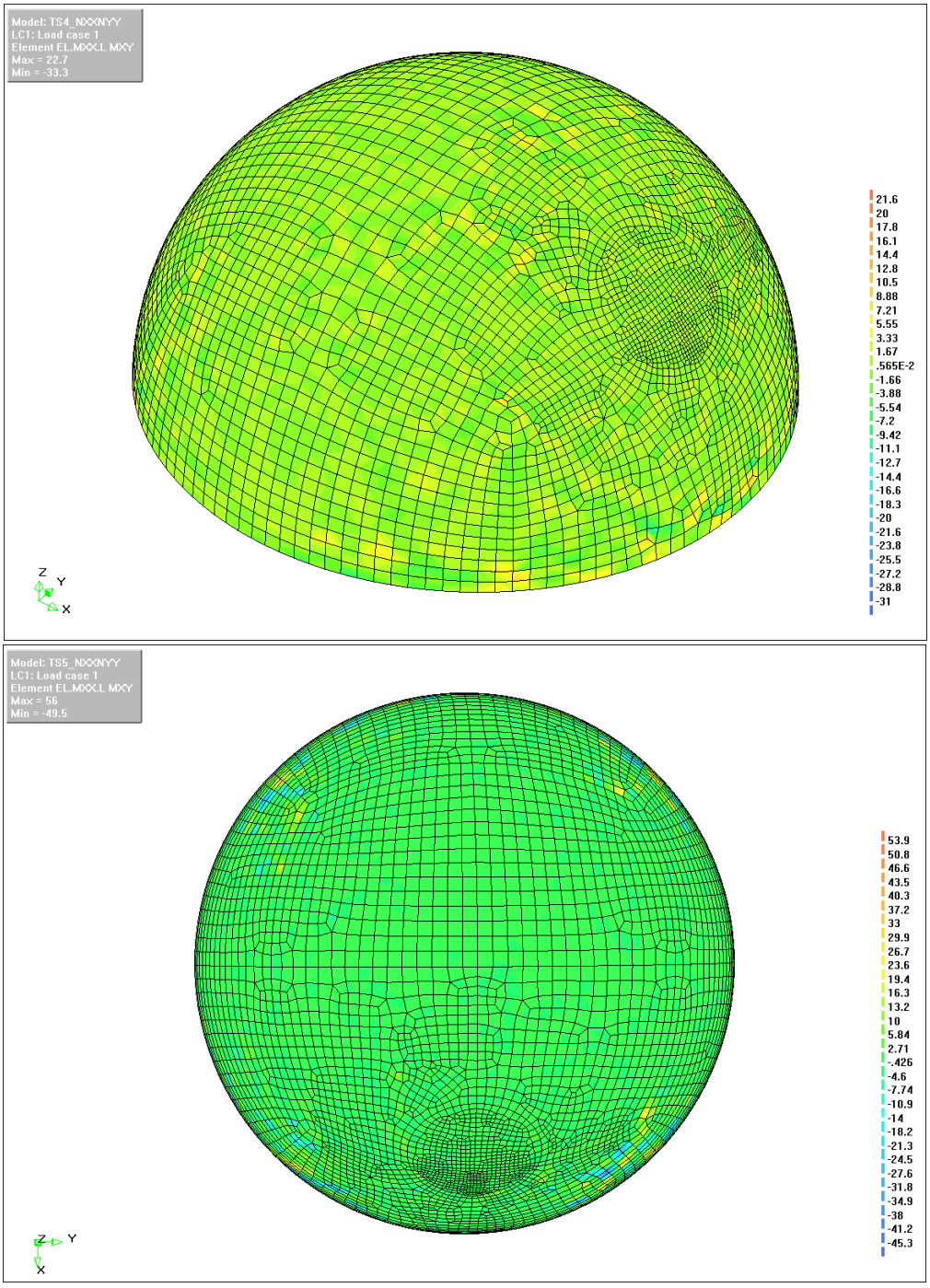

Figure 6.31: Test Shape 4 (top) and 5 (bottom), load case 1: Internal bending moments about the surface XY-plane (M_{xy}), in newton-millimeters.

DEFORMATIONS (D_{RES})

Deformations under Load Case 1 (gravity, 7.2kN/m^2) reached maximums of 2.02mm and 1.14mm for Test Shape 4 (variable thickness) and 5 (orthotropic) respectively. These small deformations are increased by a factor of 1000 to better visualize the deformed shape, as seen in Figure 6.32. Some flattening as with Test Shape 1 is seen. This flattening is irregular around the perimeter of the hemisphere causing it to appear wavy or wrinkly. This is because of the variable thickness and orthotropic stiffness, which varies the material's ability to resist bending. This waviness becomes very clear when viewing the deformations as a heat map in Figure 6.33.

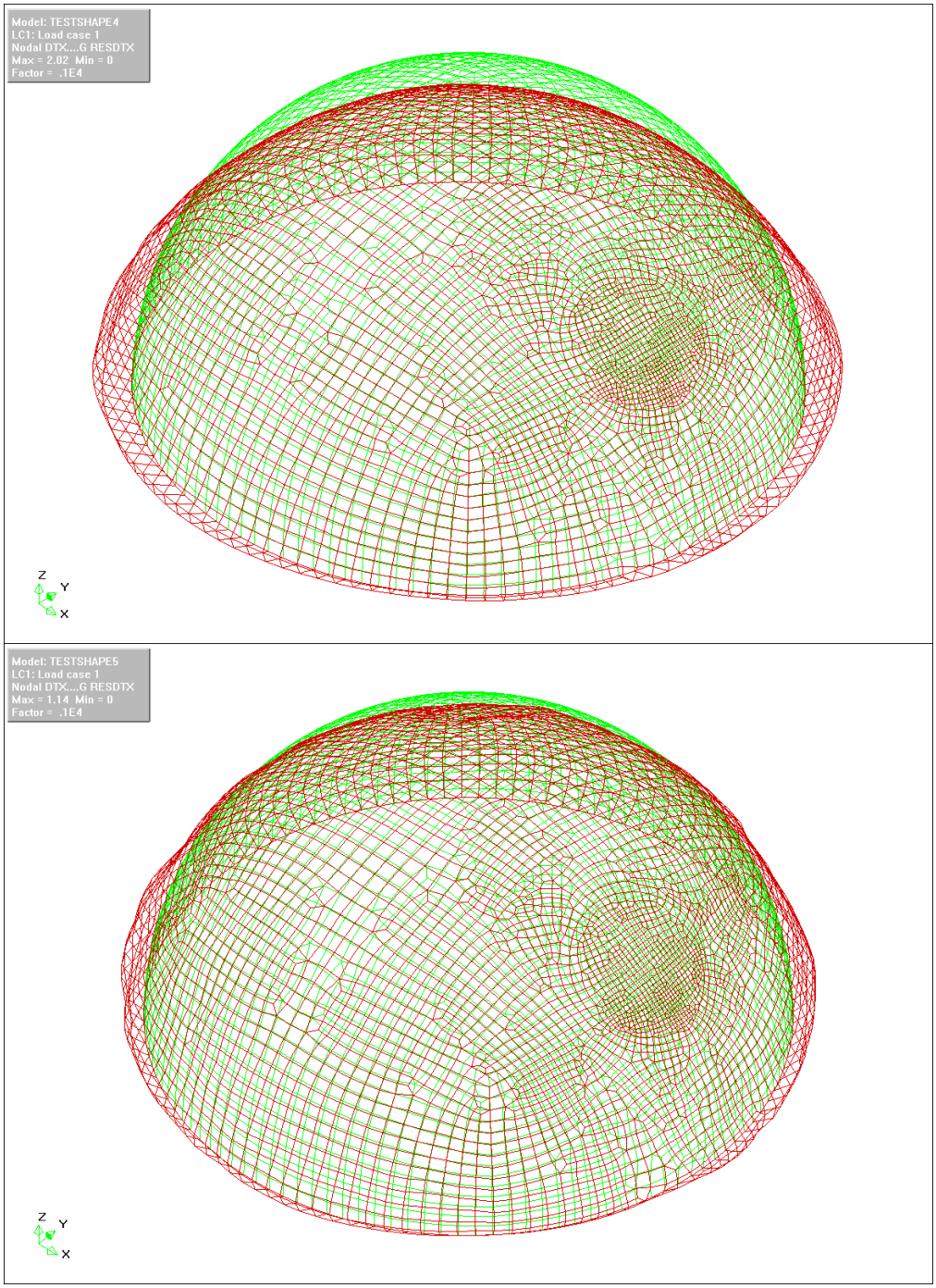

Figure 6.32: Test Shape 4 (top) and 5 (bottom), load case 1: Deformed shape resolved from each direction (D_{Res}), three-quarters top view, exaggerated by a factor of 1000.

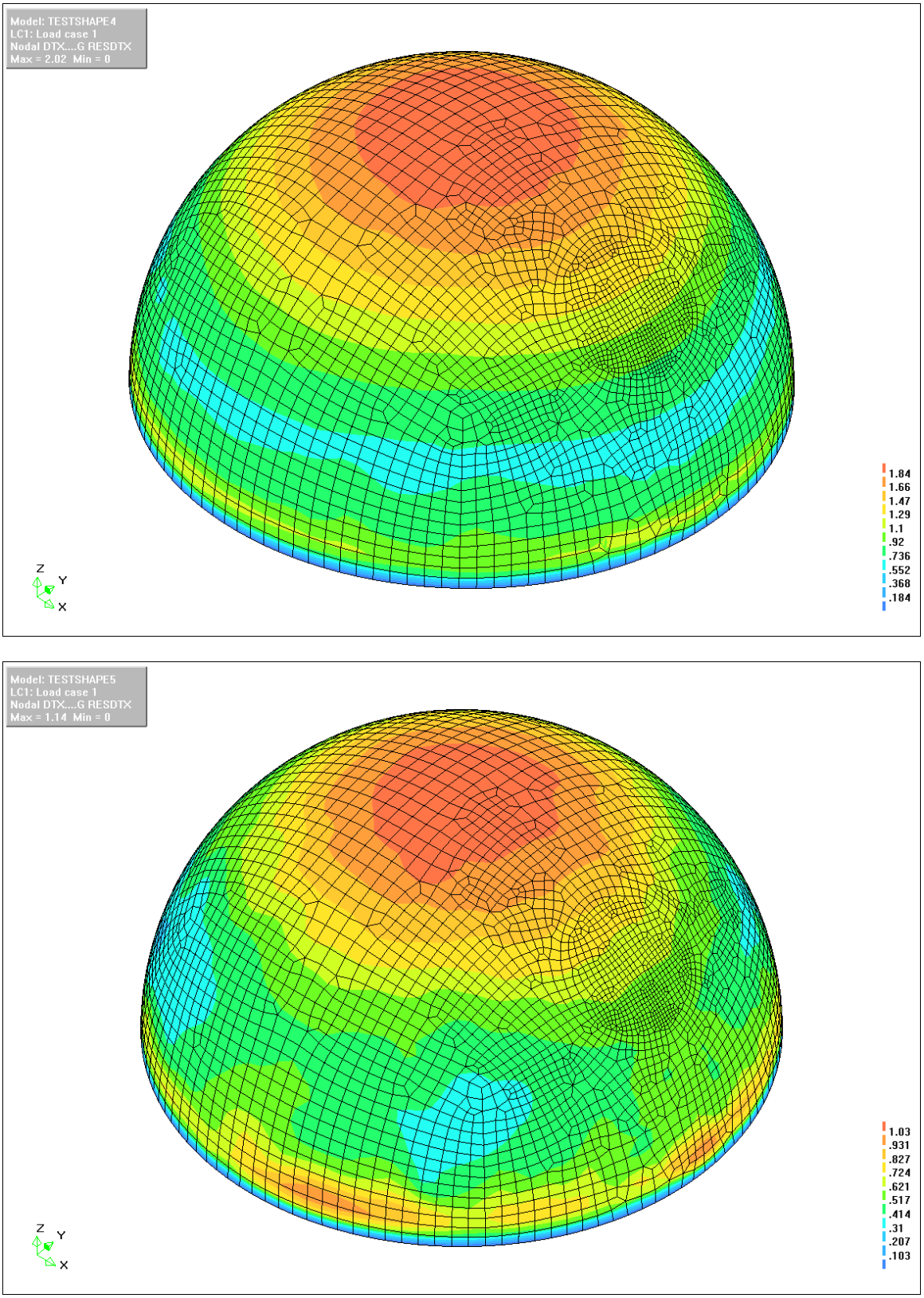

Figure 6.33: Test Shape 4 (top) and 5 (bottom), load case 1: Deformation contour heat-map resolved from each direction (D_{Res}), three-quarters top view.

COMPARISON TO ISOTROPIC TEST SHAPE 1

In order to clarify the specific behavior of constructions made with the new material Test Shape 5 should be compared against the isotropic Test Shape 1. As a general indicator of behavior the top view of both deformed test shapes is consulted, as seen below in Figure 6.34. Test Shape 1 deforms very symmetrically forming a clear circle, while Test Shape 5 deforms to a rippled, uneasy looking circle. A pattern of deformation related to the stiffness variations in Test Shape 5 would be expected, where less stiff areas would deform more. A slight effect of thickness variation on deformation is present in Test Shape 4, as seen below in Figure 6.35. This figure shows very slight indentations on the perimeter of the red deformed shape. These indentations correspond to the areas of largest shear (and therefore thickness) as seen by the red coloration in the following Figure 6.36.

The reason that no clear pattern exists in the deformed shape of Test Shape 5 may have two reasons. First, that the effect of increased thickness is hidden by the effect of increased stiffness occurring in other areas. Secondly, problems might exist with the procedure of applying the thickness and stiffness properties to the mesh in Drape and Diana, but this remains unclear.

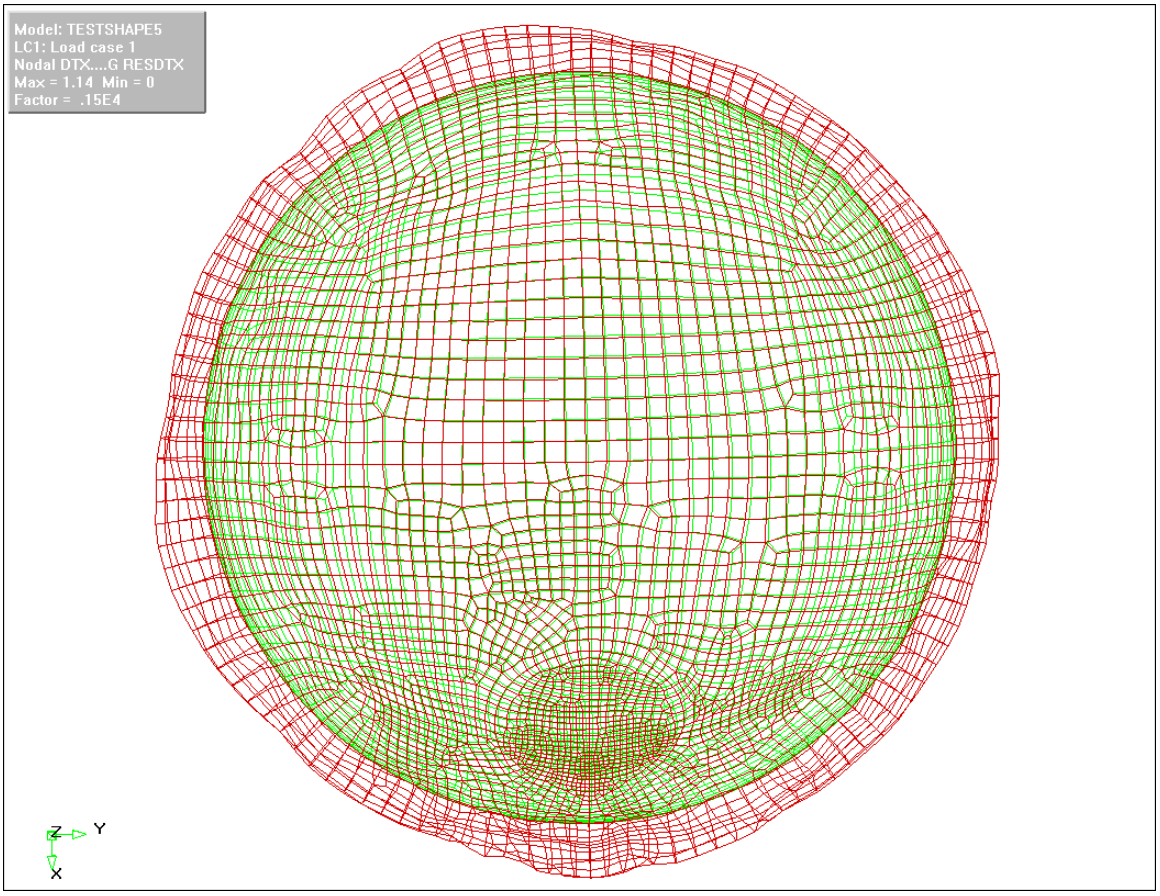

Figure 6.34: Test Shape 5, load case 1: Deformed shape resolved from each direction (D_{Res}), top view, exaggerated by a factor of 1500.

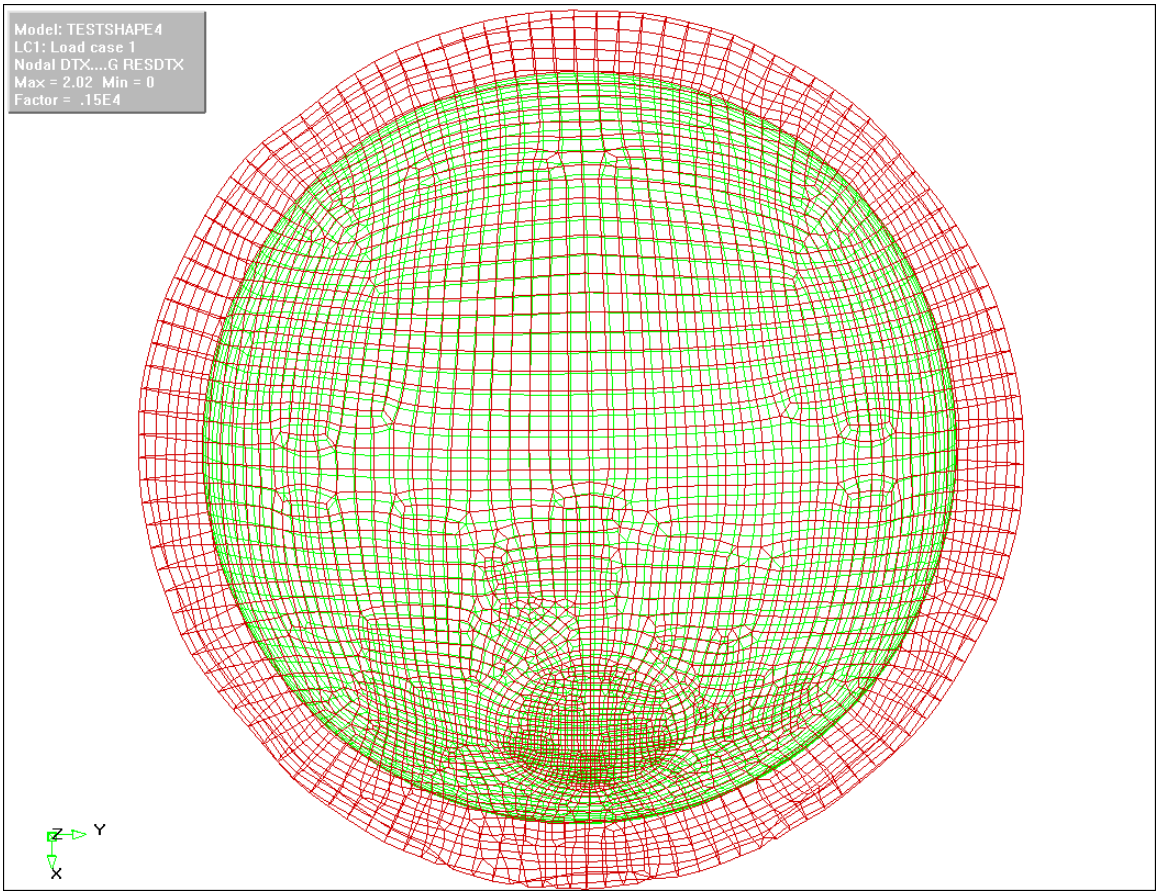

Figure 6.35: Test Shape 4, load case 1: Deformed shape resolved from each direction (D_{Res}), top view, exaggerated by a factor of 1500.

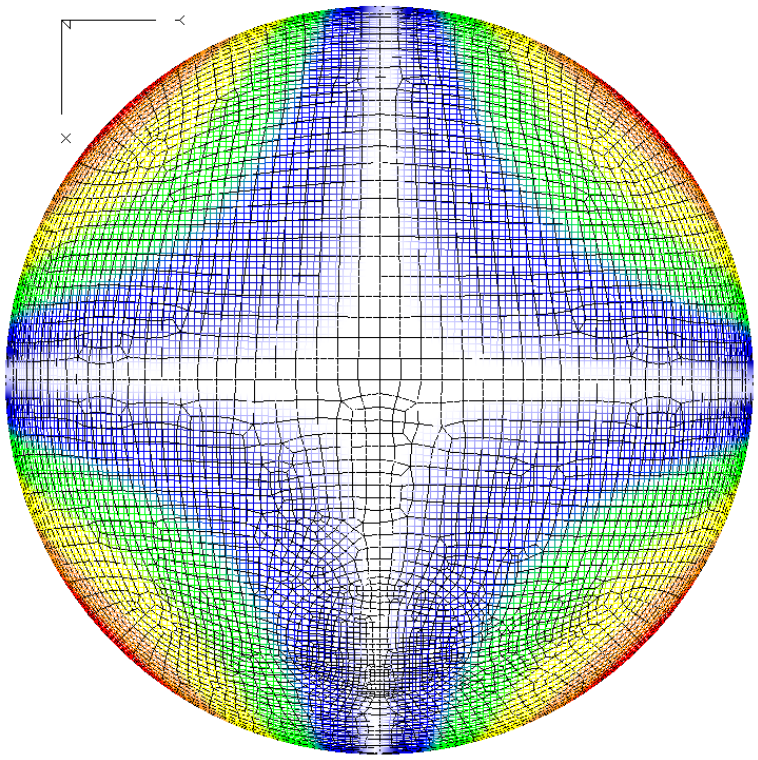

Figure 6.36: Sheared material from Drape over the test shape mesh pattern from Midas FX+, white represents areas of no shear deformation while red represents areas of greater shear deformation.

Further comparison of the two test shapes can be seen through an examination of the principle stresses. Test Shape 1 showed predictable stress distributions, large compressive arch stresses at the top and large tensile hoop stresses at the base. Test Shape 5 however shows a more smeared and splotchy stress distribution across the Test Shape for both sets of principle stresses. These results can be seen below in Figure 6.37. The "checkerboard" appearance of Test Shape 5 may be due to an error between information transfer between Drape and Diana, when applying the material properties. However the results can be read qualitatively to get insight into the behavior of the test shape with variable thickness and orthotropic properties.

Although Test Shape 5 should have greater stiffness and thickness, it has larger principle stresses accompanied with smaller deformations. Qualitatively, the stress distribution of Test Shape 5 has a pattern similar to the distribution of thickness. Below in Figure 6.37, the top right image shows a red area of larger compressive stresses to the lower left of the meshed hole and correspondingly the bottom right image shows a light blue area of lower tensile stresses in the same location. These correspond geometrically to the areas of increased thickness as seen in Figure 6.36. So, the variable thickness and orthotropic stiffness seems to have the effect of altering the load path to utilize the thicker and stiffer portions of the structure, while also leave some areas relatively weaker.

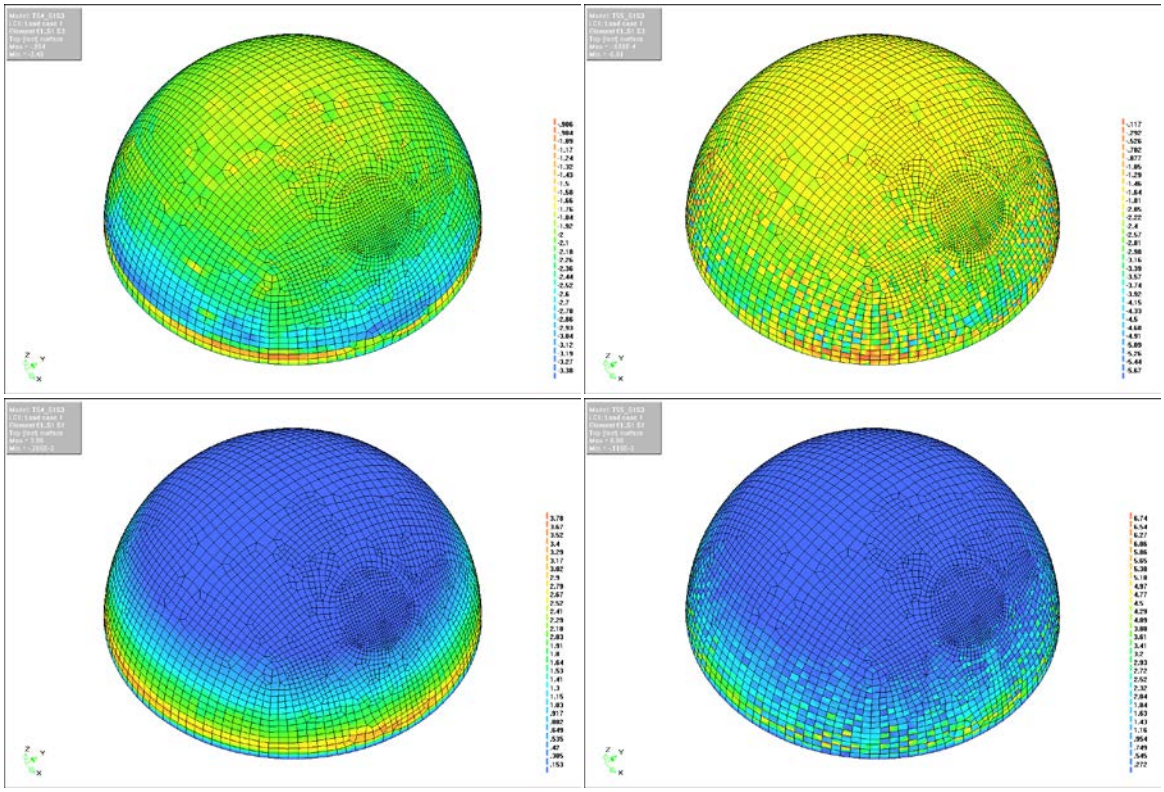

Figure 6.37: Test Shape 1 (left two), Test Shape 5 (right two), load case 1: Principle stress contoured, compression top two, tension bottom two, red represents greater magnitude stress, blue represents lesser magnitude stress.

6-5-4 NUMERICAL ANALYSIS CONCLUSION AND DISCUSSION

The test shape variations were analyzed for two reasons, first to dimension the material and secondly to get a sense of the new material's behavior. The maximum stresses and bending moments will be used to dimension the material. Those results are presented below in Table 6.5. The behavior of the material is investigated by comparing Test Shape 4 (variable thickness) and Test Shape 5 (variable thickness, orthotropic stiffness) to Test Shape 1 (uniform thickness, isotropic).

Table 6.5: Summary of test shape numerical analysis results, Test Shape 2 is grayed because it would not exist in reality, all discontinuities would require stiffening elements as considered with Test Shape 3, the results in the shaded cells are doubted, maximums are bolded and minimums underlined.

Test Shapes		S1	S3	Nxx		Nyy		Mxy	DRes
		Tens Mpa	Comp Mpa	Comp kN/m	Tens kN/m	Comp kN/m	Tens kN/m	Bend Nmm	Def mm
1	**Isotropic**	**3.94**	**3.73**	86.1	0	36.9	71.1	22.4	2.27
2	*Iso-Hole*	-	-	*181*	*37.7*	*85.8*	*104*	*449*	*34.4*
3	**Iso-Hole-Beam**	-	-	92.3	**45.4**	**79.1**	**82.4**	**189**	**8.45**
4	**Variable-Thickness**	3.86	3.46	**93**	0	37.6	80	33.3	2.02
5	**Orthotropic**	6.88	5.91	175	16.1	60.4	163	56	1.14

The non-continuous test shapes (2 and 3) were conducted so that the material could be design to a capacity which would allow for integrating windows and other features with ease. As expected, Test Shape 3, with the stiffening beam, significantly outperformed Test Shape 2. For this reason stiffening beams will be required for use around discontinuities with this material and therefore the results from Test Shape 2 will not be used.

Overall, the bending moments were quite small, the maximums being found at points of low mesh quality near the base of the hemisphere (Figure 6.18). Such areas of low mesh quality could be interpreted as irregularities in the curvature or detailing of the construction. Such areas would be expected to contain higher than normal forces and bending moments. In the future, the internal bending moments should be analyzed in Diana with non-linear analysis because as deformations grow so do bending moments and so on until equilibrium is reached. The issue of shell buckling should be investigated with research and non-linear FEM analysis. Slight geometrical imperfections or construction errors can cause buckling and greatly reduce the compressive capacity of thin shell structures, such as the ones that would be possible with this material.

Test Shape 4, with variable stiffness and isotropic stiffness, shows promising results, having similar stress values as Test Shape 1, with a lower amount of deformation. Test Shape 5, with variable thickness and orthotropic stiffness, shows unexpectedly high stresses, while having a very low amount of deformation. The reason for the increase of stress values between the two test shapes most likely comes from the addition of textile stiffness properties from Drape, although the specific reason is unclear. The results of the orthotropic analysis are doubted and will be used analyzed qualitatively, while the results of the isotropic analysis will be used quantitatively. Meaning the design stresses will come from the simpler model, but the deformation and moment distribution information will come from the orthotropic model.

Test Shape 1, 4, and 5 all approximate the reality of the situation differently, while each of them being slightly inaccurate. Test Shape 1 is the simplest and verified with analytical calculations. Test Shape 5 attempts to mimic all aspects of the material by accounting for varying thickness and stiffness. However, unknowns about the material and issues with the model prevented it from being trusted as the most realistic. Test Shape 4 partially, but reliably accounts for the material's thickness variations, while using the isotropic stiffness of the concrete. In this manner it comes closest to modeling reality.

6-6 APPLICATION OF RESULTS

For the 20 meter span of the hemispherical test shape the 20mm thickness sufficiently resisted the exaggerated loading conditions. The maximum tensile stress (3.94MPa) will be used to determine the amount of required reinforcing. The maximum compressive stress (3.73MPa) is significantly lower than maximum for normal concrete (10-40MPa). This combined with the low bending moments in the test shape mean that the cross section of the material may be able to be reduced, even by as much as half, for this small shape. For the purposes of the project the thickness will remain at 20mm, a reasonable maximum thickness for fabrication and construction. This thickness will also allow greater spans.

Table 6.6: Selected results of the test shape analysis in Diana.

Test Shapes	**S1**	**S3**	**Nxx**		**Nyy**		**Mxy**
	Tens	Comp	Comp	Tens	Comp	Tens	Bend
	Mpa	Mpa	kN/m	kN/m	kN/m	kN/m	Nm
Selected Design Values	3.94	3.73	93	45.4	79.1	82.4	0.189

6-6-1 REINFORCEMENT QUANTITY

To determine the required minimum amount of alkali resistant (AR) glass reinforcement, the stress information from the Diana FEM analysis is combined with Hegger's equation for the ultimate strength of textile reinforced concrete (TRC) in tension from Section 4-3-1. The equation is presented again below in Equation 6.4. During calculation the factor $k_{0,a}$ will be replaced with the modified version from Section 4-3-2.

$$F_{ctu} = A_t \cdot f_t \cdot k_1 \cdot k_{0,\alpha} \cdot k_2$$

with

A_t cross-sectional area of the textile reinforcement

f_t tensile strength of the filament

k_1 coefficient of efficiency

$k_{0,\alpha}$ coefficient of oblique-angled load: $k_{0,\alpha} = 1 - \frac{\alpha}{90°}$

k_2 coefficient of biaxial load: Fabric 1:

$k_2 = 1 - 22 \cdot \sigma_{c,\text{lateral}}/\sigma_{\max} \leq 1,0.$

Equation 6.4: Hegger's equation for the tensile strength of textile reinforced concrete sections [Hegger 2008, page 2053]

In order to solve for the cross-sectional area of the textile reinforcement, A_t, Equation 6.4 is rearranged as Equation 6.6. For this the minimum expected value for the other variables and the maximum for the tensile force are used. Since this is a material with a known thickness and unknown width, it is computed as the force in a unit width of the material.

$$A_t = \frac{F_{ctu}}{f_t \times k_1 \times k_{0,a} \times k_2}$$

Equation 6.5: Hegger's equation for the tensile strength of textile reinforced concrete sections (Equation 6.5) solved for cross-sectional area of the textile reinforcement.

VARIABLES

Required ultimate strength per running meter, $F_{ctu} = 3.84 \frac{N}{mm^2} \times 20mm \times 1000mm = 78.8\,kN$

Tensile strength of the filament, $f_t = 533 \frac{N}{mm^2}$

This value comes from a type of AR-glass textile used by Hegger for experiments, as presented earlier in Section 4-2-1. [Hegger 2006, Table 2]

Coefficient of efficiency, $k_{1,normal} = 0.30\,;\ k_{1,impregnated} = 0.60$

Efficiency was discussed in Section 4-3-1. Efficiency for AR-glass ranges from 19 to 40% for unimpregnated yarns and up to 66% with epoxy impregnation. It is suggested that impregnated yarn be used as reinforcement. 30% and 60% are used as conservative values for the cases with and without impregnated yarns.

Modified coefficient of oblique-angled load, $k_{0,a,Modified} = 0.000123 \times \left((-20)^2 + 20^2\right) \times \frac{1}{sin(40)} = 0.15$

This value assumes the worst case loading situation, meaning that the largest stress occurs at the smallest allowable deformation angle of 40° (although in reality 39.1°). See Section 5-1-3 for more details about the required shear angle. This value of 0.15 can be seen as the lowest point on the plot of $k_{o,a,modified}$ from Section 4-3-2.

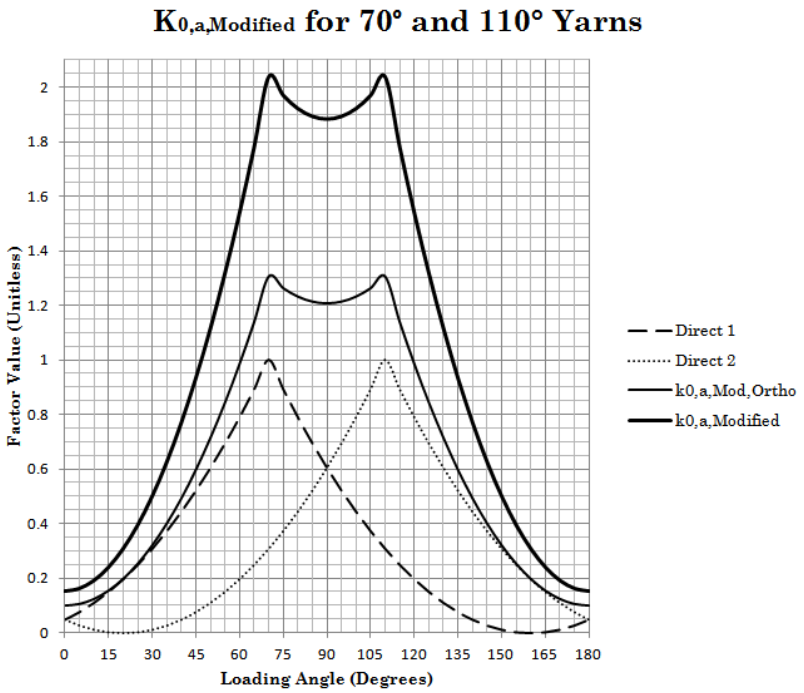

Figure 6.38: Modified coefficient of oblique-angled load for the largest sheared (40°) showing the lowest value at loading angle = 0°.

Coefficient of biaxial load, $k_2 = 1$

This value is assumed to be 1 because the textile weave properties are not decided and the other values are conservative.

SOLUTION

$$A_{t,norm} = \frac{F_{ctu}}{f_t \times k_{1,normal} \times k_{0,a} \times k_2} = \frac{78.8kN}{0.533\frac{kN}{mm^2} \times 0.30 \times 0.15 \times 1} = 3286\frac{mm^2}{running\ meter}$$

$$A_{t,imp} = \frac{F_{ctu}}{f_t \times k_{1,impregnated} \times k_{0,a} \times k_2} = \frac{78.8kN}{0.533\frac{kN}{mm^2} \times 0.60 \times 0.15 \times 1} = 1643\frac{mm^2}{running\ meter}$$

Equation 6.6: Computation of required area of reinforcement per running meter as a solution of Equation 6.5.

The required area of reinforcement is quite large either 1643 to 3286mm^2, depending on impregnation, for a meter length of the material. This equates to a reinforcement ratio of 8.23% or 16.43%, respectively, for the 20mm thickness. This would mean that probably two or three layers of textile would be required. The balance between reinforcement and the concrete cross section is visualized below, in Figure 6.39.

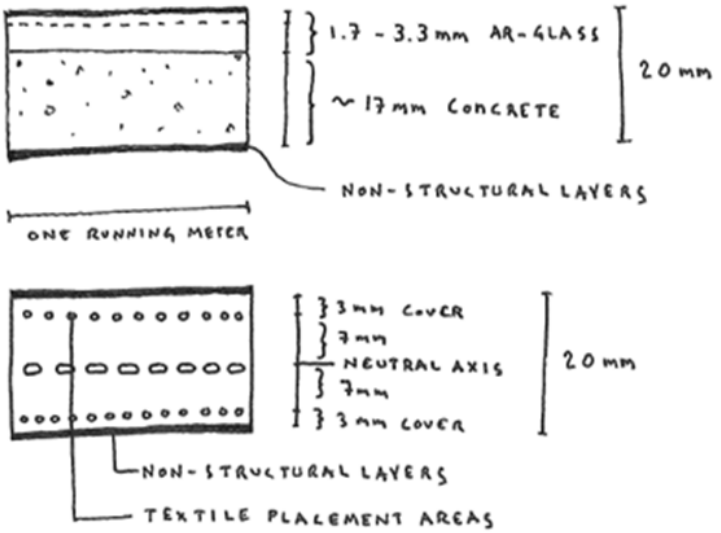

Figure 6.39: Two ways to view the reinforcement quantity: Concrete section with solid volume (top) and section with reinforcement placement (bottom).

6-6-2 MOMENT CAPACITY

To determine the maximum moment capacity of the section as reinforced by the amounts from Section 6-6-1, Hegger's equation for moment capacity from Section 4-3-1 is modified then solved for the specific placement of the reinforcement. Hegger's equation is presented again below in Equation 6.8.

$$M_u = k_{fl} \cdot F_{ctu} \cdot z$$

with

k_{fl} coefficient of the bending load depending on the fibre material:

AR-glass (chain binding): $k_{fl} = 1.0$

AR-glass (tricot binding): $k_{fl} = 1.0 + 0.15 \cdot \rho_l$

ρ_l degree of longitudinal reinforcement in %

Carbon: $k_{fl} = 1.0 + 0.4 \cdot \rho_l$

F_{ctu} according to Eq. (1)

z internal lever arm

Equation 6.7: Hegger's equation for the moment bearing capacity of textile reinforced concrete sections [Hegger 2008, page 2054]

This equation is modified to reflect the split layers of the reinforcement, giving it an equal moment resistance in both directions, but each with half the capacity. The textile binding type is unknown, so the lowest case, tricot binding, is assumed. The internal leaver arm is assumed from Figure 6.39. With these values the moment capacity of the section can be calculated, this result is seen below in Equation 6.9.

$$M_u = k_{fl} \times \frac{F_{ctu}}{2} \times z = 1 \times \frac{78.8kN}{2} \times 14mm = 552Nm$$

Equation 6.8: Solution of for the moment capacity of the concrete section. Modified from Hegger's equation for the moment bearing capacity of textile reinforced concrete sections Equation 6.8.

For one layer of textile reinforcing this value would stay the same, because the lever arm would be halved while the tensile capacity doubled. This moment capacity of 505Nm dwarfs the largest calculated moments from the FEM analysis (±0.189Nm). However, this larger capacity allows for architectural versatility, meaning flatter shapes with larger spans, beyond domes and highly curved symmetrical forms.

6-6-3 COMPARISON TO CONCRETE CANVAS

The precedent project, Concrete Canvas, is a load rated material (Section 3-1). It has been given a kilonewton rating per running meter for each thickness and in both warp and weft directions. Those results can be seen below in Figure 6.40.

CC	Thickness (mm)	Batch Roll Size (sqm)	Bulk Roll Size (sqm)	Roll Width (m)
CC5	5	10	200	1.0
CC8	8	5	125	1.1
CC13	13	N/A	80	1.1

	Tensile strength (kN/m)	
	Length direction	Width direction
CC5	6.7	3.8
CC8	8.6	6.6
CC13	19.5	12.8

Figure 6.40: The dimensions and properties of Concrete Canvas products. [Concrete Canvas]

The Concrete Canvas strength can be compared to the stresses in the test shape to determine whether it could be made from Concrete Canvas. In order to do this the calculated stresses are converted to a strength per length value by multiplying the stress by the thickness.

$$Tensile\ Strength\ per\ Length = Tensile\ Stress\ \times\ Thickness = \ 3.94\frac{N}{mm^2}\ \times\ 20mm = 78.8\frac{kN}{m}$$

Equation 6.9: Strength per length of the material for comparison to Concrete Canvas.

This resulting required strength per length value, 78.8 kN/m, is nearly four times larger than the capacity of the strongest Concrete Canvas product. This product, CC13, is 13mm thick, meaning an equivalent tensile strength would be reached with 4 layers of concrete canvas, totalling 52mm. This shows that the material will need to contain much more reinforcing material than the Concrete Canvas. Meaning it will be more expensive but higher performing and therefore more versatile.

6-6-4 DESIGN CAPACITY

A low and high strength capacity for the material will be determined for further used in designing the case study building later in Chapter 11. The assumed cross section contains 3.286mm of glass fiber and 17mm of concrete as seen in Figure 6.39. For tensile loading epoxy impregnated reinforcement is assumed with an efficiency of k_1 = 0.6 (Section 6-6-1). The compressive stress values assume high-strength concrete, as used by Hegger (Section 4-4-4), for both the low and high design values. In order to determine these values the maximum (40°) and minimum (90°) shear cases are examined across all angles of loading. These cases represent the extreme cases, so the values of all other cases will fall between them. The Modified Oblique-Loading Coefficient ($K_{0,a,Modified}$), from Section 4-3-2, for the maximum and minimum shear cases is presented below, in Figure 6.41.

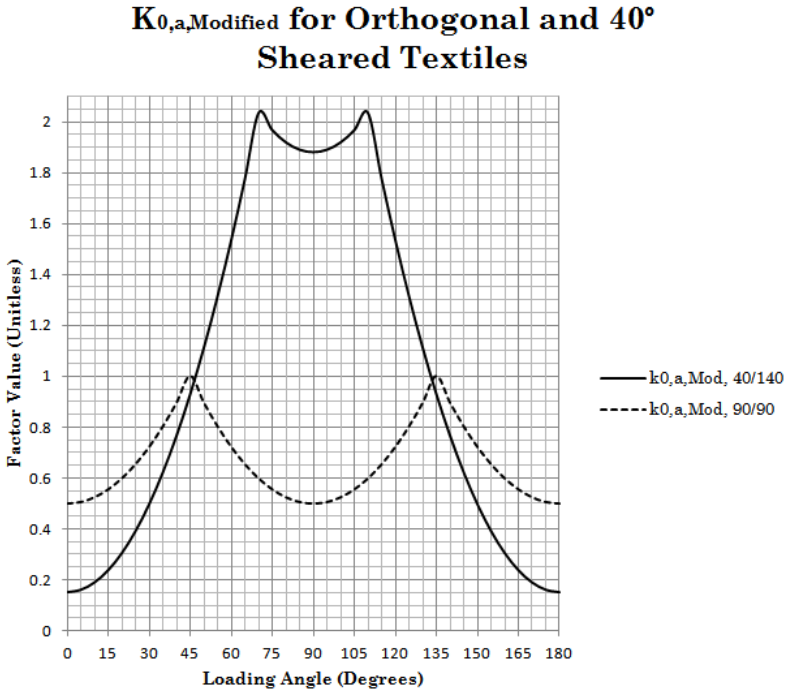

Figure 6.41: Modified Oblique-Loading Coefficient ($K_{0,a,Modified}$) for Orthogonal and 40-degree shear deformation cases.

That coefficient is used to calculate the tensile stress capacity of the material. First, Hegger's equation for the tensile strength of textile reinforced concrete sections (Equation 4.1) is simplified using the values specific for an epoxy impregnated textile, which will be used in the material, as seen in Equation 6.11. Secondly, this tensile strength value is divided by the cross sectional area of one running meter of the material, as seen in Equation 6.12. The thickness of the material is dependent upon the shear deformation angle (Section 4-2-2). The latter equation is plotted against loading angle similar to the plot for the Modified Oblique-Loading Coefficient ($K_{0,a,Modified}$) and shown in Figure 6.42.

$$\begin{aligned} F_{ctu} &= A_t \times f_t \times k_1 \times k_{0,\alpha,Modified} \times k_2 \\ &= 3286mm^2 \times 0.533\frac{kN}{mm^2} \times 0.6 \times k_{0,\alpha,Modified} \times 1.0 \\ &= 1051kN \times k_{0,\alpha,Modified} \end{aligned}$$

Equation 6.10: Material tensile force capacity in terms of the Modified Oblique-Loading Coefficient.

$$Tensile\ Stress\ Capacity\ (MPa) = \frac{F_{ctu}}{Cross\ Section\ Area} = \frac{1051kN \times k_{0,\alpha,Modified}}{1000mm \times 20mm \times (1/\sin\alpha)}$$

Equation 6.11: Material tensile stress capacity in terms of the Modified Oblique-Loading Coefficient and shear deformation angle.

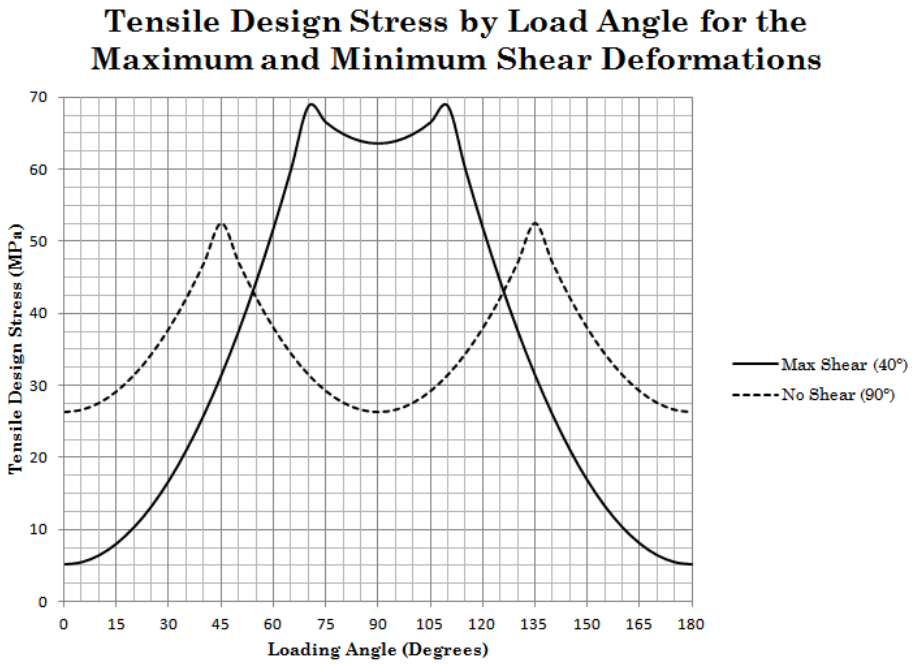

Figure 6.42: Material tensile stress capacity for Orthogonal and 40-degree shear deformation cases.

Similarly the value for moment resistance capacity is simplified and the thickness is the material is dependent upon the shear deformation angle (Section 4-2-2). It is presented below in Equation 6.13 and plotted in Figure 6.43.

$$M_u = k_{fl} \times \frac{F_{ctu}}{2} \times z = 1 \times \frac{F_{ctu}}{2} \times 14mm = F_{ctu} \times \frac{7mm}{\sin\alpha} = 1051kN \times k_{0,\alpha,Modified} \times \frac{7mm}{\sin\alpha}$$

Equation 6.12: Material tensile stress capacity in terms of the Modified Oblique-Loading Coefficient and shear deformation angle.

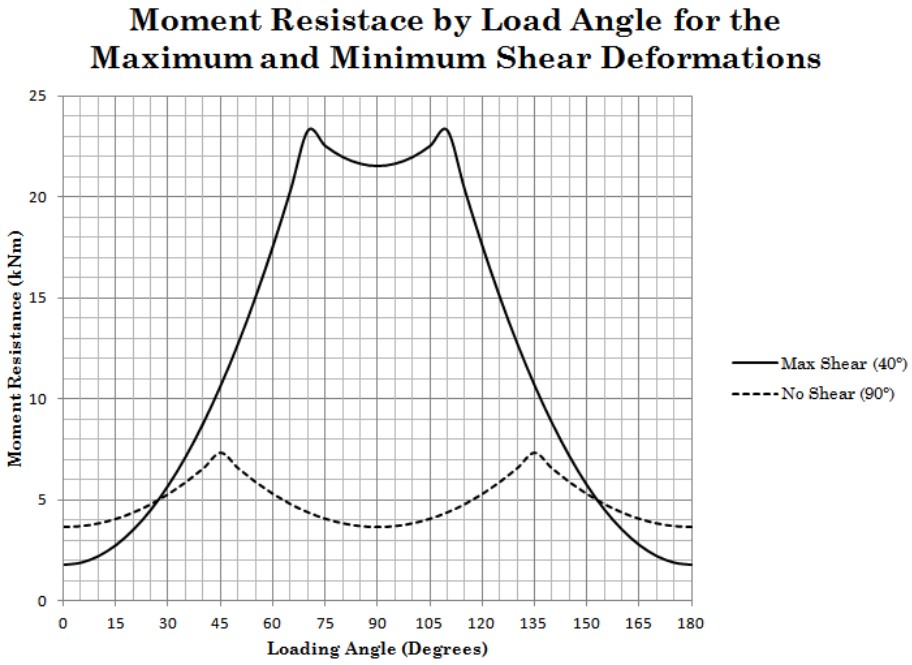

Figure 6.43: Material moment resistance for Orthogonal and 40-degree shear deformation cases.

From these plots the maximum and minimum design values are determined. They are summarized below in Table 6.7. The values for design capacity do not include any safety factors. These must be added later during the design of the structure.

Table 6.7: Material design capacity at the weakest geometry (40° shear deformation).

Design Capacity	**Stress (x,y)**		**Mxy**
	Tension (Mpa)	Compression (Mpa)	Bend Nm
Minimum	5.19	78.3	1759
Maximum	68.77	78.3	23302

6-7 CONCLUSION AND DISCUSSION

A simple geometric, hemispherical test shape was selected for the purpose of dimensioning the new material and investigating the material behavior. The isotropic test shape was modeled numerically in TNO Diana and validated with analytical calculations. Further testing investigated structural discontinuities and concluded that stiffening beams would be required for windows. The continuous test shape was then investigated with the material properties applied from the computer program Drape, first with variable thickness and later with orthotropic stiffness of the reinforcement. The results of the variable thickness model appear reasonable and are the closest representation of reality with confidence. The results of the numerical analysis were used to dimension the material. From the dimensioned material, low and high values for the material's capacity were determined.

7 ADDITIONAL TOPICS

There are additional topics in that are important to the safety and successful of implementation of the material. They are not fundamental to the early development of the project and are summarized here below.

7-1 FIRE

Fire could cause catastrophic collapse of a thin shelled structure by inflicting large deformations and altering the properties of the reinforcement. Fire will be a serious concern. It could be mitigated by thin film intumescent coatings after construction or by the addition of polypropylene fibers to the mix to guard against spalling.

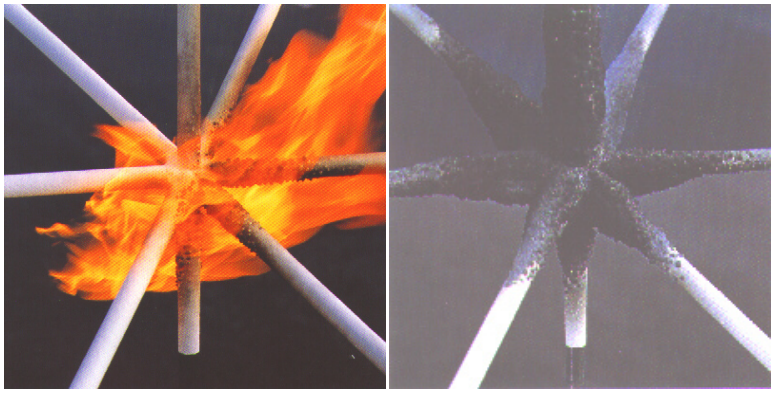

Figure 7.1: Thin-film instumescent spray fireproofing (Sika Unitherm) applied to steel pipes, being exposed to fire (left) and after fire (right). [Sika]

Concrete canvas has been tested with localized fire situation with external fuel sources. In these tests it achieved Euroclass B certification (BS EN 13501-1:2007+A1:2009) of B-s1, d0. [Concrete Canvas, 1305-CC-Data-Sheet]

Figure 7.2: Concrete Canvas Shelter with localized external fire. [Concrete Canvas]

7-2 THERMAL EXPANSION

Thermal expansion can increase stress within the material or change the curvature of the form. Glass has a thermal expansion coefficient of 5.9 * 10^{-6} m/mK. Concrete has a thermal expansion coefficient between 10 and 14.5 * 10^{-6} m/mK. This means that the concrete expansion will be partially restrained by the glass reinforcement. This restraint can be associated with an extra stress that should be considered when dimensioning the reinforcement. Expansion that causes a change in curvature can change the loading condition of the structure and therefore the stress distribution. This means that the structure should be analyzed across all expected temperatures (not just the maxima) and the maximum stresses from each case should be used for design. This could be tested in Diana by imposing thermal strains in the structure. These cases would be uniform for air temperature change or variable for sun/shade and for fire. Expansion joints could be integrated in to the construction between structural bays or the joints between elements.

7-3 CUTTING PATTERNS

Some shapes cannot be created from a single flat piece of the material. This is found out when modeling the geometry in Drape. If the shear angle is below the 40-degree minimum then cutting patterns must be used. This means that the starting geometry of the embryonic sheet will not be flat and will require special jointing. Alternatively, cutting patterns can be created for thermal expansion reasons or to simplify construction.

It is unfeasible to construct large structures from one embryonic sheet, for reasons of constructability or due to large shear deformation. Using Drape, the building-model is able to be broken into structural bays, each with its own embryonic flat sheet.

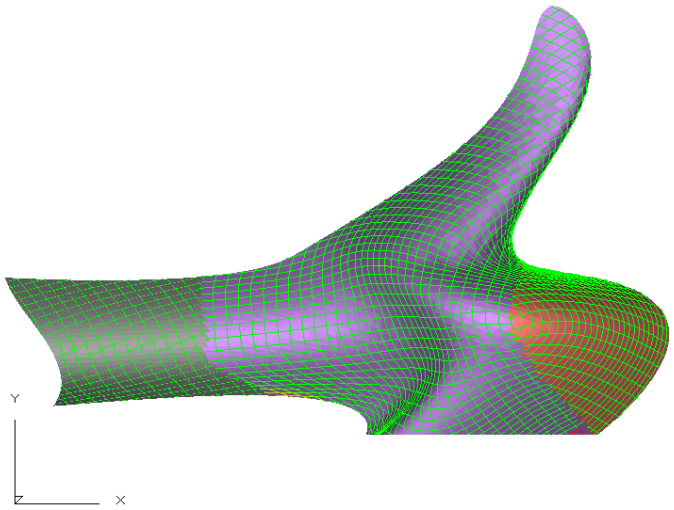

Figure 7.3: Example structure showing three bays for construction (green, purple, and red), measuring approximately 30x20 meters.

7-4 DELAMINATION

Delamination could mean significant damage during transport or construction. This would affect the structural performance of the material by altering the thickness or reinforcement placement. Physical experimentation would be the best way to investigate delamination. There is a balance between preventing delamination and allowing for thickness increase due to favorable shear deformation. Stitching or glue might be used for various layers of the material. The choice of 2D or 3D textile reinforcing would also be in question.

7-5 PRICE POINT

This material may end up being expensive because it has a large reinforcement percentage (8-16% from Section 6-6) and it require a detailed fabrication process to join the of multiple component materials. The material might enable cost savings during construction by speedy erection and reduction of building mass (through structural efficiency) leading to smaller foundations and other structural members. Concrete Canvas can be used as a price point comparison because of its similar constituent components, fabrication process, and dimensions. Concrete Canvas is also distributed in North America as Concrete Cloth. There the thickest version (13mm) can be purchased for $105 per square meter. At this price the material for the hemispherical test shape would cost about $70,000.

Figure 7.4: Examples of Concrete Cloth products with prices available from Nuna Innovations. [Nuna]

7-6 DECONSTRUCTABILITY AND REPAIR

The difficulty of deconstructing highly curved shell structures is that they have highly custom double curvature, large amounts of reinforcement, and are unstable during dismantling. These are serious concerns limiting the reuse of their structural elements beyond using them as bulk infill material for example for coastal protection.

Deconstructability generally means a reversal of the construction process. Such a reversal is not possible with one-way-curing materials such as concrete, which is proposed as the matrix material for this project. It may be possible to find a material which begins flexible, hardens, and then once again can be softened for deconstruction. This would make deconstruction and reuse of the material very practical but would probably increase its cost. Water is an example of such a material, by changing the temperature it can change from liquid to solid and then back to liquid. It is clear that water would not be appropriate for buildings because of the temperature at which this phase change occurs.

An alternative to deconstruction would be repair. Repairing existing structures requires accurate information about their structural state and expected loading conditions. Generally this information is found by non-destructive investigations such as penetrating radar/sonar and flexural load testing. By integrating sensors or other indicators about the material more accurate information could be collected in real time about the structure. More accurate information means more accurate repairs at the right time, enabling less repair material to be used. Repair of this material could come in the form of tensile ties or structural toppings. These might require connection points for ties or shear studs to be integrated into the fabrication of the elements.

7-7 SUSTAINABILITY

The sustainable design of buildings is important because of their massive scale and material requirements. The sustainability of buildings can be increased by using less CO_2 intensive materials and smart designs.

The production of high-tech synthetic and composite materials is CO_2 intensive. This could be reduced by replacing some or all of the cement with alternative alkali-active binders (Section 4-4). Yet the deconstruction and recycling of composites remains labor intensive and expensive. A possible way to circumvent their disposal would be to design the elements in such a way that they are reusable for buildings or other industries or to make the building simpler to repair (Section 7-6).

In addition to design-for-disassembly, other smart design strategies can reduce the amount of material required for the building per year of life. A simple method would be to increase the lifetime of the structure to 100 years or longer by designing in architectural and structural flexibility to accommodate future functions. Designing structures more efficiently would reduce the amount of material required to carried the same loads and in turn reduce the size of the foundation. Such an efficient design could be possible with this material by using highly curved “structurally-informed” forms (Section 1-4). Such designs are possible by the integration of smart formfinding tools early on in the design, such as Thrust Network Analysis (Section 3-7).

7-8 CONCLUSION AND DISCUSSION

Buildings are big and complex. This limited list of additional topics is only a small number facing buildings. However, the material being developed will not need to solve all of them alone. Other materials can be used to mitigate fire or thermal expansion, among others. At this stage in development it is important to acknowledge the wide set of topics but not necessary to have solutions to all of them. Structural modification and repair methods might be required to be integrated into the design of the material elements, meaning that the fabrication process or reinforcing would have to be reevaluated at a later stage.

8 PHYSICAL TESTING

Physical testing should be used to determine the specific properties of the material. Multiple scales should be used to test behavior at the material level, element level, and building level. This testing should also cover matters of fabrication, transport, and construction.

8-1 ELASTIC FOIL SHEAR ANGLE

This waterproof and airtight layer is used to contain the concrete matrix and allow erection by inflation. It is not able to deform in shear, without prestressing, however it is able to extensionally deform to approximate a sheared shape. A selection of elastic foils was provided by Vreeberg bv. These foils varied in thickness, softness, and stretch.

Table 8.1: Acquired elastic foils.

ID #	Material Color	Thickness (mm)	Notes
5821	Red	-	Solar car foil
2677	Transparent	0.2	Dentistry applications
10202	Blue	0.2	
n/a	Brown	1.0	Mix of many plastics
3371+30%	White	0.3	
n/a	Beige	-	Vacuum foil

Elastic foils are created by an extrusion process, resulting in slightly isotropic properties, much like a woven material with warp and weft. This slight isotropic property was accounted for during testing by consistently orienting the material in the testing device. These relative dimensions and orientation replicate reality as the material elements would be fabricated in long strips.

8-1-1 TEST SETUP

A simple shearing device was constructed for this test. It consists of plywood strips and bolted wing nuts. It holds samples measuring 10cm by 20cm with extra length for clamping. It was measured and marked for angles of 90°, the orientation of the textile weave, and 40°, the benchmark value for the greatest shear deformation required. (See Section 5-3-1 for more details about shear deformation.)

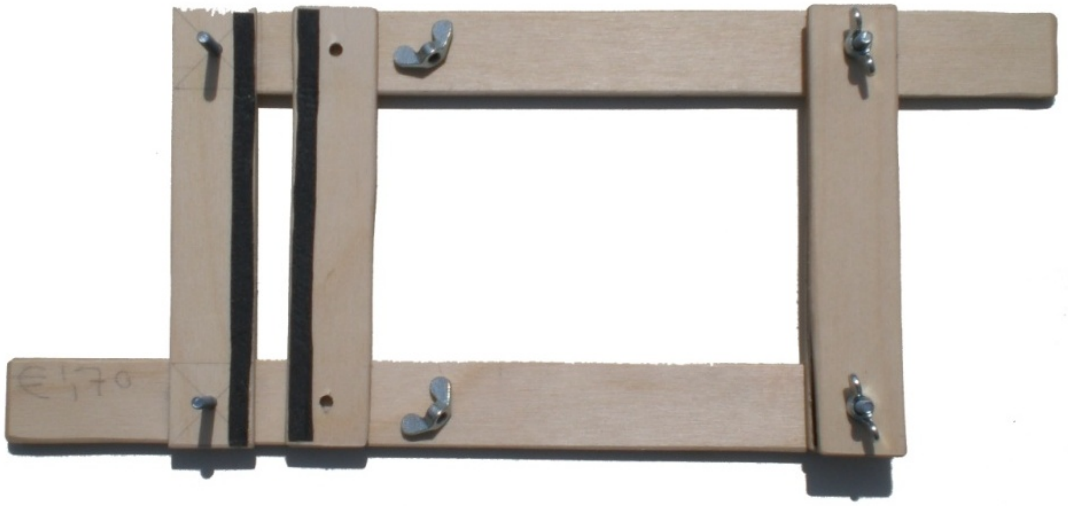

Figure 8.1: Shear testing device with one clamp disassembled, showing black rubber grip pads.

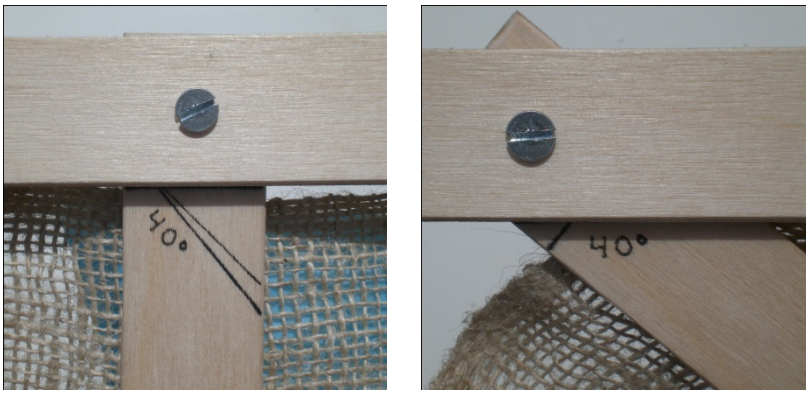

Figure 8.2: Marking on the shear testing device showing 90° and 40°.

8-1-2 TESTING

Testing is conducted by slowly shearing the device by hand until the 40° marking is reached. This process can be seen best with a material able to deform in shear, for example the burlap in Figure 8.3 below.

Figure 8.3: Deformation of a woven burlap sample from 90° down to 40°, showing slight buckling at 40°.

ROOM TEMPERATURE

The tests of the elastic films at room temperature showed significant buckling, but also a clear ability to approximate shearing through extensional deformation in two directions. An example of this can be seen in best performing elastic film in Figure 8.4 below.

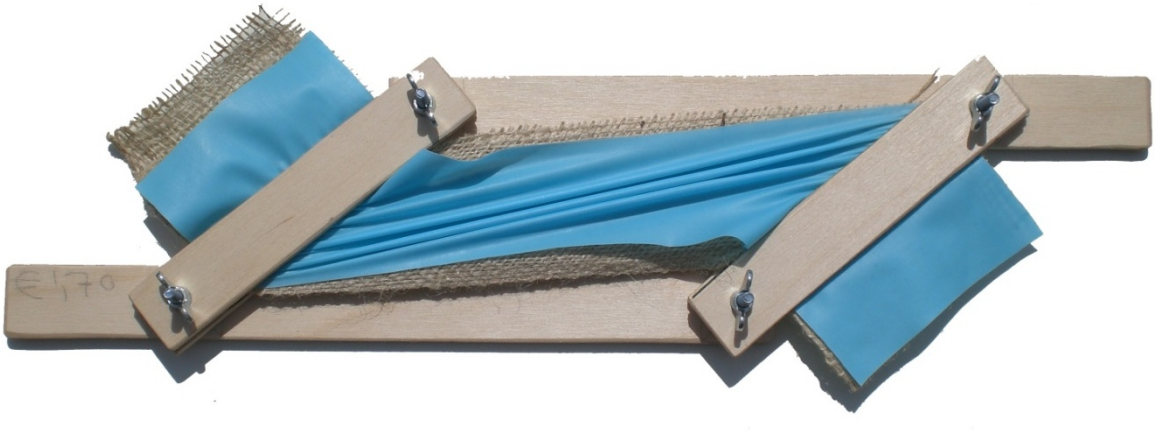

Figure 8.4: Room temperature shear deformation of a thin elastic film with burlap for comparison down to 40°.

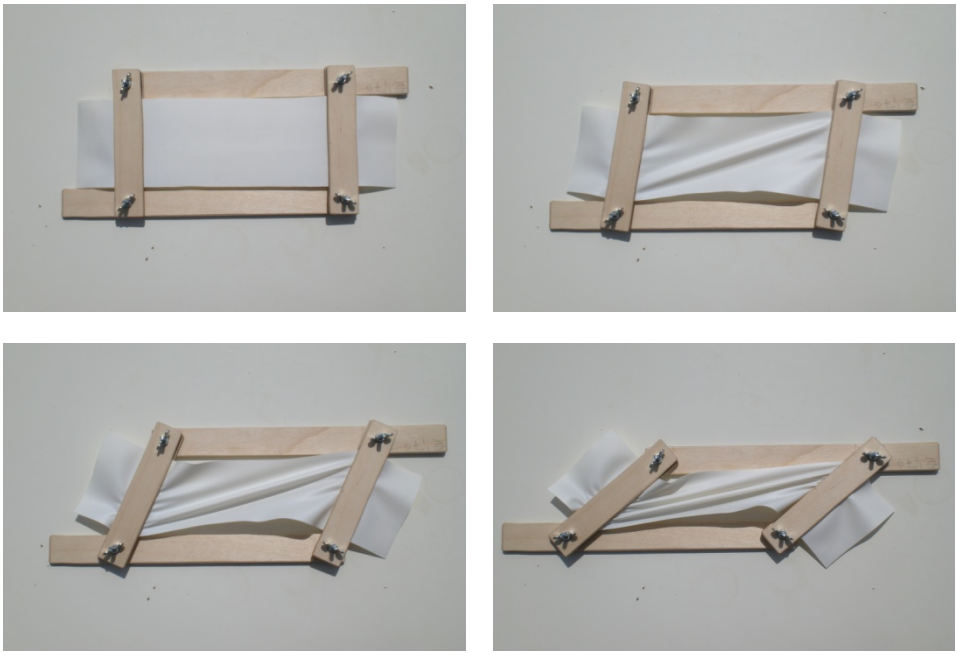

Figure 8.5: Sequential photos of buckling formation during shear deformation from 90° down to 40°.

ELEVATED TEMPERATURE

Further tests were conducted with a heat gun as an attempt to reduce buckling during shear deformation.

Figure 8.6: Black & Decker 1400 watt heat gun, which was used to locally heat the elastic foil samples.

Figure 8.7: Four elastic films shear deformed under elevated temperature conditions, showing permanent deformation.

Figure 8.8: Hole in shear deformed elastic film in elevated temperature conditions.

8-1-3 DISCUSSION

The elastic films are able to approximate shear deformations with allowable amounts of buckling if the proper material and thickness is selected. Buckling is reduced with increased temperatures at the risk of damaging the elastic film. Significant buckling should be avoided because it risks causing local irregularities in the thickness of the material. Heating could be used selectively in areas of large shear to increase in the elastic film's ability to approximate shear deformation.

This test should be recreated with a new testing device which would clamp the elastic foil at all four edges. This type of setup would be a better indicator of constrained shear. Additionally the joints of the device should be aligned with the corners of the test area of the sample. Without this the testing device will impose shear and slight amounts of extensile deformations. This was the case with the existing device. However the stretching effect was minimal because the joints were relatively close to the corners and partially canceled out by the more than sufficient elastic properties of the films. This effect can be noticed slightly in the buckling of the burlap in Figure 8.3.

These layers don't adhere very well to the concrete, which would not be a structural concern but may be an issue during transport or construction but probably just a cosmetic concern during use. This matter of delamination is discussed further in Section 7-4.

8-2 RECOMMENDED FUTURE TESTING

The material will need significantly more testing to determine its specific properties and bearing capacity. Such tests will not be conducted as part of this project, but are recommended for future development. They should be conducted mostly at full scale. The results from the full scale testing would then be used within computer modeling (such as FEM analysis within Diana). Tests at smaller scales would then be used to validate these computer models before they are applied to the design of a building. The following tests are suggested:

Material Properties (1:1)

Samples:	Flat slabs, Single curved elements Double-curved elements (positive and negative Gaussian curvature)
Tests:	Bending, Tension, Compression, and Shear

Individual joints (1:1)

Samples:	Joints alone, Joints connected to material elements, Flat and double-curved
Tests:	Bending, Tension, Compression, and Shear

Multiple Joints (1:10)

Samples:	Multiple elements connected by realistic joints, Flat and double-curved
Tests:	Test for buckling with Bending, Tension, Compression, and Shear

Building Scale (1:100)

Samples:	Building shape (not a test shape), Aerospace composites could be used to simulate elements, Scaled versions of joints would need to be developed
Tests:	Pressure differential (loading normal to surface), gravity loading (loading in global z-direction)

Non structural testing (1:1)

Samples:	Fully sealed element (dry and wet)
Tests:	Shear deformation using a deformation rig, Measure for thickness

8-2-1 FLAT ELEMENTS WITH SHEARED-REINFORCEMENT IN TENSION

Testing flat elements of the material which have undergone controlled shear-deformation would be an example of a 1:1-scale experimentation to determine the material properties. This testing would provide information about the change in tensile capacity with sheared reinforcement and could be used to adjust the approximation used to determine a value for the Modified Oblique-Loading Coefficient, from Section 4-3-2, which is more appropriate for the specific material components.

PROCEDURE

The value for the Modified Oblique-Loading Coefficient can be determined experimentally so that it accounts for all shear-deformation based changes such as the reduction of space between yarns of the textile. Hegger determined this value experimentally using Equation 8.1. [Hegger 2006] In the new version of this equation the maximum stress in the reinforcement, σ_{max} would be determined by testing non-shear-deformed sample of the material, while $\sigma_{max,\alpha}$ would represent the maximum stress in the reinforcement from the shear-deformed samples. The experimental sample size and setup could be very similar to that used by Hegger, as seen in Figure 8.9. The test would proceed much as Hegger's, the sheared material at each angle of shear-deformation would be rotated so that the angle between the reinforcement and loading angle changes from 0 to 90-degrees.

$$k_{0,\alpha} = \frac{\sigma_{max,\alpha}}{\sigma_{max}}$$

Equation 8.1: The computation of the Oblique-Loading Coefficient from experimental results. [Hegger 2006, Equation 2]

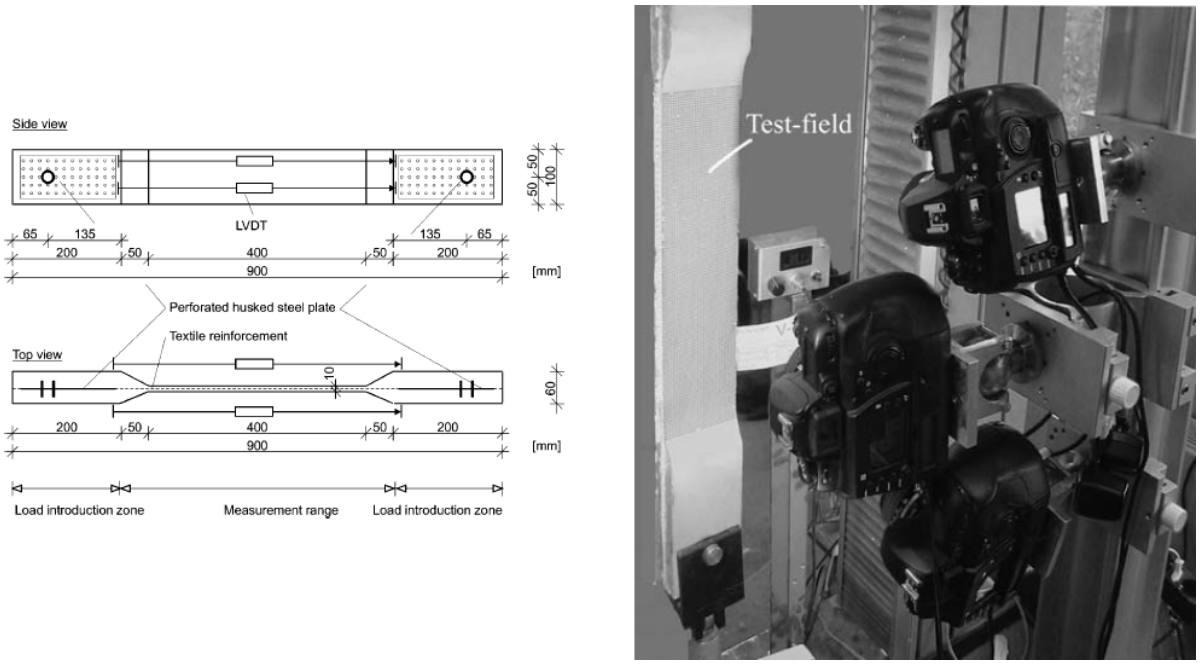

Figure 8.9: Hegger's experimental setup for the tensile testing of textile reinforced samples with oblique-oriented reinforcement. [Hegger 2006, Fig. 2 and 3]

TYPES OF SAMPLES

At least three of each type of sample should be tested to account for errors in production or testing. Both shear-deformed and non-shear deformed samples would be created. One type of sample would be used to create the baseline value of $k_{0,\alpha}$=1.0. This sample is non-sheared and has one weave direction parallel to the direction of the tensile load, as shown in Figure 8.10. Other samples would be grouped by the amount of shear-deformation. For example the 40-degree group would contain four (or more) types of samples each with a unique angle between the reinforcement and loading angle, between 0 to 90-degrees. These four example samples are diagrammed in Figure 8.11. The results of these four samples could then be plotted by loading angle and compared to the Modified Oblique-Loading Coefficient as computed analytically in Section 4-3-2. This comparison with expected results for each sample is shown in Figure 8.12.

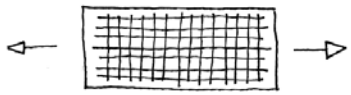

Figure 8.10: Non-sheared sample with one weave direction parallel to the direction of the tensile load.

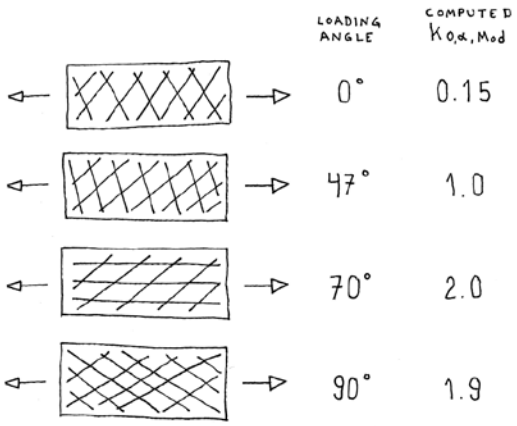

Figure 8.11: 40-degree shear-deformation group of samples each with a unique angle between the reinforcement and loading angle.

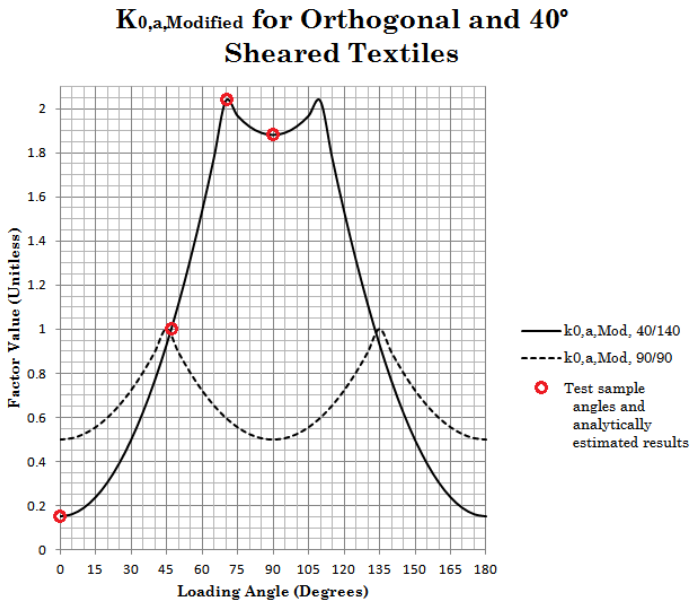

Figure 8.12: Expected results of the four samples from Figure 8.11 compared to the Modified Oblique-Loading Coefficient as computed analytically.

8-3 CONCLUSION AND DISCUSSION

The physical tests are far from complete. Priority was placed on investigating functionality of the deformation process over determining mechanical properties. Mechanical properties of textile reinforced concrete have been tested by Hegger, Kok, and others (Section 4-3). The deformation ability of the complete material should have been tested, instead of only the elastic film layer. There is concern that shear deformation might be limited by the dry concrete layers. This should be tested wet and dry. This testing would clarify the true mode of thickness increase (Section 5-1-4). The material is required to perform differently when cured and when uncured. Therefore it should be tested dry, wet, partially cured, and fully cured.

Gathering information about the joints and material would be most practical as the next step toward building design. This information would have been needed to accurately complete this project. It would identify the true bearing strength and failure mechanism (buckling) for buildings built of the material. Enough testing should be done to increase the accuracy of the computer modeling. Because of time and material constraints these tests were not conducted, instead assumptions were used in designing the case study building.

Recommendations for further testing are presented in Section 12-2-1.

9 FABRICATION AND CONSTRUCTION

Now that the expected and benchmark properties of this building have been established, the demands must be translated into physical form and method of building. The physical form will be determined primarily by the available fabrication techniques. Although the complete process of fabrication is out of the scope of this project, it can be outlined to an extent where the process appears feasible. The processing equipment and the available component materials will determine the dimensions of the product. In turn, these dimensions will be important for the specifics of transport and onsite construction.

The two proposed methods of construction, hanging and inflation, utilize the materials unique properties. These two methods are proposed in the patent (Chapter 2). Hanging utilizes the tensile strength of the material while it is still deformable. In addition to this tensile strength, inflation utilizes the airtight property of the elastic film layer (Section 5-2-3).

9-1 FABRICATION

Prefabrication of material would improve quality and reduce onsite labor. Fabrication involves knowledge about the production dimensions of the component materials as well as machinery for combining these components. Beyond this knowledge of transportation and onsite maneuverability will determine the final size and packaging of the elements.

9-1-1 WIDTH

A wider element is better for construction because it mean less jointing and less on site work, although it would be less maneuverable because of the increased mass of each element. The precedent project Concrete Canvas comes in two widths 1.0 and 1.1 meters. This demonstrates that a complex three dimensional product with dry concrete can be combined successfully at an industrial scale.

CC	Thickness (mm)	Batch Roll Size (sqm)	Bulk Roll Size (sqm)	Roll Width (m)
CC5	5	10	200	1.0
CC8	8	5	125	1.1
CC13	13	N/A	80	1.1

Figure 9.1: The dimensions of Concrete Canvas products. [Concrete Canvas]

During the course of this project a visit was made to the production facility of Vreeberg bv, in Nijkerk. Vreeberg produces the elastic foils tested in this project (Section 8-1). These foils are produced by an extrusion process and can be manufactured to near infinite lengths at widths of up to 1.1 meters. The production process creates edges on the material with different thicknesses then the middle section. These edges can be trimmed off during production if required.

Based on the elastic foil extrusion process, the produced width of the material will be set to one meter excluding one joint. Each element will overlap by one joint, so when combined each will account for one meter in width. However, wider (2+ meter) elements would be preferred to reduce the amount of jointing.

Figure 9.2: Dimensioned element cross-section.

9-1-3 LENGTH

A longer element is better for construction because it mean less jointing and less on site work. However, element weight increases with length and therefore maneuverability decreases. Heavy elements will require cranes or other lifting equipment which in turn make onsite construction more complex and expensive. The weight of the material could be reduced by using light weight aggregates in the concrete mix design. Determining a suitable element length means minimizing jointing by finding the maximum maneuverable length and weight. The best solution would be to create elements of two lengths: one which can be managed by two people and the other which is maneuverable by simple lifting equipment.

If the material section were assumed to be only 20mm and entirely made from normal cured concrete (2400kg/m^3) it would weigh 45kg/m^2. This can be compared to the similar existing product Concrete Canvas. The 13mm thick material weights 19kg/m^2. Assuming the same density a 20mm thick version would weigh 29.25kg/m^2. Even at the lowest estimate of 30 kg/m^2, the one meter wide strips could only be 4 meters long for it to be maneuverable by two people, which is far too short. The placement of longer elements would require cranes or smaller maneuverable lifting equipment. This would increase the cost of onsite production but improve quality due to the reduced jointing.

9-1-2 PRODUCTION METHOD

This material is made to be in long strips of a set width, meaning that a continuous process which combines all components would be best to enable long elements with a smaller production facility. Such a production method could use hoppers for the dry concrete and rolls for the reinforcement and other layers. In the proposed setup each component material would be produced individually and combined using an assembly line process as seen below, in Figure 9.3. This device would also be responsible for sealing the edges and affixing the joints. While this process is diagramed, its specifics will not be investigated. Instead it is assumed to be possible. Once combined, the finished material would be rolled on to large diameter spools. These are used in order to minimize delamination/damage from bending, which would occur with bending about a shorter radius. Finally these spools would be packaged and sealed with a waterproof and airtight material to prevent premature hydration of the cement.

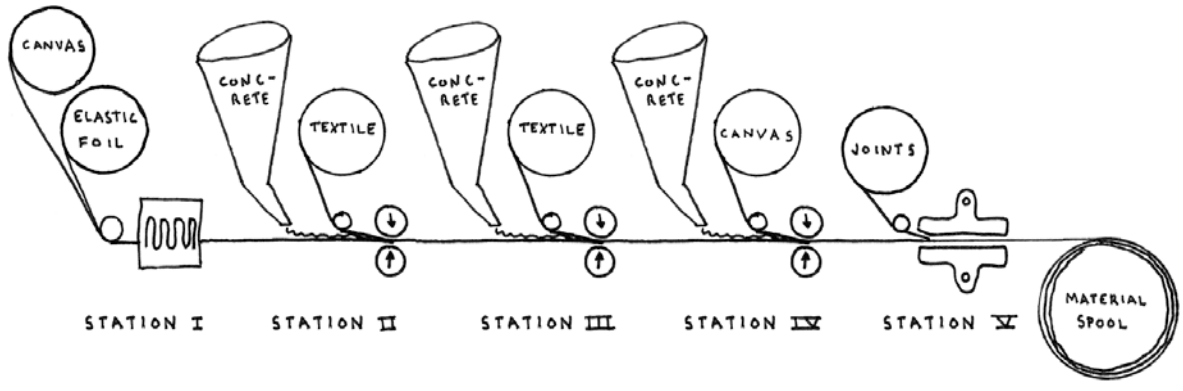

Figure 9.3: Process for combining the constituent materials. Station I: combination of elastic foil and canvas layer; II: addition of thin layer of concrete (~2mm) and pressing of textile into concrete; III: addition of thick central layer of concrete (~16mm) and pressing of textile into concrete; IV: addition of thin layer of concrete (~2mm) and pressing of durable water-permeable canvas into concrete; V: affixing of the joints to the sides of the material strip by gluing, stitching, heat sealing or other method.

9-2 FROM DIGITAL MODEL TO BUILDING BLANK

The shape of the three-dimensional building will be created digitally. From this computer model a flat "embryonic blank" will be created. This blank shows the amount of material required in terms of element length and placement. The flat shape would be created onsite by unrolling and jointing the prefabricated elements as prescribed. This assembled blank will deform during construction to create the shape prescribed by the digital model.

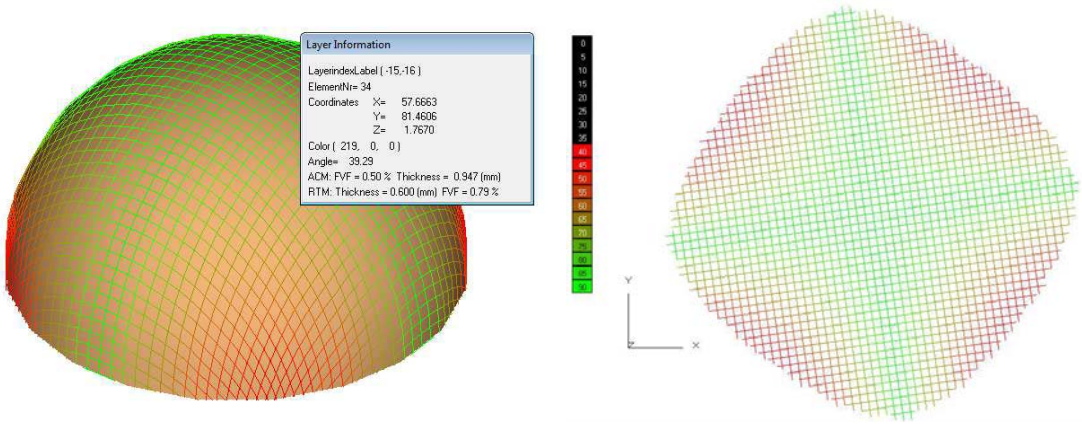

Figure 9.4: Hemisphere-shaped building and its flat "embryonic blank" showing the range of shear deformation.

The jointing process is not fully determined. It is highly dependent on the type of joint used. For more information about the joint alternatives see Section 5-3. This process might require a specialty jointing machine either to stitch the elements together or to act as the pull on a zipper.

The construction of the blank will require a larger area than the footprint of the building. This means that a separate staging area or larger building site would be required. The required staging area is reduced when multiple parts or structural bays are used because each blank will become only a part of the entire structure and can therefore be assembled one after another.

9-3 ERECTION

Erection will follow from the creation of the blank. The specifics of construction depend on the method of construction. As mentioned in the patent (Chapter 2), hanging/draping or inflation of the material will be the two methods considered. These methods can be used in combination but will be addressed individually for simplicity. Foundations should be designed to support these additional construction loads.

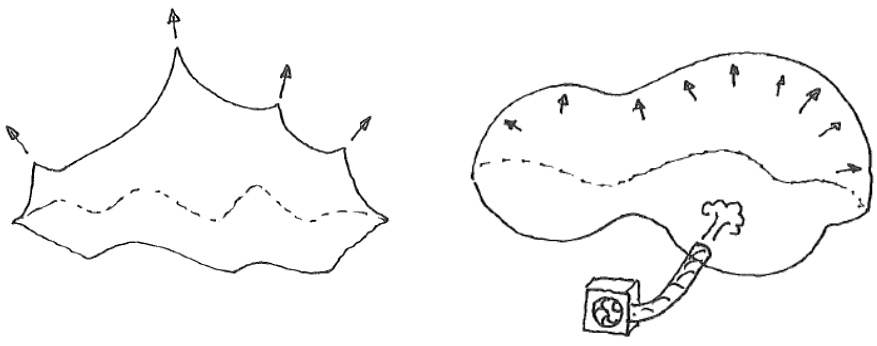

Figure 9.5: Erection methods: hanging (left) and inflation (right).

9-3-1 FOUNDATION CONNECTION

Shear deformation within the material makes it difficult to form a connection to the foundation before erection. However the areas of large shear deformation can be determined using the computer program Drape. Therefore, it is possible to account for these known deformations by pre-wrinkling the material at areas of large shear. This will have the effect of reducing slippage globally. Additionally areas of zero shear deformation can be determined and fixed to the foundation before erection. This detail of the construction method has a large potential for damage because of the friction and deformation.

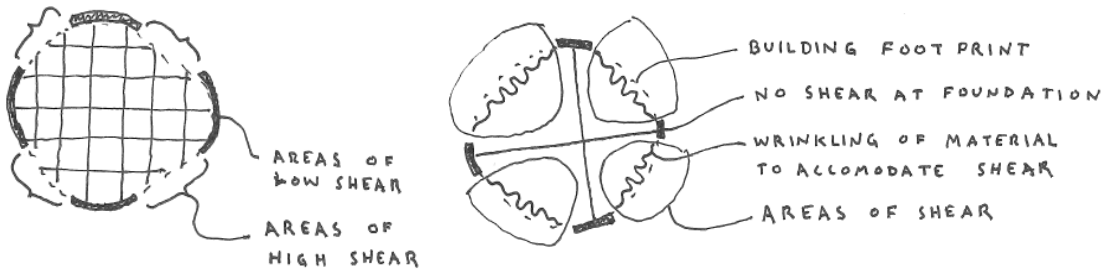

Figure 9.6: Areas of shear slippage at the foundation (left) and how to accommodate it with wrinkling (right).

9-3-2 HANGING

Hanging can mean that temporary supports are used to deform the material or that permanent structures support the material during construction. Temporary supports could be in the form of hydraulic jacks or connections suspended from cranes. A permanent structure could be an elevator shaft, floor plate, wall, or other load bearing element.

These supports could be attached from above the surface of the blank, in the case of the crane, or from below in the case of hydraulic jacks or permanent supports. Supports from below would require access to the underside of the embryonic blank. Hydraulic jacks could be installed in the foundation pit while the blank is assembled over them. Permanent supports would require the lifting of the blank and successive draping over the supports. This could be accomplished by specialty lifting equipment and completing the assembly of the blank in mid-air.

Once the supports are in place and the perimeter of the blank is secured to the corresponding foundation points, the deformation process can be completed. Some force will be required to appropriately shear-deform the material into the desired building shape. This deformation force will come from gravity and applied loads either from hydraulic jacks, cranes or through cables and winches between the material perimeter and foundation. Once properly deformed the material would be structurally connected to the foundation and permanent supports.

9-3-3 INFLATION

The inflation method of construction will require a specialty airtight foundation connection which is able to let the material slip and shift slightly as if deforms into the desired shape. Using this temporary foundation connection the blank will be secured as air is pumped into the space below the blank. This air pressure will provide the force necessary to support and deform the blank. A limited amount of air leakage between the foundation and building blank is acceptable as long as a pressure differential can be created.

The material has a mass of approximately 50kg/m^2 which means it weighs 490N/m^2 on earth. This weight-per-area can be expressed as the air pressure required to support the un-deformed material during erection. The deformed material can weigh as much as 1.56 times as much (Section 4-4-2); meaning it would require a pressure of 760 pascals. An additional force to deform the material would also be required. This force is unknown and dependant on the material's configuration. However, it is expected to be less than the force required to support the mass of the material. For the purposes of this project the expected maximum required air pressure would be approximately 800 pascals. This value is far less than required for a car tire and should be easy to achieve even with air leakages.

The air pressure within the blank will increase until the desired building form is reached. At this point the pressure should be stabilized and the material structurally connected to the foundation.

9-3-4 HYDRATION

Once the prescribed/desired shape has been reached and the material is structurally connected to the foundation and supports, it should be sprayed with water to hydrate the concrete and begin the process of hardening. The force from the jacks, cranes, or air pressure should be adjusted after hydration to insure the correct form. It may be favorable to wet the material during deformation. Wetting would have lubricating effect, reducing the friction between the particles of the dry concrete and other components (Section 4-2-1). Even once fully in place the water required for hydration is expected to reduce the force required for shear deformation because of this lubricating effect, but it also increases the mass of the material. Once these adjustments have been made the material should be left to cure for a period of time. This time until sufficient strength gain will depend on environmental conditions (temperature) as well as the properties of the concrete.

9-4 CONCLUSION AND DISCUSSION

Fabrication and production have been joined in this chapter because the limits of fabrication will influence the constructability, although some of their specifics are covered in other chapters (Chapter 5 and Section 10-1).

With any new composite material the limits of existing production methods and equipment will limit what can be made. The precedent of Concrete Canvas (Section 3-1) gives confidence to the possibility that this material will be possible to manufacture to acceptable tolerances. However, some aspects of fabrication are skimmed over, such as the connection of the joint to the textile reinforcement, deemed to be out of the scope of this project.

The material stresses during construction are very different than during use, often a full reversal from tension to compression. This imposes large structural requirements on the material which might be utilized only during construction, resulting in overdesigned elements. This is contradicts the goal of creating structurally efficient buildings. In other cases (such as hanging structures with permanent supports) the material remains similarly loaded during construction and use. In these cases the rigidity and stiffness gained during hardening would be utilized to limit deformations or to support additional constructions.

The hanging method of construction could prove to be troublesome if special care is not taken to properly orient the material. This is because the material does not significantly extend in the directions of the textile yarns, while it extends (by shear deformation) significantly diagonal to the yarn directions. This might be solvable if it can be properly secured to the foundation before deformation to control this diagonal extension. This would however impose large horizontal temporary loads on the foundation. An over-design of the foundation, as compared to the use loading, would be required for these areas. These forces and changes to the construction method could be investigated using a computer program designed for membrane structures, because during hanging the material acts as a membrane, completely in tension. EASY is the name of such a program that could be utilized.

The foundation connections will require special features to protect the material from damage during shearing and slipping. These have not been designed but could consist of rollers or plastic padding. This portion of construction imposes a durability requirement on the material's composition. This was only briefly mentioned, that woven canvas layers could be used in addition to the other functional layers for this purpose, but it should be investigated further, probably with physical experimentation.

10 FORMFINDING

Formfinding is the method of achieving the final architectural shape by balancing multiple constraints such as function, site, loading, structure, and day-lighting. It is vital to the design process, not only for architectural reasons but also for constructability. For this project the formfinding process has the added requirement of needing to mimic the way in which the material behaves during construction. This slight constraint of the architectural formfinding process is the trade off for the ease of construction that can come from using the material.

Beyond mimicking the behavior of the material, the formfinding process should create a shape that will be structurally efficient, meaning a shape with limited bending stresses. Guidelines for creating such a shape should be known by the designer. The structural efficiency of the shape can be tested during the formfinding process by using an FEM computer program or by using optimization techniques (Section 10-1-3). Additionally this process should take into account structural exceptions which might be required and would have an effect on the architecture of the building. For example a long flat span of the material might require a column or beam for support, this would influence the floor plan or useable height of the architectural interior.

The final stage of formfinding is to fit the material to the building shape. The material is assumed unable to deform to shear angles below 40 degrees. Therefore some building shapes must be created as separate structural bays to limit the extent of shear deformation. Once the material is fit to the shape, a flat “embryonic blank” can be created.

The formfinding process will be illustrated by using an example footprint from which the two construction methods can be contrasted.

10-1 MIMICKING CONSTRUCTION

The two methods of construction, hanging and inflation (Section 9-3), require different formfinding processes. These methods have been emulated using the computer program Rhinoceros and its graphical algorithm editor Grasshopper. These processes both begin with a known building footprint. This footprint is covered with a mesh anchored at its perimeter. This mesh is then fitted to match the perimeter of the footprint.

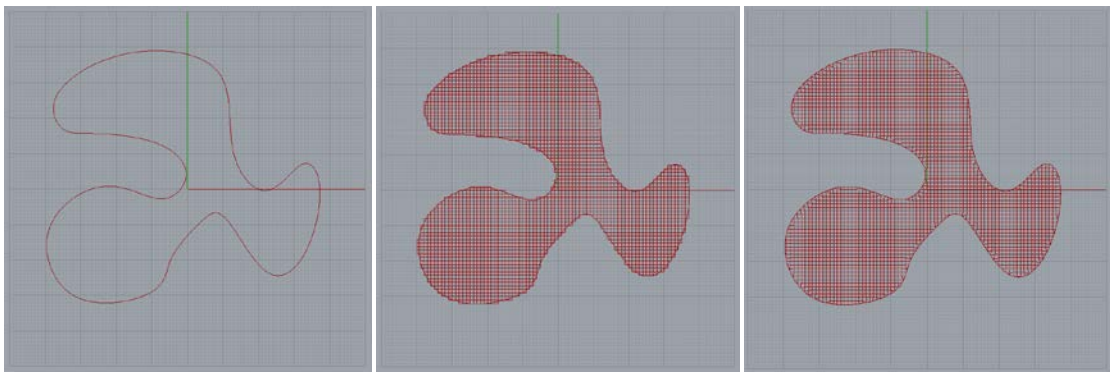

Figure 10.1: Example building footprint (left) with mesh applied (center) and mesh fitted (right).

The three-dimensional building shape is created by deforming the mesh with gravity, point loads, and internal pressure. This stage of formfinding is complete once a suitable combination of forces has been found. Using a plug-in called Kangaroo, for grasshopper, gravity and pressure forces can be applied to deform this mesh according to the construction methods. The algorithm used by Kangaroo assumes the mesh to be composed of spring elements. The resting length of these springs can be set to any absolute value or relative to the starting length.

Together pressure, gravity, and spring rest-length are the parameters that enable formfinding to mimic construction. Pressure represents internal inflation pressure (if utilized), gravity represents the weight of the material, and the spring rest-length represents the amount of material used to construct the building. These input parameters act relative to each other and are used by Kangaroo, as shown below, in Figure 10.2.

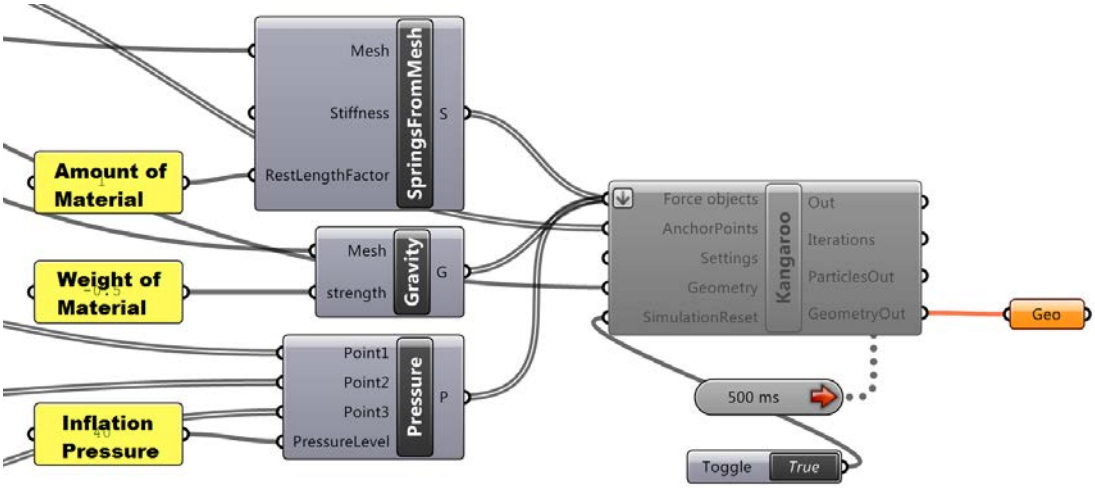

Figure 10.2: Kangaroo component for Grasshopper showing the labeled formfinding parameters.

It would be possible to set these parameters to values based on reality. For example, the mesh spring stiffness and rest length could be derived from the material's properties. Using values from reality would allow the formfinding process to more accurately emulate reality. For the purposes of this project these parameters are not strictly based on reality, but only so far that gravity is less that internal pressure. Additionally, the placement of supports and the footprint of the building would be considered formfinding parameters.

10-1-1 HANGING

Hanging forms are possible by assuming that gravity is the main force in deforming the material. To begin this process supports are placed within the footprint. The height, shape, and number of these supports can be varied. The mesh is then 'relaxed' using the Kangaroo component for Grasshopper. The results from Rhinoceros can be seen below, in Figure 10.3.

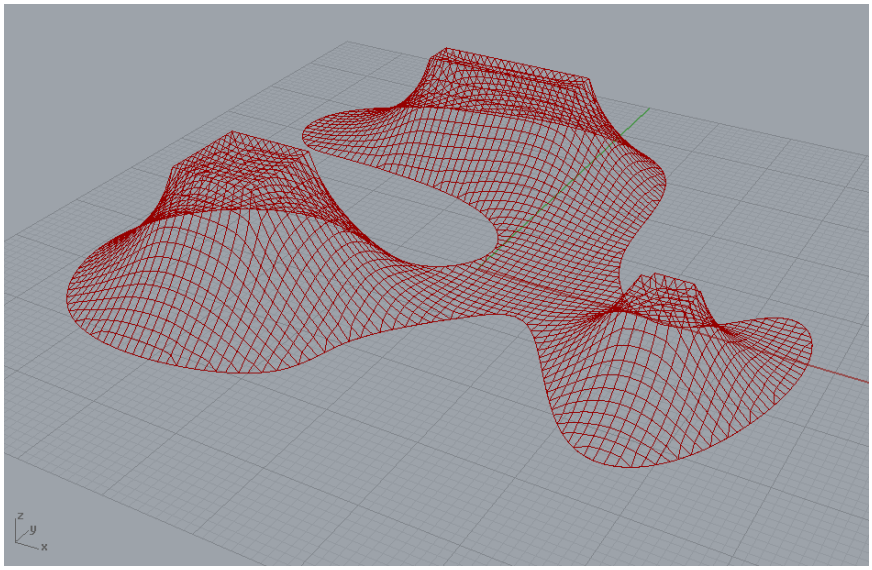

Figure 10.3: Example building footprint deformed by hanging from three permanent supports.

10-1-2 INFLATION

The principle of inflation is that air pressure within the building lifts the material until a sufficient tensile force within the material is able to cause shear deformation. To emulate the results of this process, a pressure force is applied normal to the surface to inflate the shape, while a gravity force is applied at each node in the negative Z-direction; the result it a slightly flattened bubble. The Kangaroo component for Grasshopper 'relaxes' the mesh until these forces are in equilibrium and a stable shape is found. This result from Rhinoceros can be seen below, in Figure 10.4.

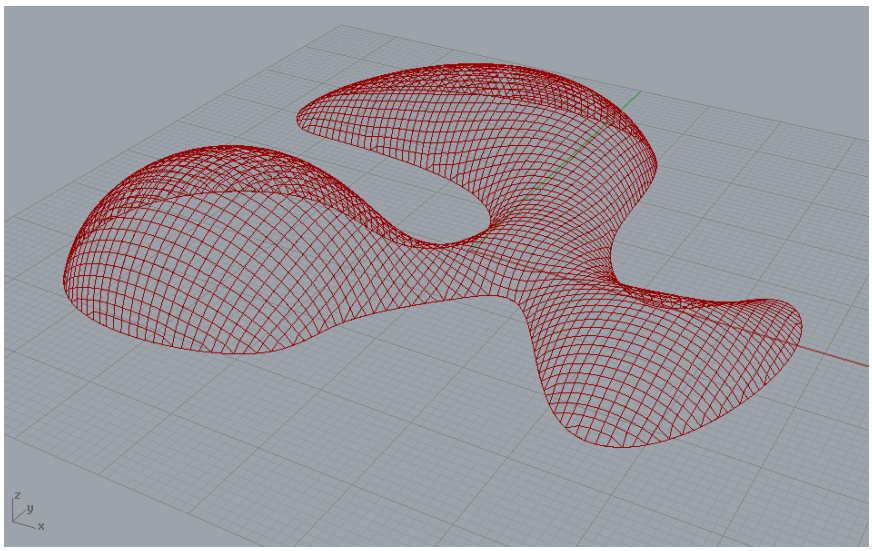

Figure 10.4: Example building footprint deformed by inflation.

10-1-3 STRUCTURAL EFFICIENCY AND OPTIMIZATION

In the future the formfinding method for this material should include a structural optimization step. Slight changes to the formfinding parameters, such as inflation pressure or placement of the hanging supports, will change the curvature of the structure and therefore the load transfer path. (Figure 10.2) An optimization process would alter these parameters, apply loads, and perform a structural calculation, then repeat until a certain combination of parameters resulted in an optimized efficient structural shape.

Such a process could be performed using genetic algorithms, such as Galapagos, the “evolutionary solver” included in Grasshopper for McNeel Rhinoceros. For this to be successful the parameters and loading conditions would need to be fine tuned. Additionally the concepts from the BLOCK research group’s Thrust Network Analysis (Section 3-7) should be included as a step within this optimization step.

Much more development is needed before structural optimization could be implemented within the formfinding process. Recommended next steps are discussed in Section 12-2-2.

10-2 STRUCTURAL BAYS

The limited deformation abilities of the material means that not all shapes can be created with a singular blank (composed of jointed elements). Instead, some buildings must be divided into separate structural bays to limit the required shear deformation (down to 40 degrees at the most).

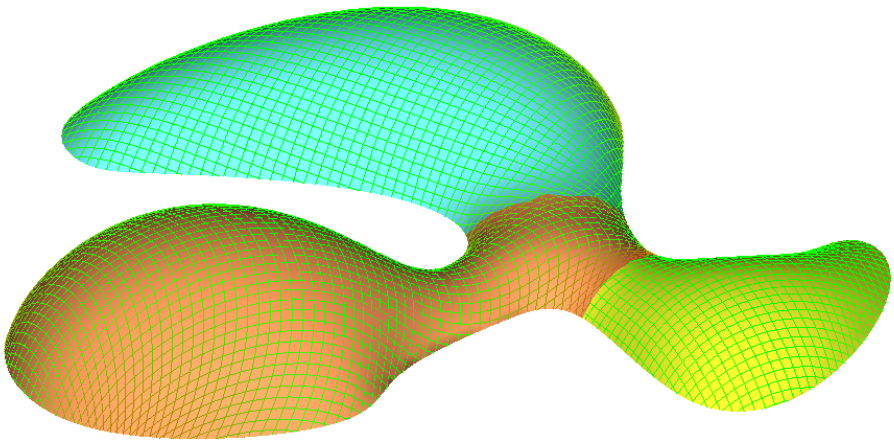

Figure 10.5: Example inflated building form divided into three structural bays.

Each bay would require its own construction process, which would most likely require additional structural elements, such as arches. These elements would be located at the seams between bays and could be temporary, only for construction, or permanent.

These seams would be good places for thermal expansion joints (Section 7-2), because each side would have a separated (partially detached) structure. Using bays the onsite construction would become more manageable by reducing the largest sized blank and therefore staging area required.

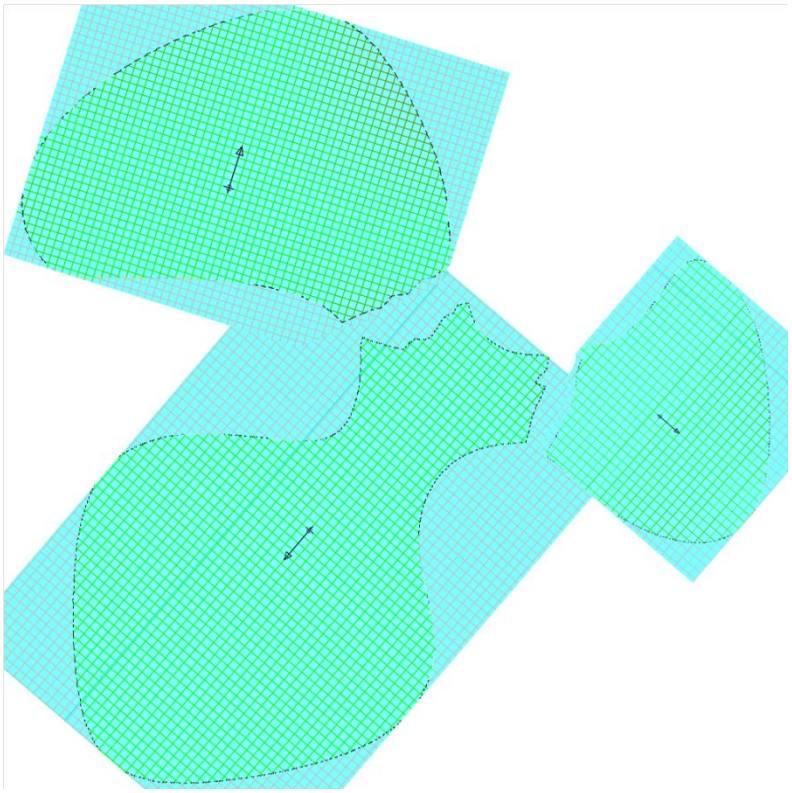

Figure 10.6: The three blanks corresponding to the structural bays of the example inflated building form, shown at relative scale with textile orientation shown by arrows.

10-3 EXCEPTIONS

Architectural features such as windows and floors are required for a well functioning building. These features represent exceptions to the continuity or loading of the structure. Windows are discontinuities which don't allow force to pass through them. Floors are loads imposed on the structure. These exceptions can either be dealt with after formfinding during structural analysis or they can be included as a step within the formfinding process.

10-3-1 IMPOSED LOADS

For a structure made from this thin material to be successful the majority of force must act in-plane. This must remain true for the structure to support floor loads without additional structural members. Such members, such as columns could be added after formfinding. In order to avoid additional members, the formfinding and therefore construction process must be modified, in order for the predominant forces to remain in-plane. One such method could be to apply a load approximately equivalent to the floor load in the opposite direction at its support points. This would likely cause the structure below the floor to become more vertical. Because the formfinding process attempts to replicate the reality of construction, this same force must be applied during construction of the structure, before the floor is added.

10-3-2 DISCONTINUITIES

Windows, doors, and overhangs are required for a well functioning building. These features represent discontinuities in the surface which have an effect on the load-bearing behavior of the building. If they are dealt with after formfinding, then the building would be erected as prescribed by formfinding and altered after erection, such as cutting the cured material to place windows. With this method these holes would require stiffening by the additional structural elements.

Alternatively, the formfinding process could be guided by structural reasons which would conflict with the methodology of construction. For example, this feature could be included in the formfinding process by using additional forces to deform the mesh into a more “shell-like” form by using Gaudi-esque catenary strategies. This would change the erection method but not require additional members. Such a change could mean the addition or temporary formwork to support the material without using inflation or hanging.

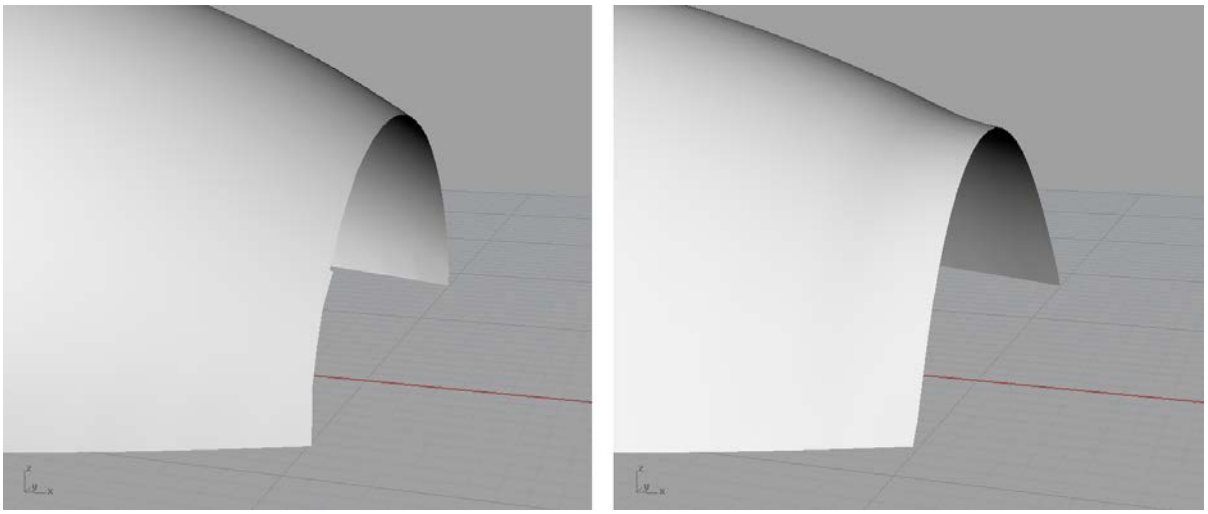

Figure 10.7: Image showing difference in cut (left) vs hung vault opening (right), notice the slight up turning of the leading edge.

10-4 CONCLUSION AND DISCUSSION

Proper formfinding is vital to creating a well constructible, efficient building from this thin material.

The process here suggests that these computer tools could be used to simulate construction. However, currently it does not do so, because many of the material properties are unknown. Creating a formfinding method that accurately simulates construction is important to insure that the constructed building matches the architectural design. To accomplish this the material properties should be investigated experimentally (Section 12-2-1).

Beyond mimicking the behavior of the material, the formfinding process should create a shape that will be structurally efficient, meaning a shape with limited bending stresses. This has not been done here, although it is suggested that inflated-dome- and hung-tent-like shapes are more structurally efficient than other kinds of freeform blob shapes. For this project, structural efficiency was found using a recursive trial-and-error method in combination with formfinding. In the future it would be possible to combine tools such as Thrust Network Analysis (Section 3-7) to imbue the formfinding with structural 'intelligence'.

At this point it the method of integrating "exceptions" such as windows and overhangs into the structural design has been messy and mostly an afterthought once the main structure has been form-found. All building will have these features and as it is currently presented they would require considerable finishing work. The purpose of this material and construction method is to reduce onsite labor. Therefore the next step towards normalizing these exceptions should be taken. In future development, the current computer tools and construction methods can be modified to make the inclusion of these "exceptions" more streamlined (Section 12-2-2).

An area of optimization yet unexplored is the placement and fitting of the actual material properties to the surface. Currently this has been done by trial-and-error in Drape. This involved manually creating structural bays along existing lines in the meshed geometry. Finding the best placement of the edges between structural bays would involve knowing the expected forces and finding arched areas or other suitable features for efficient support structures.

11 CASE STUDY BUILDING DESIGN

The specifics of building design and execution using the material and proposed formfinding and construction methods will be clarified through the design of a case study building's main structure. This chapter progresses chronologically through the design process: beginning with the architectural program, adapting this to formfinding, then a multi step numerical analysis to incorporate the new material's properties, and ending with a construction procedure.

11-1 ARCHITECTURE

The prompt for case study building is a large high profile project for a major metropolitan city. It will be a new concert hall built on an entire city block without elevation changes. Its form should be an organic freeform blob with a prominence rivaling that of any major city's concert hall, e.g.: Walt Disney Concert Hall or the Sydney Opera House. The proposed program consists of three parts: (1) concert hall and back stage, (2) space for offices and practice rooms, and (3) grand entrance with an area for coat check and congregation.

This was translated to a three-fingered floor plan, as seen below in Figure 11.1. The size of each finger representing the size of the program each would be required to fill: the largest finger for the main hall, the mid-sized for the offices, and the smallest for the entrance area.

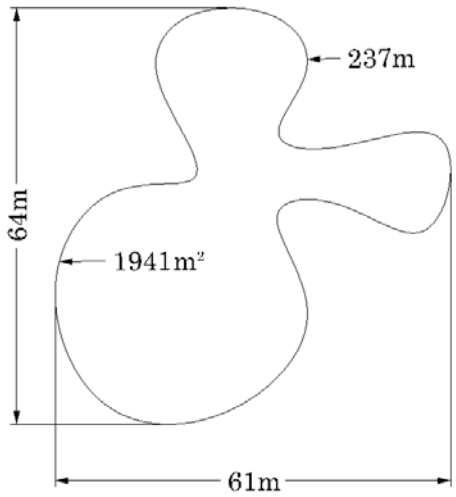

Figure 11.1: Case study building footprint dimensioned.

11-2 FORMFINDING

The formfinding processes encompasses all geometric work between the creation of the footprint curve and the input of geometry into Diana for numerical analysis. It begins with an inflation process (Section 10-1-2) and ends with a formatting of the geometry file for export.

11-2-1 INFLATION WITH GRASSHOPPER

The footprint curve (Figure 11.1) is first covered by a mesh, that mesh is fitted to the curve, as seen below in Figure 11.2, and then it's deformed by inflation. The inflation parameters for Grasshopper have been adjusted by trial and error until a suitable height (16m) for the main hall has been achieved. The inflation process occurs dynamically in Rhinoceros. This process is visualized as a series of intermediary screen captures, in Figure 11.3.

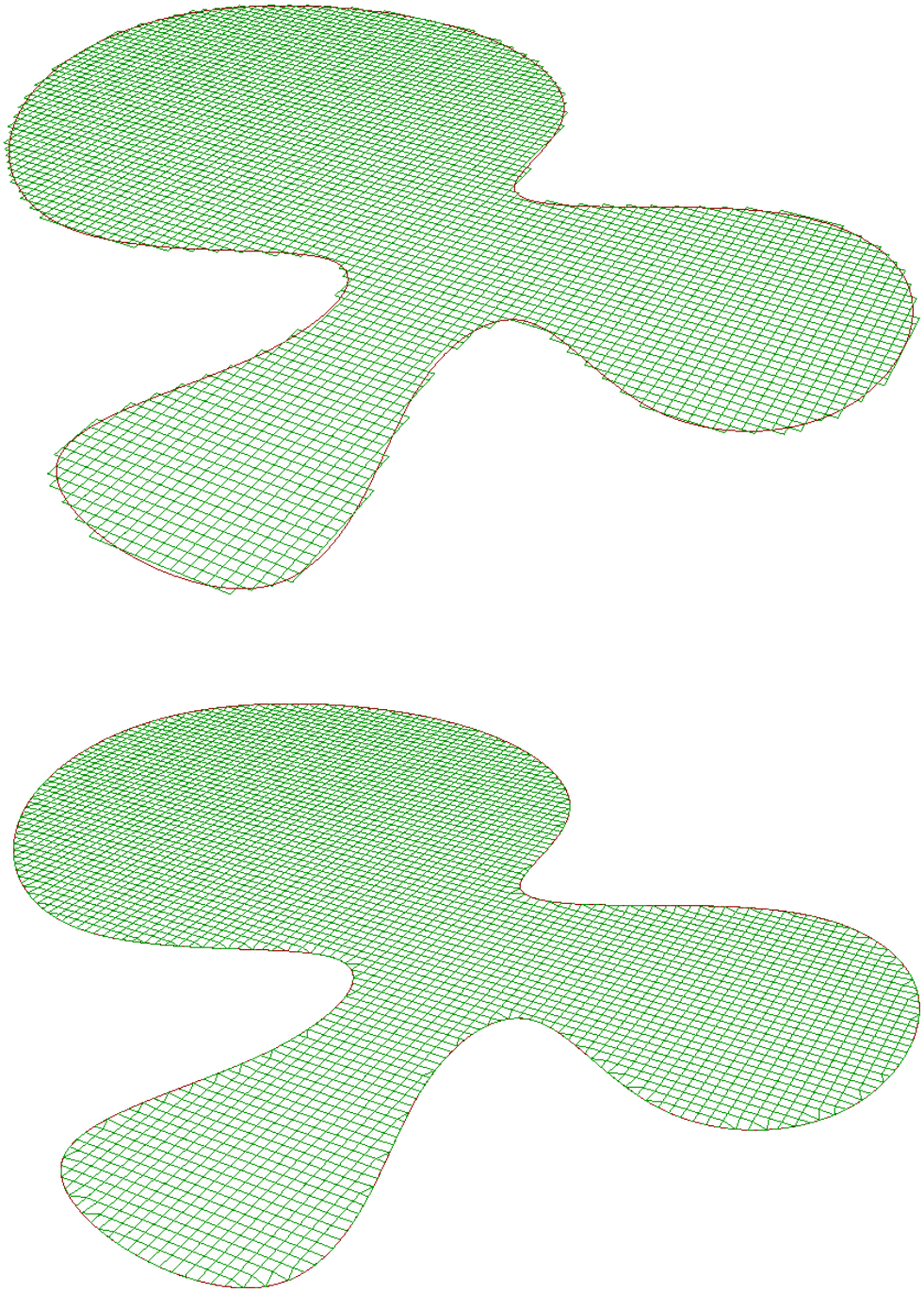

Figure 11.2: Footprint curve and mesh before (top) and after fitting (bottom).

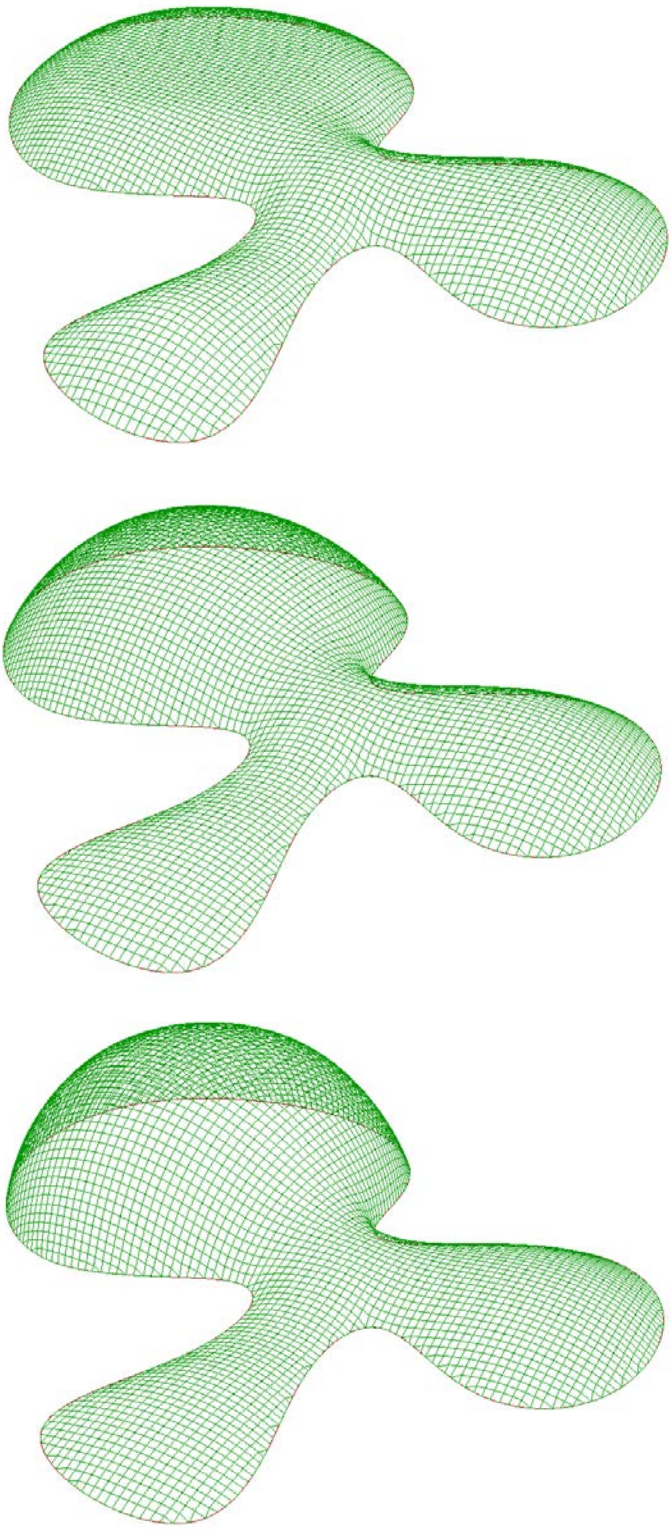

Figure 11.3: Intermediate steps of inflation in Rhinoceros by the Grasshopper formfinding definition.

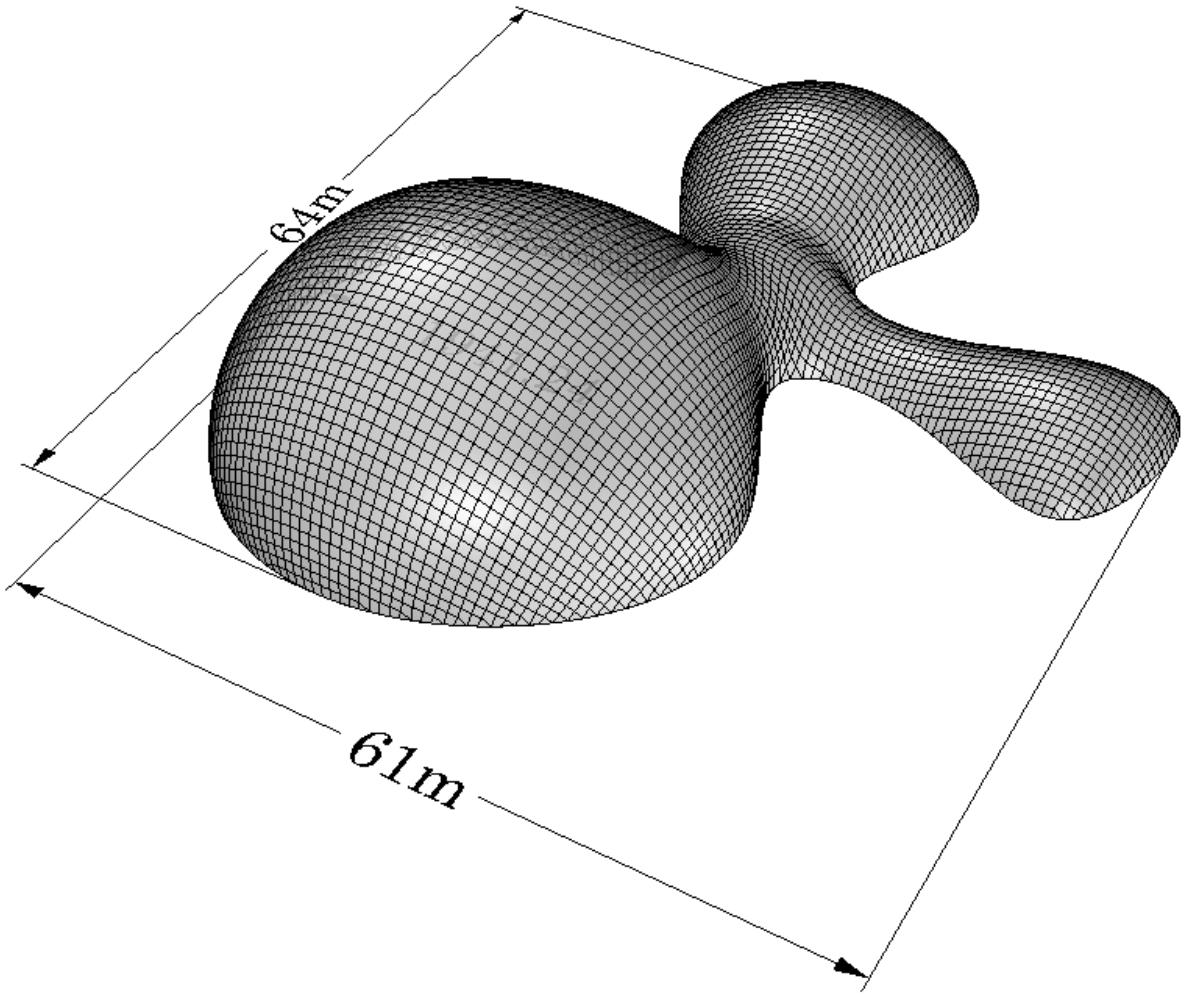

Figure 11.4: Case Study Building: Three-quarters top view dimensioned.

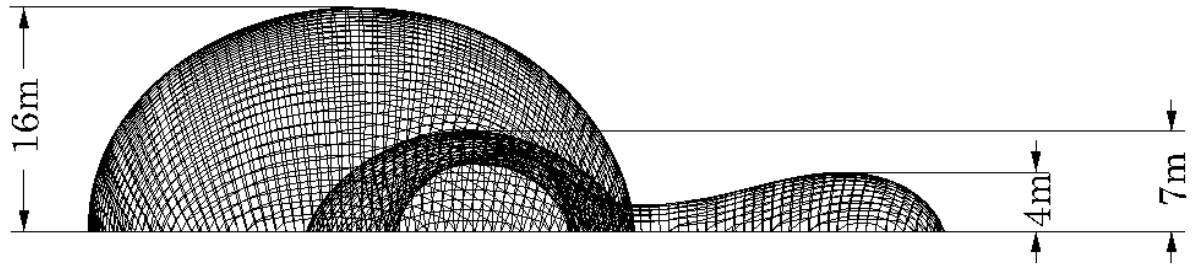

Figure 11.5: Case Study Building: Front elevation dimensioned.

11-2-3 SHAPE REVIEW

As mentioned in Section 1-4, not all freeform shapes are structurally efficient. Although the Case Study Building geometry was created without being explicitly “structurally informed”, it has been created using a method (inflation) which favors dome-like shapes, which are naturally efficient because of their curvature. The Case Study Building has a large nearly-flat top caused by the parameter representing the material self-weight (Section 10-1). This area may be subject to relatively large bending forces because of its low curvature. Over all the geometry appears suitable because of its visual similarity to domes and barrel vaults. Not only should the structure be sufficiently structurally efficient, but also it should be a good test of the new material. For this purpose it was important to include multiple kinds of curved surfaces: anticlastic, synclastic, monoclastic, and flat-inclined areas. The curvature of the surface can be quantified by to values: Gaussian curvature and mean curvature. Figure 11.6 shows the Gaussian curvature, which indicated the type of curved surface. The blue areas represent anticlastic curvature while green represents relatively monoclastic curvature and red represents higher levels of synclastic curvature. Figure 11.7 shows mean curvature, where blue and green represent the near-flat areas of the surface. Some background information about curvature is located in Section 4-1-1.

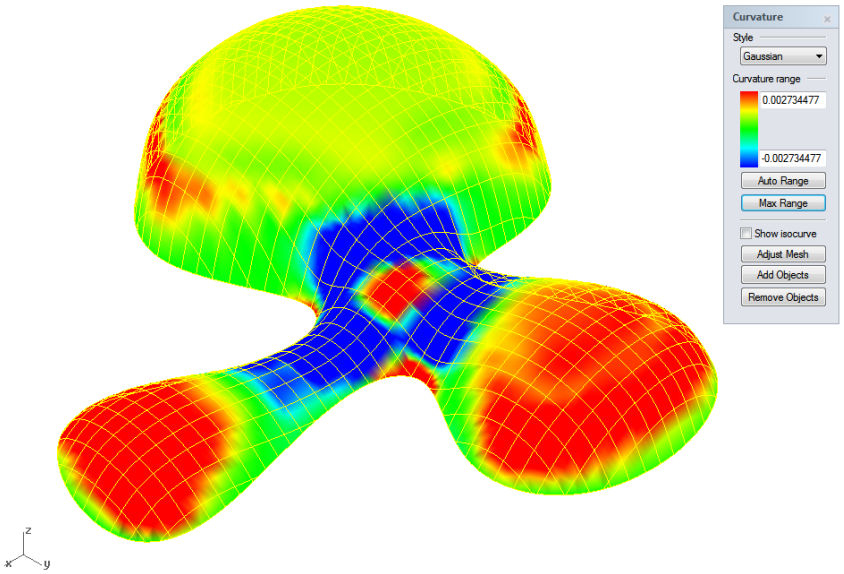

Figure 11.6: Gaussian curvature of the Case Study Building.

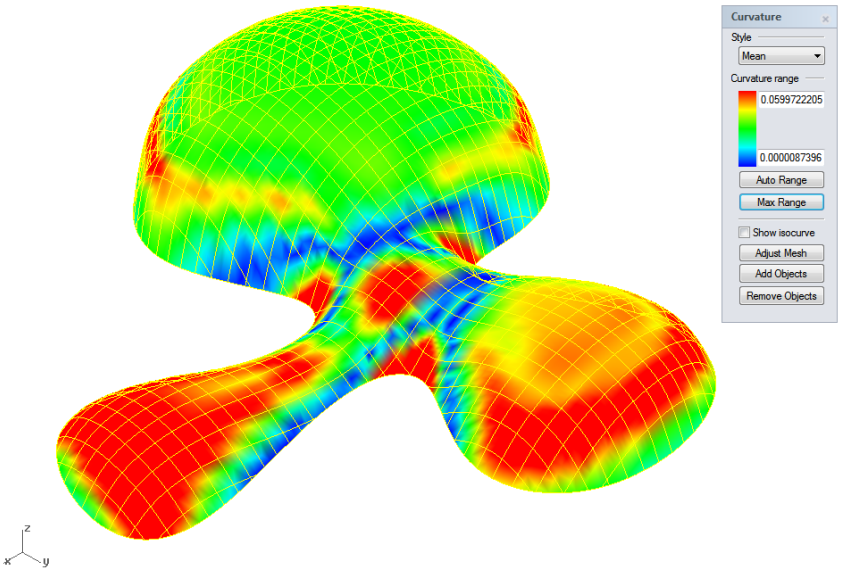

Figure 11.7: Mean curvature of the Case Study Building.

11-2-4 SHAPE FORMATTING

The formfinding definition in Grasshopper creates the geometry in the form of a “mesh” which is constructed from lines and nodes. However, Midas FX+ requires the geometry to be in the form of a “surface” which is constructed from curves and control points. Therefore, a function within Rhinoceros is used to create a surface which approximates the mesh from the formfinding process. The result of this function, Patch, can be seen below in Figure 11.8. This figure also includes a square cutting surface at Z=0, which will later be used by FX+ to create the shape for numerical analysis.

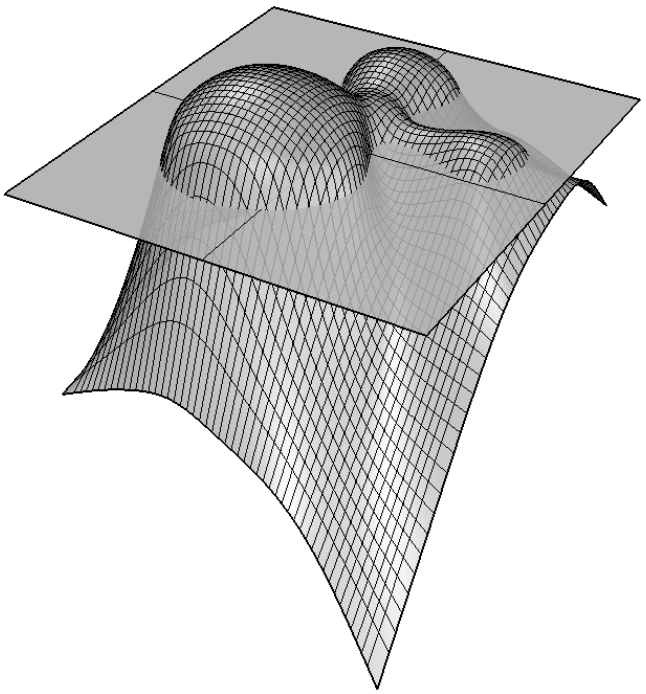

Figure 11.8: Patch surface approximation of the mesh created with Grasshopper and cutting surface at Z=0.

11-3 NUMERICAL ANALYSIS OVERVIEW

The FEM numerical analysis is performed in Diana. The material for the Case Study Building is assumed to be 20mm thick concrete with isotropic properties. It is loaded with a distributed gravity load of -7.2kN/m^2 in the Z-direction representing an exaggerated self-weight and a wind load of ±2.0kN/m^2 normal to the surface.

Table 11.1 Case Study Building load cases.

Load Case	Direction	Force	Rational
1: Gravity	Z	-0.0072 N/mm^2	Force of 300mm concrete = material + topping
2: Wind	Surface Normal	±0.002 N/mm^2	Exaggerated pressure and suction of 2kN/m^2
3: Construction	Surface Normal	+0.002 N/mm^2	Extra inflation pressure during construction

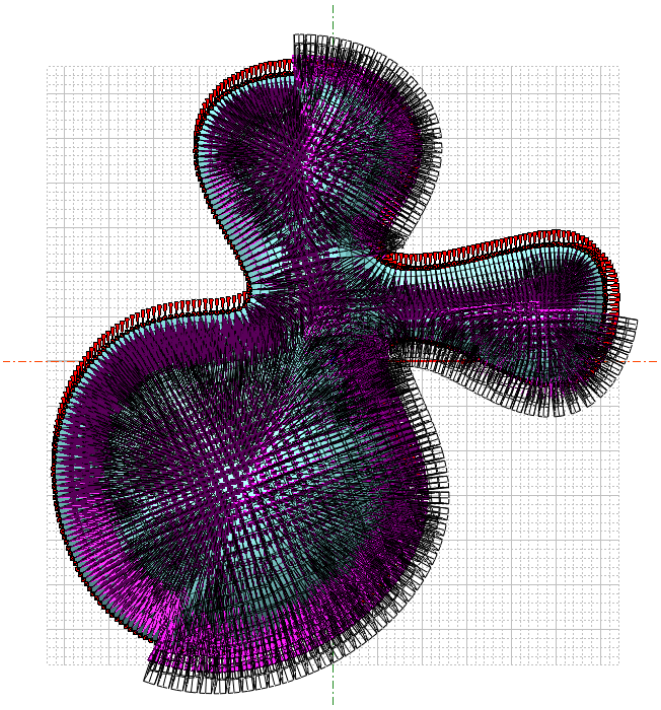

Figure 11.9: Load distribution for load case 2: Wind.

The building will be analyzed as a continuous structure although it would most likely involved discontinuities such as doors and windows. The reason for this is simplicity, to maintain the focus of the design on the material characteristics by eliminating these structural exceptions. First a uniform thickness, isotropic version of the building will be analyzed to establish a baseline of loaded behavior. These results will be used to create a second isotropic model with varying thickness, as if it were constructed of multiple layers of the material. Lastly this variable thickness model will be adapted in Drape to incorporate the specific orthotropic material characteristics of thickness and stiffness. This adapted orthotropic model will be the final model analyzed. By including the material information, this last orthotropic model aims to represent reality most closely. However since the specific material properties are unknown and over-estimated for this project, reality will most likely be somewhere between the isotropic and orthotropic models. The field of possible numerical models for the Case Study Building is shown in Figure 11.10. The computational element mesh for these models is created from the formfound geometry (Figure 11.8), which is imported to Midas FX+ where it is cut and meshed (Section 6-4-3). The result of this meshing can be seen in Figure 11.11.

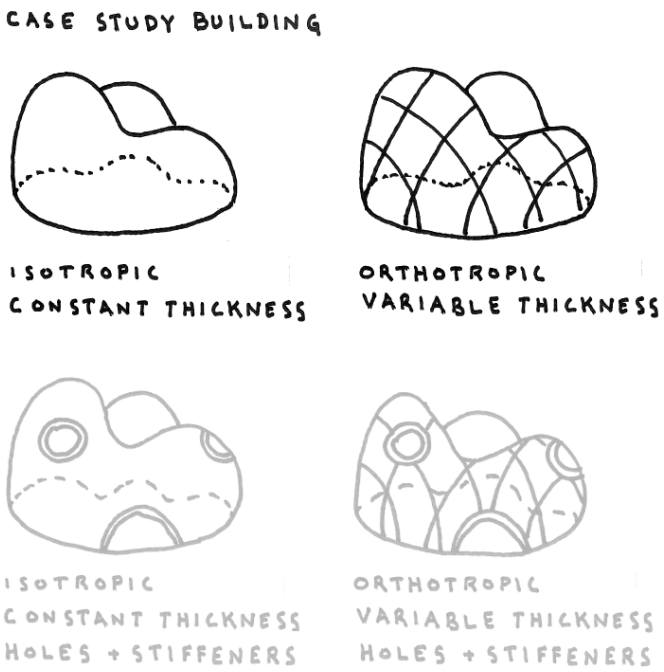

Figure 11.10: Field of numerical models for the Case Study Building, the top two will be created, the bottom two will not be.

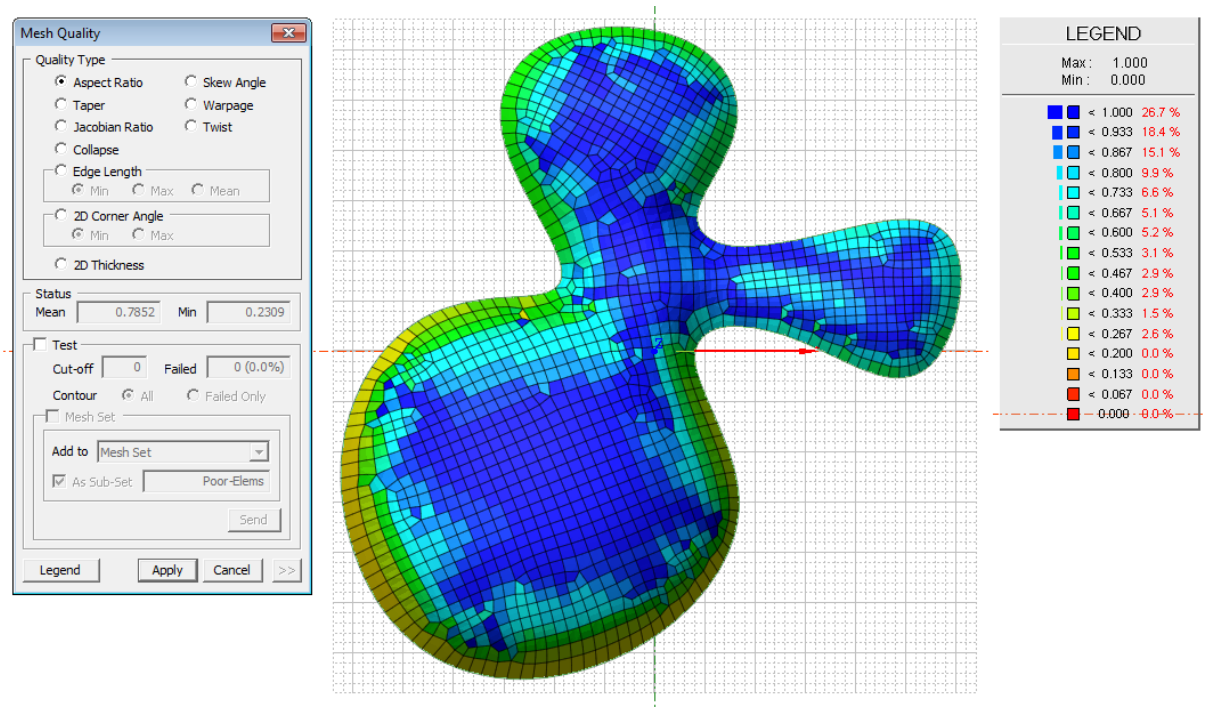

Figure 11.11: FEM meshing of the Case Study Building in Midas FX+ for numerical analysis in Diana.

11-4 INITIAL NUMERICAL ANALYSIS (CSB #1)

11-4-1 PRINCIPAL STRESSES (S_1 AND S_3)

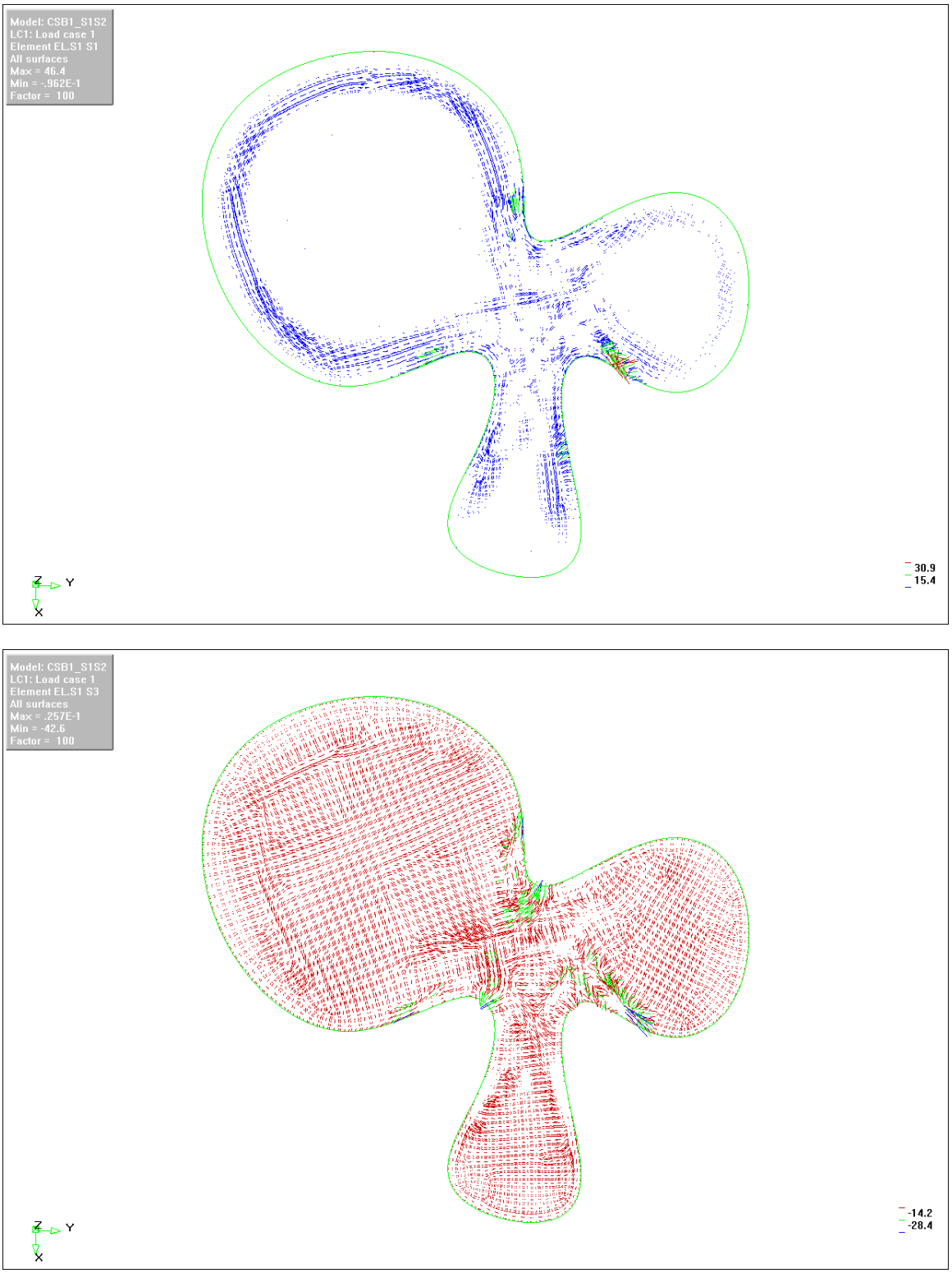

Figure 11.12: Case Study Building, load case 1: Principle stress vectors for tension (top) and compression (bottom).

11-4-2 INTERNAL FORCES (N_{XX} AND N_{YY})

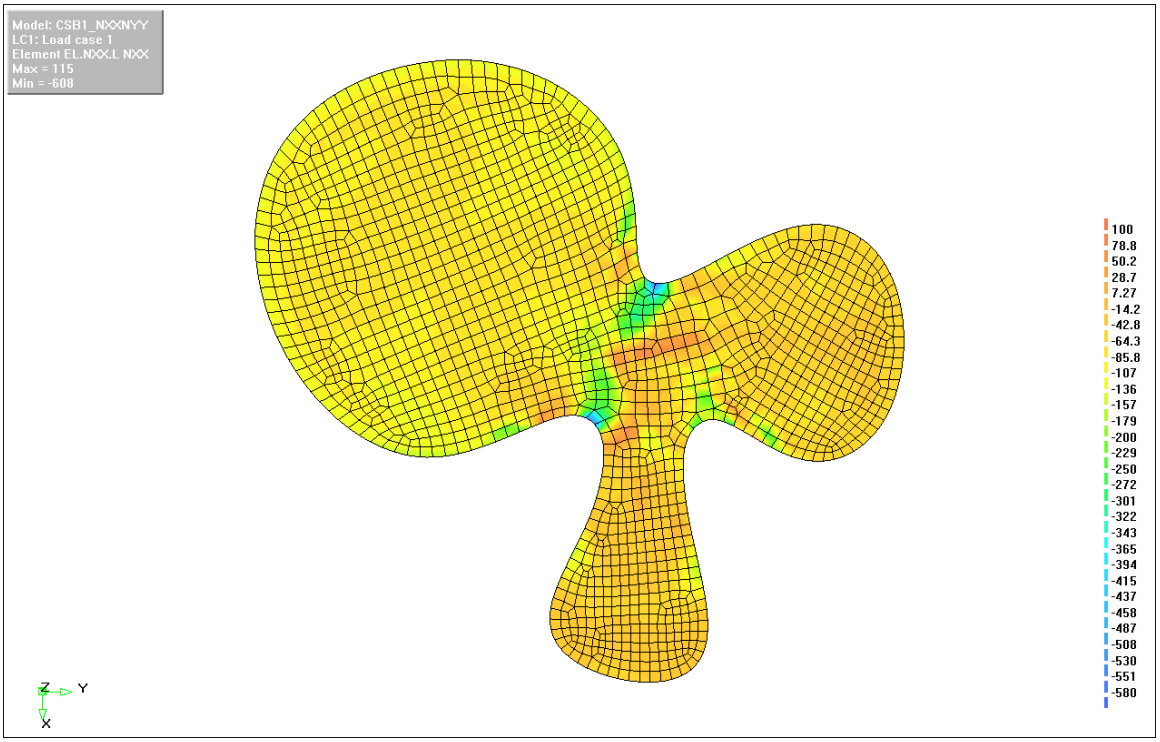

Figure 11.13: Case Study Building, load case 1: Internal (arch) forces in the surface X-direction (N_{xx}), in kilonewtons per meter, negative values represent compression.

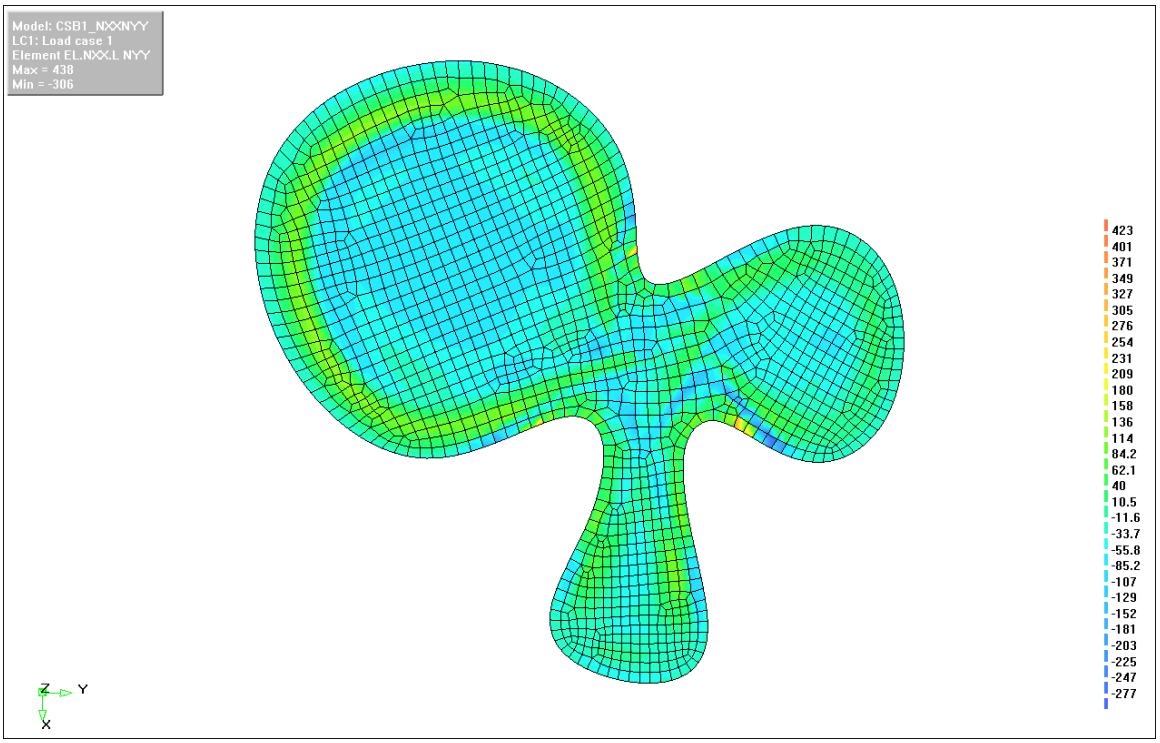

Figure 11.14: Case Study Building, load case 1: Internal (hoop) forces in the surface X-direction (N_{yy}), in kilonewtons per meter, negative values represent compression.

11-4-3 INTERNAL MOMENTS (M_{XY})

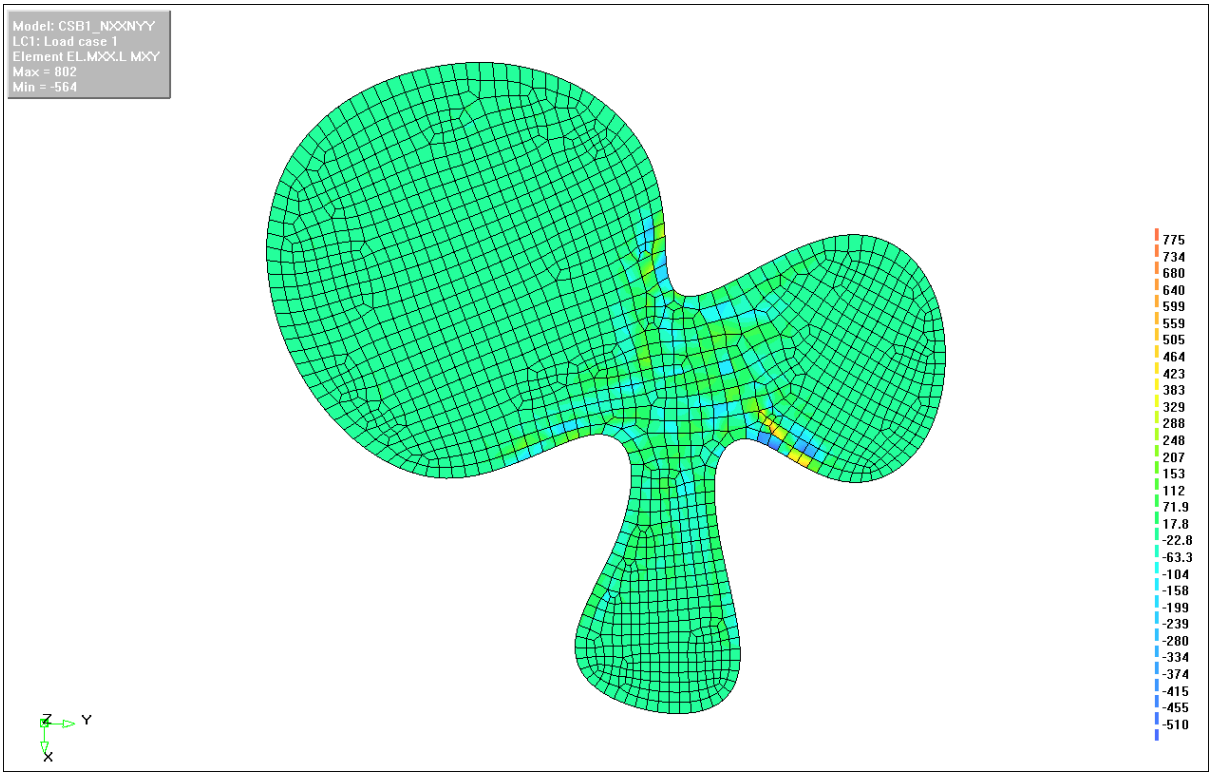

Figure 11.15: Case Study Building, load case 1: Internal bending moments about the surface XY-plane (M_{xy}), in newton-millimeters.

11-4-4 DEFORMATIONS (D_{RES})

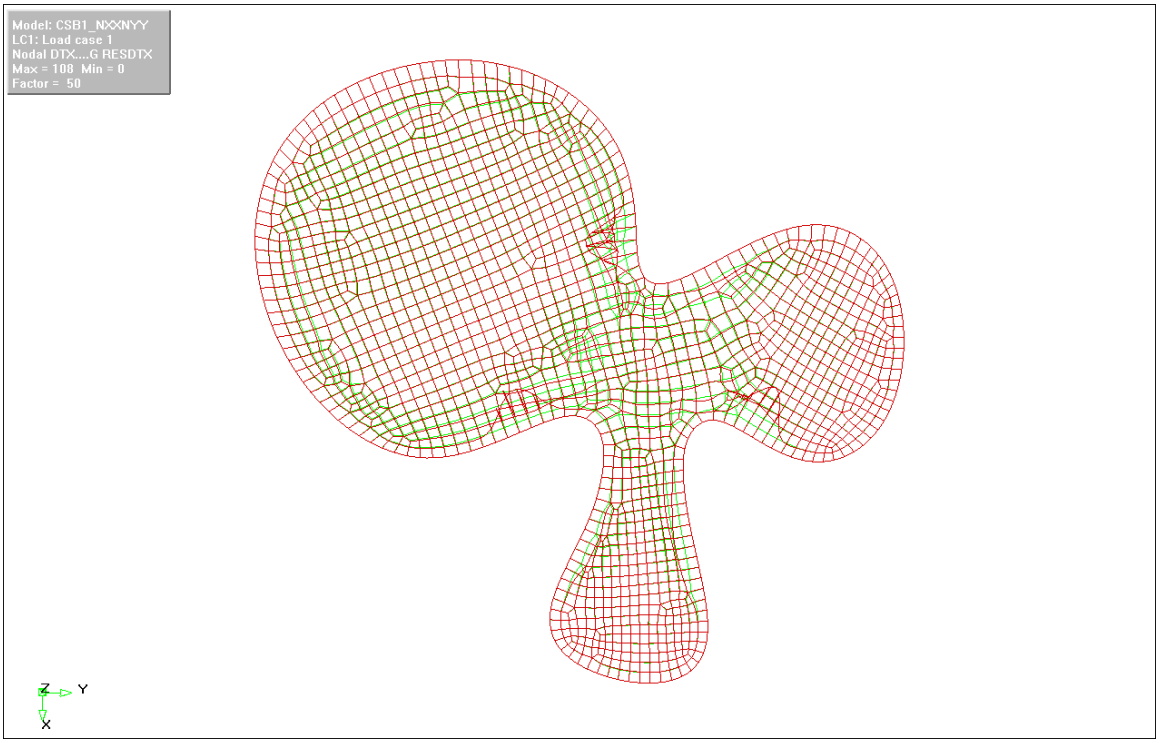

Figure 11.16: Case Study Building, load case 1: Deformed shape resolved from each direction (D_{Res}), three-quarters top view, exaggerated by a factor of 1000.

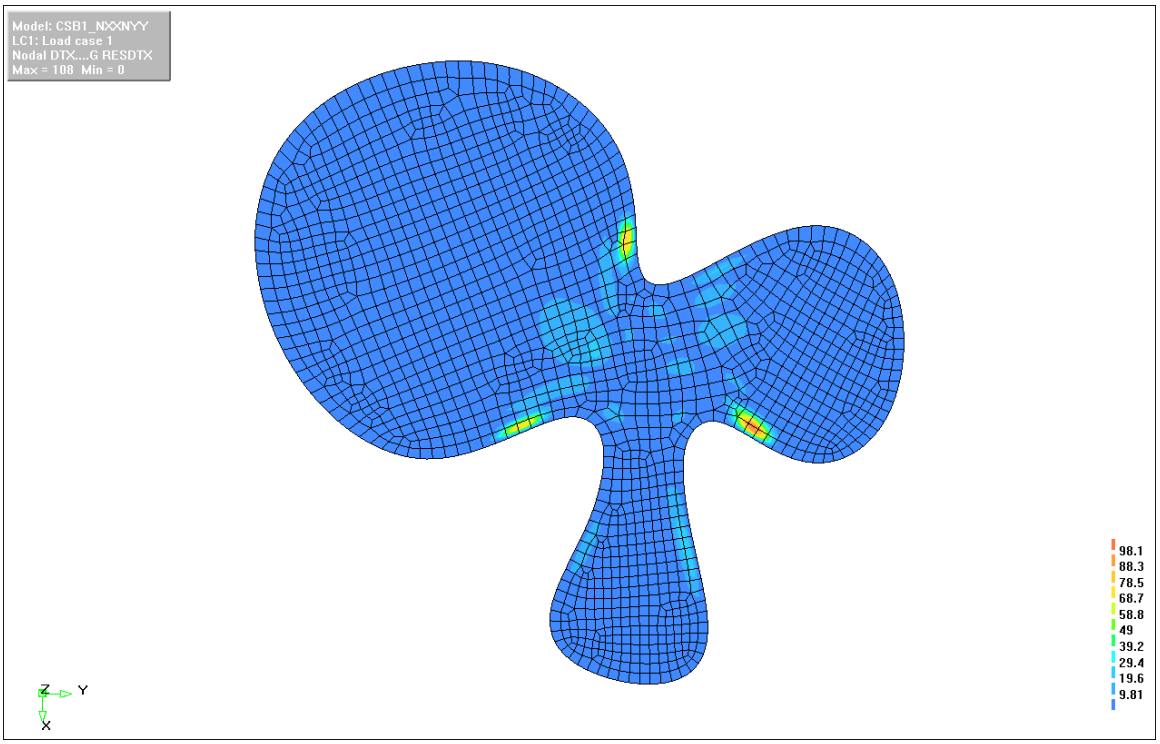

Figure 11.17 Case Study Building, load case 1: Deformation contour heat-map resolved from each direction (D_{Res}), three-quarters top view.

11-5 THICKNESS INCREASE

A proposed method for dealing with stresses which exceed the capacity of the base thickness (20mm) of the material is to layer the material (Section 5-4-2). Two arrangements of thickness increase by layer have been selected and are shown below, in Figure 11.18.

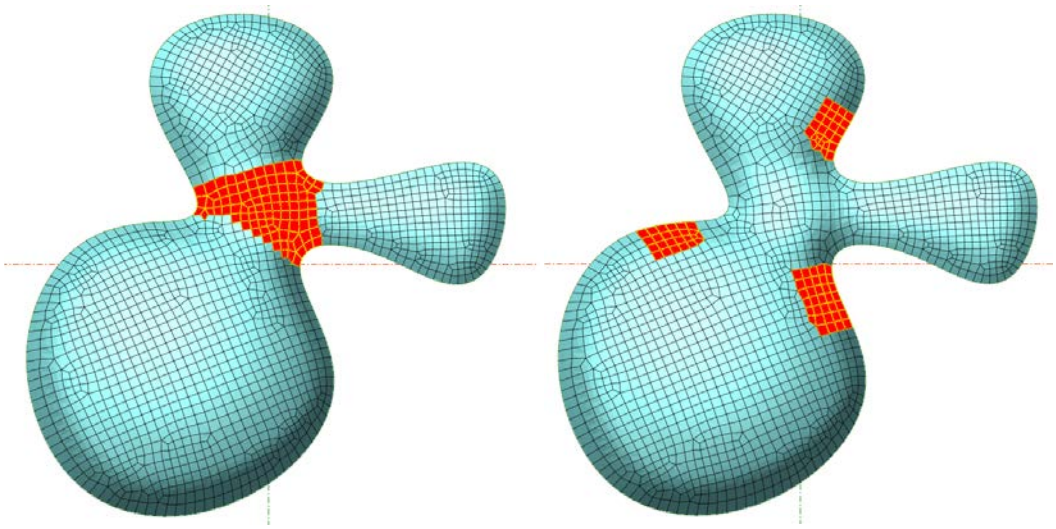

Figure 11.18: Two options for areas of thickness increase for the Case Study Building, Saddle (left) and Patches (right), top view.

The first option, Saddle, where thickness increase was concentrated in the central section, was the first to be analyzed, but ultimately not selected. It performed poorly even at four layers (80mm) of material. The rational for increasing thickness in this region was to isolate the fingers as individual domes. This large thickness increase only slightly decreased the overall deformation of the structure, from 108mm to 102mm, as shown below in Figure 11.19. The second option, Patches, had superior performance with only one additional layer (40mm) of thickness increase, which decreased the overall deformation from 108mm to an acceptable 26.7mm. It will be covered in the following section, 11.6.

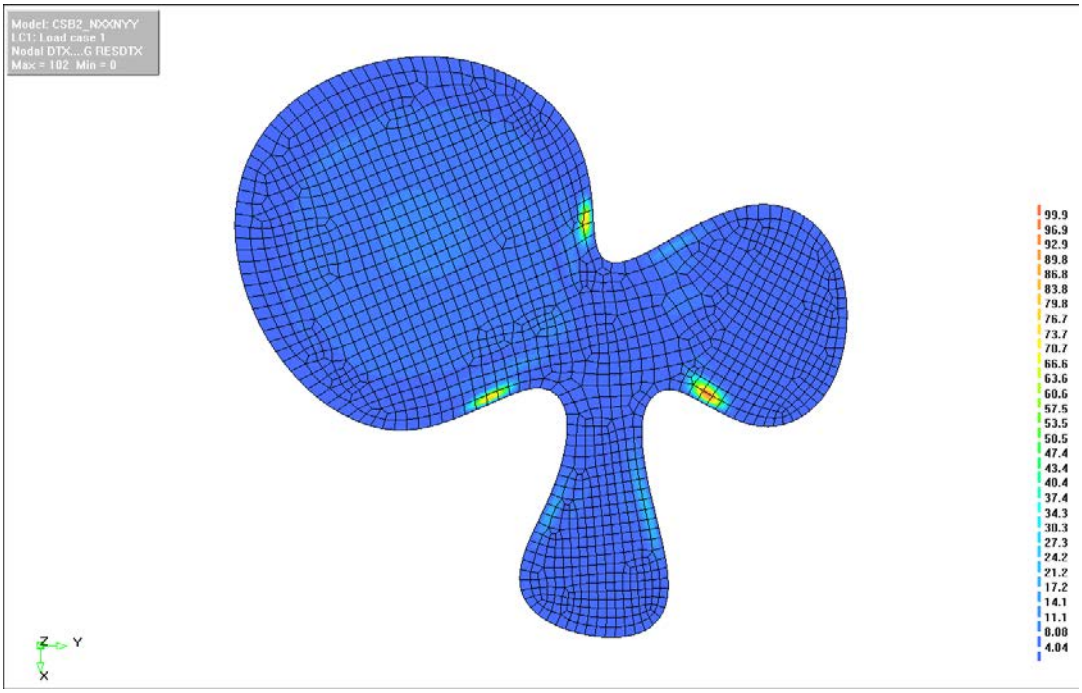

Figure 11.19: Thickness increase option 1, Saddle, load case 1: Deformation contours. (Case Study Building #2)

11-6 ISOTROPIC NUMERICAL ANALYSIS (CSB #3)

This model of the Case Study Building treats the material as isotopic concrete with a constant thickness (20mm) except for the layered areas which have a constant thickness equal to two layers of material (40mm). The areas of increased thickness are shown, at the right of Figure 11.18.

11-6-1 PRINCIPAL STRESSES (S_1 AND S_3)

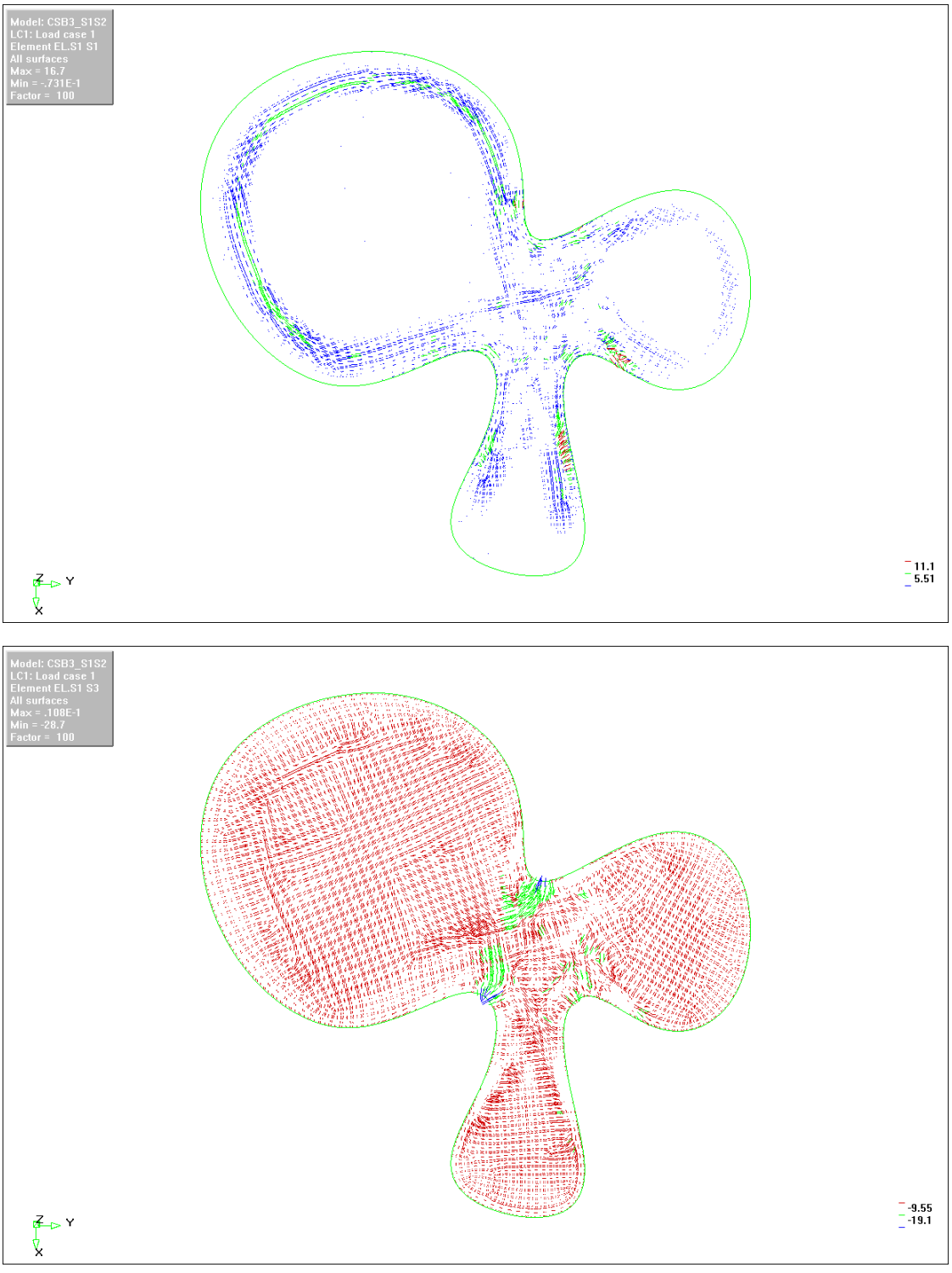

Figure 11.20: Case Study Building, load case 1: Principle stress vectors for tension (top) and compression (bottom).

11-6-2 INTERNAL FORCES (N_{XX} AND N_{YY})

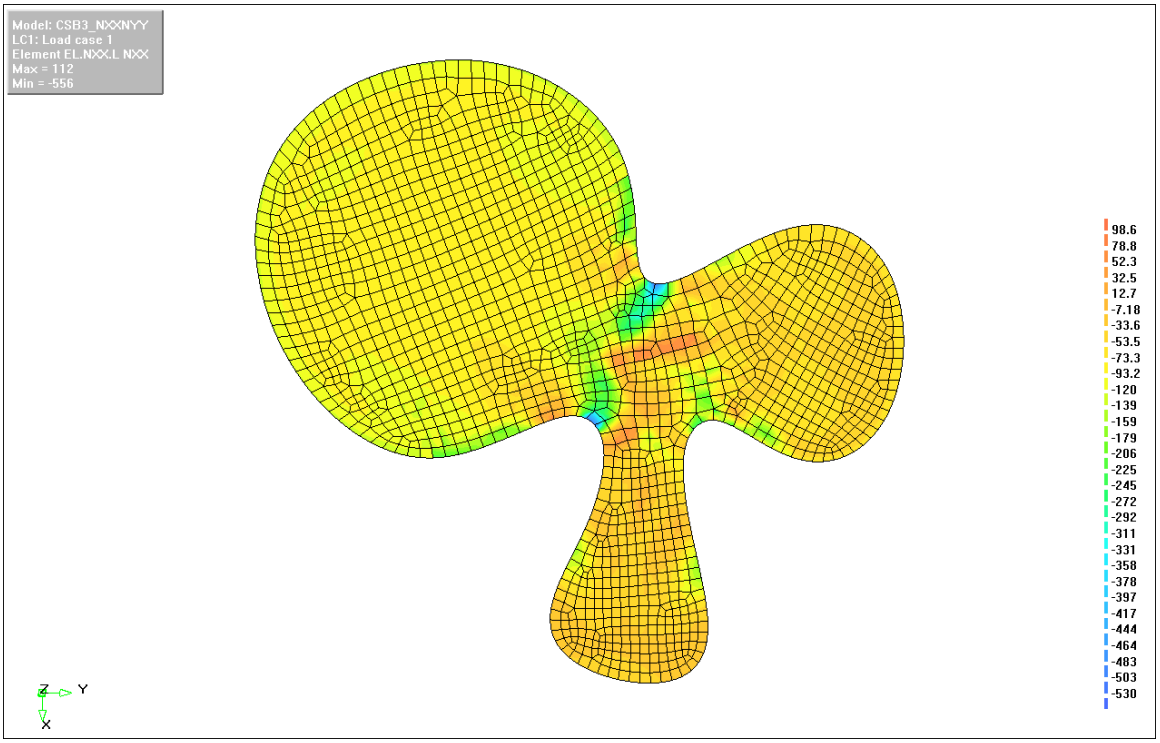

Figure 11.21: Case Study Building, load case 1: Internal (arch) forces in the surface X-direction (N_{xx}), in kilonewtons per meter, negative values represent compression.

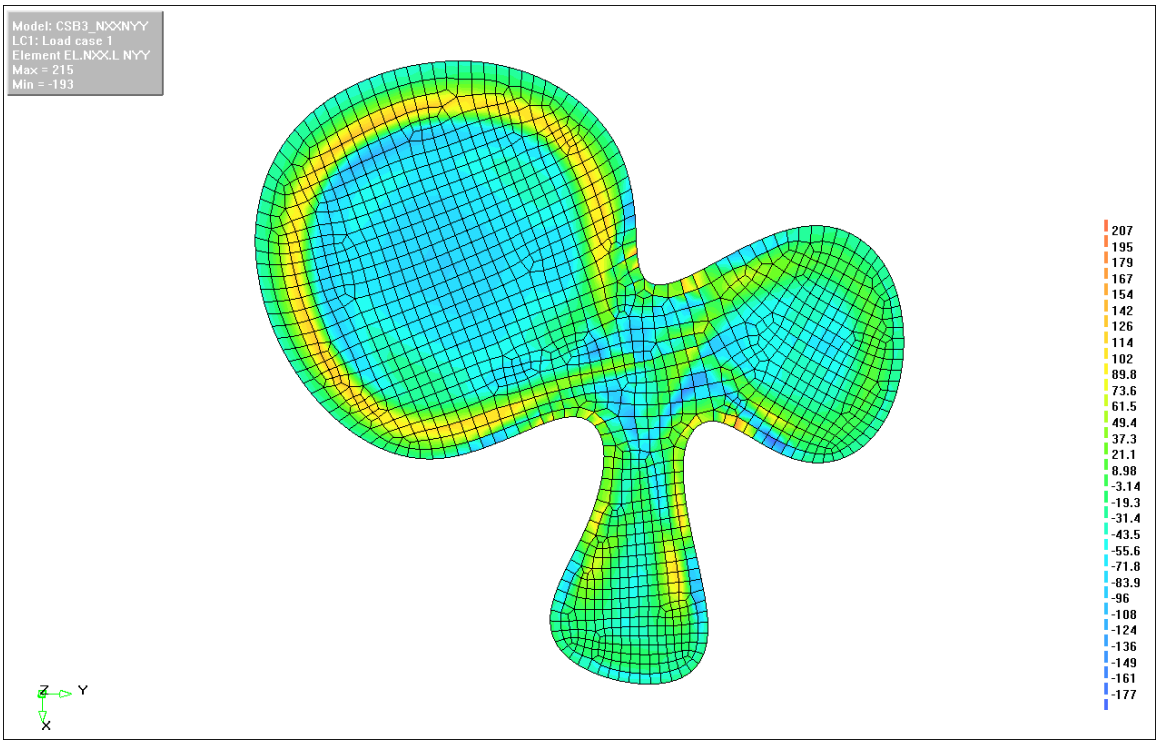

Figure 11.22: Case Study Building, load case 1: Internal (hoop) forces in the surface X-direction (N_{yy}), in kilonewtons per meter, negative values represent compression.

11-6-3 INTERNAL MOMENTS (M_{XY})

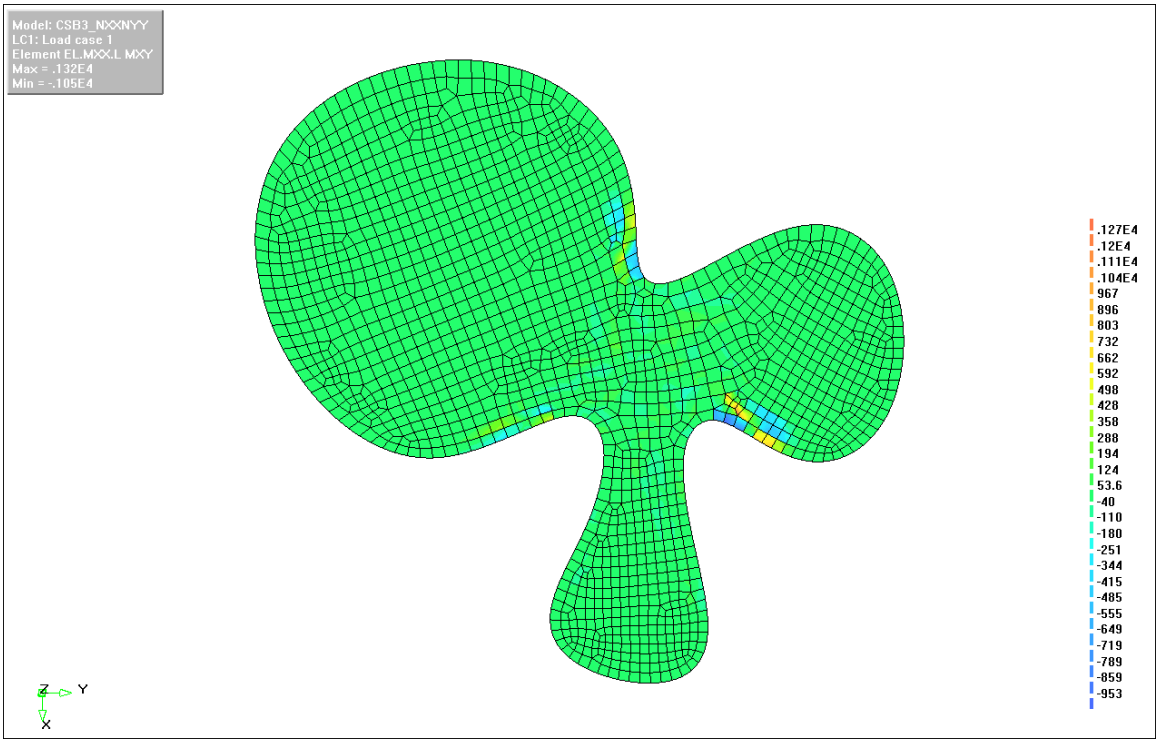

Figure 11.23: Case Study Building, load case 1: Internal bending moments about the surface XY-plane (M_{xy}), in newton-millimeters.

11-6-4 DEFORMATIONS (D_{RES})

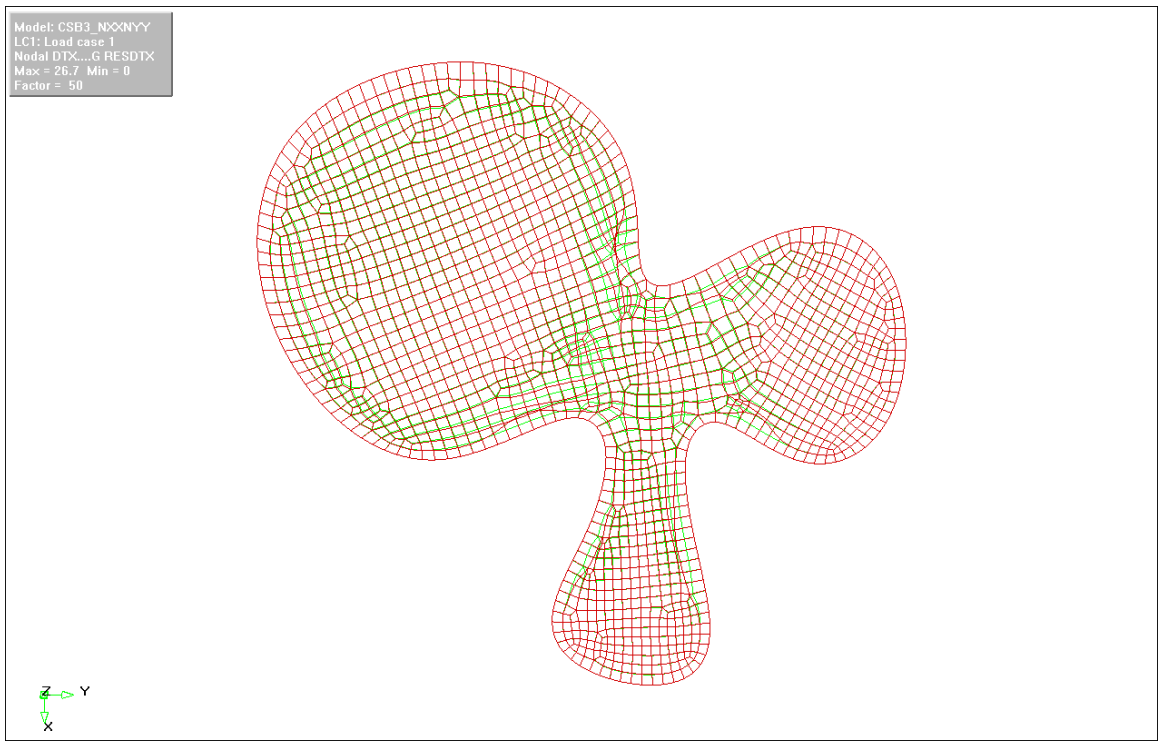

Figure 11.24: Case Study Building, load case 1: Deformed shape resolved from each direction (D_{Res}), three-quarters top view, exaggerated by a factor of 1000.

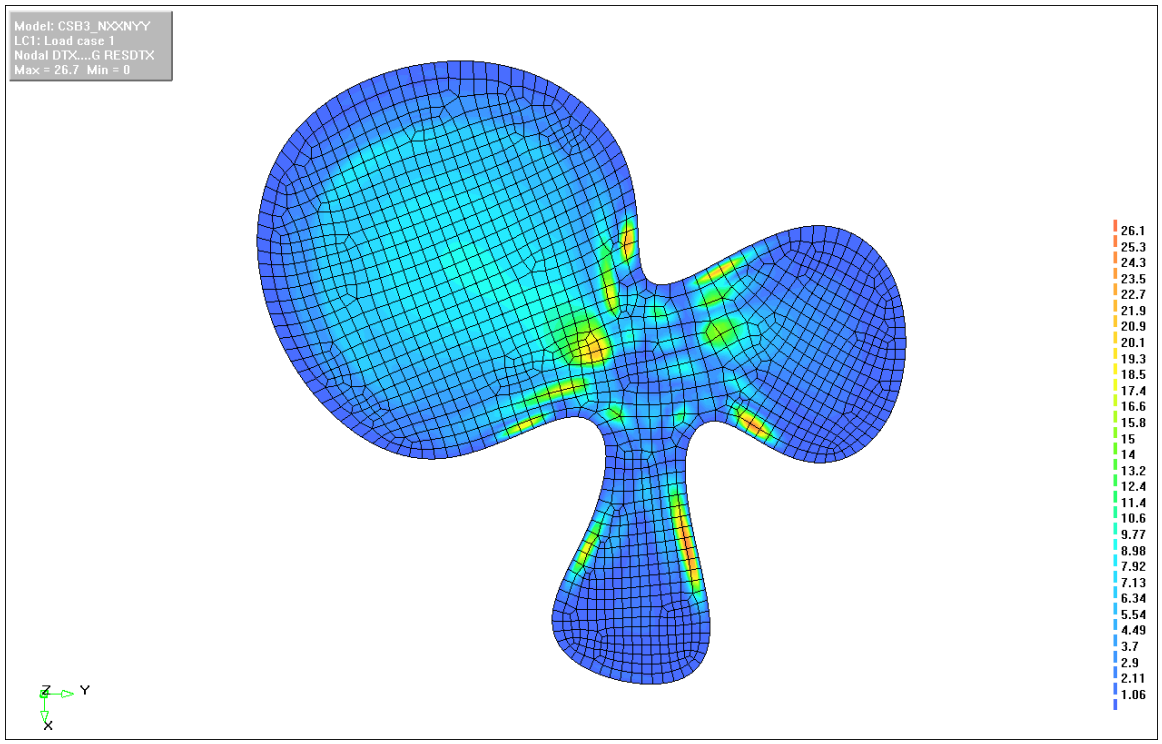

Figure 11.25: Case Study Building, load case 1: Deformation contour heat-map resolved from each direction (D_{Res}), three-quarters top view.

11-7 DRAPING

The Case Study Building is broken in to three structural bays (Section 10-2) in order to limit the shear deformation and enable construction. Drape is used for this as well as to apply the deformed-material's characteristics and add the additional layers to the model for analysis in Diana. The topology of the structural bays and the relative placement of the additional layers are shown below in Figure 11.26. Then the material properties are selected, similar to the process for the test shape in Section 6-4-7, this is shown in Figure 11.27. Drape applies a textile, representing the reinforcement of the new material, to each structural bay. This process is modified and repeated until each bay is successfully covered without the material shearing below an angle of 40-degrees, as outlined in Section 5-1-3. The result of this process is shown below in Figure 11.28.

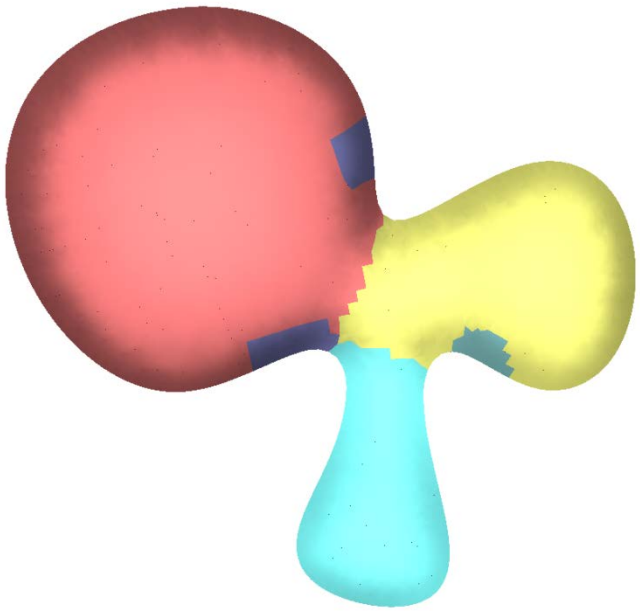

Figure 11.26: Case Study Building divided in to structural bays (red, yellow, and blue), showing the three double layered areas (dark blue).

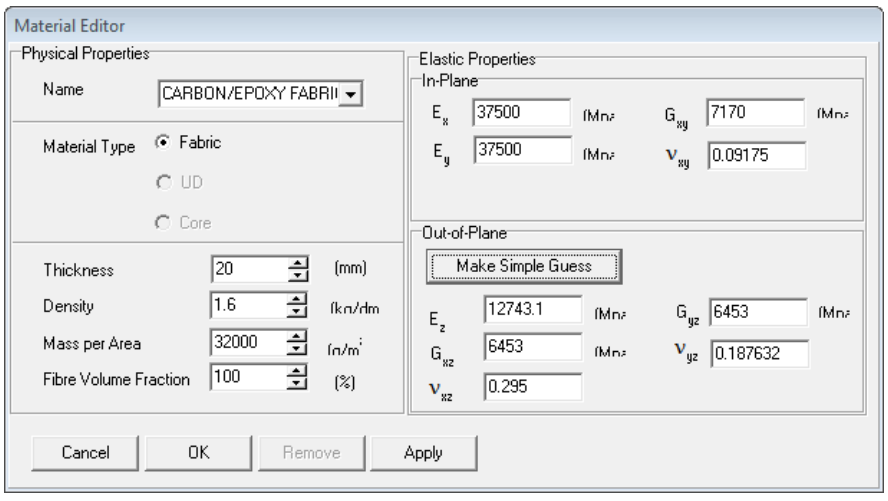

Figure 11.27: Material properties for a single layer of the undeformed material in Drape.

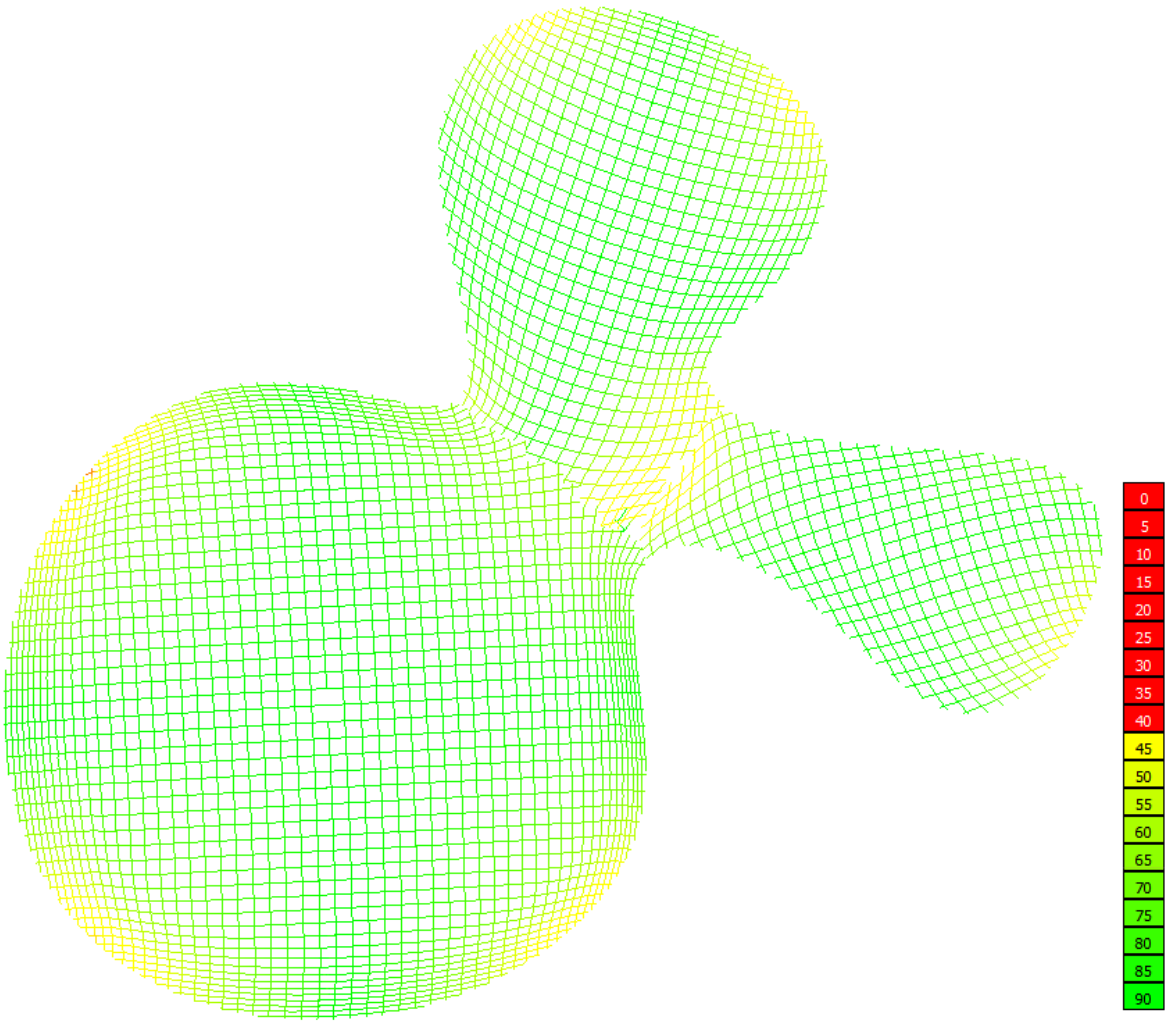

Figure 11.28: Case Study Building covered with the one-meter wide material in Drape, color shows deformed angle between reinforcement, red represents angles at or below 40°.

11-8 VARIABLE THICKNESS (CSB #4)

The variable thickness is determined by the computer program Drape. It computes thickness bases on the angle of shear deformation. This is explained in Section 4-2-2.

11-8-1 PRINCIPAL STRESSES (S_1 AND S_3)

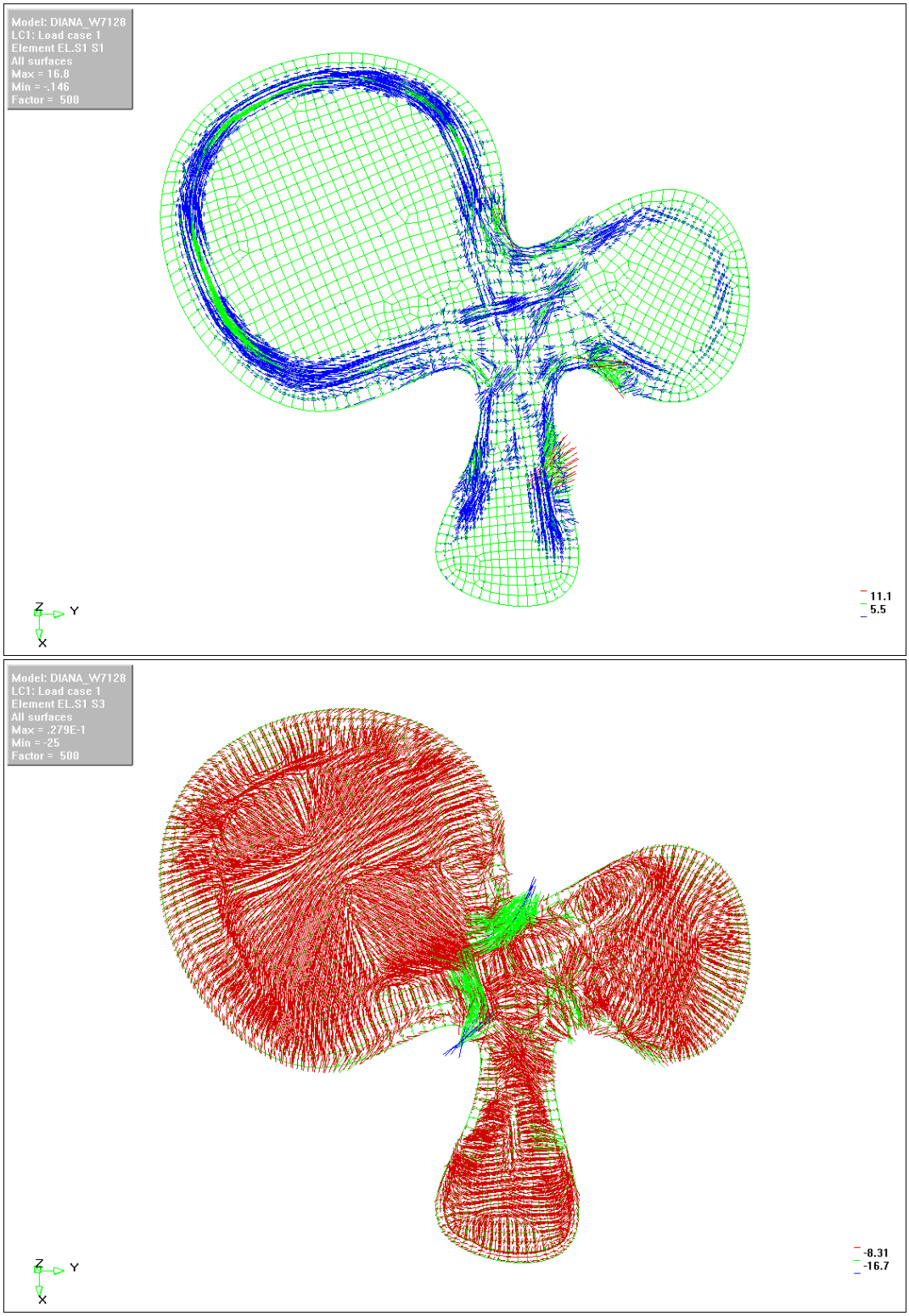

Figure 11.29: Case Study Building, Variable Thickness, load case 1: Principle stress vectors for tension (top) and compression (bottom), top view.

11-8-2 INTERNAL FORCES (N_{XX} AND N_{YY})

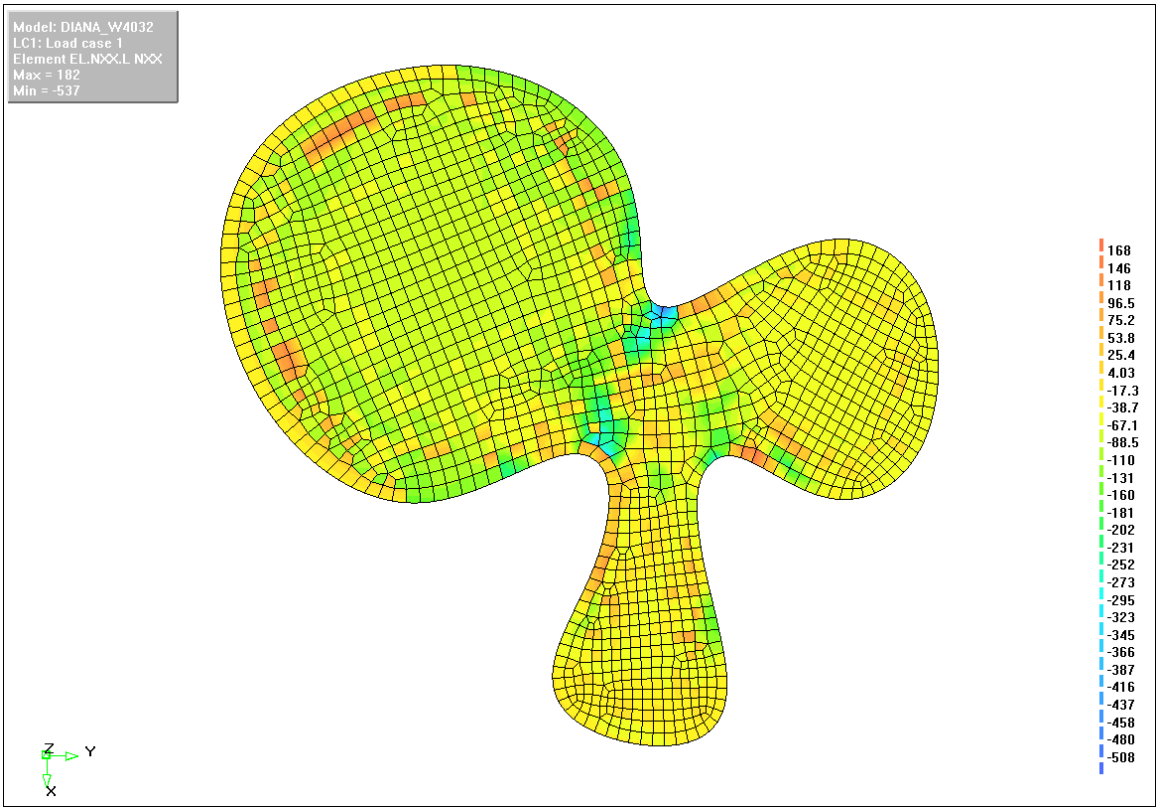

Figure 11.30: Case Study Building, Variable Thickness, load case 1: Internal (arch) forces in the surface X-direction (N_{xx}), in kilonewtons per meter, negative values represent compression, top view.

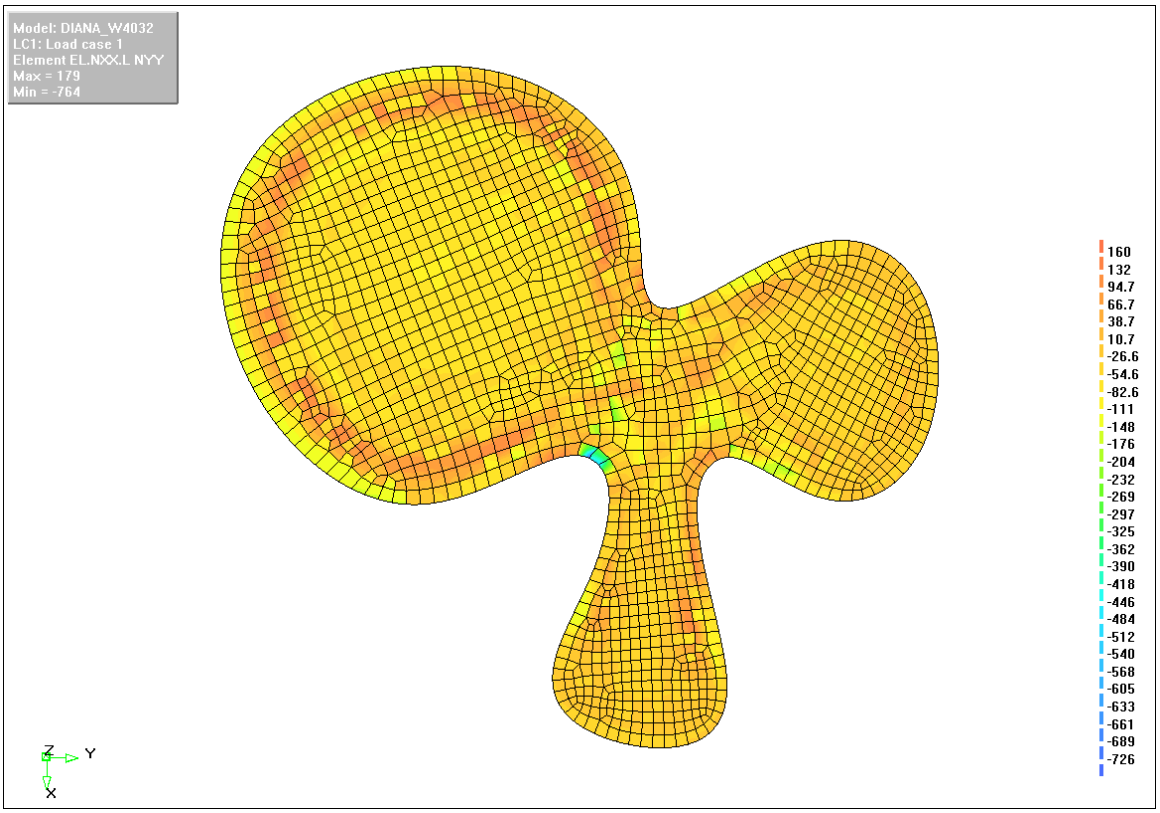

Figure 11.31: Case Study Building, Variable Thickness, load case 1: Internal (hoop) forces in the surface X-direction (N_{yy}), in kilonewtons per meter, negative values represent compression, top view.

11-8-3 INTERNAL MOMENTS (M_{XY})

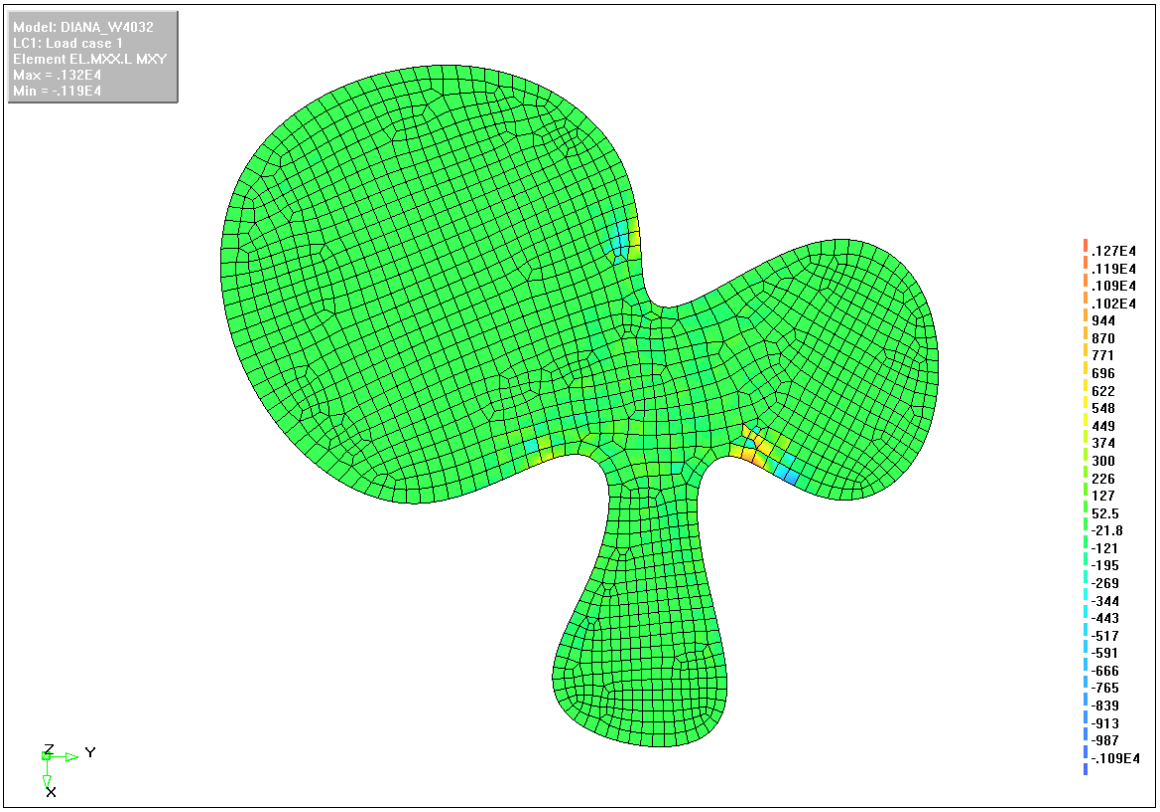

Figure 11.32: Case Study Building, Variable Thickness, load case 1: Internal bending moments about the surface XY-plane (M_{xy}), in newton-millimeters, top view.

11-8-4 DEFORMATIONS (D_{RES})

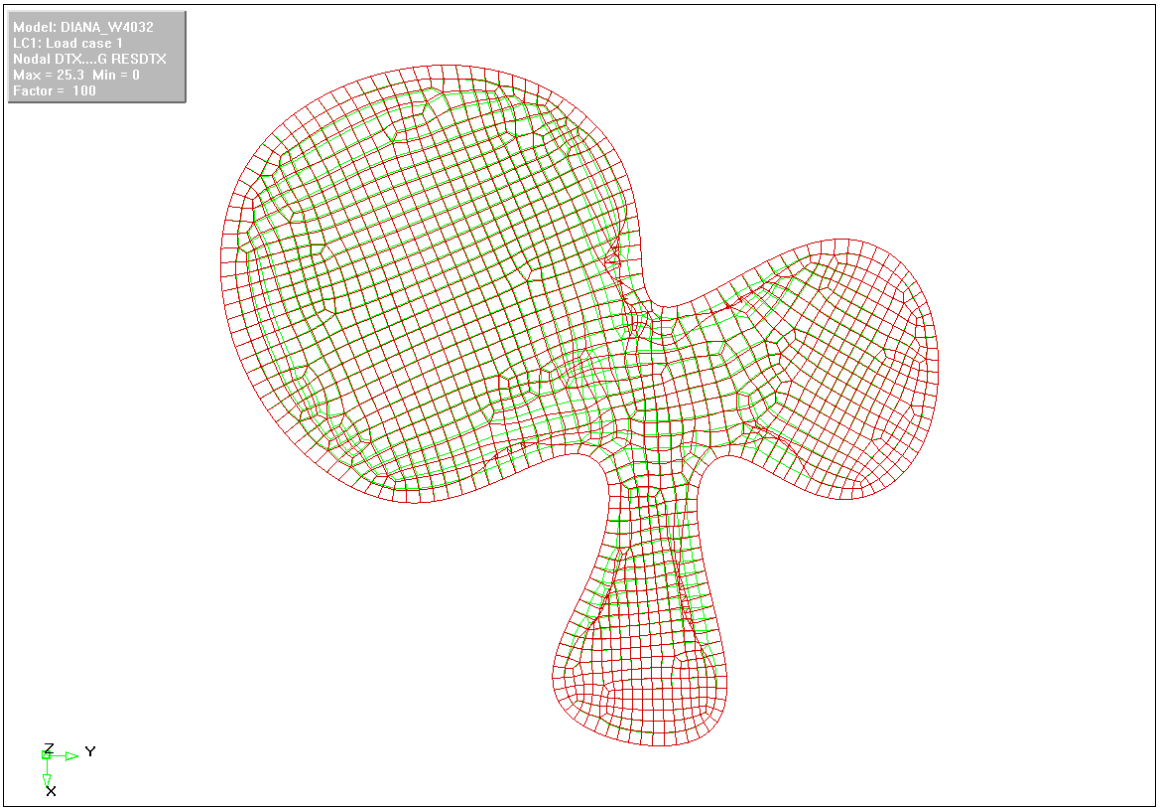

Figure 11.33: Case Study Building, Variable Thickness, load case 1: Deformed shape resolved from each direction (D_{Res}), top view, exaggerated by a factor of 100.

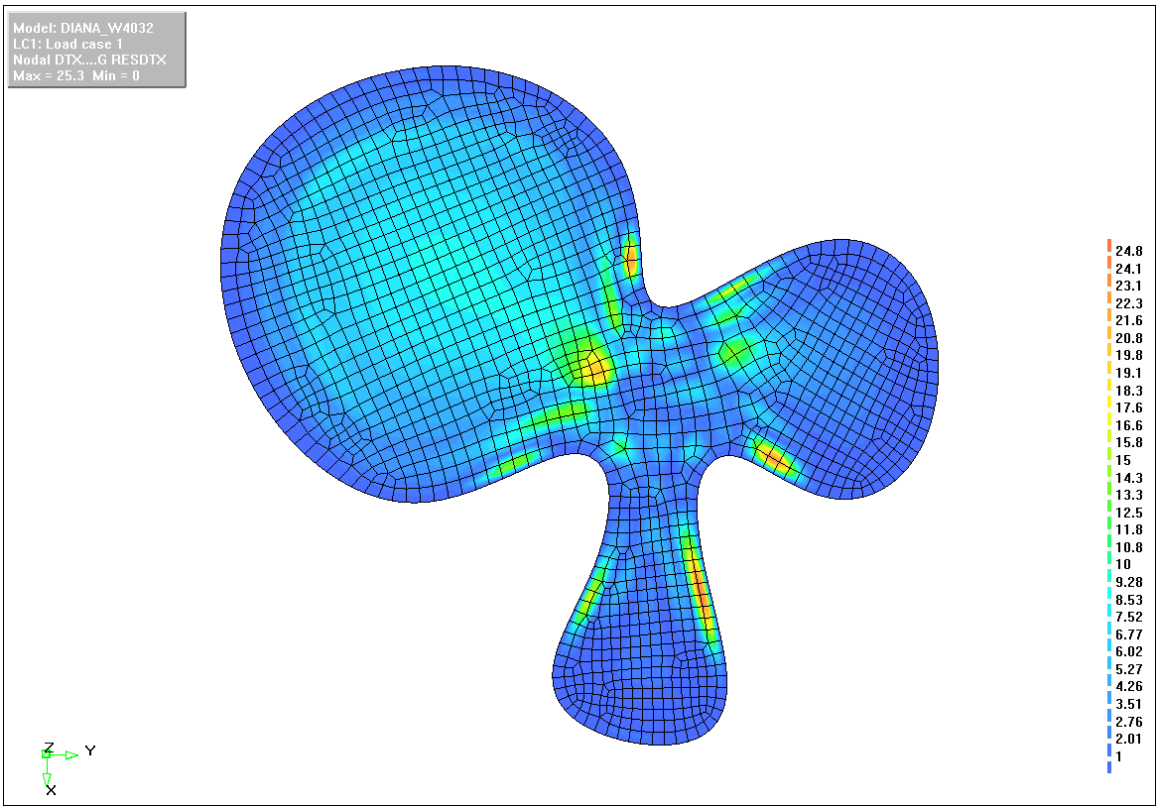

Figure 11.34: Case Study Building, Variable Thickness, load case 1: Deformation contour heat-map resolved from each direction (D_{Res}), top view.

11-9 ORTHOTROPIC NUMERICAL ANALYSIS (CSB #5)

After the Case Study Building model has been created with the material properties using Drape, it is analyzed once more in Diana.

11-9-1 PRINCIPAL STRESSES (S_1 AND S_3)

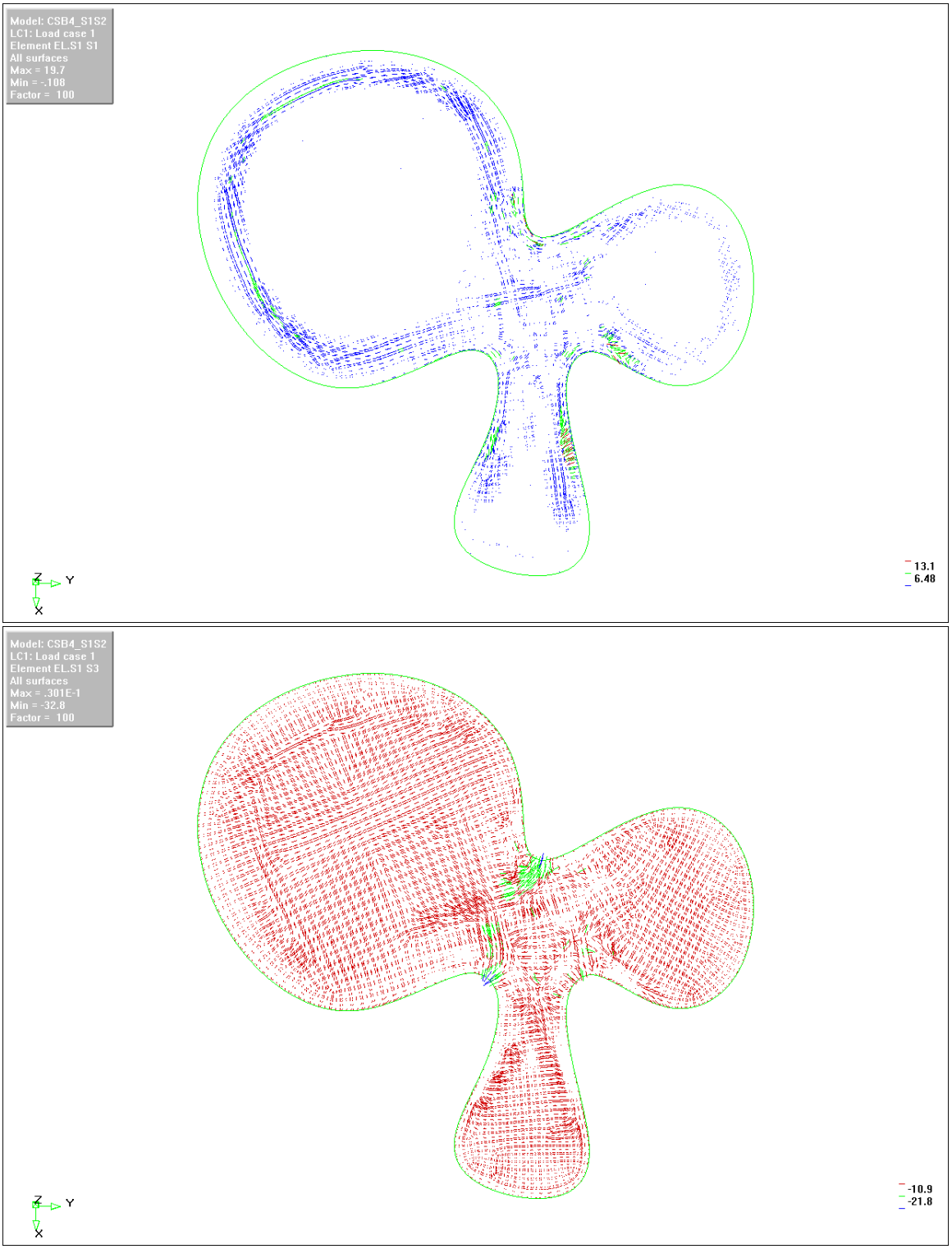

Figure 11.35: Case Study Building, load case 1: Principle stress vectors for tension (top) and compression (bottom).

11-9-2 INTERNAL FORCES (N_{XX} AND N_{YY})

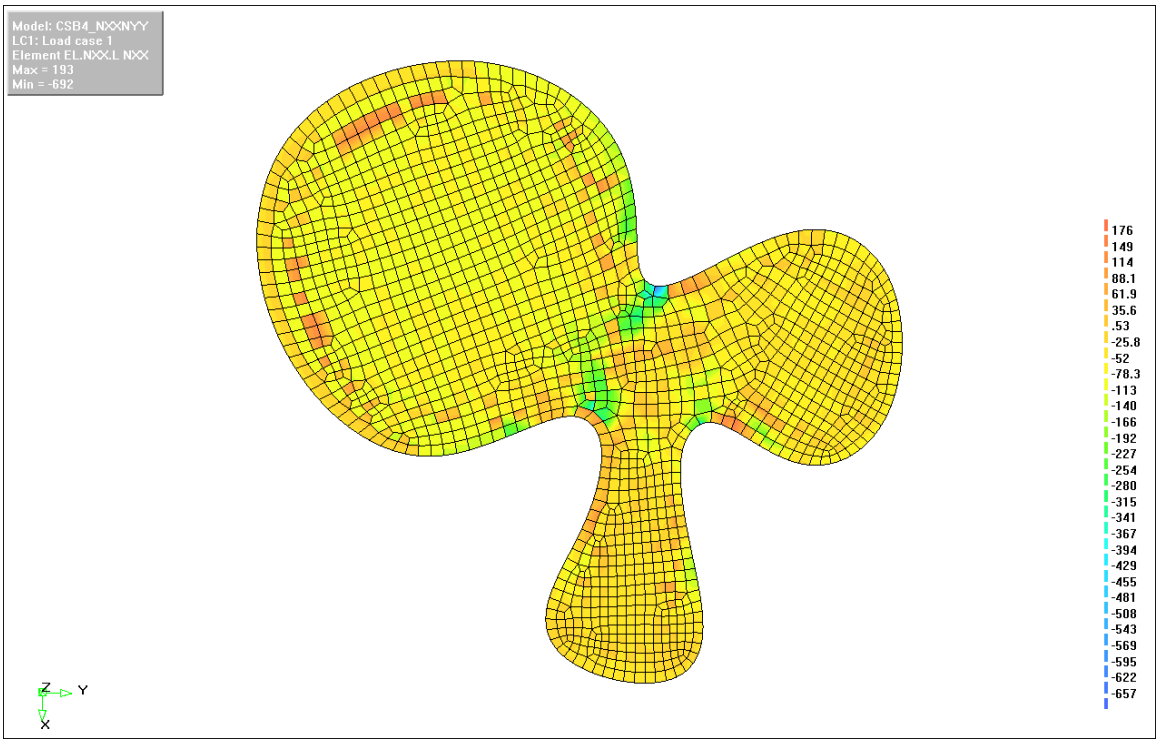

Figure 11.36: Case Study Building, load case 1: Internal (arch) forces in the surface X-direction (N_{xx}), in kilonewtons per meter, negative values represent compression.

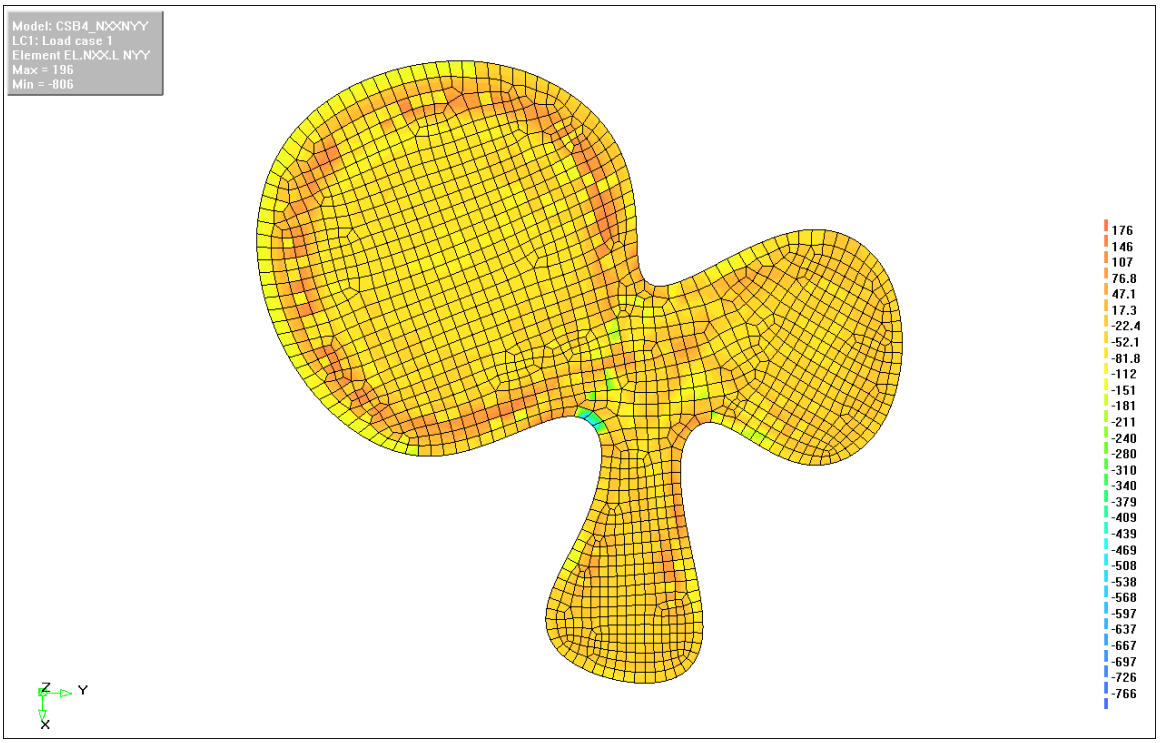

Figure 11.37: Case Study Building, load case 1: Internal (hoop) forces in the surface X-direction (N_{yy}), in kilonewtons per meter, negative values represent compression.

11-9-3 INTERNAL MOMENTS (M_{XY})

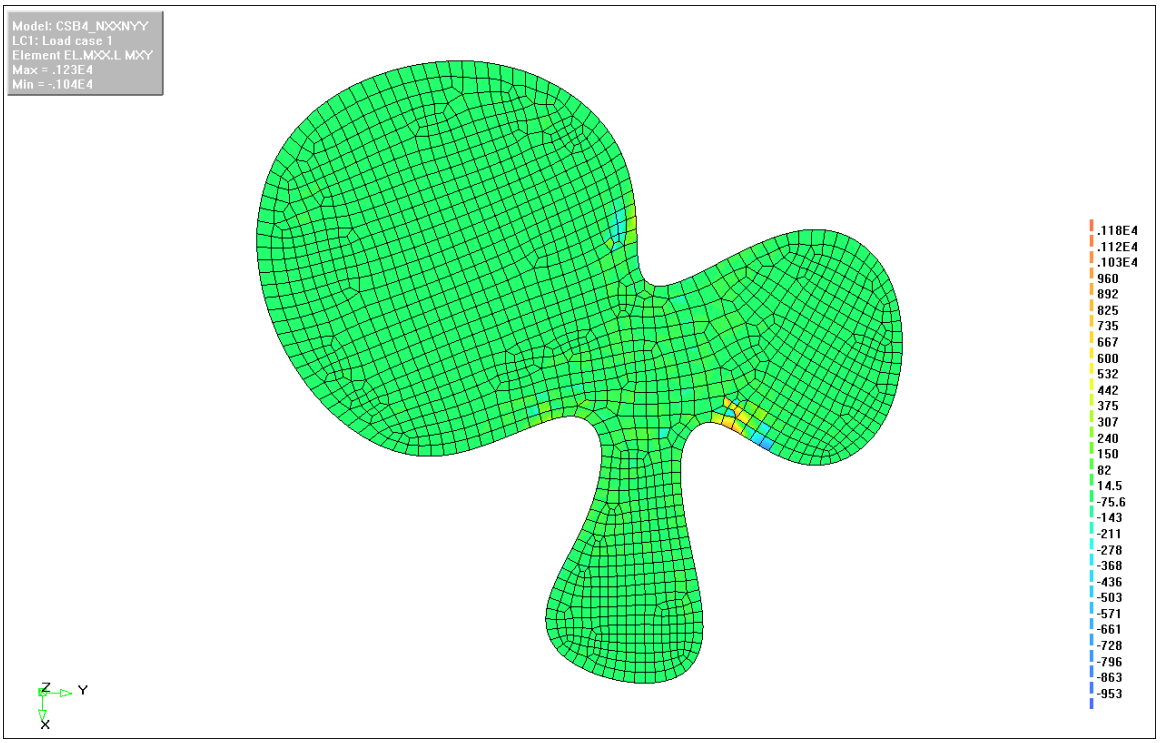

Figure 11.38: Case Study Building, load case 1: Internal bending moments about the surface XY-plane (M_{xy}), in newton-millimeters.

11-9-4 DEFORMATIONS (D_{RES})

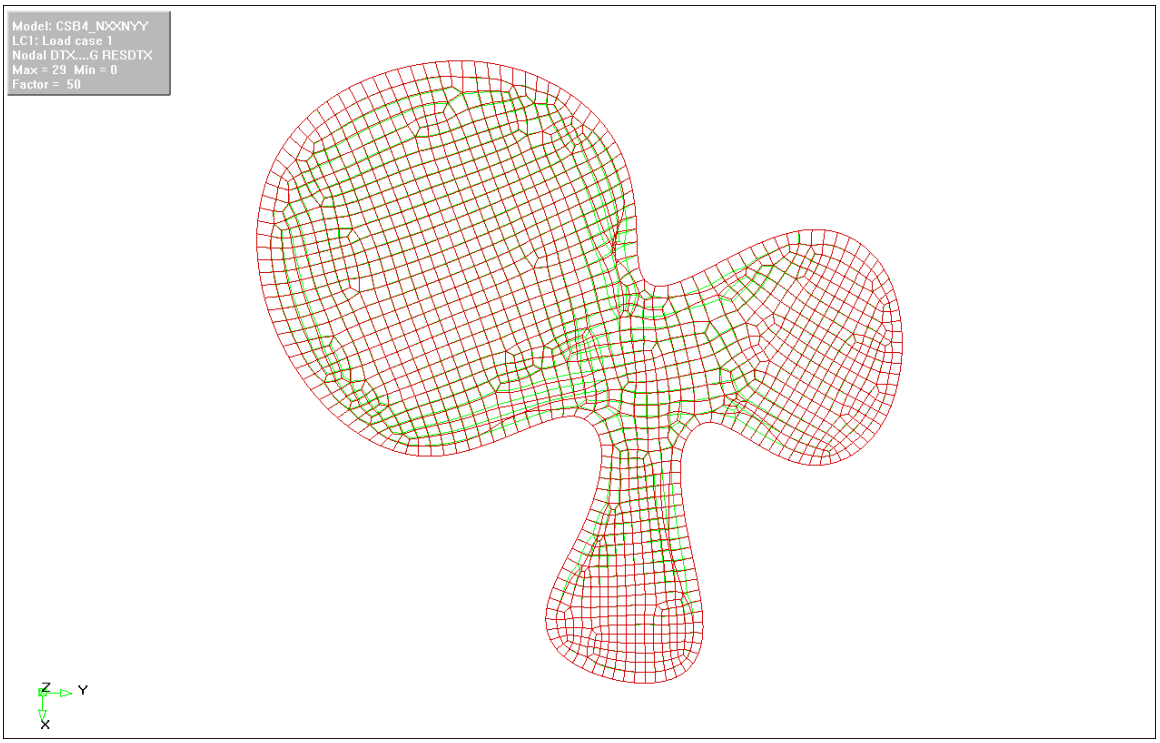

Figure 11.39: Case Study Building, load case 1: Deformed shape resolved from each direction (D_{Res}), top view, exaggerated by a factor of 50.

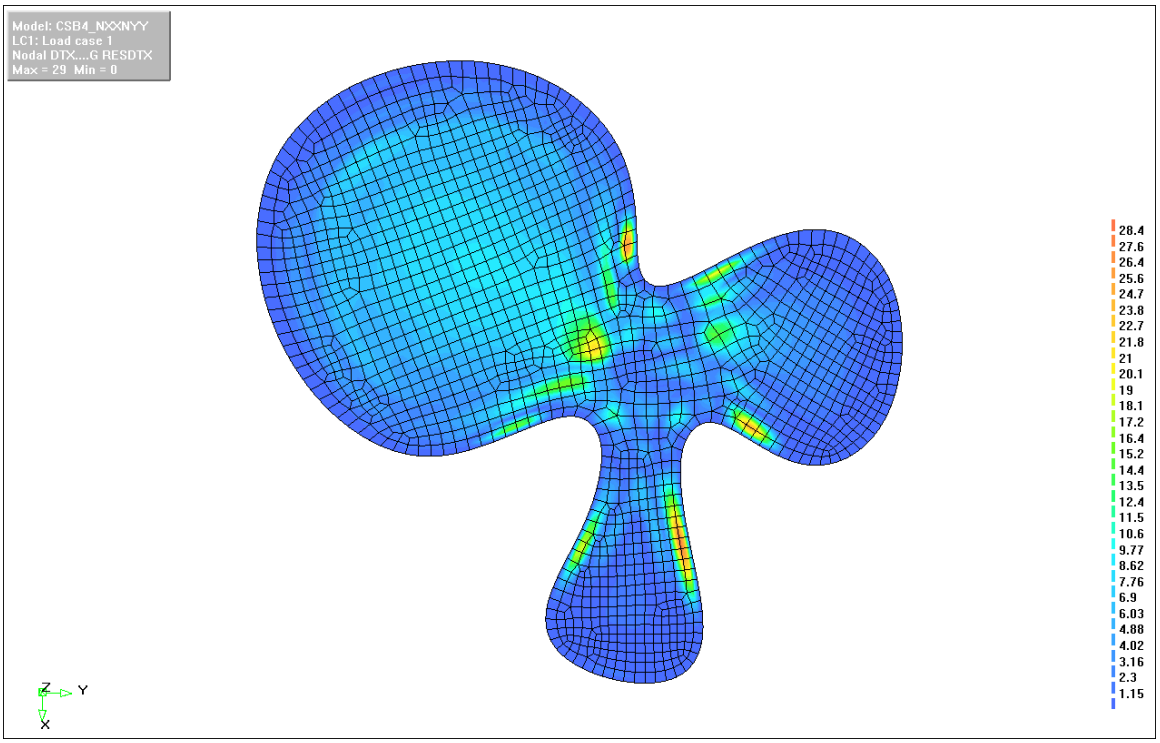

Figure 11.40: Case Study Building, load case 1: Deformation contour heat-map resolved from each direction (D_{Res}), top view.

11-10 STRESS CHECKS

The case study building is constructed of the same type of material as determined from the test shape in Section 6-6-4. The assumed cross section contains 3.286mm of glass fiber and 17mm of concrete. The largest compressive stress of all models (42.6MPa) was found to be significantly under the maximum compressive stress of the fine-grained concrete as described by Hegger (78.3MPa, Section 4-4-4) and therefore won't be analyzed further. For tensile loading epoxy impregnated reinforcement is assumed with an efficiency of k_1 = 0.6 (Section 6-6-1). The compressive stress values assume high-strength concrete, as used by Hegger (Section 4-4-4). Equations 6.10 and 6.11 for determining the tensile stress capacity are reproduced here as Equations 11.1 and 11.2. The tensile stress capacity is determined by the shear angle of the material and loading angle (by way of the Modified Oblique-Loading Coefficient, $k_{0,\alpha,Modified}$).

$$\begin{aligned} F_{ctu} &= A_t \times f_t \times k_1 \times k_{0,\alpha,Modified} \times k_2 \\ &= 3286mm^2 \times 0.533\frac{kN}{mm^2} \times 0.6 \times k_{0,\alpha,Modified} \times 1.0 \\ &= 1051kN \times k_{0,\alpha,Modified} \end{aligned}$$

Equation 11.1: Material tensile force capacity in terms of the Modified Oblique-Loading Coefficient.

$$Tensile\ Stress\ Capacity\ (MPa) = \frac{F_{ctu}}{Cross\ Section\ Area} = \frac{1051kN \times k_{0,\alpha,Modified}}{1000mm \times 20mm \times (1/\sin\alpha)}$$

Equation 11.2: Material tensile stress capacity (of the entire material) in terms of the Modified Oblique-Loading Coefficient and shear deformation angle.

Every element used in the FEM calculation (Figure 11-11) should be calculated for its specific combination of loading direction and reinforcement shearing, this is unfeasible by hand and will not be performed. Instead three critical points will be examined. These points involve either large shear deformations or large stresses. This process should be computerized and included within the software package that is used to formfind, drape, and analyze buildings built with the new material (Section 12-2-2). An illustration of the differing orientation between primary stresses and reinforcement direction geometrically overlayed over an element is shown in Figure 11.41 below.

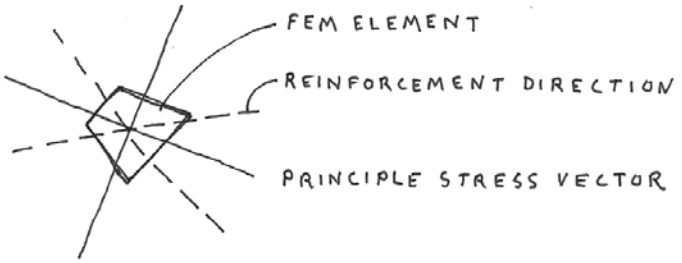

Figure 11.41: An element showing the differing orientation between primary stresses and reinforcement direction, geometrically overlayed.

The three selected points are investigated by closer examining the geometrical overlay of the primary stresses and sheared reinforcement orientation at each point. An overview of the building showing the overlay and the three selected points is shown in Figure 11.42. The data from this closer examination is then used to create and analyze a graph made using Equation 11.2. This graph is shown in Figure 11.43 and a summary of the results at each point is show in Table 11.2.

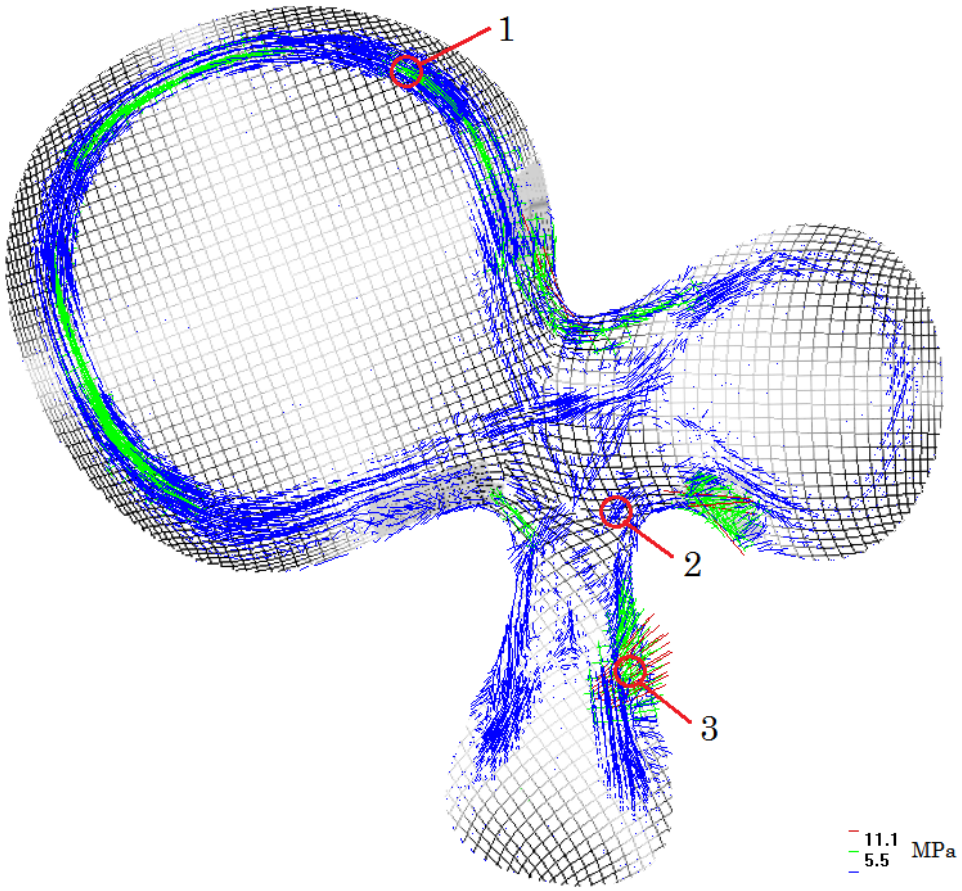

Figure 11.42: The Case Study Building with the primary stresses and sheared reinforcement geometrically overlayed, showing the three points for investigation during stress checks.

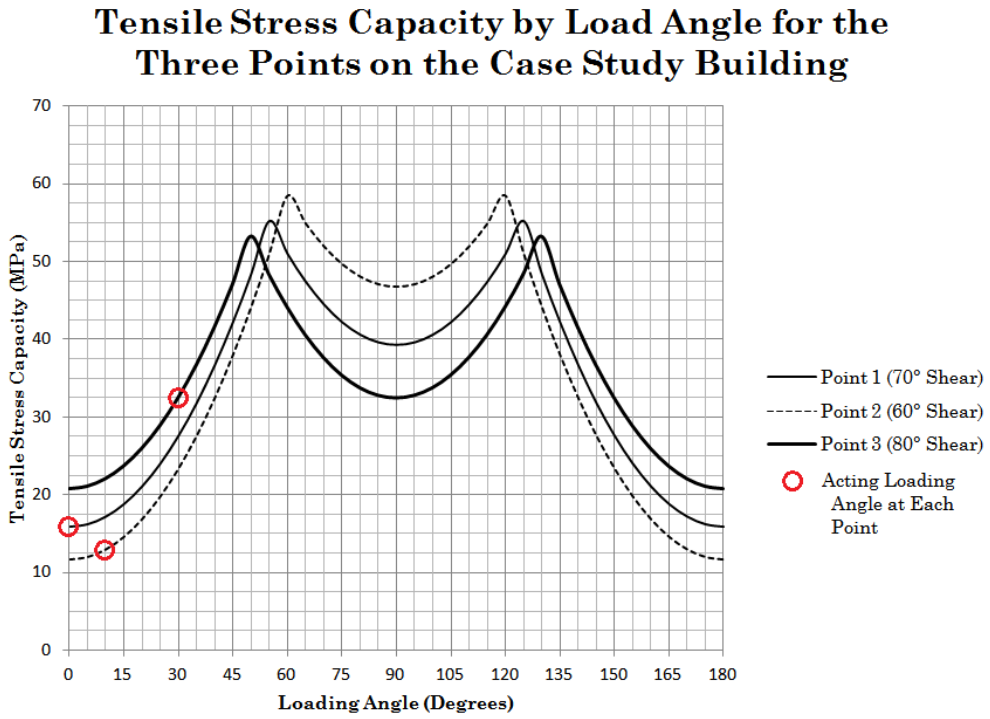

Figure 11.43: Tensile stress capacity for three points on the case study building, constructed Equation 11.2.

Table 11.2: Points for stress check inspection on the Case Study Building.

Point for Inspection	Shear Angle	Thickness (mm)	Loading Angle	Max Stress (MPa)	Capacity (MPa)	Safety Factor
1	70°	21	0°	11.1	15.9	1.43
2	60°	23	10°	5.5	13.0	2.36
6	80°	20	30°	16.8	32.4	1.93

While the safety factor at these three critical points is quite low (1.43 to 2.36) the rest of the structure has significantly larger values. The oversized loading (-7.2kN/m^2 in the Z-direction) was meant to push the structure to greater deformations and stresses. When an actual building is to be design using this material more realistic loading conditions should be used and greater safety factors at the critical points would be required. As the first investigation into the application of this material, the results show that the material is of sufficient capacity.

11-11 FOUNDATION DESIGN

The foundation must withstand loads during construction and during use. The loads during construction can be significantly different than during use, in both magnitude and direction. Therefore the foundation must be designed for both load cases. This could be solved using temporary or permanent solutions. Only a procedural outline of the foundation design will be covered here, as the foundation strategy is not unique for buildings made from this material. The foundation design begins with analyzing the reaction forces at the foundation-structure connection for each of the three loading cases. The connection to the foundation during construction is covered in Section 9-3-1.

The loading on the foundation is included in the numerical analysis of the orthotropic model (Section 11-8). Each of the approximately 200 support points in the model applies a load to the foundation in three directions X, Y, and Z. This loading is shown as component vectors for each direction, X and Y are represented by vector line, while Z is represented by a colored spot. The lengths and sizes of each indicator are proportional to its magnitude. For the Z-direction blue spots represent uplifting forces in the positive Z-direction. The set of forces for loading during construction is shown below, in Figure 11.44. The set of forces for loading during use is shown below, in Figure 11.45. The vectors are at the same relative scale (0.05) and in the same units (newtons). The forces during use are significantly larger than in construction and act in very similar directions. This indicates that the low levels of force on the foundation might not result in a significant overdesign and capacity useable only during construction. An appropriate foundation design could be created from the force information contained within these two figures.

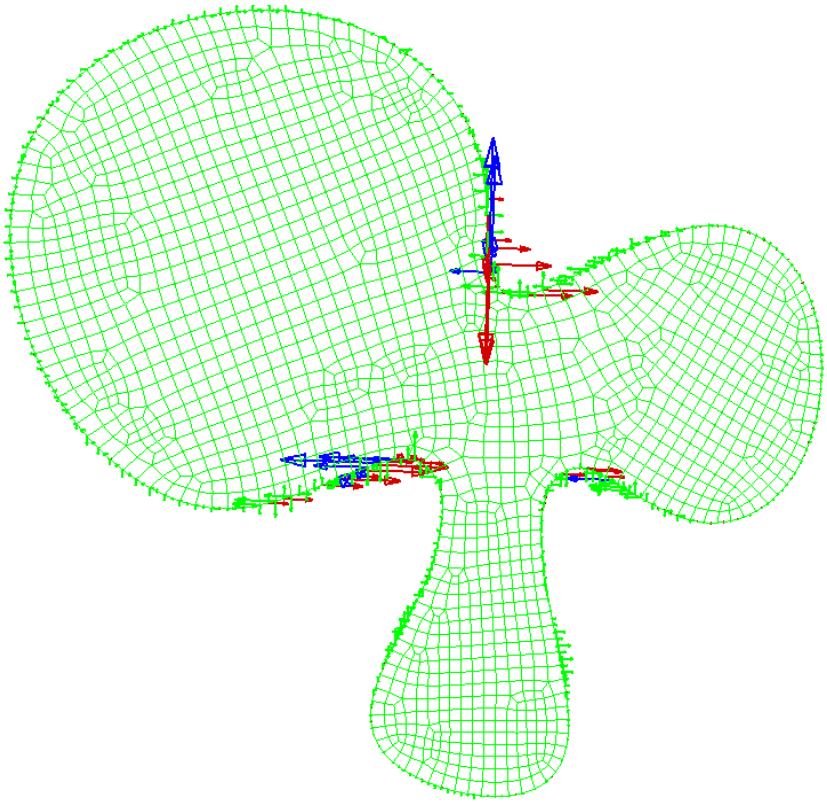

Figure 11.44: Foundation loading during construction, showing X, Y, and Z components, results from load case 3. (Case Study Building #6)

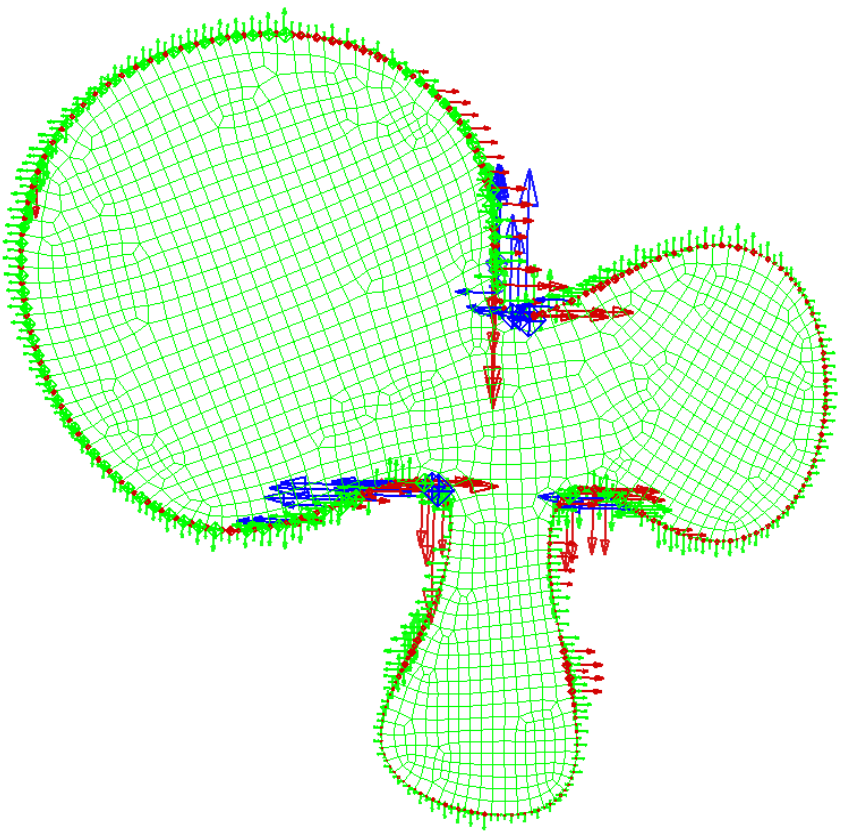

Figure 11.45: Foundation loading during use, showing X, Y, and Z components, results from load case 1 and 2.

11-12 CONSTRUCTION

The construction process will continue as described generally in Section 9-3 and specifically by the method of inflation described in Section 9-3-3. To begin the process of construction the site will be cleared and the foundation and basement levels constructed. Following this, a temporary construction will be required for the area of the building where the three structural bays meet (Figure 11.26). This construction will support the separate blanks as they shear to fit together and contain some sort of an airtight bladder to create an airtight seal. On a semi-level staging area, rolls of the new material will be brought to site, and joined to create the blank for the large structural bay. While still flat, the additional layers of material will be jointed to the blank in the appropriate two places. Fans or air compressors will then be used to inflate the blank to its appropriate shape. The thicker areas with multiple layers will likely require more force for shear deformation, which could be applied by cranes or jacks. Wetting should be used to ease shear deformation. Either at the same time or in the following days, the remaining two structural bays will be inflated from their blanks. Once in place, fully hydrated and cured, the air pressure can be released and the building is ready for finishing layers to be added.

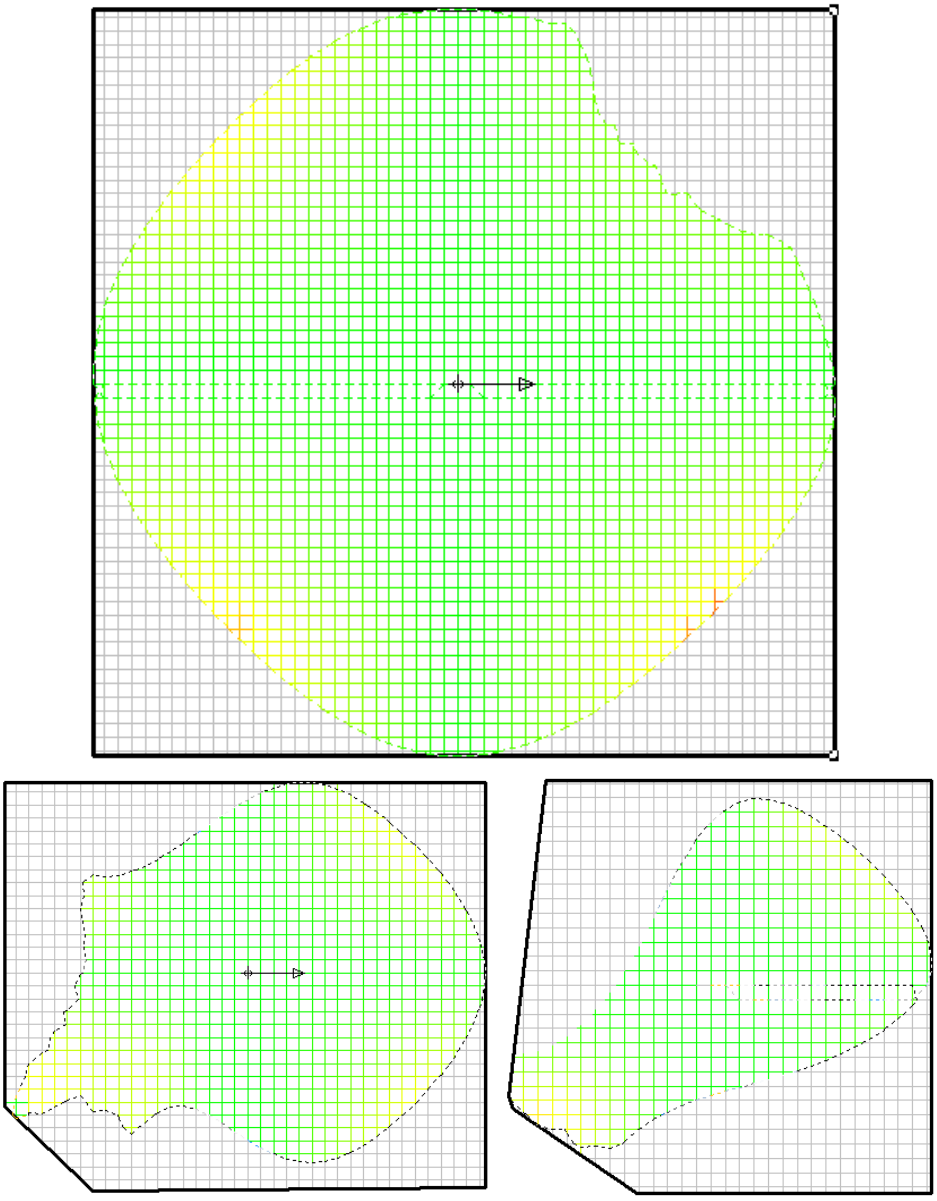

Figure 11.43: The flat material "blanks" which will be deformed by inflation to create the building shape, Large (top), Mid (bottom left), and Small (bottom, right).

11-13 CONCLUSION AND DISCUSSION

The architectural function of the Case Study Building was decided to be a concert hall which could utilize the large cavernous freeform spaces (Section 11-1). Such a large prestigious building would have rivals that are of equally freeform and blob-like. From this functional concept a footprint was created and the formfinding process added the inhabitable volume above (Section 11-2). This double-curved, three dimensional surface was analyzed using a finite element method (FEM) computer program called Diana, first as an isotropic concrete shell for general behavior (Section 11-4). These results were used to identify areas of the structure which would be constructed with two layers of the material (Section 11-5). The surface was then analyzed with this increased thickness (Section 11-6) and found to have increased performance. The shear-deformed properties of the material were added to the surface by using the computer program Drape (Section 11-7) and it was once more analyzed with Diana (Section 11-8). These results were used to analyze the stresses at three critical points (Section 11-10). Further, the process of construction (Section 11-10) and the design of the foundation (Section 11-11) are discussed.

The design of the Case Study Building illuminated some important points of the material and design process. Firstly, layering of the material to achieve increased thickness is effective at decreasing moments, distributing stress, and decreasing deformation. Additionally it is a method very simple to integrate into the design of structures made with this new material. It should be investigated further whether this thickness increase is best to be done in layers of the base material or by thicker versions of the material. The areas where the thickness change occurs could be an area of concentrated stresses and should be investigated further experimentally.

Secondly, the stress checks (Section 11-10) suggest that shear-deformation angle could be used strategically when determining the material draping scheme. Large shearing could be planned for areas of high loading in certain directions. This would be accomplished by changing the initial orientation of the material when draping.

Lastly, the orthotropic numerical analysis (Section 11-9) seems to have some issues with unexpectedly large local force values. This could be because the material properties in Drape are not sufficiently transferred to the material properties of the FEM model in Diana perhaps due to the difference in the alignment of local coordinate systems. It this could be done with confidence, such a model would provide more realistic results about the behavior of the structure because it includes angle dependant values of stiffness caused by the orientation of the reinforcement.

A summary of the results of the numerical analysis for each case study building is shown in Table 11.3.

Table 11.3: Summary of Case Study Building numerical analysis results, the grayed cell is thought to be an error caused by local axis misalignment and is removed from the results, Case Study Building 6 is grayed because it represents a special case therefore it is only considered for its limiting (maximum) values and not its minimum values (representing performance), maximums are bolded and minimums underlined.

Case Study Building		S1	S3	Nxx		Nyy		Mxy	DRes
		Tens	Comp	Comp	Tens	Comp	Tens	Bend	Def
		Mpa	Mpa	kN/m	kN/m	kN/m	kN/m	Nmm	mm
1	**Uniform**	**46.4**	**42.6**	608	115	306	**438**	802	**108**
2	**Saddle (80mm)**	45.5	40.4	**761**	122	299	427	1310	102
3	**Patches (40mm)**	16.7	28.6	556	112	193	215	**1320**	26.7
4	**Variable Thickness**	16.8	25	537	**182**	**763**	179	**1320**	25.3
5	**Draped**	19.7	32.8	692	193	*806*	196	1230	29
6	***Construction***	*16.2*	*12.8*	*279*	*115*	*241*	*159*	*602*	*16.2*

12 CONCLUSION

This chapter will present the successful portions of the entire project, discuss its shortcomings, and propose next steps for realizing this new material and method of construction.

12-1 DISCUSSION

This project began as the realization of a patented material but expanded include the material development as well as a digital design process. This increased scope was necessary to fully envisioning a functioning material. However in splitting its focus it leaves two open ends to the project. Both sides of the project explore the specifics of using shear deformation to create double curvature. This is the innovative feature of the patented material. The materialization and design process can differ from the methods described in the patent but always enable the property of shear-deformation.

12-1-1 GENERAL

Buildings are big and complex and therefore have many requirements placed on them. This material will never be able to fulfill all of them. It should focus on what it does well and find solutions or exceptions for the requirements preventing its usage. Its power is that it acts as a load-bearing surface and can therefore be very efficient if designed properly. However, this strength is also a weakness because of its lack of transparency, an often sought after feature for large public buildings.

Other topics such as fire performance, thermal expansion, and waterproofing, among others can be solved using other materials. At this stage in development it is important to acknowledge the wide set of topics but not necessary to have solutions to all of them. Structural modification and repair methods might be required to be integrated into the design of the material elements, meaning that the fabrication process or reinforcing would have to be reconsidered at a later stage.

This project should have searched for collaboration and inspiration from manufacturers of existing products to gain insight into the fabrication process. Collaboration with Concrete Canvas could have simplified the material development process significantly. It is possible that Concrete Canvas has a capacity for shear deformation. Although its capacity would most likely be insufficient to form the hemispherical test shape it would still be valuable for testing. Inspiration from other jointed systems or other industries should be searched, instead of the imagined joints currently proposed.

During FEM analysis, the wind loading case was not limiting and therefore not considered during the design and dimensioning process. The largest internal forces and stresses came from the gravity loading situation. Moments from both loading cases were much less than the capacity and therefore not addressed during the design.

During the course of the numerical analyses only two load cases were used, gravity and wind, but not together. Furthermore only the gravity case was discussed in the report because it was the limiting case. New loading cases and combinations of cases should be applied to account for thermal expansion, live loads, floor loads, and others.

12-1-2 MATERIAL REALIZATION

Although this project proposes a material configuration with specific materials, it more importantly aims to create a foundation for the behavior of a shear deforming material. The suggested materialization and configuration relies on established materials, glass fiber and fine-grained concrete, instead of using newer materials which might have mechanical or sustainability benefits. For this a collection of many more types of materials is required, namely types of foams and 3D woven textiles. They could be the most promising type of reinforcement because they are very stable and would resist delaminating. However, this configuration should be reevaluated after further physical testing inspection.

With the conservative base configuration chosen, material properties could be estimated, although they were often estimated differently throughout the course of the project. For example, the inputs for Drape and Diana use different stiffness properties (Young's Modulus and orientation) than those prescribed by the examples of Hegger. Hegger's experiments formed the basis of strength calculations for the material. This required a significant modification to one of Hegger's coefficients to enable the calculation with shear-deformed reinforcement.

The physical testing performed during this project was insufficient to determine many important properties of the shear deformed material. New testing should be conducted to update the assumptions taken about the strength, minimum shear angle, required deformation force, and extent thickness increase. The lower bound of shear deformation was set by the hemispherical test shape. However, the majority of the surface requires significantly less severe shear deformation. Many freeform buildings could be constructed entirely without ever reaching this lower bound of shear deformation. Therefore those areas of high shear deformation could be treated as exceptional and handled by alternative structures. This would ease the requirements of the new material, perhaps making it easier to realize.

Buckling of the material was not evaluated even though it represents a considerable concern for thin shell structures. Buckling would occur at imperfections, joints, or with uneven loading situations. This could have been investigated further by using a nonlinear structural analysis in Diana or by applying knowledge about shell buckling. Even more simply, exaggerating the wind loading case might have been sufficient to create large-scale buckling like behavior because of additional bending moments.

12-1-3 DIGITAL DESIGN PROCESS

Properties about shear-deformation are required at each stage of digital design and analysis. During formfinding, the force required for shear deformation and during analysis, the shear angle, thickness increase, and reinforcement orientation are required. Currently only Drape contains all of this information and during each other stage it must be approximated or roughly imported.

This loss of information did not prevent the project from progressing but did weaken its representation of reality. For formfinding this meant that the found geometry was less like the real process of construction because it did not include the force required for shear deformation. For analysis this meant that the angle between reinforcement and primary stress vectors could not be directly investigated making the process of stress checks more difficult and less accurate. Additionally, the link between formfinding (in Rhinoceros and Grasshopper) and FEM analysis (in Diana/FX+) is an approximation using the Patch command to create a surface from a meshes. This slightly alters the geometry and causes winkling where it was not prescribed, so the shape being analyzed is not exactly same shape which was created in the formfinding process.

The formfinding process had many of its own assumptions most importantly the balance between internal stiffness, gravity loading, and inflation pressure. Ideally this formfinding process would mimic reality, but this was not yet accomplished. Structural efficiency is not accounted for in the formfinding process, although, it is suggested that inflated-dome- and hung-tent-like shapes are more structurally efficient than other kinds of freeform blob shapes. For this project, structural efficiency was found using a recursive trial-and-error method in combination with formfinding. In the future it would be possible to combine tools such as Thrust Network Analysis, from the BLOCK Research Group (Section 3-7), to imbue the formfinding with structural 'intelligence'.

Draping of the material is also an area of optimization yet unexplored. It would involve the placement and fitting of the actual material properties to the surface. Currently this has been done by trial-and-error in Drape but does not include the increasing force required for shear deformation (Figure 4.9). High areas severe shear could be aligned with areas of high stresses. Edges between structural bays could be created in locations of no shear for easier construction or with low stresses.

12-1-4 CONSTRUCTION

The forces during construction are significantly different than during use, particularly for the inflation method. These hanging and inflation forces should be considered during the formfinding process more adequately. Large tensile forces during construction may cause delamination or other destruction to the cross-section of the material.

As mentioned, the material stresses change dramatically, often a full reversal from tension to compression. As it stands now, this imposes large structural requirements on the material which might be utilized only during construction, resulting in overdesigned elements. This is contradicts the goal of creating structurally efficient buildings. In other cases (such as hanging structures with permanent supports) the material remains similarly loaded during construction and use. In these cases the rigidity and stiffness gained during hardening would be utilized to limit deformations or to support additional constructions.

Although possibly more efficient, the hanging method of construction could prove to be troublesome if special care is not taken to properly orient the material. This is because the material does not significantly extend in the directions of the textile yarns, while it extends (by shear deformation) significantly diagonal to the yarn directions. This might be solvable if it can be properly secured to the foundation before deformation to control this diagonal extension. This would however impose large horizontal temporary loads on the foundation. An over-design of the foundation, as compared to the use loading, would be required for these areas. These forces and changes to the construction method could be investigated using a computer program designed for membrane structures, because during hanging the material acts as a membrane, completely in tension. EASY is the name of such a program that could be utilized.

The foundation connections will require special features to protect the material from damage during shearing and slipping. These have not been designed but could consist of rollers or plastic padding. This portion of construction imposes a durability requirement on the material's composition. This was only briefly mentioned, that woven canvas layers could be used in addition to the other functional layers for this purpose, but it should be investigated further, probably with physical experimentation.

12-2 NEXT STEPS

This project outlines the required knowledge for building with a shear deforming material, yet such a material remains unrealized and the design process remains complex and does not properly mimic reality. The next steps should address these two areas. The material should be investigated by physical testing of prototypes, while the design process by the streamlining of the computer tools. This project used computer tools to get an idea of the required material properties, therefore the next step should be to realize the material and settle its properties. After this experimentation, the computer tools can use the results to better mimic reality.

Additionally a case study building that is created using the hanging method instead of the inflation method should be designed. This very different digital design process would behave differently and would place different requirements on the material.

12-2-1 MATERIAL TESTING

The material should be redesigned with a broader set of material and configuration options and then tested for the following:

- Jointing and buckling
- Thickness increase behavior
- Required force for shear deformation
- Behavior during construction loading
- Shear loading to update the Modified Oblique-Angled Loading Coefficient

This project only had time to test the deformation ability the elastic film layer (Section 8-1), instead of the material as a whole. There is concern that shear deformation might be limited by the dry concrete layers. This should be tested wet and dry. This testing would clarify the true mode of thickness increase. The material is required to perform differently when cured and when uncured. Therefore it should be tested dry, wet, partially cured, and fully cured.

Gathering information about the joints and material would be most practical as the next step toward building design. This information would have been needed to accurately complete this project. It would identify the true bearing strength and failure mechanism for buildings built of the material (which would probably be buckling). Physical testing of the joints could be performed at multiple scales. Enough testing should be done to increase the accuracy of the computer modeling.

12-2-2 STREAMLINED COMPUTER TOOLS

A significant hurdle during this project was getting the various computer programs to communicate effectively and reliably. A next step should therefore be to streamline this process as well as to improve upon it by including more information about the material properties and architectural features. This would mean a formfinding process that not only considers the method of construction but also the force required to deform the material and opens up the possibility of optimization. This will vary with shear angle, number of layers, hydration, and other factors. Then this formfinding process should be linked to Diana and Rhinoceros using “surfaces” instead of “mesh” geometry. In summary these next steps are:

- Formfinding with material properties and construction behavior
- Formfinding to include doors and windows
- Optimization using Drape, formfinding, and Thrust Network Analysis
- Linking of shear deformation information to analysis (in Diana) and stress checks

At this point the method of integrating “exceptions” such as windows and overhangs into the structural design has been messy and mostly an afterthought once the main structure has been form-found. All building will have these features and as it is currently presented they would require considerable finishing work. The purpose of this material and construction method is to reduce onsite labor. Therefore the next step towards normalizing these exceptions should be taken.

The formfinding process should include information about the shear deformed material and construction method so that the found-geometry will be easy to implement during structural analysis. In this project the structural analysis was performed by geometrically overlaying both sets of data about shear-deformation and stresses. An example of these data overlaid is shown in Figure 12.1. Additionally, architectural flexibility should be maintained as the design process progresses, for example by the use of parametric software and a cross referenced modeling environment.

Work from the BLOCK Research Group, utilizing Thrust Network Analysis, provides a computer tool which links material properties to formfinding. Such a tool shows the possibility of designing with building elements of known strengths instead of designing building elements to match forces derived from the design. This reversal of the traditional design process would be very important to designing with the new material being developed, which has limited, predetermined properties.

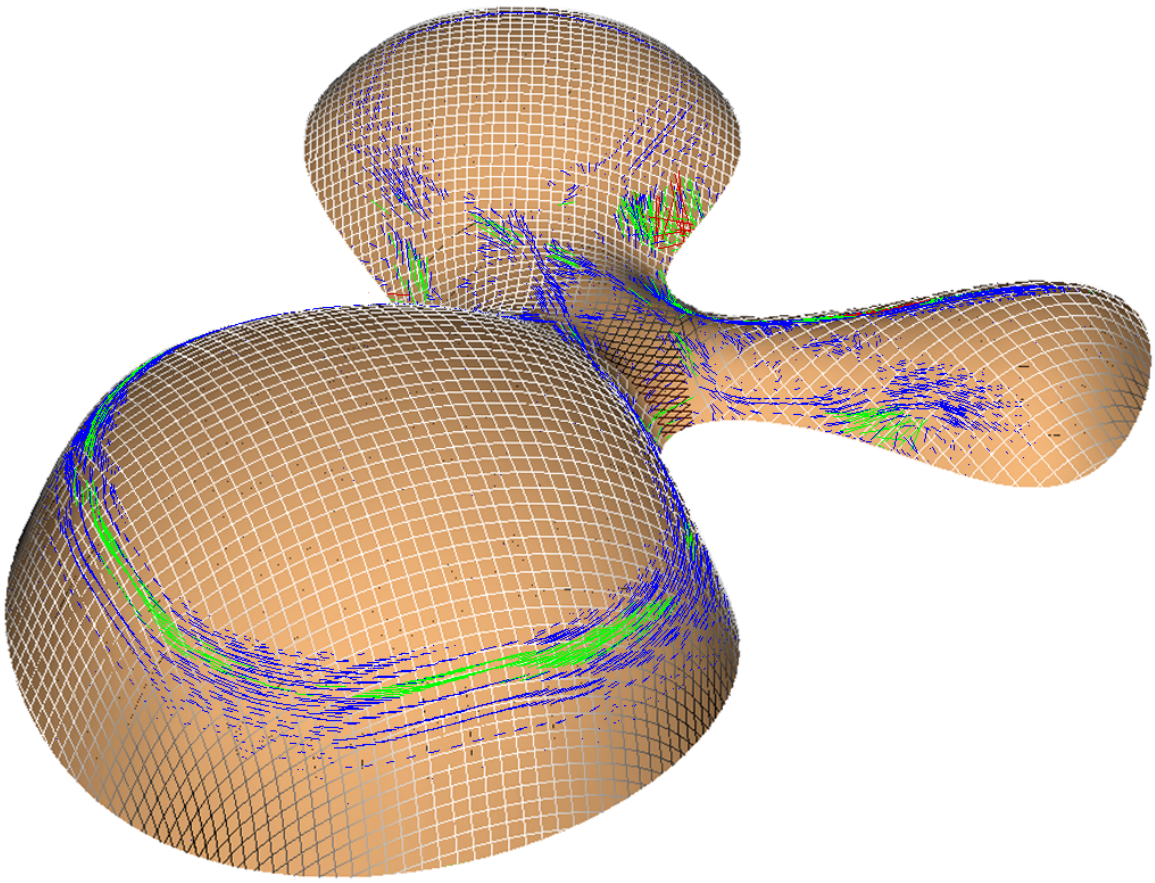

Figure 12.1: Three-quarters top view of the case study building showing shear-deformation and primary stress vectors.

12-3 FINAL REMARK

Seeing issues such as cost and joint detailing, this material has many hurdles to overcome before becoming a reality. It provides an easy to construction solution for making certain kinds blob/freeform buildings. It however could be classified as a cheaper method for making worse buildings, as compared to more labor intensive construction methods, such as traditional formwork and concrete construction. If this material has one positive aspect, it can hope to enable the creation and inspire the design of structurally efficient buildings. However, it might be better to design efficient shell structures and construct them of reinforced concrete the labor intensive way, albeit more expensive.

All in all, this project represents the base layer of information for designing a building from a shear deforming material. It takes many assumptions and lacks the real-world information to be useful for designing a building. The broadened scope of the project suggests that it should be possible to accurately design and create thin, double-curved, freeform structures with a shear-deforming material if additional physical testing and a redevelopment of the digital design process occur.

Ultimately the success of such a material will depend greatly on the willingness of architects to utilize such a material and the continuing popularity of freeform, blob-like buildings.

List of Conclusions

- This project suggests that a shear-deforming material for double curved structures is possible
    - It would measure 20mm thick and increase up to 30mm when fully shear-deformed
    - A large reinforcement percentage (16%) is required (more similar to the aerospace industry, which inspired this material, than to the construction industry where it will be used)
- Fabrication is possible is 1m widths and very long (20m+) lengths from precedent project
    - Joints between elements and foundations have been outlined
- Simple geometrical shapes, such as a hemisphere, can be constructed continuously
    - Larger complex geometries will require multiple pieces to limit shear-deformation
    - The material should be layered, or a thicker version used, to enable larger spans
    - Spans of up to 30 meters might be possible
- Digital, parametric formfinding methods were developed to mimic construction
    - Inflation and hanging methods of construction are applicable
    - Parameters such as material-weight, inflation-pressure, and amount of material are used to control the formfinding process
- Additional topics preventing realization were outlined, such as fire, cost, and sustainability
- Research on textile reinforced concrete was modified to enable structural analysis
- A large high-profile, concert hall, case study building was designed as a conclusion to the research
- Further areas of computer tool integration and material development are required and have been outlined

REFERENCES

TEXTS

Bergsma, O.K.. Three Dimensional Simulation of Fabric Draping. Den Haag: CIP-Data Koninklijke Bibliotheek, 1995. Web.

Chudoba, R.. "ORICRETE: Modeling support for design and manufacturing of folded concrete structures." Advances in Engineering Software: n. pag. Web. 4 Aug. 2014.

Concrete Canvas. http://www.concretecanvas.com/concrete-canvas/general/what-is-it

Eigenraam, Peter. Flexible mould for production of double-curved concrete elements. Masters Thesis: Delft University of Technology, 2013. Web.

Formtexx: Quote from http://www.e-architect.co.uk/products/formtexx.htm

Hegger, J., and S. Voss. "Investigations on the bearing behaviour and application potential of textile reinforced concrete." Engineering Structures: 2050-2056. Web.

Hegger, J., and S. Voss. "Load–bearing behaviour and simulation of textile reinforced concrete." Materials and Structures: 765-776. Web.

Kok, Marijn. Textile reinforced double curved concrete elements: Manufacturing free-form architecture with a flexible mould. Masters Thesis: Delft University of Technology, 2013. Web.

NL2003576C: Beukers, A., and O.K. Bergsma. Sheet-Like Building Material. NL Octrooicentrum, assignee. Patent NL2003576C. 6 Apr. 2011. Print.

Provis, John L.; -van Deventer, Jannie S.J. RILEM State-of-the-Art Reports. Alkali Activated Materials. 2014. Springer Netherlands. IBSN: 978-94-007-7672-2_1

Schipper, R.. "Manufacturing Double Curved Precast Concrete Panels." Concrete Plant International 1 Aug. 2011: 32-38. Scan.

West, Mark. Thin-Shell Concrete from Fabric Molds. C.A.S.T. The Centre for Architectural Structures and Technology: University of Manitoba Faculty of Architecture, 2009. Web.

IMAGES

Aistleitner, Christoph; Schneider, Marion. Kunsthaus Graz in Graz, Austria, Europe; seen from "Schloßberg" mountain Photograph. 2008. http://en.wikipedia.org/wiki/File:Graz_Kunsthaus_3.jpg

Albertini, C., and Montagnani, M.. "Study of the true tensile stress-strain diagram of plain concrete with real size aggregate ; need for and design of a large Hopkinson bar bundle." Le Journal de Physique IV: C8-113-C8-118. Web.

Barhum, R.. "Mechanical Behaviour under Tensile Loading of Textile Reinforced Concrete with Short Fibres." Colloquium on Textile Reinforced Structures 6 (CTRS6): 175-186. Web.

Bergsma, O.K.. Three Dimensional Simulation of Fabric Draping. Den Haag: CIP-Data Koninklijke Bibliotheek, 1995. Print.

China Beihai. Fiberglass 3D GRP reinforced foam cement board. Photo. http://www.fiberglassfiber.com/Item/Show.asp?m=5&d=344

Colocho. Inside view of the Biosphere in Montréal, Quebec. Photograph. 2006. http://en.wikipedia.org/wiki/File:Biosph%C3%A8re_int%C3%A9rieur.JPG

Concrete Canvas. http://www.concretecanvas.com/concrete-canvas/general/what-is-it

Edkins, Keith. Long distance view of The Sage Gateshead from an upper storey of the 55 Degrees North apartment block at the Swan House Roundabout in Newcastle. Photograph. 2004. http://en.wikipedia.org/wiki/File:The_Sage_Gateshead_2004.jpg

Emporis; Adams, Victor B. Rebar sticking out from a concrete column. Image ID: 630230. Photograph. 2008. http://www.emporis.com/images/details/630230

Epfll Alain Herzog. Rolex Learning Center. Photograph. July 2009. Web, Wikipedia, http://en.wikipedia.org/wiki/File:Rolex_Learning_Center_07-2009.jpg (accessed March 2014).

Fczarnowski. Rome - Pantheon, oculus. Photograph. 2010. http://en.wikipedia.org/wiki/File:Pantheon_chiesa,_Roma_fc07.jpg

Furuti, C.A. [Flattened orange peel.] Photograph. 2011. http://www.progonos.com/furuti/MapProj/Normal/CartDef/MapDef/mapDef.html

GS Consulting. [Laminated glass fabric.] Photograph. http://d2n4wb9orp1vta.cloudfront.net/resources/images/cdn/cms/0613CT_Roundup_transparent.jpg

Haas, A.M. "Design of thin concrete shells Vol. 1 Positive curvature index." Wiley, 1962.

Hagens, Wouter. Expo 1958 Philips Pavilion. Photograph. 1958. http://en.wikipedia.org/wiki/File:Expo58_building_Philips.jpg

Hegger, J., and S. Voss. "Investigations on the bearing behaviour and application potential of textile reinforced concrete." Engineering Structures: 2050-2056. Print.

Hegger, J., and S. Voss. "Load–bearing behaviour and simulation of textile reinforced concrete." Materials and Structures: 765-776. Web.

Huijben, F., F. van Herwijnen, and R. Nijsse. "Concrete Shell Structures Revisited: Introducing a 'Low-Tech' Construction Method using Vaccumatics Formwork." International Conference on Textile Composites and Inflatable Structures Structural Membranes 2011. Web.

Kapoutrocknroll. [Louis Vuitton Foundation under construction]. Photograph. 6 February 2009. Web, Skyscrapercity, http://www.skyscrapercity.com/showthread.php?t=401966 and http://img859.imageshack.us/img859/9206/img20120131145442.jpg (accessed March 2014).

Lightweight Structures BV. Schematic of the vacuum form process. http://www.lightweight-structures.com/vacuum-forming-of-thermoplastic-composites/index.html

Lightweight Structures BV: http://www.lightweight-structures.com/vacuum-forming-of-thermoplastic-composites/index.html

Mayer, Thomas. Neuer Zollhof Dusseldorf, the new emblem of the city, office buildings, architect Frank O. Gehry. Image number: 001AA19990901A0021. Photograph. 1999. http://thomasmayerarchive.de/details.php?image_id=27353

NL2003576C: Beukers, A., and O.K. Bergsma. Sheet-Like Building Material. NL Octrooicentrum, assignee. Patent NL2003576C. 6 Apr. 2011. Print.

Nuna Innovations. http://store.nunainnovations.com/concrete-cloth/

Parabeam. 3D Glass Fabric. Photo. http://www.parabeam.nl/standard-fabrics

Piéton. Fondation Louis Vuitton pour la Création, #24359. 11 June 2011. Web, PSS Architecture Forum, http://www.pss-archi.eu/photos/membres/390/l/1321118652lcl.jpg (accessed March 2014).

Provis, John L.; -van Deventer, Jannie S.J. RILEM State-of-the-Art Reports. Alkali Activated Materials. 2014. Springer Netherlands. IBSN: 978-94-007-7672-2_1

Rippmann, M. and Block, P.Funicular Shell Design ExplorationProceedings of the 33rd Annual Conference of the ACADIAWaterloo/Buffalo/Nottingham, Canada2013.

Sika 1990 http://deu.sika.com/dms/getdocument.get/bb73cb5c-79d0-31fa-ac98-b5c5f45fd1df/Brosch%C3%BCre%20Sika%20Unitherm%20GB%2012%20S.pdf

Stockton, Jon. Experience Music Project and Science Fiction Museum and Hall of Fame, Seattle. Photograph. 2006. http://en.wikipedia.org/wiki/File:ExperienceMusicProject.jpg

Unknown1. [Sicli Company building.] Photograph. http://1.bp.blogspot.com/_xJWa77A8OSw/SuaRrNdApII/AAAAAAAAFFk/3qO_VmTvvZg/s400/isler+Sicil+Materiel+Incendie+SA-1.jpg

Unknown2. Photograph of Hegger's Ice Tents. From a conference paper somewhere.

Unknown3. Beachball. Photograph. http://german.inflatable-watertoy.com/china-no_giftige_gro_e_aufblasbare_wasserb_lle_f_rdernder_wasser_ball_pvcs_f_r_kinder-624684.html

West, Mark. Thin-Shell Concrete from Fabric Molds. C.A.S.T. The Centre for Architectural Structures and Technology: University of Manitoba Faculty of Architecture, 2009. Web.

A APPENDIX